RICE UNIVERSITY

Modeling Protein Flexibility Using Collective Modes of Motion: Applications to Drug Design

by

Miguel L. Teodoro

A THESIS SUBMITTED
IN PARTIAL FULFILLMENT OF THE
REQUIREMENTS FOR THE DEGREE

Doctor of Philosophy

APPROVED, THESIS COMMITTEE:

____
Lydia E. Kavraki, Associate Professor,
Computer Science and Bioengineering

____
Kevin R. MacKenzie, Assistant Professor,
Biochemistry and Cell Biology

____
Seiichi Matsuda, Associate Professor
Biochemistry and Cell Biology

____
John S. Olson, Dorothy and Ralph Looney
Professor, Biochemistry and Cell Biology

____
George N. Phillips, Jr., Adjunct Professor,
Biochemistry and Cell Biology

HOUSTON, TEXAS

AUGUST, 2003

Abstract

This work shows how to decrease the complexity of modeling flexibility in proteins by reducing the number of dimensions necessary to model important macromolecular motions such as the induced fit process. Induced fit occurs during the binding of a protein to other proteins, nucleic acids or small molecules (ligands) and is a critical part of protein function. It is now widely accepted that conformational changes of proteins can affect their ability to bind other molecules and that any progress in modeling protein motion and flexibility will contribute to the understanding of key biological functions. However, modeling protein flexibility has proven a very difficult task. Experimental laboratory methods such as X-ray crystallography produce rather limited information, while computational methods such as molecular dynamics are too slow for routine use with large systems. In this work we show how to use the Principal Component Analysis method, a dimensionality reduction technique, to transform the original high-dimensional representation of protein motion into a lower dimensional representation that captures the dominant modes of motions of proteins. For a medium-sized protein this corresponds to reducing a problem with a few thousand degrees of freedom to one with less than fifty. Although there is inevitably some loss in accuracy, we show that we can approximate conformations that have been observed in laboratory experiments, starting from different initial conformations and working in a drastically reduced search space. As shown in this work, the accuracy of protein approximations using this method is similar to the tolerance of current rigid protein docking programs to structural variations in receptor models.

Acknowledgements

First and foremost, I would like to thank my advisors Dr. George Phillips and Dr. Lydia Kavraki. Dr. George Phillips provided me with the necessary freedom to pursue diverse research topics. His invaluable supervision and insight allowed me to find the perfect project. Dr. Lydia Kavraki has been an extraordinary mentor and friend. It has been a pleasure and honor to work with her. I thank them, as well as my previous advisors, Dr. Helena Santos and Dr. António Xavier, for making me a better scientist.

I would like to thank the remaining members of my thesis committee, Dr. Kevin MacKenzie, Dr. Seiichi Matsuda, and Dr. John Olson for continued guidance and many helpful suggestions. I am also grateful to all the past and present members of the Kavraki and Phillips labs for making Rice a fun place to be.

This body of work would not have been possible without financial support from the PRAXIS XXI program from the Portuguese Foundation for Science and Technology, the Keck Center for Computational Biology, the Whitaker Foundation, the National Science Foundation, the Texas Advanced Technology Program, and an Autrey Fellowship Award from Rice University.

Finally I would like to thank my parents, Luis and Conceição and my wife, Rosinha, for their love and support of my education and personal growth.

.

Table of Contents

List of Tables

List of Figures

Chapter 1.

Introduction

1.1. Protein Modeling and Pharmaceutical Drug Design

The three-dimensional structures of protein and nucleic acid molecules are being determined at increasingly faster rates by X-ray crystallography and Nuclear Magnetic Resonance. These large molecules play a role in almost all biological processes either directly, or indirectly by acting as regulators. As a result, biomacromolecules are key targets for drug design. The rapid generation of quality lead compounds is a major hurdle in the design of therapeutics, so that accurate automated procedures would be of tremendous value to the pharmaceutical and other biotechnology companies. However, designing a drug based on the knowledge of the target receptor structure as determined by current experimental techniques is a process prone to error. The two major reasons responsible for failures are imperfect energy models when scoring potential ligand/receptor complexes (Muegge and Rarey 2001; Halperin, Ma et al. 2002; Shoichet, McGovern et al. 2002), and the inability of current methods to predict conformational changes that occur during the binding process not only for the ligand, but also for the receptor (Carlson 2002; Teodoro and Kavraki 2003). Although the latter problem has been partially solved by incorporating ligand flexibility in search methods, predicting receptor structural rearrangements is a very complex problem which has not been solved. The focus of the work reported in this dissertation is to develop a method which can account for receptor conformational changes that occur during the binding process.

1.2. Induced Fit Binding

Induced fit binding is the process by which both receptor and ligand change their conformation from the native form in solution to a new minimum energy conformation which takes into account the interaction of the two molecules. Because induced fit is a common occurrence in biological systems, in order to be able to accurately predict docked conformations between a protein and a ligand it is often necessary to model this effect (Murray, Baxter et al. 1999). Taking into account the receptor flexibility in structural-based drug design is a natural step in the evolution of this field and can lead to new classes of drugs which can be effective with lower dosages and with fewer side effects (Kaul, Cinti et al. 1999). From an industrial point of view the development of new classes of drugs is also important because it reduces the probability of intellectual property conflicts with previous patents.

Induced fit conformational changes have been observed experimentally for a large number of systems. A few examples are thymidylate synthase (Weichsel and Montfort 1995), chaperonin GroEL (Fenton, Kashi et al. 1994), cyclooxygenase-2 (Luong, Miller et al. 1996), lipoprotein (a) (Fless, Furbee et al. 1996), thrombin (Banner and Hadvary 1991), cytochrome c peroxidase (Cao, Musah et al. 1998), phosphofructokinase (Auzat, Gawlita et al. 1995), dihydrofolate reductase (Bystroff and Kraut 1991), HIV-1 protease (Appelt 1993), aldose reductase, maltose binding protein

(Spurlino, Lu et al. 1991; Sharff, Rodseth et al. 1992), and many others. For this study we decided to use the last four proteins as models systems. For more information on these proteins and their conformational changes upon binding see Appendix A.

1.3. The Curse of Dimensionality

Current docking programs used commonly in academic and industrial settings can account for the flexibility of the ligand during induced fit binding. This is carried out by modeling the degrees of freedom of the ligand explicitly. The degrees of freedom can be represented by the Cartesian coordinates of every atom in the ligand molecule. The resulting search space has (3 × N) + 6 degrees of freedom, where N is the number of atoms in the ligand and the extra 6 six degrees of freedom account for rotation and translation of the ligand relative to the receptor. The dimensionality of the problem can be further simplified by considering that bond angles and bond lengths are fixed. In this case the flexibility of the ligand can be modeled exclusively with torsions around single bonds. As a result the total number of internal degrees of freedom that need to be modeled for a traditional ligand is approximately 10 to 20. Although high, the dimension of the search space is within the capabilities of modern optimization methods such as genetic algorithms (for more information see Appendix C.).

Including the receptor flexibility in current docking programs by modeling the protein in the same way as the ligand is currently impossible. Instead of 10 to 20 degrees of freedom, the search space would be composed of hundreds or even thousands of degrees of freedom. The dimensionality of such a search space is well beyond the capabilities of current computational methods. Given the impossibility of modeling the receptor using the same methods as the ligand it is imperative to find alternative docking methods that can be used in structure-based drug design.

1.4. About This Project

In this project we propose a method to reduce the dimensionality of the protein flexibility space that can be applied to modeling conformational rearrangements such as induced fit changes upon ligand binding. Unlike other current methods which reduce the dimensionality of the search space by considering only a few degrees of freedom in a very limited region of the receptor, our method is able to consider the flexibility of the protein as a whole. The method described in this work is based on the calculation of a small set of collective degrees of freedom that account for most of the conformational variance of the protein.

This work is organized as follows. In Chapter 2 we review current protein flexibility models which can be used in the context of structure-based drug design. In Chapter 3 we carry out a quantitative assessment of the tolerance of current rigid-protein / flexible ligand docking methods to receptor conformational changes. Chapter 4 describes how to obtain a reduced set of collective degrees of freedom that explain protein flexibility using principal components analysis. The method is applied to three different model proteins: HIV-1 protease, aldose reductase and maltose binding protein. Finally in Chapter 5 we explore three different methods of incorporating the information obtained about protein flexibility in structure-based drug design.

Chapter 2.

Background - Protein Flexibility Models in Structure-Based Drug Design

2.1. Introduction

The ability to predict the bound conformations and interaction energy between small organic molecules and biological receptors, such as proteins and DNA, is of extreme physiological and pharmacological importance. Hence, there has been a considerable effort from both academia and industry to develop computational methods that can be used to determine the affinity with which a ligand will bind a target receptor. These methods usually include docking algorithms that compute the three dimensional structure of the complex as would it be determined experimentally using X-ray crystallography or Nuclear Magnetic Resonance (NMR) methods. Docking entails determining not only the identity and three dimensional structure of the bound ligand, but also how the binding process affects the conformation of the receptor. Here we review the different receptor flexibility representations that have been proposed to study receptor conformational changes in the context of structure based drug design.

A central paradigm which was used in the development of the first docking programs was the lock-and-key model first described by Fischer (Fischer 1894). In this model the three dimensional structure of the receptor and the ligand complement each other in the same way that a lock complements a key. According to this model, one could find a good drug candidate by searching a database of small molecules for one that complemented the three dimensional structure of a given receptor. This rigid matching was supported by several studies of complexes of proteolytic enzymes with small protein inhibitors (Blow 1976; Huber and Bode 1978; Hubbard, Campbell et al. 1991) and from the first example of an antibody-protein complex (Amit, Mariuzza et al. 1986). However, subsequent work has confirmed that the lock-and-key model is not the most correct description for ligand binding. A more accurate view of this process was first presented by Koshland (Koshland 1958) in the induced fit model. In this model the three dimensional structure of the ligand and the receptor adapt to each other during the binding process. It is important to note that not only the structure of the ligand but also the structure of the receptor changes during the binding process. This occurs because the introduction of a ligand modifies the chemical and structural environment of the receptor. As a result, the unbound protein conformational substates, corresponding to the low energy regions of the protein energy landscape, are likely to change. The induced fit model is supported by multiple observations in many different proteins including streptavidin (Weber, Ohlendorf et al. 1989), HIV-1 protease (Wlodawer and Vondrasek 1998), DHFR (Bystroff and Kraut 1991), aldose reductase (Wilson, Tarle et al. 1993). The qualitative and quantitative effects of ligand-induced changes in proteins have been described previously (Betts and Sternberg 1999; Murray, Baxter et al. 1999; Najmanovich, Kuttner et al. 2000; Zhao, Goodsell et al. 2001; Fradera, Cruz et al. 2002) and explain the ability of a protein to bind multiple drugs with considerably different three dimensional shapes (Wlodawer and Vondrasek 1998; Vazquez-Laslop, Zheleznova et al. 2000).

A more modern, but not contradictory, model for protein/ligand binding considers the binding process as a selection of a particular receptor conformation from an ensemble of metastable states (Ma, Kumar et al. 1999; Ma, Wolfson et al. 2001; Bursavich and Rich 2002; Ma, Shatsky et al. 2002). The protein exists as a family of similar conformations in a hierarchical energy landscape (Verkhivker, Bouzida et al. 2002). Successful binding shifts the dynamic population equilibrium in favor of the bound receptor conformation. This model of ligand binding suggests that for the design of novel inhibitors we may need to explore receptor conformations beyond the narrow scope of the conformational ensemble presently determined using experimental methods. This is important for drug design because it clearly illustrates the need to consider protein flexibility and the existence of multiple receptor conformations. It also provides a justification for higher affinity inhibitors that do not mimic substrates at their transition state. Additionally, if a protein exists in a population of states as discussed in (Carlson and McCammon 2000; Ma, Shatsky et al. 2002) then one could either design a moderate affinity ligand for a highly populated conformer (lower energy) or a high affinity ligand for a less populated conformer (higher energy).

Although it has been clearly established that a protein is able to undergo conformational changes during the binding process, most docking studies consider the protein as a rigid structure. The reason for this crude approximation is the extraordinary increase in computational complexity that is required to include the degrees of freedom of a protein in a modeling study. Pioneer efforts in the docking area (Holtje and Kier 1974; Kier and Aldrich 1974) were limited not only in methodology but also in computational capability. In the 1980s Kuntz and coworkers developed the program DOCK (Kuntz, Blaney et al. 1982) which made structure-based drug design a staple of current pharmaceutical research methods. Currently available docking software includes improved versions of the original DOCK(Ewing and Kuntz 1997), FlexX (Rarey, Kramer et al. 1996) and Autodock (Morris, Goodsell et al. 1998), among many others, to computationally predict the spatial conformation and affinity of bound complexes between a flexible ligand and a rigid receptor. These programs use different search methods and scoring functions. A review of these is beyond the scope of this chapter. For recent reviews on docking methods and scoring functions see (Gane and Dean 2000; Klebe 2000; Muegge and Rarey 2001; Halperin, Ma et al. 2002; Shoichet, McGovern et al. 2002).

The three dimensional conformation of a molecule can be represented by the values corresponding to its degrees of freedom. These are usually the Cartesian coordinates of its individual atoms or alternatively the values for its internal degrees of freedom. The latter are bond lengths, bond angles and dihedral angles (i.e., torsions around single bonds). A common approximation when modeling organic molecules is to consider that bond lengths and bond angles are constant and only dihedral angles are free to change. Even when using this approximation, a protein can have thousands of degrees of freedom whereas a small organic molecule can be usually modeled using only five to twenty degrees of freedom. In the last decade, with the advent of improved computational capabilities, researchers have been trying to solve the high dimensional problem of modeling protein flexibility in docking applications. The effect of protein flexibility on structure based drug design has been reviewed by Carlson *et al.* (Carlson and McCammon 2000; Carlson 2002; Carlson 2002).

There is currently no computationally efficient docking method that is able to screen a large database of potential ligands against a target receptor while considering the full flexibility of both ligand and receptor. In order for this process to become efficient, it is necessary to find a representation for protein flexibility that avoids the direct search of a solution space comprised of thousands of degrees of freedom. Here we review the different representations that have been used to incorporate protein flexibility in the modeling of protein/ligand interactions. A common theme behind all these approaches is that the accuracy of the results is usually directly proportional to the computational complexity of the representation. We tried to group the different types of flexibility representations models into categories that illustrate some of the key ideas that have been presented in the literature in recent years. However it is important to note that the boundaries between these categories are not rigid and in fact several of the publications referenced below could easily fall in more than one category.

2.2. Flexibility Representations

2.2.1. Soft Receptors

Perhaps the simplest solution to represent some degree of receptor flexibility in docking applications is the use of soft receptors. Soft receptors can be easily generated by relaxing the high energy penalty that the system incurs when an atom in the ligand overlaps an atom in the receptor structure. By reducing the van der Waals contributions to the total energy score the receptor is in practice made softer, thus allowing, for example, a larger ligand to fit in a binding site determined experimentally for a smaller molecule (see Figure 2.1.). The rationale behind this approach is that the receptor structure has some inherent flexibility which allows it to adapt to slightly differently shaped ligands by resorting to small variations in the orientation of binding site chains and backbone positions. If the change in the receptor conformation is small enough, it is assumed that the receptor is capable of such a conformational change, given its large number of degrees of freedom, even though the conformational change itself is not modeled explicitly. It is also assumed that the change in protein conformation does not incur a sufficiently high energetic penalty to offset the improved interaction energy between the ligand and the receptor. The main advantage of using soft receptors is ease of implementation (docking algorithms stay unchanged) and speed (the cost of evaluating the scoring function is the same as for the rigid case).

The first use of a soft docking approach was by Jiang *et al.* (Jiang and Kim 1991). Their method consisted of constructing a three dimensional cube representation of the molecular volumes and surfaces. These were matched geometrically in a first phase. In a second phase they were scored in accordance to the favorable energetic interactions in the buried surface areas. Schnecke *et al.* (Schnecke, Swanson et al. 1998) also allowed for some tolerance when calculating van der Waals overlaps between atoms.

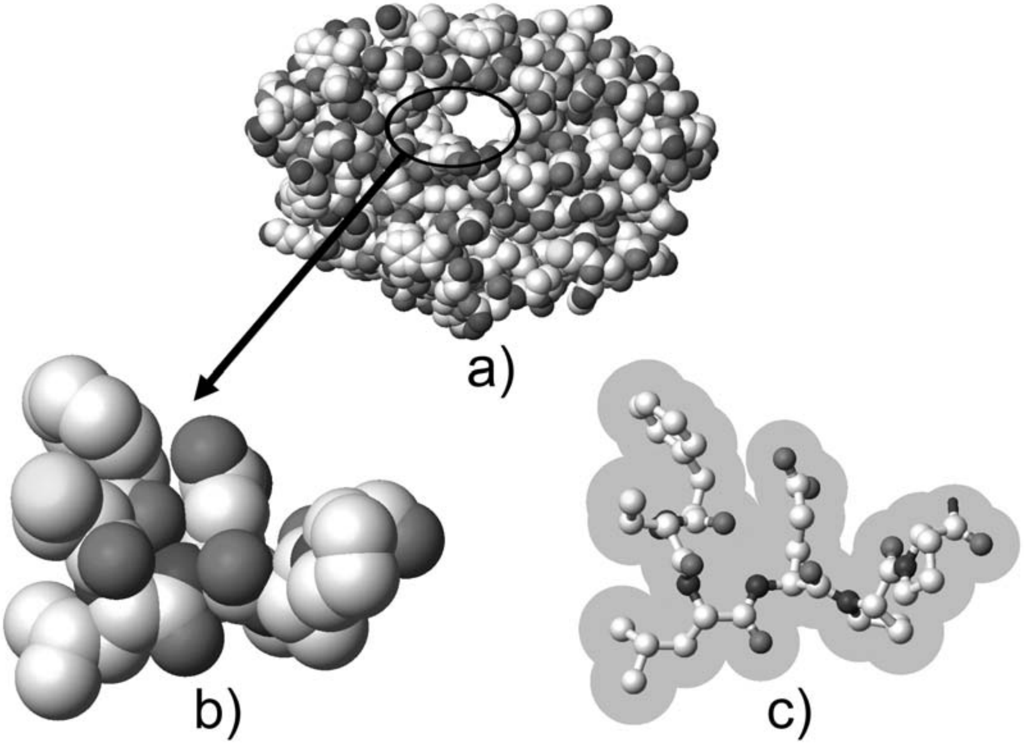

Figure 2.1 – a) Three dimensional van der Waals representation of a target receptor. b) Close up image of a section of the binding site. For the purposes of rigid protein docking, the receptor is commonly described by the union of the volumes occupied by its atoms. The steric collision of any atom of the candidate ligand with the atoms of the receptor will result in a high energetic penalty. c) Same section of the binding site as shown in b) but with reduced radii for the atoms in the receptor. This type of soft representation allows ligand atoms to enter the shaded area without incurring a high energetic penalty.

Another use of soft docking models is to improve convergence during energy minimization of the complex by avoiding local minima. Apostolakis *et al.* (Apostolakis, Pluckthun et al. 1998) developed a docking approach that is based on a combination of Monte Carlo and shifted nonbonded interactions minimization. In the initial stages of the conformational search the ligand is allowed to overlap with the receptor and nonbonded energy terms are modified to avoid high energy gradients. During the course of the minimization the interactions are then gradually restored to their original values simulating a ligand that is gradually exposed to the field of the receptor. This allows initial ligand/receptor conformations, which due to steric clashes would result in a very high energy penalty, to slowly adapt to each other in a complementary conformation without overlaps. One potential pitfall of this approach is the possibility that the ligand may become interlocked with the protein, leading to failure of the docking procedure to arrive at the minimal energy configuration.

Although the use of soft receptors presents a number of advantages such as ease of implementation and computation speed, it also makes use of conformational and energetic assumptions that are difficult to verify. This can easily result in errors, especially if the soft region is made excessively large to account for larger conformational changes on the part of the receptor.

2.2.2. Selection of Specific Degrees of Freedom

In order to reduce the complexity of modeling the very large dimensional space representing the full flexibility of the protein, it is possible to obtain an approximate solution by selecting only a few degrees of freedom to model explicitly. The degrees of freedom chosen usually correspond to rotations around single bonds (see Figure 2.2). The reason for this choice is that these degrees of freedom are usually considered the natural degrees of freedom in molecules. Rotations around bonds lead to deviations from ideal geometry that result in a small energy penalty when compared to deviations from ideality in bond lengths and bond angles. This assumption is in good agreement with current modeling force fields such as CHARMM (MacKerell, Bashford et al. 1998) and AMBER (Cornell, Cieplak et al. 1995). Choosing which torsional degrees of freedom to model is usually the most difficult part of this method because it requires a considerable amount of *a priori* knowledge of alternative binding modes for a given receptor. This knowledge is usually a result of the availability of experimental structures obtained under different conditions or using different ligands. If multiple experimental structures are not available some insight can be obtained from simulation methods such as Monte Carlo (MC) or molecular dynamics (MD). The torsions chosen are usually rotations of aminoacid side chains in the binding site of the receptor protein. It is also common to further reduce the search space by using rotamer libraries for the aminoacid side chains (Tuffery, Etchebest et al. 1991; Lovell, Word et al. 2000; Dunbrack 2002).

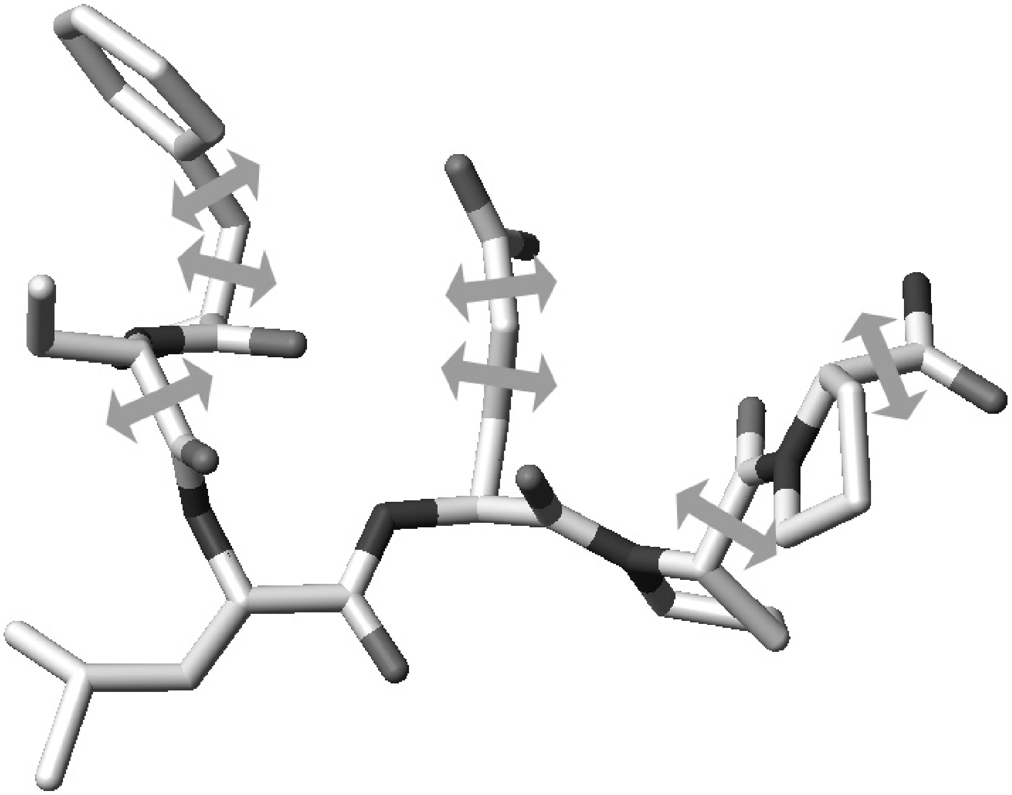

Figure 2.2 – Stick representation of the same binding site section as shown in Figure 2.1. In order to approximate the flexibility of the receptor it is possible to carefully select a few degrees of freedom. These are usually select torsional angles of sidechains in the binding site that have been determined to be critical in the induced fit effect for a specific receptor. In this example the selected torsional angles are represented by arrows.

The first application of using select degrees of freedom to model receptor flexibility was carried out by Leach (Leach 1994). This work made use of the Dead End Elimination (DEE) (Desmet, DeMaeyer et al. 1992) and the A* algorithm (Hart, N.J. et al. 1968) to explore the conformational space for the degrees of freedom for both ligand and receptor. The DEE states that a rotamer *r* of residue *i* (i_r) is incompatible with the global energy minimum structure if it satisfies the following inequality:

$$E_{i_r,rigid} + \sum_j \min_s \varepsilon_{i_r,j_s} > E_{i_t,rigid} + \sum_j \max_s \varepsilon_{i_t,j_s} ,$$

where $E_{i_r,rigid}$ and $E_{i_t,rigid}$ are the interaction energies between rotamer conformations i_r and i_t and the rigid part of the protein, respectively, $\min_s \varepsilon_{i_r,j_s}$ is the minimum interaction energy between rotamer *r* of residue *i* with all permitted rotamers *s* of residue *j*, and $\max_s \varepsilon_{i_t,j_s}$ is the corresponding maximum value for rotamer i_t. The A* (pronounced "A star") algorithm is a well known and well studied best-first search algorithm that works by expansion of graph nodes, always expanding the current fringe node that seems to be along the best path from the start node to the goal node. Besides using these two methods Leach also introduced an energy threshold to the global minimum and returned all structures under this threshold as potential binding candidates. The purpose of the threshold is to take into account the fact that the true global energy minimum of the bound complex does not necessarily correspond to that of the force field. This work was later extended by Leach and Lemon (Leach and Lemon 1998) to explore the conformational space of whole proteins. Schaffer *et al.* (Schaffer and Verkhivker 1998) also used DEE to perform flexible docking of two HIV-1 protease inhibitors with mutants of this protein. The DEE algorithm was applied using a rotamer library to perform discrete optimization of all possible combinations of side chain conformations in the binding site. The best solutions were later optimized in conjunction with the ligand using a Monte Carlo simulated annealing technique. This two step method leads to a solution that is not restricted to the dihedral values present in the rotamer library and is also of lower energy. More recently Althaus *et al.* (Althaus, Kohlbacher et al. 2002) also used two alternative combinatorial optimization methods to solve the side chain conformation problem. The first method consists of a heuristic multi-greedy approach, which is faster but does not necessarily produce an optimal solution. The second method is able to find the global minimum energy conformation and is based on a branch-and-cut algorithm and integer linear programming.

In the program GOLD, Jones *et al.* (Jones, Willett et al. 1997) use a genetic algorithm (GA) to dock a flexible ligand to a semi-flexible protein. GAs are an optimization method that derive their behavior from a metaphor of the process of evolution. A solution to a problem is encoded in a chromosome and a fitness score is assigned to it based on the relative merit of the solution. A population of chromosomes then goes through a process of evolution in which only the fittest solutions “survive”. This program takes into account not only the position and conformation of the ligand but also the hydrogen bonding network in the binding site. This was achieved by encoding orientation information for donor hydrogen atoms and acceptors in the GA chromosome. This type of conformational information is very important because if the starting point for a docking study is a rigid crystallographic structure, the orientations of hydroxyl groups will be undetermined. Being able to model these orientations explicitly removes any bias that might result from positioning hydroxyl groups based upon a known ligand. One limitation of this work is that the binding site still remains essentially rigid because protein conformational changes are limited to a few terminal bonds. This program performed very well for hydrophilic ligands but encountered some difficulties when trying to dock hydrophobic ligands due to the reduced contribution of hydrogen bonding to the binding process.

In SPECITOPE Schnecke *et al.* (Schnecke, Swanson et al. 1998) also make use of side chain rotations in the late stages of docking to remove steric overlaps between the protein side chains and the ligand. If an overlap clash is detected, the program attempts to remove it by rotating the side chain through the minimal angle that resolves the clash. The single bond closest to the bumping atoms in the side chain is used first to resolve the overlap. If a bump free conformation cannot be generated with this rotation, the next rotatable bond closer to the ligand backbone is rotated. This procedure will miss potential combinations of side chain conformations that do not overlap with the ligand and is not capable of finding the minimum energy conformation. Nevertheless, it will successfully resolve many cases of overlap.

Anderson *et al.* (Anderson, O'Neil et al. 2001) introduced the algorithm SOFTSPOTS that addresses the problem of knowing which rotational degrees of freedom should be selected to represent receptor flexibility. Using a single protein structure, this algorithm is capable of identifying regions of high flexibility. The results were combined with a second algorithm named PLASTIC that provides a collection of possible conformations based on rotamer libraries effectively reducing the bias caused by structures of proteins co-crystallized with inhibitors. More recently, Kayrys *et al.* (Kairys and Gilson 2002) have improved the Mining Minima optimizer method, first described by David *et al.* (David, Luo et al. 2001), to include select side chain degrees of freedom in the docking simulation of several proteins and ligands.

A common theme among the work described in this section is that receptor side chain conformations are modeled using torsional degrees of freedom. In order to make the calculation of interaction energies more efficient it would be desirable to work with a force field that is also described in terms of internal coordinates to avoid repeated conversion between two coordinate systems. Use of internal coordinate force fields also leads to more efficient convergence of energy optimizations. Abagyan *et al.* described a method to carry out flexible protein-ligand docking by global energy optimization in internal coordinates (Totrov and Abagyan 1997) and more recently described a method to accurately "project" a Cartesian force field onto an internal coordinate molecular model with fixed-bond geometry (Katritch, Totrov et al. 2003).

2.2.3. Multiple Receptor Structures

One possible way to represent a flexible receptor for drug design applications is the use of multiple static receptor structures (see Figure 2.3). This concept is supported by the currently accepted model that proteins in solution do not exist in a single minimum energy static conformation but are in fact constantly jumping between low energy conformational substates (Noguti and Go 1989; Frauenfelder, Sligar et al. 1991; Andrews, Romo et al. 1998; Kitao, Hayward et al. 1998). In this way the best description for a protein structure is that of a conformational ensemble (Bursavich and Rich 2002; Rich, Bursavich et al. 2002) of slightly different protein structures coexisting in a low energy region of the potential energy surface. Moreover the binding process can be thought of as not exactly an induced fit model as first described by Koshland (Koshland 1958) but more like a selection of a particular substate from the conformational ensemble that best complements the shape of a specific ligand (Ma, Kumar et al. 1999).

The use of multiple static conformations for docking gives rise to two critical questions. The first question is "How can we obtain a representative subset of the conformational ensemble typical of a given receptor?" Currently, the three dimensional structure of macromolecules can be determined experimentally using X-ray crystallography or NMR, or generated via computational methods such as Monte Carlo or molecular dynamics simulations. Simulations typically use as a starting point a structure determined by one of the experimental methods. Ideally we would like to use a sampling that provides the most extensive coverage of the structure space. Comparisons between traditional molecular simulations and experimental techniques (Clarage, Romo et al. 1995; Philippopoulos and Lim 1999) indicate that X-ray crystallography and NMR structures seem to provide better coverage. However this balance can potentially change due to advances in computational methods (Karplus and McCammon 2002). Another limitation in choosing data sources is availability. Although experimental data is preferable, the monetary and time cost of determining multiple structures experimentally is significantly higher than obtaining the same amount of data computationally. The second critical question is “What is the best way of combining this large amount of structural information for a docking study?”. This question also remains open. Current approaches use diverse ways of combining multiple structures as discussed below.

The first use of multiple structures for a drug design applications was by Pang and Kozikowski (Pang and Kozikowski 1994) to study the binding of huperzine A (HA) to acetylcholinesterase (AChE). In this study the authors ran a short molecular dynamics simulation (40 ps) of AChE from which they extracted 69 conformations that were docked to HA using rigid docking. This study successfully predicted that HA binds to the bottom of the binding cavity of AChE (the gorge). More recently, other studies (Kua, Zhang et al. 2002; Lin, Perryman et al. 2002) have exploited similar approaches but used a larger number of structures, longer molecular dynamics sampling, and more accurate simulation conditions. Instead of resorting to computational methods to derive structural data Knegtel *et al.* (Knegtel, Kuntz et al. 1997) used a family of structures from an NMR structural determination or, as an alternative, several crystal structures of the same protein system. In that study the authors combined the different structures into a single interaction energy grid to be used for rigid receptor docking by the DOCK program. Interaction energy grids are calculated by placing a probe atom at discrete points in the space around a target protein and assigning to the grid point the value of the interaction energy between the probe and protein. This grid is then utilized as a fast lookup table for interaction energy calculations, effectively reducing the cost of computation from quadratic to linear. The averaged grids were constructed using energy-weighted and geometry-weighted averaging methods. The main limitation of these averaging approaches is that they can lead to loss of geometric accuracy. The binding energies computed from the composite grid are also less favorable than for individual grids for each protein in the ensemble. In the case of geometry-weighted averaging, the binding site can become too permissive in terms of the size of the ligand that it can accommodate. Sudbeck *et al.* (Sudbeck, Mao et al. 1998) superimposed the crystal structures of nine inhibitor complexes of HIV reverse transcriptase to generate a composite binding site that summarized its unique critical features. The overlaid coordinates of the nine different inhibitors were used to generate a combined molecular surface defining an enlarged binding pocket that represented the plasticity of the receptor. The combined binding pocket was used to verify the results obtained from the docking of small molecules to a single structure of reverse transcriptase through a conjugate gradient minimization method for the ligand and all residues within 5 Å. This study resulted in the development of two new inhibitors. Multiple crystal structures of HIV-1 protease were also used by Bouzida *et al.* (Bouzida, Rejto et al. 1999) to account for receptor flexibility. Broughton *et al.* (Broughton 2000) used different conformation snapshots from a short molecular dynamics simulation of dihydrofolate reductase to generate interactions grids that were also combined into a single grid by means of a weighted average method. Before the calculation of the grids, the structures were superimposed using the bound inhibitors as a reference.

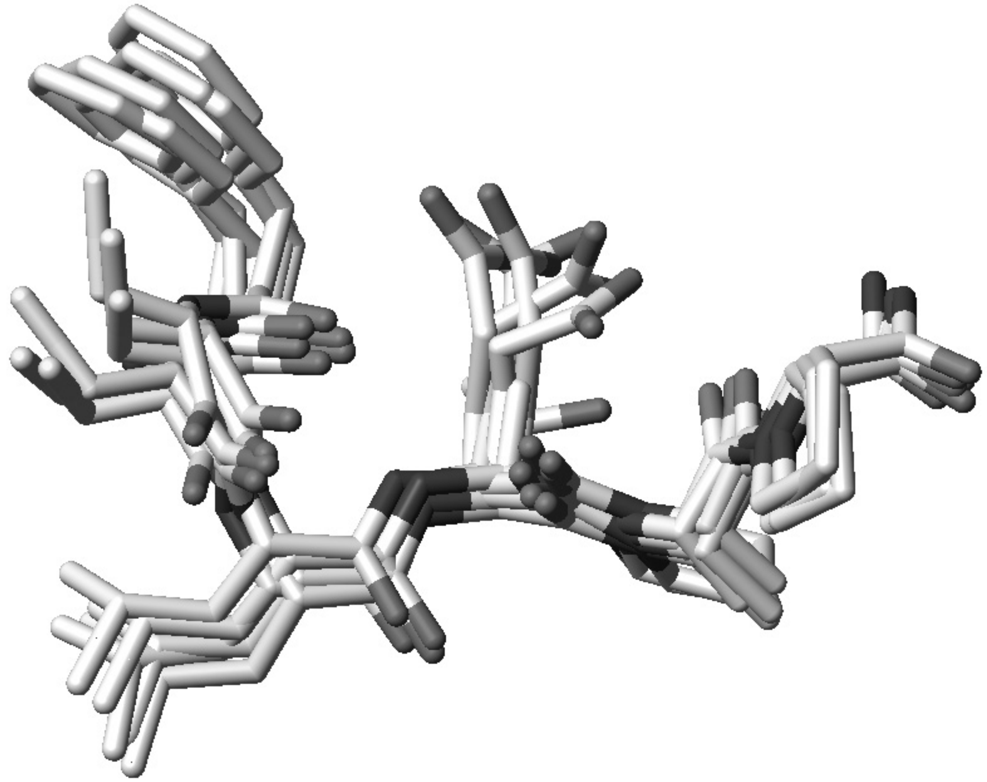

Figure 2.3 – Superposition of multiple conformers of the same binding site section as shown in Figure 2.1. As an alternative to considering the target protein as a single three dimensional structure, it is possible to combine information from multiple protein conformations in a drug design effort. These can be either considered individually as rigid representatives of the conformational ensemble or can be combined into a single representation that preserves the most relevant structural information.

As mentioned earlier one of the methods of combining multiple receptor structures is to create an average grid for the protein/ligand interaction potential (Knegtel, Kuntz et al. 1997). Osterberg *et al.* (Osterberg, Morris et al. 2002) analyzed this problem in depth by using HIV-1 protease as a model system and comparing four different grid averaging methods. The fist two naïve methods consisted of a mean grid that takes a simple point-by-point average across all the grids, and a minimum grid that takes the minimum value across all the grids. Both methods performed poorly. The third approach is similar to that described by Knegtel *et al.* (Knegtel, Kuntz et al. 1997) and consists of a weighted averaging scheme. In this case if one or more of the grids contain a favorable, negative value, their weights will dominate the average. On the other hand, if all the grids contain unfavorable positive values, all will have identical small weights resulting in an unfavorable region representing all grids. The fourth averaging scheme is similar to the previous one but uses a Boltzmann assumption to calculate the weight based on the interaction energy. The last two averaging schemes were able to efficiently represent multiple structures in a single grid and the docking results were satisfactory. However, as the authors point, out this method for incorporation of conformational flexibility can introduce potentially dangerous artifacts such as positive interaction regions for mutually exclusive solutions.

A different way of considering protein flexibility as represented in interaction grids for multiple static structures is GRID/CPCA (Consensus Principal Component Analysis). This method, introduced by Kastenholz *et al.* (Kastenholz, Pastor et al. 2000) in the study of serine proteases, is an extension of GRID/PCA (Pastor and Cruciani

1995), and can be used to identify selectivity features for a receptor. One of the main advantages of this method over its predecessor is that it allows the inclusion of more that two structures in the PCA calculation. Moreover, when several structures are used, it allows for some averaging of individual structures, reducing differences that might be present due to experimental variations but are not relevant to the specificity features of the receptors.

In the program FlexE, Claussen *et al.* (Claussen, Buning et al. 2001) introduced a new method of combining multiple receptor structures to represent a flexible binding site. The algorithm starts by superimposing the set of conformations available for a given receptor and merging similar parts of the structures. Dissimilar substructures are treated as independent alternatives and FlexE selects the combination of substructures that best complements conformations of the ligand with respect to the scoring function. In practice, this results in the generation of alternative receptor conformations that were not present in the initial set but may constitute valid docking targets.

More recently Moreno and León (Moreno and Leon 2002) introduced a new receptor representation that allows the use of an ensemble of protein structures as input to DOCK instead of a single rigid structure. In this approach, an ensemble of protein/inhibitor complex structures is used to construct a set of templates of attached points (one for each type of amino acid) located in positions suitable for interactions with ligand atoms. The combination of templates gives a description of a flexible binding site. The authors propose the method of attached points as an alternative to

SPHGEN (Bolin, Filman et al. 1982; DesJarlais, Sheridan et al. 1988) or SURFSPH (Oshiro and Kuntz 1998) to generate a binding site descriptor.

Multiple protein structures can be used not only to generate flexible receptor representations for docking purposes, but also to generate pharmacophores. A pharmacophore is a template for the desired ligand. The pharmacophore is represented by a set of features that an effective ligand should possess and a set of spatial constraints among the features. The features can be specific atoms, positive or negative charges, hydrophobic or hydrophilic centers, hydrogen bond donors or acceptors, and others. The spatial arrangement of the features represents the relative 3D placements of these features in the docked conformation of the ligand. Carlson *et al.* introduced the concept of a dynamic pharmacophore by combining sets of structures derived by either X-ray crystallography (Carlson, Masukawa et al. 1999) or snapshots of a molecular dynamics simulation (Carlson, Masukawa et al. 2000). Potential sites of interest in the receptor binding site are determined by running a multi-unit Monte Carlo minimization using probe molecules for the different features of interest. The results of these simulations for each conformer are then overlaid. This procedure reveals conserved binding regions that are highly occupied during the molecular dynamics simulation despite the flexibility of the receptor. The conserved features define the dynamic pharmacophore. Studies similar to dynamic pharmacophore identification were performed by Stultz and Karplus (Stultz and Karplus 1999) using a combination of the Multiple Copy Simultaneous Search (MCSS) and Locally Enhanced Sampling (LES) methods (Roitberg and Elber 1991). Their protocol uses quenched molecular dynamics to identify energetically favorable positions and orientations of small functional groups in a flexible binding site. In this method multiple copies of the functional groups are distributed in the binding site and quenched to find energy minima. These functional groups can later be used as building blocks for larger ligands.

One of the main advantages of using multiple structures instead of using a selection of degrees of freedom to represent protein flexibility is that the flexible region is not limited to a specific small region of the protein. Multiple structures allow the consideration of the full flexibility of the protein without the exponential blow up in terms of computational cost that would derive from including all the degrees of freedom of the protein. On the other hand, flexibility is modeled implicitly and as such only a small fraction of the conformational space of the receptor is represented. In addition, the method by which the multiple receptor structures are combined has a drastic influence on the possible results of the docking computation.

2.2.4. Molecular Simulations

To simulate the binding process with as much detail as possible and avoid some of the limitations of previous flexibility models one can use force field based atomistic simulation methods such as Monte Carlo or molecular dynamics (see Figure 2.4.). Whereas molecular dynamics applies the laws of classical mechanics to compute the motion of the particles in a molecular system, Monte Carlo methods are so called because they are based on a random sampling of the conformational space. The main advantage of Monte Carlo or molecular dynamics flexibility representations in docking studies is that they are very accurate and can model explicitly all degrees of freedom of the system including the solvent if necessary. Unfortunately, the high level of accuracy in the modeling process comes with a prohibitive computational cost. For example, in the case of molecular dynamics, state of the art protein simulations can only simulate periods ranging from 10 to 100 ns, even when using large parallel computers or clusters. Given that diffusion and binding of ligands takes place over a longer time span, it is clear that these simulations techniques cannot be used as a general method to screen large databases of compounds in the near future. It is however possible to carry out approximations that reduce the computational expense and lead to insights that would be impossible to gain using less flexible receptor representations. The cost of carrying out the computational approximations is usually a loss in accuracy.

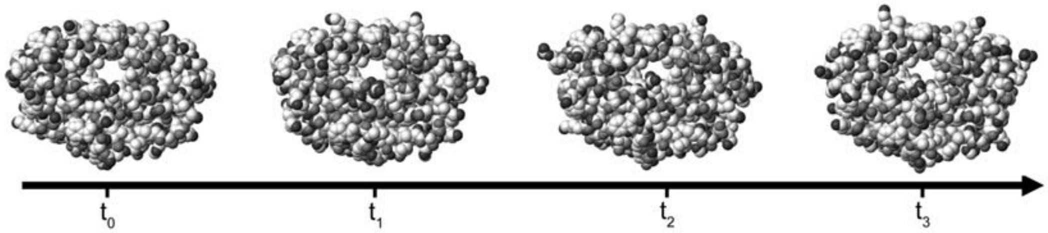

Figure 2.4 – Molecular simulations can give a description of the full protein flexibility as it interacts with a ligand. Molecular dynamics applies the laws of classical mechanics to compute the motion of particles in a molecular system. Alternatively, the different conformational snapshots obtained at times t_0, t_1, etc., can be used as multiple protein structures representing the conformational ensemble.

In order to address the time sampling limitations of traditional molecular dynamics Di Nola *et al.* (Di Nola, Roccatano et al. 1994) used a modified temperature coupling scheme to perform the docking of phosphocholine onto immunoglobulin McPC603. Instead of coupling the whole system to the same temperature bath, Di Nola used a regular coupling temperature to the internal degrees of freedom of the ligand and a very high temperature (1300-1700 K) for the translational modes. In practice, this allows the ligand to sample the surface of a protein receptor much faster and without disturbing internal motions. This method was extended later by Mangoni *et al.* (Mangoni, Roccatano et al. 1999) to also include the flexibility of the receptor, which was also coupled to the lower temperature bath (300 K). In order to further reduce the computational cost of the simulation, the protein simulation was restricted to a sphere of 20 Å around the chain oxygen of the phosphocholine molecule in the crystallographic position. The remaining part of the protein was kept rigid. The same approach of restricting the full molecular simulation to the vicinity of the binding site was used by Luty *et al.* (Luty, Wasserman et al. 1995) to simulate the docking of benzamidine to trypsin and by Wasserman *et al.* (Wasserman and Hodge 1996) to simulate the docking of L-leucine hydroxamic acid to thermolysin. Given and Gilson (Given and Gilson 1998) also restricted flexibility to the binding site area of HIV-1 protease within the context of a hierarchical docking protocol. In this method conformations are evolved in stages, with the lowest energy conformations from one stage serving as starting points for the next. The focus of this study was not to develop a computationally efficient method but rather generate a picture of the ligand-binding energy surface with different energy functions.

A different approach to enhance the sampling rate of force field based simulations methods is to smooth the potential energy surface in order to increase the rate of transition between metastable conformations. Nakajima *et al.* (Nakajima, Higoa et al. 1997; Nakajima, Nakamura et al. 1997) used the method of multicanonical molecular dynamics simulation based on the work of Berg *et al.* (Berg and Neuhaus 1992) to simulate the binding of a short proline-rich peptide to a Src homology 3 (SH3) domain. In this method the simulation is carried out in a deformed energy surface characterized by a flatter energy distribution resulting in much faster sampling of the conformational space of the ligand and the binding site of SH3. Pak and Wang (Pak and Wang 2000) applied the Tsallis transformation to the non bonded interaction potential of the CHARMM force field and ran dynamics simulations with infrequent *q*-jumping and *q*-relaxation between the normal and the smooth energy surface. By combining potential smoothing and restriction of the flexibility of the receptor to aminoacid side chains in the binding site, it was possible to successfully simulate the formation of streptavidin/biotin and protein kinase C/phorbol-13-acetate complexes. More recently, Zhu *et al.* (Zhu, Fan et al. 2001) introduced the program F-DycoBlock that performs the docking of a flexible ligand to a flexible receptor using multiple-copy stochastic molecular dynamics. In this method several copies of the ligand molecule are simulated simultaneously. These copies are constructed in a special way because they do not interact with each other. The protein moves in the mean field of all ligand copies. In this study the authors also used four different types of receptor flexibility: all-atom restrained, backbone restrained, intramolecular hydrogen-bond restrained and active-site flexible.

The alternative to the use of molecular dynamics is the use of Monte Carlo based methods. In (Caflisch, Fischer et al. 1997) Caflisch *et al.* extended the Monte Carlo minimization approach to take into account receptor flexibility by the use of a flexible enzyme binding site whose side chains are submitted to random perturbations. This work used the Metropolis Monte Carlo method for global optimization, combined with a conjugate gradient minimization scheme for local optimization. Solute-solvent energies were calculated by solving the finite-difference linearized Poisson-Boltzmann equation. Trosset and Scheraga developed the PRODOCK package for docking (Trosset and Scheraga 1999). The global optimization method used in this tool is the scaled collective variables Monte Carlo method developed by Noguti and Go (Noguti and Go 1985) with energy minimization after each Monte Carlo step. The minimization step was greatly improved by the use of a grid based energy evaluation technique using Bézier splines (Trosset and Scheraga 1998; Trosset and Scheraga 1999) and the use of collective degrees of freedom. One of the main problems with conventional simulation methods is the propensity for the system to get trapped in local minima, leading to a computationally inefficient sampling of the energy landscape. In order to minimize this problem, Verkhivker et al. (Verkhivker, Rejto et al. 2001) made use of parallel simulated tempering dynamics to investigate the specificity of binding and mechanisms of inhibitor resistance in HIV-1 protease. Parallel tempering is a replica-exchange

Monte Carlo method that simulates several copies of the protein simultaneously using different temperatures and periodically exchanges conformations at neighboring temperatures. This process enhances conformational sampling by facilitating escape from local minima.

An innovative approach to predicting the binding conformation of a flexible ligand in a flexible binding pocket by combining the simulated annealing and the crystallographic refinement search methods was recently introduced by Ota and Agard (Ota and Agard 2001). This scheme starts by using a shrunken ligand for which the bond lengths and the non bonded interactions have been greatly reduced. The ligand is then grown in the binding site using a simulated annealing protocol to search for a bound conformation. This procedure is repeated several times and a pseudo electron density map is calculated by averaging amplitudes and phases calculated from each structure. The final bound conformation is determined by conventional crystallographic refinement using the calculated structure factors. This method has the advantages of being able to model individual water molecules relevant to the binding configuration and providing a series of crystallographic measures, such as B-factors, that facilitate the comparison with X-ray crystallographic data. Unfortunately, due to the high computational cost, this technique is not suitable for large scale database screening but could be useful in the late stages of a docking study.

2.2.5 Collective Degrees of Freedom

An alternative representation for protein flexibility is the use of collective degrees of freedom. This approach enables the representation of full protein flexibility, including loops and domains, without a dramatic increase in computational cost. Collective degrees of freedom are not native degrees of freedom of molecules. Instead they consist of global protein motions that result from a simultaneous change of all or part of the native degrees of freedom of the receptor.

Collective degrees of freedom can be determined using different methods. One method is the calculation of normal modes for the receptor (Levy and Karplus 1979; Go, Noguti et al. 1983; Levitt, Sander et al. 1985). Normal modes are simple harmonic oscillations about a local energy minimum, which depends on the structure of the receptor and the energy function. For a purely harmonic energy function, any motion can be exactly expressed as a superposition of normal modes. In proteins, the lowest frequency modes correspond to delocalized motions, in which a large number of atoms oscillate with considerable amplitude. The highest frequency motions are more localized such as the stretching of bonds. By assuming that the protein is at an energy minimum, we can represent its flexibility by using the low frequency normal modes as degrees of freedom for the system. Zacharias and Sklenar (Zacharias and Sklenar 1999) applied a method similar to normal mode analysis to derive a series of harmonic modes that were used to account for receptor flexibility in the binding of a small ligand to DNA. This in practice reduced the number of degrees of freedom of the DNA molecule from 822 (3×276 atoms – 6) to between 5 and 40. Keseru and Kolossvary also used a normal mode based model (Kolossvary and Guida 1999; Kolossvary and Keseru 2001) to study inhibitor binding to HIV integrase (Keseru and Kolossvary 2001).

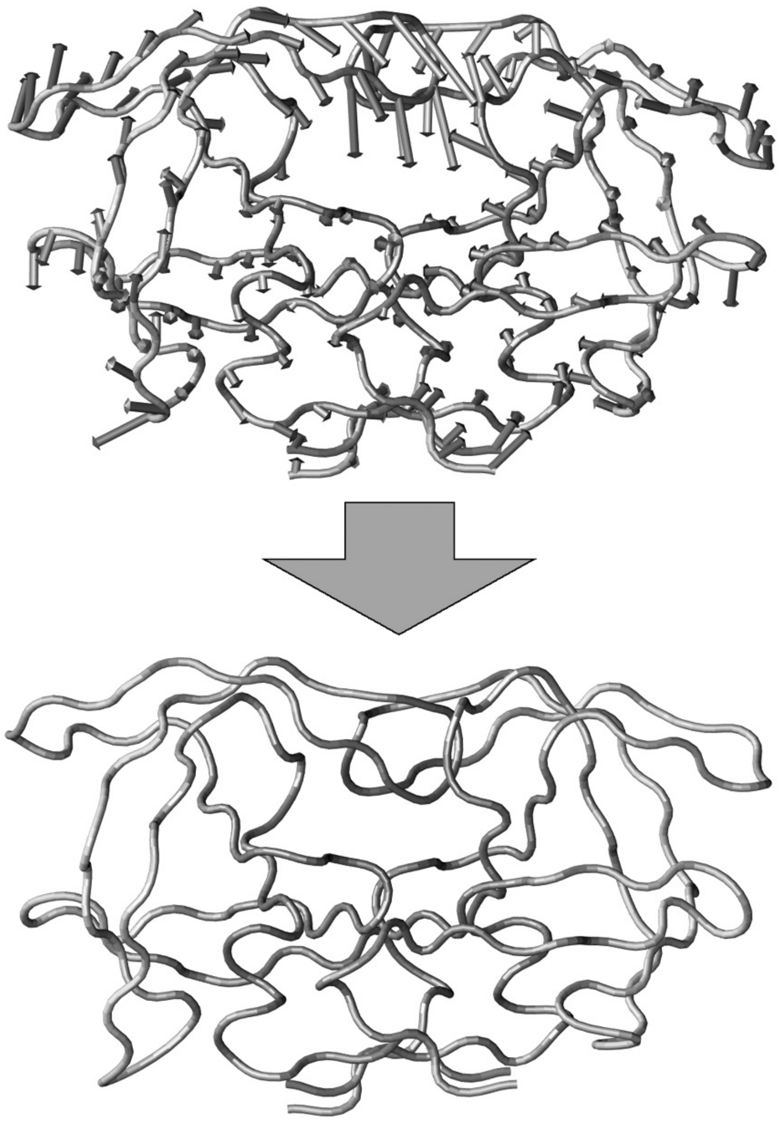

Figure 2.5 – Representation of a collective degree of freedom for HIV-1 protease. Full protein flexibility can be represented in a low dimensional space using collective degrees of freedom. One method to obtain these is Principal Component Analysis. Principal components correspond to a concerted motion of the protein. The first principal component for HIV-1 protease is indicated by the arrows (top). By following this collective degree of freedom it is possible to generate alternative conformations for the receptor (bottom).

An alternative method of calculating collective degrees of freedom for macromolecules is the use of dimensional reduction methods. The most commonly used dimensional reduction method for the study of protein motions is principal component analysis (PCA). This method was first applied by Garcia (Garcia 1992) in order to identify high-amplitude modes of fluctuations in macromolecular dynamics simulations. It has also been used to identify and study protein conformational substates (Romo, Clarage et al. 1995; Caves, Evanseck et al. 1998; Kitao and Go 1999), as a possible method to extend the timescale of molecular dynamics simulations (Amadei, Linssen et al. 1993; Amadei, Linssen et al. 1996; Abseher and Nilges 2000) and as a method to perform conformational sampling (de Groot, Amadei et al. 1996; de Groot, Amadei et al. 1996; Abseher and Nilges 2000). In Chapter 4, we present a protocol (Teodoro, Phillips et al. 2003) based on PCA to derive a reduced basis representation of protein flexibility that can be used to decrease the complexity of modeling protein/ligand interactions. The most significant principal components have a direct physical interpretation. They correspond to a concerted motion of the protein where all the atoms move in specific spatial directions and with fixed ratios in overall displacement. An example is provided in Figure 2.5,. where the directions and ratios are indicated by the direction and size of the arrows, respectively. By considering only the most significant principal components as the valuable degrees of freedom of the system, it is possible to cut down an initial search space of thousands of degrees of freedom to less than fifty. This is achievable because the fifty most significant principal components usually account for 80-90% of the overall conformational variance of the system. The PCA approach avoids some of the limitations of normal modes such as deficient solvent modeling and existence of multiple energy minima during a large motion. The last limitation contradicts the initial assumption of a single well energy potential.

An alternative representation of receptor flexibility that uses a concept similar to collective degrees of freedom, is based on the concept of molecular hinges (Sandak, Nussinov et al. 1995; Sandak, Nussinov et al. 1998; Sandak, Wolfson et al. 1998). This research is based on methods from the fields of computer vision and robotics. The hinge-bending approach was originally used to model flexibility of the ligand, but the roles of the ligand and the protein can be swapped since the mathematical problem is symmetrical. Hinges are articulation points placed at specific locations in the protein that allow for relative movement of domains or substructural parts. A few simultaneous hinges can be modeled. These hinge points do not correspond to single degrees of freedom of the original model but are instead articulations that are allowed to rotate in three dimensions, implicitly representing rotations about consecutive or nearby bonds. The ligand is also considered flexible and the search for a docking conformation is done simultaneously, mimicking the induced fit process. Like pliers closing on a screw, the receptor adapts its shape to that of the ligand. This method does not model conformational changes for sidechains explicitly. However, it models large conformational changes efficiently and can be easily combined with some of the methods described above in order to model conformational changes for specific areas of the receptor at an atomistic level. One of the main problems of the molecular hinges approach is determining the location of the hinges. Recently, Jacobs *et al.* (Jacobs, Rader et al. 2001) introduced a flexibility prediction algorithm based on graph theory which can help solve this problem. The algorithm computes a constraint network for the protein defined by the bonds (covalent and hydrogen) and salt bridges and identifies all the rigid and flexible substructures in the protein, including overconstrained regions and underconstrained or flexible regions.

Using collective degrees of freedom as a flexibility representation has a number of advantages and disadvantages. One advantage is that protein flexibility is not limited to a specific small region of the protein as was the case when using only select degrees of freedom. Furthermore, because only a few independent degrees of freedom are used in the optimization procedure, the computational cost is similar to using only select degrees of freedom and is much less than the cost of techniques that consider all degrees of freedom, such as traditional molecular dynamics or Monte Carlo. On the other hand, the degrees of freedom that are searched during the drug design procedure are not the native degrees of freedom of the protein, but collective modes of motion that try to account for most of the variance observed during protein motion. This may result in a loss of accuracy and difficulty in obtaining exact solutions. For example, there may not exist a combination of values for the reduced basis formed by the most significant collective degrees of freedom that results in the exact placement of all binding site sidechains, as observed in an experimentally determined structure. However, this is probably a minor problem since exact solutions are rarely obtained using other methods, either. As shown in (Teodoro, Phillips et al. 2003) and Chapter 5, it is possible to obtain very good approximations using only a small number of collective degrees of freedom. Furthermore, in order to avoid high energy penalties that might result from van der Waals clashes, it is possible to combine collective modes of motion with either a soft receptor representation or with a post-processing minimization procedure.

2.3. Summary

The problem of incorporating receptor flexibility in routine *in silico* screening of databases of small chemical compounds for the purposes of structure based drug design is still an unsolved problem. The main reason behind this difficulty is the large number of degrees of freedom that have to be considered to represent receptor flexibility. In this chapter we reviewed protein flexibility models that have been developed to limit the number of additional search parameters. These models can be roughly divided into five different categories. These are a) use of soft receptors which relax energetic penalties due to steric clashes, b) selection of a few critical degrees of freedom in the receptor binding site, c) use of multiple receptor structures either individually or by combining them using an averaging scheme, d) use of modified molecular simulation methods, and e) use of collective degrees of freedom as a new basis of representation for protein flexibility. All these flexible receptor models strive to balance an improvement in the accuracy of the binding predictions with an increase in computational cost.

Chapter 3.

Tolerance Assessment of Rigid-Protein Docking Methods to Induced Fit Effects

3.1. Introduction

A major advance in pharmaceutical drug discovery has been the ability to computationally determine the three dimensional conformation of the complex formed between a small ligand and a large biomacromolecule (Kuntz, Blaney et al. 1982). This procedure, known as docking, led to a novel method for developing drugs. Instead of physically screening millions of chemical compounds in the laboratory in search of pharmacological activity, it was now possible to carry out the same tests *in silico* at a fraction of the initial cost. Using the new method, large databases of chemically diverse small molecules are screened to determine which are able to bind effectively to a target receptor. The best candidates are then later optimized using both computational and experimental methods to produce drug candidates that must undergo further laboratory and clinical trials before final approval. During the last two decades we have seen the emergence of different algorithms and software packages for docking. For recent reviews on docking methods see (Muegge and Rarey 2001; Halperin, Ma et al. 2002). However, the development of docking methods is still a work in progress and these software packages will often fail to predict the three dimensional structures and affinities of the bound complexes. The most common reasons for failure are oversimplified energy models, poor solvent modeling and lack of representation for receptor flexibility. In Chapter 3 we will focus on the last problem and perform a quantitative assessment of the consequences of modeling the receptor as a rigid structure.

Due to computational limitations, the first generation of docking programs followed the lock-and-key model first described by Fischer (Fischer 1894). In this model the three dimensional structure of the receptor and the ligand complement each other in the same way that a lock complements a key. The role of the docking programs was to find the best geometric and chemical match between two rigid structures. Unfortunately, the lock-and-key model is a crude approximation of the binding process which is better described by an induced-fit process (Koshland 1958) in which the three dimensional structure of the ligand and the receptor adapt to each other during binding. To partially address this limitation, the second generation of docking programs modeled some of the induced-fit effect by considering a flexible ligand binding to a rigid receptor. This is a reasonable approximation because the ligand is usually the more flexible of the two molecules. Furthermore, ligand flexibility can be usually modeled using only 5 to 15 degrees of freedom, whereas the full flexibility of a large biomacromolecule can require the inclusion of more than 1000 degrees of freedom (Teodoro, Phillips et al. 2001). Although, such a level of complexity is currently computationally intractable a number of approximations have been proposed to overcome this problem and are being used to develop a third generation of docking programs which are able to model the flexibility of both the ligand and the receptor. For an extensive review of current protein flexibility for structure-based drug design see Chapter 2.

Although we are now starting to see the emergence of the third generation of docking programs, second generation programs are still the most used in both academia and industry settings. In practice, second generation programs are still computationally more efficient than those that try to account for protein flexibility. Given the widespread use and availability of second generation programs we decided to quantitatively evaluate the extent to which the rigid-receptor/flexible-ligand docking model can be used effectively. For this purpose we selected two commonly used docking programs, Autodock (Morris, Goodsell et al. 1998), and DOCK (Ewing and Kuntz 1997), and three protein models for which protein flexibility has been shown to play a critical role during the binding process, HIV-1 protease (Wlodawer and Vondrasek 1998), dihydrofolate reductase (DHFR) (Bystroff and Kraut 1991) and aldose reductase (Wilson, Tarle et al. 1993). We used both docking programs to determine if accurate docking results could be obtained for increasingly different binding site conformations from the ones determined experimentally using X-ray crystallography. Our work extends an earlier investigation by Murray *et al* (Murray, Baxter et al. 1999) in which the authors tested whether the assumption of a rigid enzyme compromises the accuracy of docking results. That test was carried out using all-pairs docking for a series of three proteins. Murray *et al* determined that that the assumption of a rigid active site can lead to errors in identification of the correct binding mode and the assessment of binding affinity but did not quantitatively determine to what extent current programs are able to deal with receptor model errors.

In the present work we try to address the following question: “What is the level of similarity necessary between a receptor structural model and the actual experimental structure to obtain useful results using second generation docking programs?”. This is an important question because in practical docking applications the receptor model is often an approximation of the real three dimensional conformation of the receptor when bound with the small molecule used for the docking trial. The measure of receptor similarity used in this work is the Root Mean Square Deviation (RMSD) for the atoms that constitute the binding site of the different protein models. Our objective in this work is not to evaluate the efficacy of different docking programs in dealing with the flexible receptor problem. Our main objectives are to quantify the limitations of second generation docking programs and to understand the range of problems that should be addressed by third generation programs.

3.2. Materials and Methods

3.2.1. Model Systems

The coordinates for the model systems used in this study were all determined using X-ray crystallography and obtained from the Protein Data Bank (PDB) (Berman, Westbrook et al. 2000). The PDB codes are 1HVR (Lam, Jadhav et al. 1994) (HIV-1 protease complex with Xk263 of Dupont Merck), 4DFR (Bolin, Filman et al. 1982) (dihydrofolate reductase complex with methotrexate), and 1AH3 (Urzhumtsev, Tete-Favier et al. 1997) (aldose reductase complex with tolrestat).

3.2.2. Conformational Sampling

Conformational sampling of the receptor structures was obtained using a simple molecular dynamics based method. Molecular dynamics has been often used as a method to model the conformational flexibility of the receptor during binding processes (Di Nola, Roccatano et al. 1994; Luty, Wasserman et al. 1995; Wasserman and Hodge 1996; Mangoni, Roccatano et al. 1999; Pak and Wang 2000). In this study we used high temperature molecular dynamics (Bruccoleri and Karplus 1990). The advantages of this technique are its simplicity and high computational efficiency. In contrast to earlier studies, the objective of the molecular dynamics step is not to exhaustively explore the conformational space of the protein as it binds to a ligand. We used molecular dynamics in order to obtain a small set of alternative protein conformations that represented different levels of similarity from the original X-ray structure. Simulations were carried out using the NAMD2 program (Kalé, Skeel et al. 1999) and the CHARMM forcefield (MacKerell, Bashford et al. 1998). The receptor structures were prepared by removing ligands (Xk263, methotrexate, and tolrestat) and water molecules. After an initial minimization using a conjugate gradient method, the receptor structures were simulated at a temperature of 800K for 50ps using a 1fs integration timestep. Non-bonded interactions were truncated at distances larger than 12Å. To avoid a discontinuity in the non-bonded potential at the cutoff distance a switching function was used starting at 9Å. Conformational snapshots were written to disk every 100fs. The high temperature simulation was run 20 times for each system using different random seeds for initial velocity assignment to improve the conformational sampling. The conformational snapshots for the 20 simulations were combined into a single large pool and were superimposed on the original crystal structure using a least squares procedure (Kabsch 1976).

Although the whole protein was simulated using molecular dynamics, we restricted the analysis of the results to the residues that constitute the binding site region of the three proteins. The reason is that conformational changes at the level of the binding site play the most significant role in determining the results of docking. The residues were chosen by visual inspection of the experimental bound conformations. The residues considered for each protein are shown in Table 3.1.

Protein	Residues included in RMSD calculation
HIV-1 Protease (PDB code: 1HVR)	8, 23, 25, 27-32 , 47-50, 80-84 (monomers A and B)
Dihydrofolate Reductase (PDB code: 4DFR)	5, 7, 27, 28, 31, 32, 46, 49, 50, 52, 54, 57, 94
Aldose Reductase (PDB code: 1AH3)	20, 47, 48, 79, 110, 111, 113, 115, 122, 130, 219, 298, 300, 302, 303

Table 3.1 – Residue numbers included in binding site RMSD calculation.

From the pool obtained using molecular dynamics we formed 10 groups of 10 structures, such that structures in the same group had similar RMSD to the X-ray structure. The RMSD groups considered were from 0.1Å to 1.9Å in steps of 0.2Å.

Figure 3.1 illustrates the conformational variation present in the different RMSD groups for HIV-1 protease. The selected RMSD range of conformational variation was in accordance to what was observed in many cases for proteins deposited in the PDB (Berman, Westbrook et al. 2000). It is common for proteins to differ by as much as 2Å RMSD between their bound and unbound forms or even when bound to different ligands. In some cases, such as the protein calmodulin, conformational changes upon binding are much larger than 2Å. We decided not to include such large conformational changes in our study since they are usually beyond what can be tackled using second generation docking program.

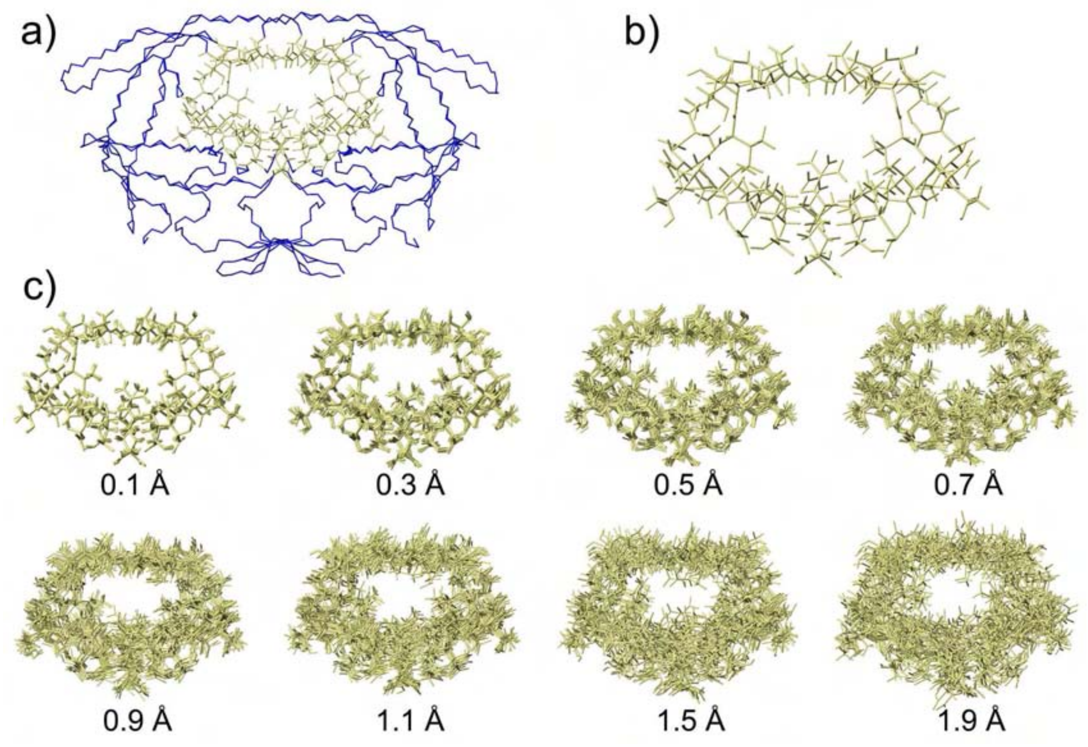

Figure 3.1 - Conformational sampling of binding site conformations. a) The experimentally determined structure of the model proteins (HIV-1 protease shown) was used as a starting point for a high temperature molecular dynamics simulation. The entire protein backbone is shown in blue and the residues defining the shape of the binding site are highlighted in yellow. In b) we show a magnified view of the binding site displaying only the residues used for the RMSD calculations. c) The multiple conformational snapshots resulting from the sampling simulations were sorted and grouped according to the RMSD to the original experimental structure. In c) we show the superposition of 10 representative structures for eight different similarity groups. Structures from these groups were subsequently used for docking as representatives of different levels of conformational flexibility.

3.2.3. Autodock

Ligand and protein input files were prepared as suggested in the Autodock manual. Ligand atom coordinates were obtained from the original PDB files. Hydrogen atom coordinates and Gasteiger-Marsili (Gasteiger and Marsili 1980) charges for all ligand atoms were calculated using SYBYL V6.8 (Tripos Associates, St Louis, MO). In order to test the effects of ligand flexibility on the docking results ligand input files were prepared for different degrees of conformational flexibility. Xk263 was modeled using 0, 4, and 10 degrees of freedom. Methotrexate was modeled using 0, 4, and 12 degrees of freedom. Tolrestat was modeled using 0 and 6 degrees of freedom. The bonds which were defined to be rotatable on the different levels of flexibility are illustrated in Figure 3.2. In the case where 0 degrees of freedom were used to model the flexibility of the ligand (i.e., rigid ligand), the ligand conformation was taken directly from the original X-ray structure.

Protein atom coordinates were obtained from the snapshots of the molecular dynamics simulations. All hydrogen atoms were removed from the protein. SYBYL was then used to re-add polar hydrogens and to assign Kollman united-atom partial charges to the protein. Atomic solvation parameters and fragmental volumes were assigned to the protein atoms using ADDSOL. The resulting structures were used to calculate interaction energy grid maps using AutoGrid. Grids were calculated for an axis aligned cube of side 22.5Å centered on the geometric center of the ligand in the original crystal structure. Grid spacing was 0.375Å. Default AutoGrid values were used for the remaining parameters. The resulting grids and the ligand files were used as input for Autodock V3.0.5. Docking was carried out using the Lamarckian Genetic Algorithm (LGA) search method. The following values were used for the genetic algorithm parameters: the number of individuals in population was 50; the maximum number of energy evaluations was 1500000; the maximum number of generations was 27000; the elitism was 1; the rate of gene mutation was 0.02; the rate of crossover was 0.80; the number of generations for picking worst individual was 10; the mean of Cauchy distribution for gene mutation was 0; the variance of Cauchy distribution for gene mutation was 1. Local search was carried out using the pseudo Solis and Wets local optimizer using the following parameter values: the maximum number of iterations per local search was 300; the probability of performing local search on an individual in the population was 0.06; the maximum number of consecutive successes or failures before doubling or halving the local search step size, ρ, was 4, in both cases; and the lower bound on ρ, the termination criterion for the local search, was 0.01. The search for a docked conformation was repeated 10 times for each initial protein conformation. The results reported refer to the conformation with the lowest interaction energy score as reported by Autodock. RMSD values reported are from the ligand coordinates in the lowest energy conformation using as reference the crystallographic coordinates of the ligand.

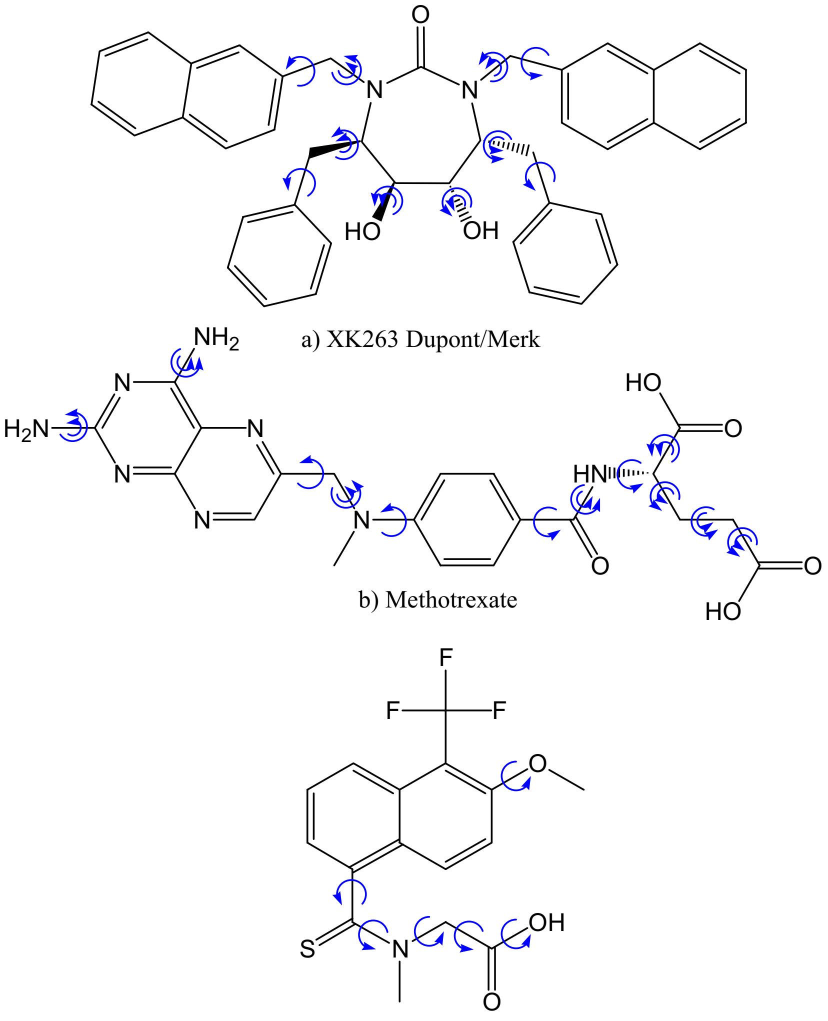

a) XK263 Dupont/Merk

b) Methotrexate

c) Tolrestat

Figure 3.2 - Ligands and degrees of freedom used in docking. For the case of rigid ligand docking all torsional degrees of freedom were set to the values found in the experimental structure. For the case of flexible ligand docking the arrows indicate the torsional degrees of freedom allowed to vary during the flexible ligand conformational search. In cases a) and b) where more than one level of conformational flexibility was explored, the bonds labeled with the single arrows indicate the degrees of freedom searched in the least flexible model and the bonds labeled with double arrows indicate the degrees of freedom that were added for the most flexible model.

3.2.4. Dock

Ligand and protein input files were prepared in the same manner was described above for Autodock with the exception that all hydrogens were added to the protein representation as required by DOCK. Spheres characterizing the binding site were generated using the program SPHGEN as described in (Kuntz, Blaney et al. 1982) and edited in order to remove spheres far from the binding site. Interaction energy scoring grids were generated using the program GRID. The grid size and positions were calculated such that they would enclose the cluster of spheres representing the binding site. An extra margin of 5Å in all directions was added to the grid sizes. The size of the grids computed was variable but was approximately the size of the grids computed for scoring in Autodock. Grid spacing was 0.300Å. Default GRID values were used for the remaining parameters. The resulting grids and the ligand files were used as input for DOCK V4.0. The following values were used for the DOCK parameters: the maximum number of orientations tried was 10,000 using automated matching and a matching tolerance of 0.25Å. Default values were used for the remaining docking parameters. Torsion minimization was used in the case of flexible ligand models. One cycle of minimization was also used to adjust the orientation and conformation of the ligand and improve its interaction energy score. The minimization used a maximum of 100 steps, an initial translation step of 0.5Å, an initial rotation step of 0.1 degrees, and an initial torsion step of 10 degrees. The reported results refer to the conformation with the lowest interaction energy score as reported by DOCK.

3.3. Results and Discussion

The original experimentally determined conformation and the derived structures obtained using high temperature molecular dynamics were used as input for the docking programs Autodock and DOCK. This corresponded to 101 alternative receptor conformations considered for each of the proteins. Alternative levels of ligand flexibility were also tested. The results for the docking experiments are shown in Figures 3.3 through 3.5. Each of the plots contains the following information. The axis of abscissas represents the different conformational variation groups. The 100 computationally generated protein conformations are grouped in 10 sets according to the RMSD values of non-hydrogen atoms of residues that constitute the binding site using as a reference the crystal structure. On the right axis of ordinates and shown in open circles connected by lines is the average interaction energy score for each conformational group. On the left axis of ordinates and shown using filled rhombs are the ligand RMSD values for the lowest energy docked solution using as a reference the position of the ligand in the crystal structure. The circle and the cross over the left axis of ordinates indicate the interaction energy score and ligand RMSD using the experimental receptor conformation, respectively. Theoretically, if docking programs were able to reproduce exactly experimental ligand bound conformations the ligand RMSD value should be 0.0Å. Due to errors and approximations present in interaction energy scoring functions the conformation corresponding to the global minimum of the scoring function never matches exactly the conformation determined experimentally. Nevertheless, this value is usually very close to the experimental value. The ligand

RMSD values we obtained for docking with the crystal structure of HIV-1 protease, DHFR, and aldose reductase using Autodock are 0.36Å, 0.60Å, and 0.69Å respectively. The same values using the DOCK program are 0.25Å, 0.69Å, and 0.53Å. These numbers provide a baseline for what are the best results that can be expected using the above model systems. In this study we considered that any result better than 1.5Å corresponds to the correct docked orientation. This value is similar to values chosen for other docking studies(Rarey, Kramer et al. 1996; Jones, Willett et al. 1997; Paul and Rognan 2002). Furthermore, in order to avoid any bias we did not select the solution with lowest ligand RMSD as the best solution from each docking run. The best solution selected was the one with the lowest interaction energy value.

Figure 3.3 shows the results obtained for both rigid and flexible ligand models using the Autodock program. The rationale for testing the effects of ligand flexibility in conjunction with receptor flexibility was to assess to what extent a flexible ligand model would compensate for changes in the receptor. For example, conformational changes in the receptor could be such that the original three dimensional shape of the ligand could not fit into the binding site cavity without leading to steric clashes resulting in a high energetic penalty. However, a flexible ligand might still lead to a good three dimensional shape complementarity by changing its internal degrees of freedom by a small amount in order to adapt to the new receptor shape. We also used the rigid ligand model to compare whether it would be more adversely affected by changes in the receptor. Furthermore, the use of multiple low energy ligand conformers to represent a ligand in a rigid-protein/rigid-ligand virtual screening effort is still a common practice. Such approach reduces the dimensionality of the conformational space that needs to be explored in the search for the minimum energy docked conformation. In practice we observed only small differences in the results between the rigid and moderately flexible (4 to 6 degrees of freedom) ligand models. This is due mainly to the fact that the conformation of the ligand used for the rigid docking was taken directly from the crystal structure. As such, the values for its torsional degrees of freedom are already at its optimum values which facilitated the docking search. When a flexible ligand was used the conformational search ended up with a very similar solution to the rigid ligand conformation. This type of result was independent of the docking program used as can be seen from Figure 3.5. Another observation common to all protein systems is that correct docked solutions show an increase in average ligand RMSD for more flexible ligand models. This is not an indication that the docking solution is worse. It is caused by small differences from the crystal structure in the values obtained for the internal degrees of freedom which lead to an increase in ligand RMSD. The increase in ligand RMSD is particularly noticeable for DHFR. For this protein the average ligand RMSD for the 0.1Å receptor RMSD group are 0.59Å, 0.70Å, and 1.23Å for the 0, 4, and 12 degrees of freedom models, respectively. However a visual inspection of the results clearly indicates that in all solutions the generally correct docked conformation was obtained.

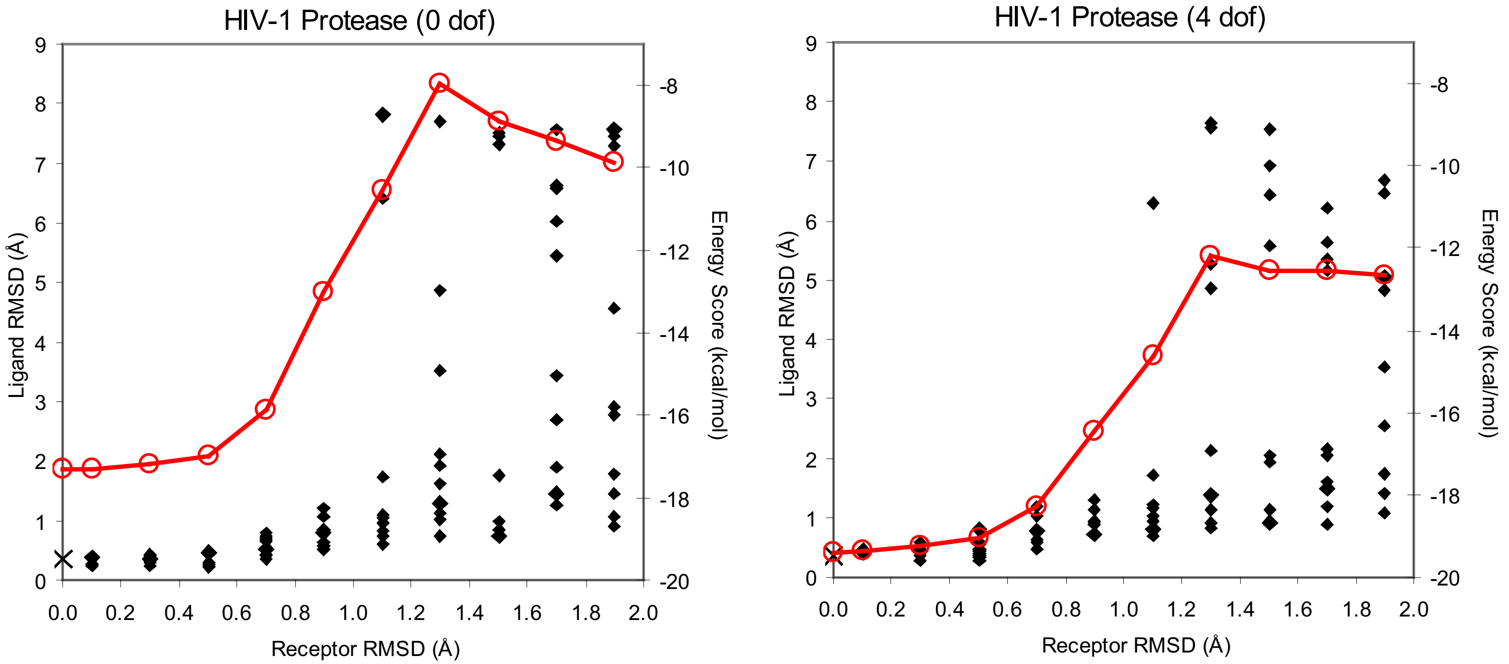

Figure 3.3-a) – Autodock docking results for HIV-1 protease using a rigid (left column) or a flexible ligand (right column). The axis of abscissas represents the different conformational variation groups for the protein. Each conformational group contains 10 representative structures. The RMSD values are for the non-hydrogen atom coordinates of the residues that constitute the binding site using as a reference the crystal structure. On the right axis of ordinates and shown in open circles in the plot is the average interaction energy score for each conformational group. On the left axis of ordinates and shown using filled rhombs are the ligand RMSD values for the lowest energy docked solution using as a reference the position of the ligand in the crystal structure. The cross over the left axis of ordinates indicates the ligand RMSD docking solution using the original receptor structure.

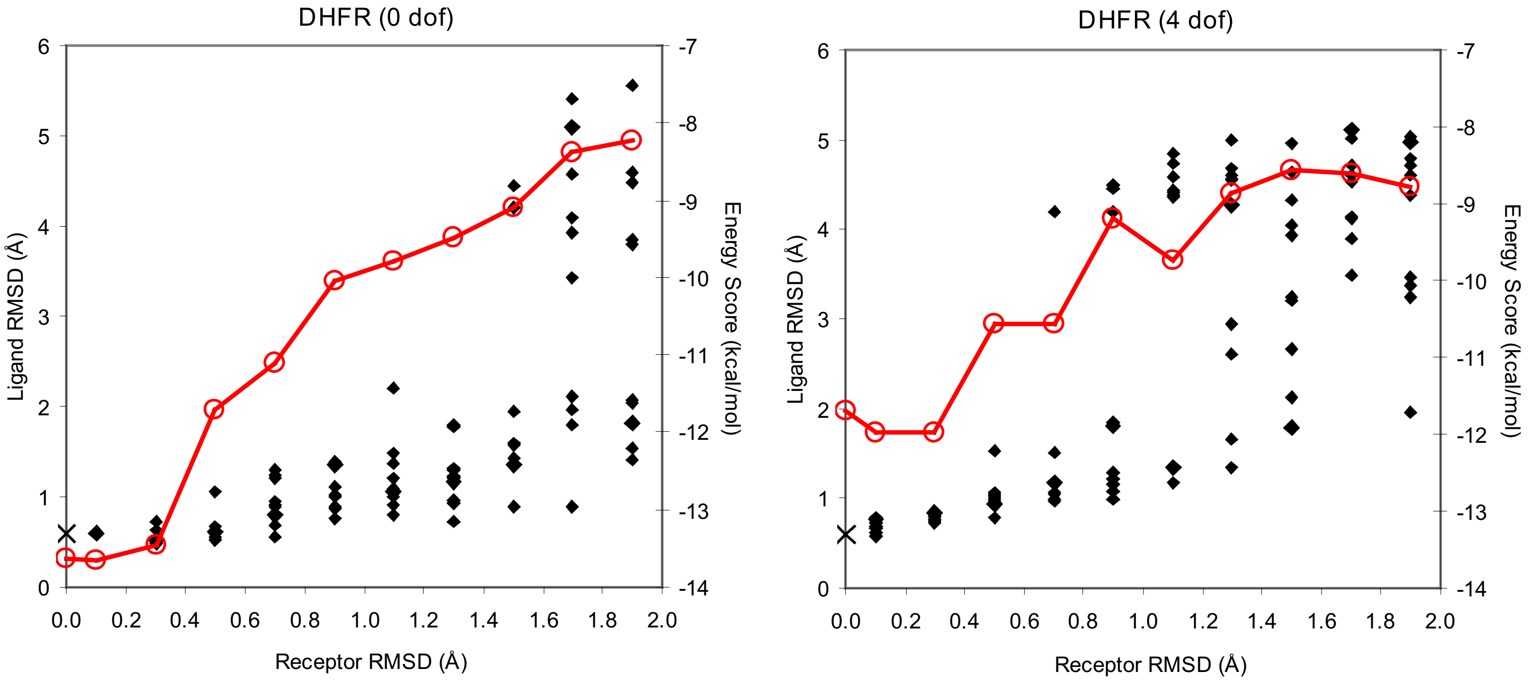

Figure 3.3–b) - Autodock docking results for DHFR using a rigid (left column) or a flexible ligand (right column). The data representation is the same as for Figure 3.3-a).

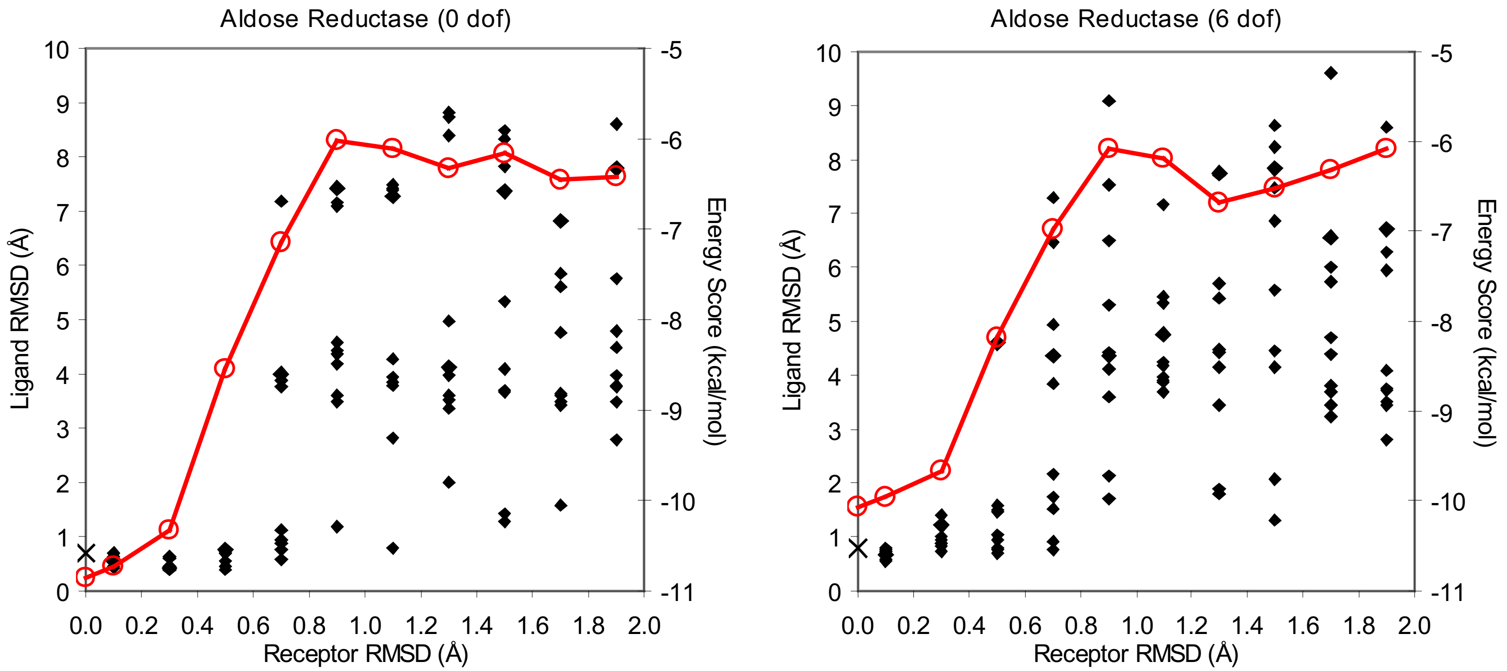

Figure 3.3-c) - Autodock docking results for aldose reductase using a rigid (left column) or a flexible ligand (right column). The data representation is the same as for Figure 3.3-a).

In almost all cases where the rigid ligand model could not be fitted in the binding site cavity the same occurred for the flexible case. This occurred because the change in the receptor shape was such that it drastically affected the three dimensional properties of the binding site. An example of such change is a reorientation of a sidechain in the center of the binding site of aldose reductase such that the binding cavity was approximately divided into two smaller cavities. In these types of situations, ligand flexibility is not sufficient to compensate for the receptor changes therefore negating the advantages of this model. In addition, we also observed that the increase in dimensionality of the search space due to the extra degrees of freedom in the ligand sometimes resulted in failure to find the correct ligand conformation even when we knew it existed because it was found using the rigid search. This type of behavior is evident when we compare the results for the docking of HIV-1 protease and DHFR using the moderate (4 torsional degrees of freedom) shown in Figures 3.3-a) and 3.3-b) and very flexible ligand models (10 and 12 torsional degrees of freedom, respectively) shown in Figure 3.4. In the case of HIV-1 protease the total number of docked solutions with ligand RMSD below 1.5Å falls from 73 to 69. This effect is even more noticeable for DHFR in which the increase in the search space is larger. In this case the number of correct solutions falls from 43 to 35. The main conclusion from these observations should not be that using flexible ligand models for docking is a wasted effort. In the specific case of the present study we are trying to evaluate only the effects of receptor flexibility on docking results. As such we are starting our ligand conformational search from the known experimental conformation and, in the case of the flexible model, letting the ligand adapt to changes in the shape of the receptor. The main observation from the ligand flexibility results is that, for that case of the receptor/ligand pairs used in this study, ligand flexibility did not play a major role in the docking results and the advantages obtained from the flexible model are lost by the increase in the search space given equal computing time.

The results obtained for the average lowest energy score for each conformational set show the same general behavior for all protein models, docking programs and ligand flexibility levels. For very small receptor RMSD, the energy score is usually very similar to the score obtained using the original crystal structure (results not shown). As the receptor RMSD increases we observe an increase in energy. The increase in energy is always initiated even at receptor RMSD levels for which the docking results as determined by the ligand RMSD score are still very good. This behavior reflects the fact that although the ligand is still located in the correct area of the binding site, the interactions it is forming with the protein are not as strong as in the crystal structure. For very large receptor deviations the average interaction energy reaches a plateau similar to the ligand RMSD values. This reflects final docked orientations for the ligand which bind weakly and are very different from the original.

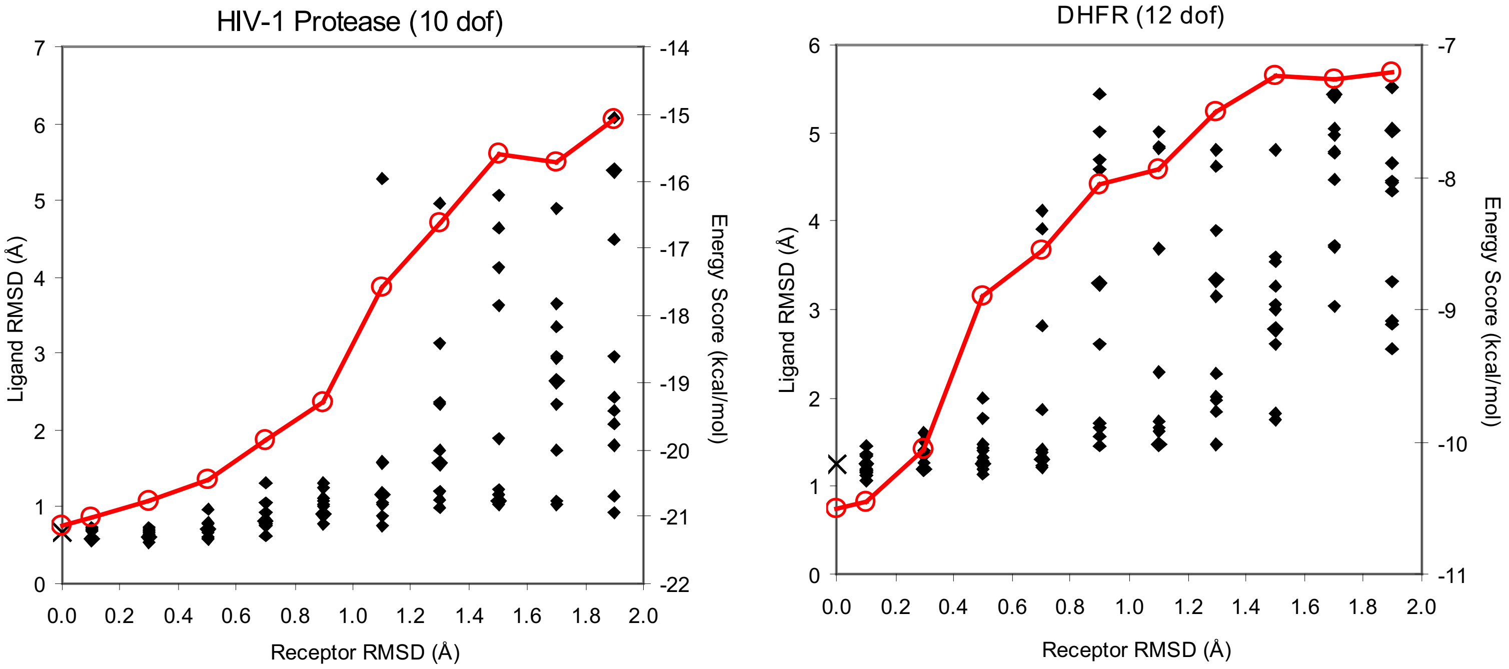

Figure 3.4 - Autodock docking results for HIV-1 protease (left) and DHFR (right) using a very flexible ligand model. The data representation is the same as for Figure 3.3-a).

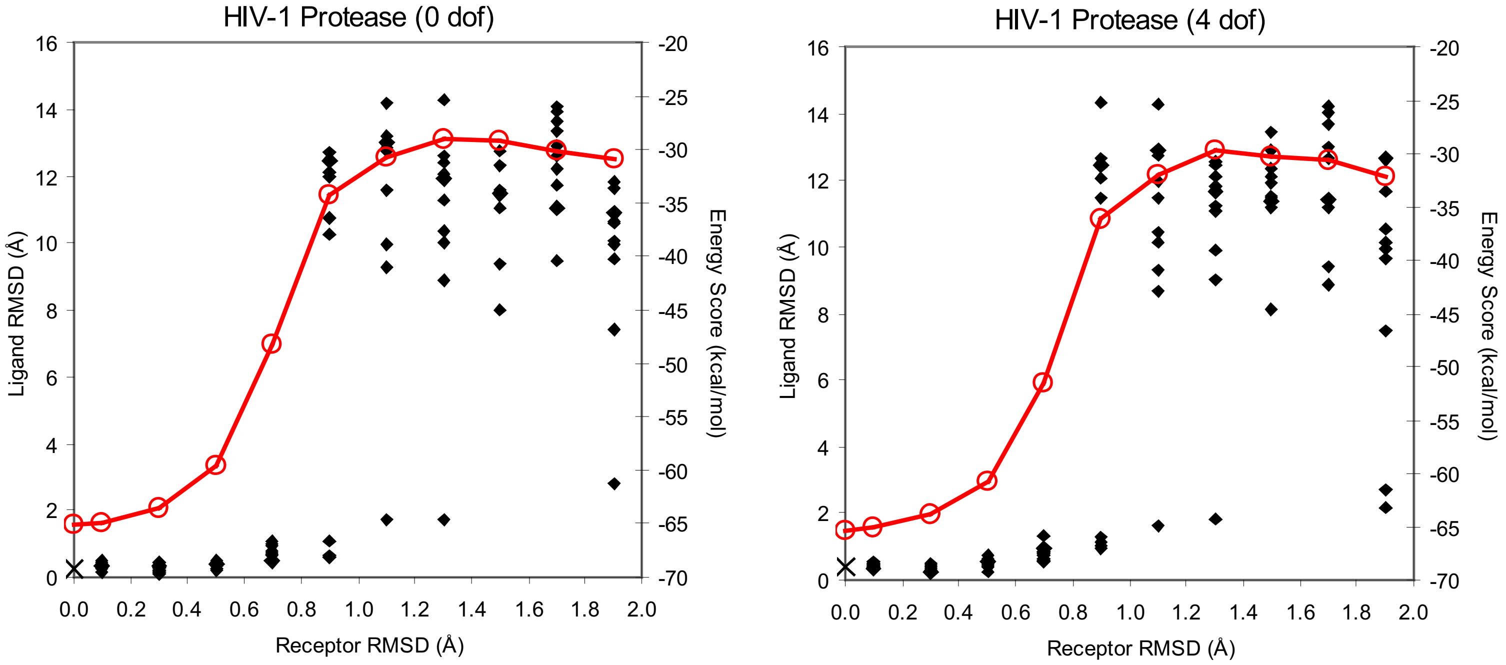

Figure 3.5-a) - DOCK docking results for HIV-1 protease using a rigid (left column) or a flexible ligand (right column). The data representation is the same as for Figure 3.3-a).

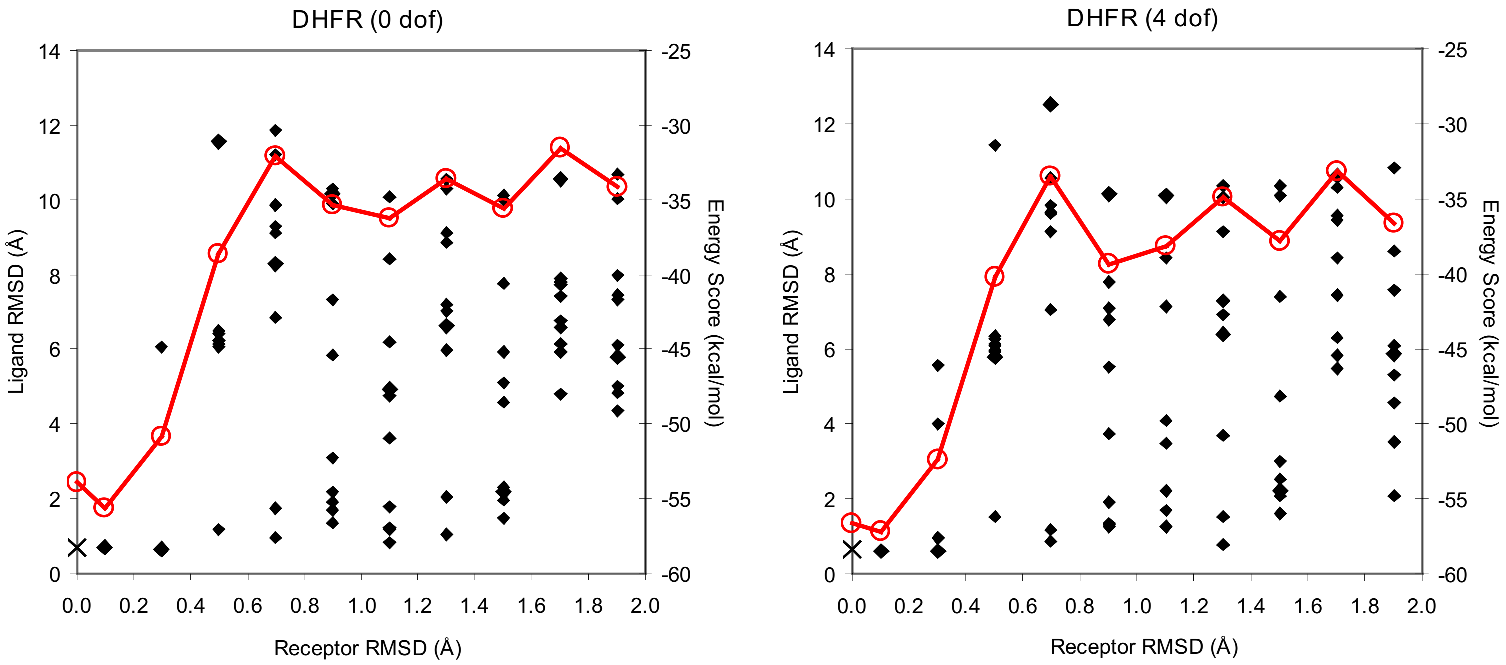

Figure 3.5-b) - DOCK docking results for DHFR using a rigid (left column) or a flexible ligand (right column). The data representation is the same as for Figure 3.3-a).

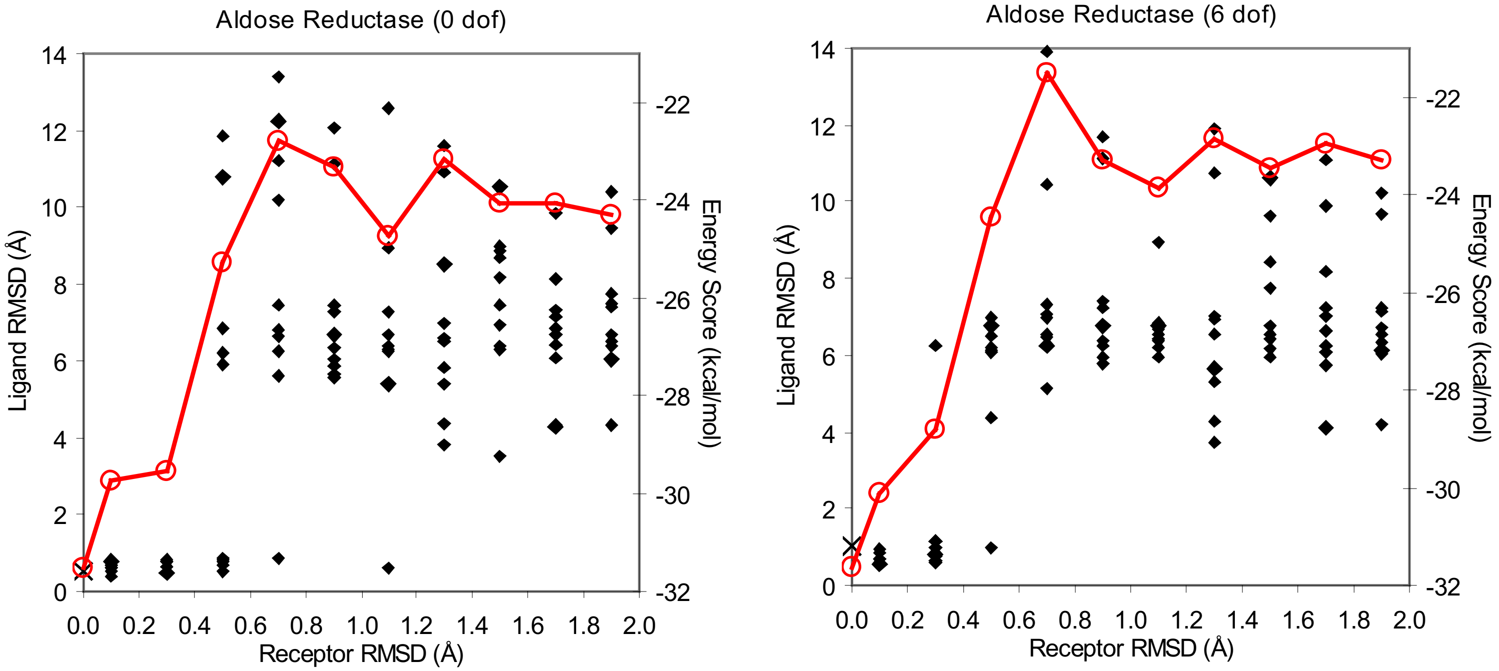

Figure 3.5-c) - DOCK docking results for aldose reductase using a rigid (left column) or a flexible ligand (right column). The data representation is the same as for Figure 3.3-a).

One of the main motivations for this study was to determine what level of receptor similarity is necessary between a structural model and the actual experimental structure in order to obtain a correct docking result. This type of information is valuable because it is common practice in virtual screening to use as a target, a receptor structural model that differs from what would be the actual experimental structure bound to the ligand being tested. This receptor model can originate from an experimental structure of a complex with another ligand or from a homology model. The results we obtained are clearly protein dependent. Using the Autodock program we can observe from Figure 3.3 that, whereas for HIV-1 protease all structures in the conformational sets with receptor RMSD lower than 1.0Å are able to correctly dock rigid models of XK263, for aldose reductase there are 14 structural models that fail to find the correct docked conformation for a rigid model of tolrestat. Using a flexible model of tolrestat there are 20 failed dockings. From the plots in Figure 3.3 we can derive that HIV-1 protease docking seems to be very tolerant of variations in the conformation of the receptor. In fact almost all of the docking experiments with receptor models for which the RMSD to the crystal structure is less than 1.2Å result in correct docking results. In the case of aldose reductase this number drops to 0.6Å. DHFR results are similar to HIV-1 protease, but there is a larger difference depending on the level of flexibility of the ligand model. Whereas most results below 1.4Å receptor RMSD find ligand conformations similar to the one observed in the experimental structure in the rigid ligand case, this threshold drops to approximately 0.8Å in the flexible case. The results using DOCK (Figure 3.4) for HIV-1 protease and for aldose reductase show a similar behavior although with different threshold values. HIV-1 protease and aldose reductase show correct results up to 0.8Å and 0.4Å receptor RMSD respectively. On the other hand the results seem to be minimally affected by the presence of ligand flexibility. These types of differences between docking programs are not significant and are fairly dependent on the input parameter values chosen to run the program. Due to the fact that there we were not trying to compare docking programs we decided to use the recommended parameters by the authors of these programs. The largest difference in results between Autodock and DOCK was for DHFR. In this case there are several positive results for receptor conformations as different as 1.5Å but there are also several docking failures for values as low as 0.3Å. The worse results are due to some difficulty in the DOCK scoring function in identifying the correct docked conformation as the one with lowest interaction energy. For the case of DHFR it was common to find the correct docked conformation as a lower ranking conformation in terms of energy score. Autodock and DOCK use very different scoring functions and as such it is not surprising to see cases in which one of the scoring functions works better than other for a particular protein system. Energy scoring functions are probably the most critical part of a docking system and problems like these are common. For recent reviews on this topic see (Tame 1999; Gohlke and Klebe 2001; Muegge and Rarey 2001; Halperin, Ma et al. 2002).

The results obtained in the present study clearly indicate that the effectiveness of second generation docking programs in dealing with receptor flexibility is protein dependent. This provides further insight into why structure-based drug design efforts have encountered mixed results when applied to the development of new pharmaceutical drugs. If the working receptor model conformation is fairly similar (approximately less than 0.5Å RMSD) to the actual conformation of the receptor when bound to the specific drug being screened, then second generation docking programs are a very effective discovery tool. However, as the errors in the receptor model increase, the chances to obtain correct results will be reduced by different amounts depending on the protein. The fact that HIV-1 protease seems to be a particular tolerant system to the receptor conformation may explain the success in developing drugs for this protein using structure-based drug design methods (Wlodawer and Vondrasek 1998). Although defining an exact set of rules that could determine how docking results would be affected by errors in the conformation of the receptor would contitute valuable information, such a set cannot be derived using exclusively the results of this study. The effects will depend on the specific protein, ligand, and docking program and deriving these exact rules would require a very large computing effort using a large number of model systems and a comprehensive statistical analysis. Nevertheless, even using a limited number of receptor models such as in this study it is possible to observe that proteins with large binding sites that form several favorable contacts with large ligands, such as HIV-1 protease, are less affected by variations in receptor shape. The absolute values for the interaction energies for the different proteins are a good indicator of the tolerance for conformational variation in the receptor. Another way of interpreting this result is to consider that receptor/ligand pairs that bind with high affinity correspond to deep wells in the interaction energy landscape of the docking search space. Variations at the level of the receptor correspond in practice to a smoothing of this space. If the energy well is not very deep in relation to the rest of the space then smoothing of the interaction energy function will quickly result in the occurrence of a lot of incorrect docked solutions. This type of behavior was observed when docking DHFR to methotrexate using DOCK. This study also showed that although receptor conformational differences below approximately 0.5Å RMSD do not pose a problem, differences above 1.5Å RMSD are unlikely to be well modeled using second generation programs.

3.4. Summary

In this chapter we assessed the level of similarity necessary between a receptor structural model and the actual experimental structure to obtain correct docking results using two current docking packages. The programs used are second generation programs that follow the rigid protein/flexible ligand model. This information is important due to the widespread use of this type of docking software in pharmaceutical structure-based drug design. Moreover, it is common in virtual screening to use receptor models that originate from an experimental structure of the unligated receptor or from a complex with another ligand. These experimentally determined receptor models, as well as those derived computationally using methods such as homology modeling, contain variations from the actual docked conformation which can easily be as large as 2.0Å RMSD. Our results show that the effectiveness of DOCK and Autodock in addressing this problem is protein dependent. However, we observed that independently of the protein system, receptor errors below approximately 0.5Å RMSD do not pose a problem, whereas errors above 1.5Å RMSD will likely result in docking failures.

Chapter 4.

Calculation of Protein Collective Modes of Motion Using Dimensional Reduction Methods

4.1. Introduction

The functions of proteins can be as varied as enzymatic catalysis, mechanical support, immune protection and generation and transmission of nerve impulses among many others. Today there is a large body of knowledge available on protein structure and function as a result of several decades of intense research by scientists worldwide. This information is expected to grow at an even faster pace in the coming years due to new efforts in large-scale proteomics and structural genomics projects. In order to make the best use of the exponential increase in the amount of data available, it is imperative that we develop automated methods for extracting relevant information from large amounts of protein structural data. The focus of this chapter is on how to obtain a reduced representation of protein flexibility from raw protein structural data.

Current structural biology experimental methods are restricted in the amount of information they can provide regarding protein motions because they were designed mainly to determine the three-dimensional static representation of a molecule. The two most common methods in use today are protein X-ray crystallography (Rhodes 1993) and nuclear magnetic resonance (NMR) (Wüthrich 1986). The output of these techniques is a set of {x, y, z} coordinate values for each atom in a protein. Neither of these methods is able to provide us with a full description, at atomic resolution, of the structural changes that proteins undergo in a timescale relevant to their function. Such information would be ideal to understand and model proteins. The alternative to experimental methods is to use computational methods based on classical (Brooks, Montgomery et al. 1988) or quantum mechanics (Gogonea, Suarez et al. 2001) to approximate protein flexibility. However these computations are prohibitively expensive and are not suitable for potential target applications such as the ones described in the previous paragraph. One of the reasons why the above computational methods are expensive is that they try to simulate all possible motions of the protein based on physical laws. For the case of molecular dynamics, the timestep for the numerical integration of such simulations needs to be small (in the order of femtoseconds), while relevant motions occur in a much longer timescale (microseconds to milliseconds). It is unrealistic to expect that one could routinely use molecular dynamics or quantum mechanics methods to simulate large conformational rearrangements of molecules. A medium sized protein can have as many as several thousand atoms and each atom can move along three degrees of freedom. Even when considering more restricted versions of protein flexibility that take into account only internal torsional degrees of freedom, or restrict the degrees of freedom to take only a set of discrete values, exploring the conformational space of these proteins is still a formidable combinatorial search problem (Finn and Kavraki 1999).

The method presented in this chapter addresses the high-dimensionality problem by transforming the basis of representation of molecular motion. Whereas in the standard representation all degrees of freedom (the {x, y, z} values for each atom) of the molecule were of equal importance, in the new representation the new degrees of freedom will be linear combinations of the original variables in such way that some degrees of freedom are significantly more representative of protein flexibility than others. As a result, we can approximate the total molecular flexibility by truncating the new basis of representation and considering only the most significant degrees of freedom. The remaining degrees of freedom can be disregarded resulting in only a small inaccuracy in the molecular representation. Transformed degrees of freedom will no longer be single atom movements along the Cartesian axes but collective motions affecting the entire configuration of the protein. The main tradeoff of this method is that there is some loss of information due to truncation (of the new basis) but this factor is outweighed by the ability to effectively model protein flexibility in a subspace of largely reduced dimensionality. We also show that results are acceptable, consistent with experimental laboratory results, and help shed light on the mechanisms of biomolecular processes.

4.2. Background

4.2.1. Dimensional Reduction Methods

Dimensionality reduction techniques aim to determine the underlying true dimensionality of a discrete sampling X of an n-dimensional space. That is, if X is embedded in a subspace of dimensionality m, where m<n, then we can find a mapping $F: X \rightarrow Y$ such that $Y \subset B$ and B is an m-dimensional manifold. Dimensionality reduction

methods can be divided into two types: linear and non-linear. The two most commonly used linear methods to find such mappings are Multi-Dimensional Scaling (MDS) and Principal Component Analysis (PCA).

MDS encompasses a variety of multivariate data analysis techniques that were originally developed in mathematical psychology (Shepard 1962; Kruskal 1964) to search for a low-dimensional representation of high-dimensional data. The search is carried out such that the distances between the objects in the lower dimensional space match as well as possible, under some similarity measure between points in the original high-dimensional space.

PCA is a widely used technique for dimensionality reduction. This method, which was first proposed by Pearson (Pearson 1901) and further developed by Hotelling (Hotelling 1933), involves a mathematical procedure that transforms the original high-dimensional set of (possibly) correlated variables into a reduced set of uncorrelated variables called principal components. These are linear combinations of the original values in which the first principal component accounts for most of the variance in the original data, and each subsequent component accounts for as much of the remaining variance as possible. Note that if the similarity measure of MDS corresponds to the Euclidean distances then the results of MDS are equivalent to PCA. The MDS and PCA dimensionality reduction methods are fast to compute, simple to implement, and since their optimizations do not involve local minima, they are guaranteed to discover the dimensionality of a discrete sample of data on a linear subspace of the original space.

One of the limitations of methods such as MDS and PCA is that their effectiveness is restricted by the fact that they are globally linear methods. As a result, if the original data is inherently non-linear these methods will represent the true reduced manifold in a subspace of higher dimension than necessary in order to cover non-linearity. This problem is likely to occur with protein motion data (Garcia 1992). To overcome this limitation several methods for non-linear dimensionality reduction have been proposed in recent years. Among these are principal curves (Hastie and Stuetzle 1989; Tibshirani 1992), multi-layer auto-associative neural networks (Kramer 1991), local PCA (Kambhatla and Leen 1997; Meinicke and Ritter 1999), mixtures of principal components formulated within a maximum-likelihood framework (Tipping and Bishop 1999), generative topographic mapping (Bishop, Svensen et al. 1998), and genetic algorithms (Raymer, Punch et al. 2000). More recently Tenenbaum *et al* proposed the isomap method (Tenenbaum, de Silva et al. 2000) and Roweis and Saul proposed the locally linear embedding method (Roweis and Saul 2000). The main advantage of the last two methods is that the optimization procedure used to find the low-dimensional embedding of the data does not involve local minima. In general the main disadvantages of non-linear versus linear dimensionality reduction methods are increased computational cost, difficulty of implementation, and problematic convergence. The development of new methods for dimensionality reduction is an active research area.

4.2.2. Collective Coordinate Representation of Protein Dynamics

The application of dimensionality reduction methods, namely PCA, to macromolecular structural data was first described by Garcia in order to identify high-amplitude modes of fluctuations in macromolecular dynamics simulations (Garcia 1992). It as also been used to identify and study protein conformational substates (Romo, Clarage et al. 1995; Caves, Evanseck et al. 1998; Kitao and Go 1999), to identify domain motions (Chillemi, Falconi et al. 1997), as a possible method to extend the timescale of molecular dynamics simulations (Amadei, Linssen et al. 1993; Amadei, Linssen et al. 1996), and as a method to perform conformational sampling (de Groot, Amadei et al. 1996; de Groot, Amadei et al. 1996). The validity of the method has also been established by comparison with laboratory experimentally derived data (van Aalten, Conn et al. 1997; de Groot, Hayward et al. 1998). As a substitute to the use of direct coordinate information for the computation of the principal components it is also possible to use this method with atomic distances information (Abseher and Nilges 1998). An alternative approach to determine collective modes for proteins uses normal mode analysis (Levy and Karplus 1979; Go, Noguti et al. 1983; Levitt, Sander et al. 1985; Case 1994) and can also serve as a basis for modeling the flexibility of large molecules (Kolossvary and Guida 1999; Zacharias and Sklenar 1999; Keseru and Kolossvary 2001; Kolossvary and Keseru 2001). Normal mode analysis is a direct way to analyze vibrational motions. To determine the vibrational motions of a molecular system, the eigenvalues and the eigenvectors of a mass weighted matrix of the second derivatives of the potential function are computed. The eigenvectors correspond to collective motions of the molecule and the eigenvalues are proportional to the squares of the vibrational frequencies. Direct comparisons of PCA and normal modes based methods have been published (Hayward, Kitao et al. 1997; van Aalten, de Groot et al. 1997). The PCA approach described in this chapter avoids some of the limitations of normal modes such as lack of solvent modeling, assumption that the potential energy varies quadratically, and existence of multiple energy minima during large conformational transitions. In contrast to previously published work, we focus on the interpretation of the principal components as biologically relevant motions and on how combinations of a reduced number of these motions can approximate alternative conformations of the protein. More recently other collective coordinate models such as the Gaussian network (Bahar, Erman et al. 1999), the "Jumping-Among- Minima" (Kitao, Hayward et al. 1998), and space warping (Jaqaman and Ortoleva 2002) have been applied to the study of proteins and DNA. For general reviews on the use of collective coordinate representations to model biomacromolecules see (Hayward and Go 1995; Kitao and Go 1999; Lafontaine and Lavery 1999).

4.3. Methods

4.3.1. Molecular Dynamics Data

Molecular dynamics simulations were carried out using similar protocols for all model systems. The protocol for HIV-1 protease will be described in detail and specific differences will be shown in parentheses. The HIV-1 protease simulation was computed using the program NAMD2 (Kalé, Skeel et al. 1999) and the Charmm22 parameter set

(MacKerell, Bashford et al. 1998). The starting coordinates for HIV-1 protease used in the simulations originated from the crystal structure published by Miller and collaborators (Miller, Schneider et al. 1989) with Protein Data Bank (Berman, Westbrook et al. 2000) code 4HVP (1AH4 for aldose reductase and 1JW4 for maltose binding protein). The ligand (N-Acetyl-Thr-Ile-Nle-Ψ(CH2-NH)-Nle-Gln-Arg amide) coordinates were removed from the structure but crystallographically observed waters were kept. Information about hydrogen atom positions was added using the HBUILD module of the program XPLOR v3.851 (Brünger 1992).

The model was hydrated by inserting the protein in an equilibrated periodic boundary cell of dimensions 77.625×62.100×62.100 Å^3 (77.625×77.625×77.625 for aldose reductase and 93.150×77.625×62.100 for maltose binding protein) containing 10,000 water molecules represented by the TIP3 water model box (15625 for aldose reductase and 15000 for maltose binding protein). The water boxes were generated by replicating along the Cartesian axes a previously equilibrated water box of size 15.525×15.525×15.525Å^3 containing 125 water molecules. The small box was replicated as many times as needed in order to reach the final cell dimensions. The protein was inserted in the center of the box with its longest axis aligned with the longest axis of the water box. Every atom in the protein was checked for collisions against the water oxygen atoms in the water molecules and in case of collision (threshold distance = 2.3 Å) the water molecule was removed. This resulted in the removal of 1184 water molecules from the box (1981 for aldose reductase and 2561 for maltose binding protein). The presence of solvent is necessary in order to simulate the protein in conditions as similar as possible to its natural environment. Although it was common in the early days of protein simulation to carry out molecular dynamics simulations of proteins in vacuum, this was done solely to avoid the increased computation of simulating explicitly solvent motion. Modern versions of popular forcefields such as Charmm (MacKerell, Bashford et al. 1998) and Amber (Cornell, Cieplak et al. 1995) were parameterized in such a way that explicit solvent models must be used in order to achieve the most accurate results. The use of explicit solvent is particularly important in the context of the present work, where ultimate objective of running the simulations is to determine a representation for the flexibility of the protein using collective modes of motion. Hayward and coworkers (Hayward, Kitao et al. 1993) have studied the effects of solvent on the collective motions of globular proteins and determined that its presence is important for the accurate computation of collective modes.

The charges on the resulting model were balanced by substituting 24 chloride and 18 sodium ions for 42 randomly selected waters in the model (31 Cl^- / 30 Na^+ for aldose reductase and 51 Cl^- / 43 Na^+ for maltose binding protein). The introduction of salt ions is necessary to maintain a stable protein structure (Ibragimova and Wade 1998) and avoid certain simulation artifacts such as unnaturally strong interactions between aminoacid side chains (Pfeiffer, Fushman et al. 1999). The charge distribution on the model was equilibrated in a process analogous to quenched minimization. The first step after introduction of the ions was to carry out 500 steps of conjugate gradient minimization to remove any steric clashes between the protein, solvent atoms, and salt ions. The minimization was carried out using fixed coordinates for the protein atoms in order to avoid artificial deformations in the initial protein model due to the ad-hoc placement of solvent atoms. Using again fixed coordinates for the protein atoms we heated the system to 1000K and simulated the solvent motion for 50 ps of simulation. This step was designed to redistribute the positions of the salt ions in the water box. The solvent was then gradually cooled to 300K during 40 ps and then simulated for another 30 ps at this temperature. This method of assigning positions to counter ions is different from what is usually described in the literature. The usual method calculates the electrostatic field around the protein and places counter ions at maxima and minima of potential. The traditional method results in a placement of atoms corresponding to a local minimum of the potential interaction energy between the protein and the counter ions. The method we used achieves approximately the same results and is less labor intensive.

After equilibration of the solvent, we equilibrated the entire system. The first step was to carry out 500 steps of conjugate gradient minimization on all atoms. The purpose of this step was to remove any bad contacts between the solvent and the protein and also within the protein. This step is always necessary because it is common for experimentally determined structures (especially the ones determined at low resolution) to exhibit local atomic interactions that are rather unfavorable according to the simulation forcefield. If the simulation is started directly from the experimentally determined structure it is likely that it would quickly become unstable. The minimization is followed by a gradual heating of the system from 0 K to 300K over the period of 40 ps followed by an extra 40 ps of simulation at 300K. The simulation was then carried out for a total of 1.4 ns (1.0 ns for aldose reductase and 1.6 ns for maltose binding protein). The choice of simulation time was determined according to previously published studies (Amadei, Ceruso et al. 1999) that indicate that simulations of a few hundreds of picoseconds are in general sufficient to provide a stable and statistically reliable definition of the collective modes of motion. The integration timestep for the simulation was 2 fs. The ShakeH algorithm (Ryckaert, Ciccotti et al. 1977) was used to restrain hydrogen atom positions. A cutoff of 8.5 Å was used for van der Waals interactions with a switching function starting at a cutoff of 8.0 Å. Full electrostatic interaction were taken into account in our simulations by using the particle-mesh Ewald method (Darden, York et al. 1993; Essman, Perera et al. 1995). The temperature of the system was kept at approximately 300K and the pressure was kept at 1 atm through the use of the Berendsen coupling algorithms (Berendsen, Postma et al. 1984). The coupling constant used in conjunction with the Berendsen temperature-coupling algorithm was 0.10 for the protein atoms and 0.50 for the water atoms. The Berendsen pressure compressibility was 0.000049 bar $^{-1}$, the relaxation time was 500 fs, and the number of time steps between applying pressure scaling was 12. Coordinates describing the time evolution of the system were written to a file every 100 fs.

4.3.2. Experimental Data

For comparison purposes we carried out the dimensional reduction analysis using exclusively experimentally derived data. Such analysis is possible for only a few model systems. Of the model systems used in this study, HIV-1 protease is the one for which more structures were determined experimentally using X-ray crystallography. For this calculation we used 135 structures determined under different experimental conditions and bound to different ligands (see Apendix B. for full list of structures). Prior to determination of the dimensional reduction calculation all the structures were backbone aligned using the structure with PDB code 4HVP as reference.

4.3.3. Principal Components Analysis and Singular Value Decomposition

In this chapter we focus our analysis on the application of PCA to protein structural data. For our study we chose PCA as the dimensionality reduction technique because it is very well established and efficient algorithms with guaranteed convergence for its computation are readily available. PCA has the advantage over other available methods that the principal components have a direct physical interpretation. As explained later, PCA expresses a new basis for protein motion in terms of the left singular vectors of the matrix of conformational data. The left singular vectors with largest singular values correspond to the principal components. When the principal components are mapped back to the protein structure under investigation, they relate to actual protein movements also known as modes of motion. It is now possible to define a lower dimensional subspace of protein motion spanned by the principal components and use these to project the initial high-dimensional data onto this subspace. The inverse operation can also be carried out and it is possible to recover the high-dimensional space with minimal reconstruction error. By contrast, recovering the high-dimensional representation is not readily achievable when using MDS because the definition of the low-dimensional subspace is implicit in the projection and is not defined directly by the left singular vectors as is the case for PCA.

The quality of the dimensionality reduction obtained using PCA can be seen as an upper bound on how much we can reduce the representation of conformational flexibility in proteins. The reason for this is that PCA is a linear dimensionality reduction technique and protein motion is in general non-linear (Garcia 1992). Hence, it should be possible to obtain an even lower dimensional representation using non-linear methods. However, we wanted to test the overall approach before proceeding to more expensive methods. For non-linear methods, the inverse mapping needs to be obtained using for example a neural network approach but the feasibility and efficiency of these mappings has not been tested so far. There is active research in this area and our work will benefit from any progress.

In PCA, principal components are determined so that the 1st principal component $PC_{(1)}$ is a linear combination of the initial variables A_j, with j=1, 2, … , n. That is

$$PC_{(1)} = w_{(1)1}A_1 + w_{(1)2}A_2 + \ldots + w_{(1)n}A_n\,,$$

where the weights $w_{(1)1}$, $w_{(1)2}$, … , $w_{(1)n}$ have been chosen to maximize the ratio of variance of $PC_{(1)}$ to the total variation, under the constraint

$$\sum_{j=1}^{n} \left(w_{(1)j} \right)^2 = 1\,.$$

Other principal components $PC_{(p)}$ are similarly linear combinations of the observed variables which are uncorrelated with $PC_{(1)}$, …, $PC_{(p-1)}$, and account for most of the remaining total variation. Although it is possible to determine as many principal components as the number of original variables, this method is typically used to determine the smallest number of uncorrelated principal components that explain a large percentage of the total variation in the data. The exact number of principal components chosen is application dependent and constitutes a truncated basis of representation.

The data used as input for PCA was generated using either the molecular dynamics simulations described above or experimental data obtained using X-ray crystallography. The data is in the form of several conformational vectors corresponding to different structural conformations that are sampled during the simulation. We will call the vector collection of all vectors the conformational vector set. Each conformational vector in the conformational vector set has dimension 3N where N is the number of atoms in the protein being studied and is of the form $[x_1, y_1, z_1, x_2, y_2, z_2,\ldots, x_N, y_N, z_N]$, where $[x_i, y_i, z_i]$ corresponds to Cartesian coordinate information for the i^{th} atom. In order to be used for the computation of principal components the data must be in the form of atomic displacement vectors. The first step in the generation of the atomic displacement vectors is to determine the average protein vector for each conformational vector set. This was achieved by first removing the translational and rotational degrees of freedom from the considered molecule by doing a rigid least squares fit (Kabsch 1976) of all the structures to one of the structures in the vector set and then averaging the values for each of the 3N degrees of freedom. The resulting average structure vector is then subtracted from all other structures in the conformational vector set to compute the final atomic displacement vectors.

In this work we use the singular value decomposition (SVD) as an efficient computational method to calculate the principal components (Romo 1998). The SVD of a matrix, A, is defined as:

$$A = U \Sigma V^T,$$

where U and V are orthonormal matrices and Σ is a nonnegative diagonal matrix whose diagonal elements are the singular values of A. The columns of matrices U and V are called the left and right singular vectors, respectively. The square of each singular value corresponds to the variance of the data in A along its corresponding left singular vector and the trace of Σ is the total variance in A. For our purposes, matrix A is constructed by the column-wise concatenation of all atomic displacement vectors. If there are m conformations of size 3N in the vector set, this results in a matrix of size $3N\times m$. The left singular vectors of the SVD of A are equivalent to the principal components (Romo 1998) and will span the space sampled by the original data. The right singular vectors are projections of the original data along the principal components. The right singular vectors also provide useful molecular information by helping to identify preferred protein conformations (Romo, Clarage et al. 1995; Teodoro, Phillips et al. 2000).

Another common nomenclature used in PCA is to refer to the principal components as eigenvectors and to the singular values as eigenvalues. The eigenvectors are the same as the left singular vectors and the eigenvalues are the square of the singular values. These names are used because it is also common to calculate the PCA by determining the eigenvectors and eigenvalues of the covariance matrix of conformational data. In the results and discussion section of this chapter we will refer to the results of the PCA calculation using the eigenvalues / eigenvectors / right singular vectors terminology.

The PCA for the molecular dynamics data was calculated at three different levels of detail: backbone, binding site, and all-atoms. For the case of the binding site calculation only the atoms of residues forming the binding site were used for the construction of matrix A. The residues used for each protein were chosen by visual inspection and are shown in Figure 4.1 and Table 4.1.

Protein	**Residues included in binding site PCA analysis**
HIV-1 Protease	8, 23, 25, 27-32 , 47-50, 80-84 (monomers A and B)
Aldose Reductase	20, 47, 48, 79, 110, 111, 113, 115, 122, 130, 219, 298, 300, 302, 303
Maltose Binding Protein	12, 14, 15, 44, 62, 63, 65, 66, 111, 153, 154, 155, 156, 230, 340

Table 4.1 – Residue numbers included in the binding site PCA analysis.

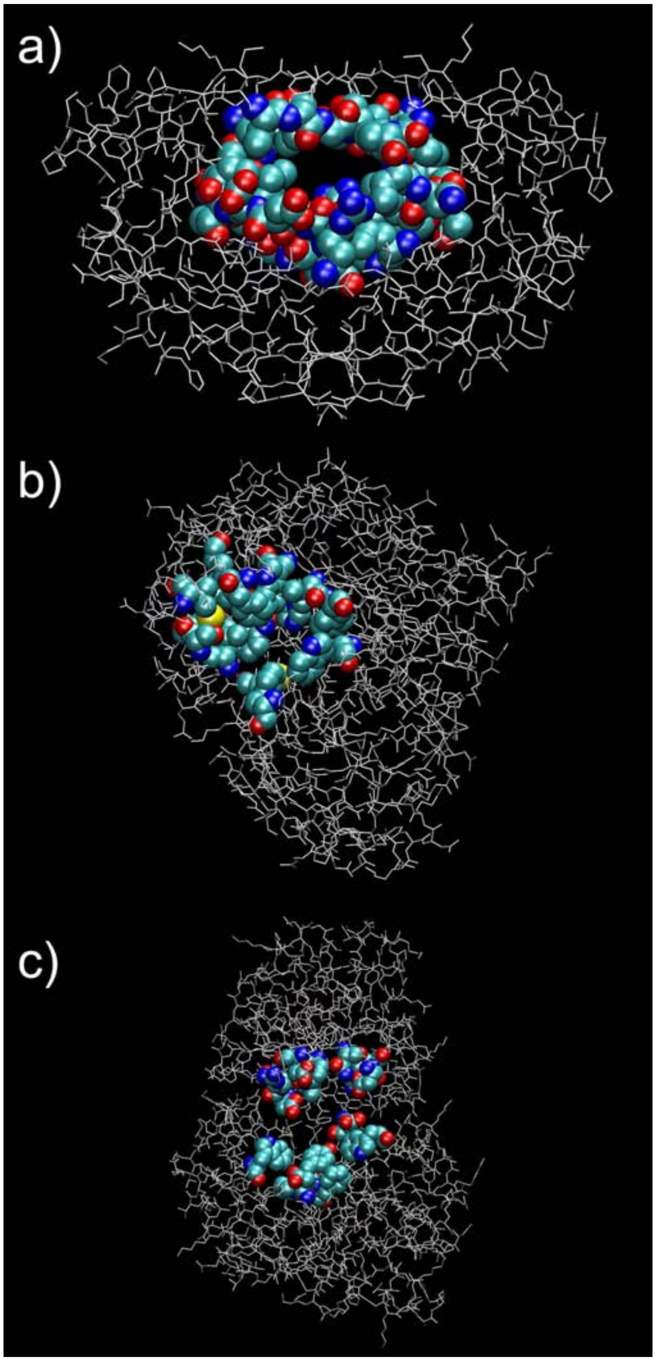

Figure 4.1 – Binding site atoms used for PCA. The atoms used for the PCA calculation are shown using VDW representation for a) HIV-1 protease, b) aldose reductase, and c) maltose binding protein.

The SVD of matrix A was computed using two distinct methods. In the initial phases of this project we used the built in function `SingularValues[]` in the program *Mathematica* (Wolfram 1999) to carry out the computation. Unfortunately, *Mathematica* relies on its internal algorithms for memory management and used considerably more computer memory than what was theoretically necessary for the SVD computation. In practice this limited the use of the Mathematica implementation only to the smallest SVD problems in this chapter such as the computation of modes of motion for the backbone of HIV-1 protease. In order to address this limitation we wrote the program *svd*. The program *svd* is written in the language C++ and calculates the singular value decomposition for a molecular dynamics trajectory. This program is built on top of the optimized Intel BLAS (Basic Linear Algebra Subroutines) library and the ARPACK++ library. The BLAS library is a series of optimized functions for calculations involving vectors and matrices. ARPACK++ is an object-oriented version of the ARPACK package developed by Danny Sorensen at Rice University (Lehoucq, Sorensen et al. 1998). ARPACK is a collection of Fortran77 subroutines designed to solve large-scale eigenvalue problems. It is based upon an algorithmic variant of the Arnoldi process called the Implicitly Restarted Arnoldi Method (Lehoucq and Sorensen 1996). The package is designed to compute a few eigenvalues and corresponding eigenvectors of a general n by n matrix. This also presented another advantage in comparison with the built in functions in Mathematica that can only compute the full decomposition of the input matrix. An (extremely) optimized program such as *svd* was able to improve the memory requirements for the computation approximately 4 fold and the computation speed by more than an order of magnitude when compared to *Mathematica*. Furthermore the program was parallelized using the pthreads library to run in parallel on shared memory multiprocessor machines. This allowed us to achieve approximately another 3 fold speedup in computation time on 4 processor machines.

4.4. Results and Discussion

4.4.1. Molecular Dynamics

Prior to the actual collection of the data that is going to be used for the dimensional reduction procedure, it is necessary in all molecular dynamics simulation to perform an equilibration of the simulation system. During this period the structure is going to assume a slightly different conformation from what was observed in the original model determined experimentally by X-ray crystallography. The main reason for this effect is probably related to errors and approximations that are common in forcefields currently in use for the simulation of biological systems. Some approximations, such as the lack of molecular polarization, are necessary in order to speed up the simulations and extend them to useful timescales. Another source for the RMSD differences to the experimental structure observed after the equilibration period may be due to the fact that the protein is being simulated in an environment which is significantly different from the one in which the experimental structure was determined. Namely, there are no direct contacts with other proteins in the environment and there is no addition of any crystallization agents. As such, it is possible that the differences observed may be at least partly due to real variations corresponding to different protein environments. A similar argument is often used in part to justify structural differences observed when the same protein is determined using both NMR and X-ray crystallography. For the purposes of molecular simulation, it is defendable that the starting structures should originate from NMR methods given the higher similarity in the protein environment. However, for the purposes of this study, we decided to use exclusively X-ray crystallography derived data given the much larger amount of data available. The RMSD values for the three model systems after the different phases that precede the actual simulation of the proteins are show in Table 4.2.

Protein	**HIV-1 Protease**	**Aldose Reductase**	**Maltose Binding Protein**
RMSD after minimization (Å)	0.173	0.198	0.220
RMSD after heating phase (Å)	0.978	0.774	1.012
RMSD after equilibration (Å)	1.300	0.959	1.283

Table 4.2 – C-α RMSD values for different phases of the simulation. The X-ray crystal structure (4HVP) was used as reference.

The deviation level from the original crystal structure after minimization is similar for the three proteins. The initial conjugate gradient minimization leads to a very small structural change from the initial structure. The values range from 0.173 Å for the case of HIV-1 protease to 0.220 Å for maltose binding protein. The structural changes correspond mostly to removal of bad contacts, reorientation of charged atoms on aminoacid sidechains to form better interactions with other aminoacids and/or the solvent, and a very small variation at the backbone level to adjust the structure to a local energy minimum in the forcefield. The step that causes the largest deviations from the experimental structure is the heating phase. During this phase the atoms have more kinetic energy available, which allows them to escape the local energy minimum that was reached during the initial minimization. During this phase the protein system will migrate to lower potential energy regions of the conformational state space. During this period and also during the equilibration phase the energy of the system has to be kept constant through periodic adjustments of atomic velocities. This is done by periodically reassigning atomic velocities corresponding to the simulation temperature from a Boltzmann distribution. Without this procedure the temperature of the simulation system would start to climb uncontrollably and eventually lead to protein denaturation or even instability of the numerical integration due to very high atomic displacements during each integration timestep. During the equilibration phase, the simulation is run in approximately the same conditions as in the production phase. In this step we looked for convergence of certain parameters of the simulation such as temperature, pressure, and RMSD deviation for the protein. At the end of this phase the values for C-α RMSD ranged from 0.959 for aldose reductase to 1.300 to HIV-1 protease. The difference between the values observed for aldose reductase in relation to the other two proteins is likely due to the fact that this protein is in general significantly less flexible. As such, it is also expected that this protein displays the lower RMSD deviations for both equilibration and simulation of the model system.

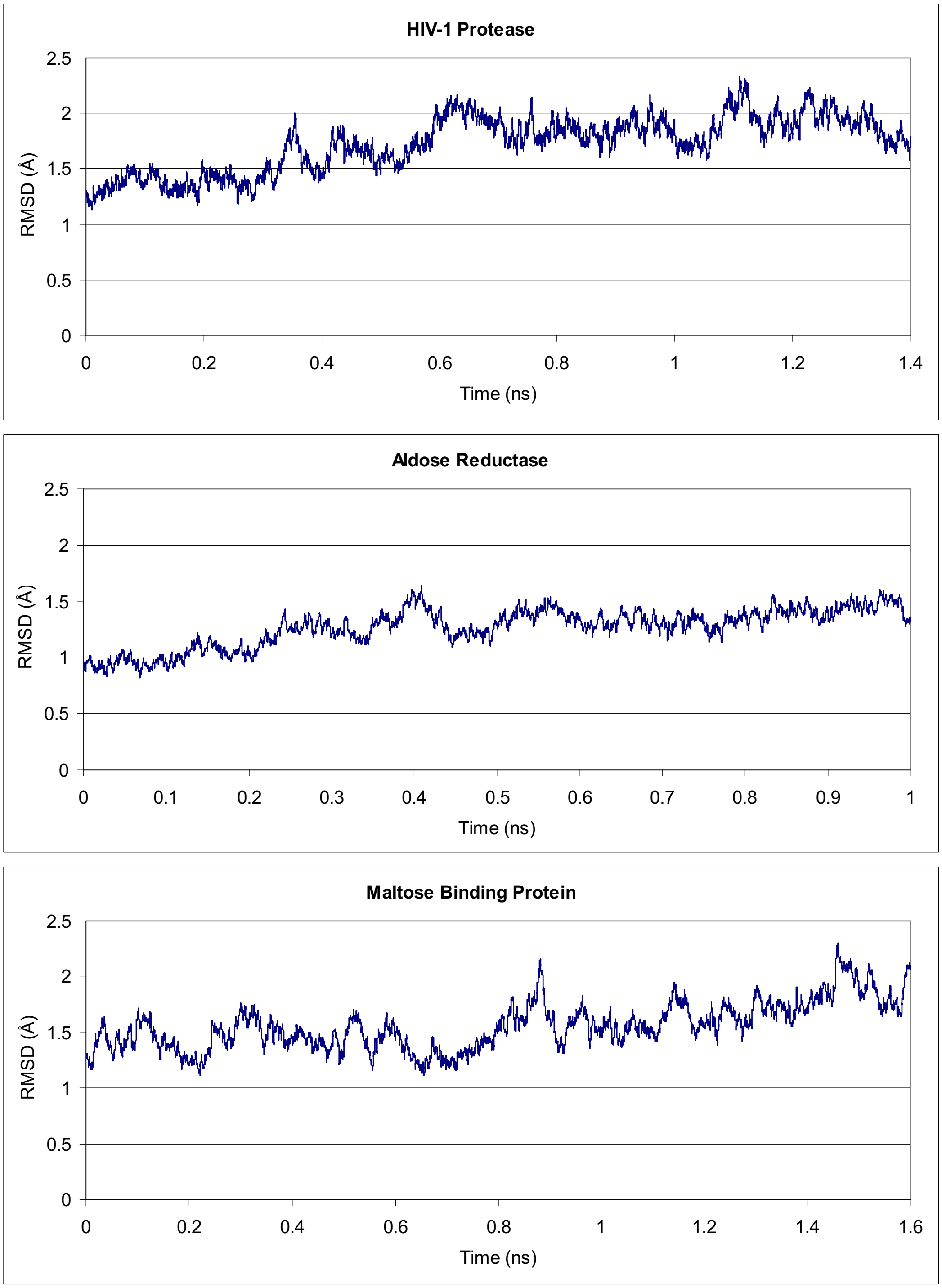

Figure 4.2 – α-Carbon RMSD progression for the molecular dynamics simulations of the three model systems.

The RMS deviations versus the original crystal structure during the production part of the simulation are shown in Figure 4.2. The plots show that all proteins are stable during the simulation period. The average RMSD values for the first 100 ps of simulation are 1.351 Å, 0.948 Å, and 1.405 Å for HIV-1 protease, aldose reductase, and maltose binding protein, respectively. The same values for the last 100 ps of simulation are 1.837 Å, 1.454 Å, and 1.849 Å. The overall level of conformational variation is approximately the same for all protein systems. The change in conformation that is observed for proteins is not due to simulation instability and is within the ranges normally observed for these types of simulations.

The RMSD changes shown in Figure 4.2 during the simulation correspond in large part to changes at the level of the binding site. However, this information is not clearly observable just by visualizing the output of the simulation. Although, especially for the case of HIV-1 protease, it is possible to observe by visualization of the raw data a larger flexibility component at the level of the binding site, this is not immediately clear for the other two cases. This is the main reason why we decided to use a dimensional reduction methodology in the present work. The purpose of this technique is to help understand what the most important components of protein flexibility are. In addition the PCA method provides us with an abstract and compact flexibility representation that enables the use of its results in modeling studies such as structure-based drug design.

4.4.2. Backbone PCA

One of the advantages of the dimensional reduction method using PCA is the ability to carry out the data analysis at different levels of detail and focusing on different parts of the protein. Although an analysis consisting of all the atoms in the protein provides us with information regarding all levels of detail, such as backbone or binding site, it is also computationally more expensive and often unnecessary. In this section we will analyze the results of studying the flexibility of the protein at the backbone level. In this computation we included as part of the backbone atoms the N, CA, and C atoms. The O, HN, and H were not included because their positions can be readily approximated from the other three. Alternatively, we could have chosen to represent the backbone using only the CA atoms. The backbone representation chosen for this study uses 9 degrees of freedom per aminoacid. As such the total number of degrees of freedom is 1782 for HIV-1 protease, 2835 for aldose reductase, and 3330 for maltose binding protein. If we had used all the atoms in the proteins these numbers would have been 9360, 15732, and 17211, respectively.

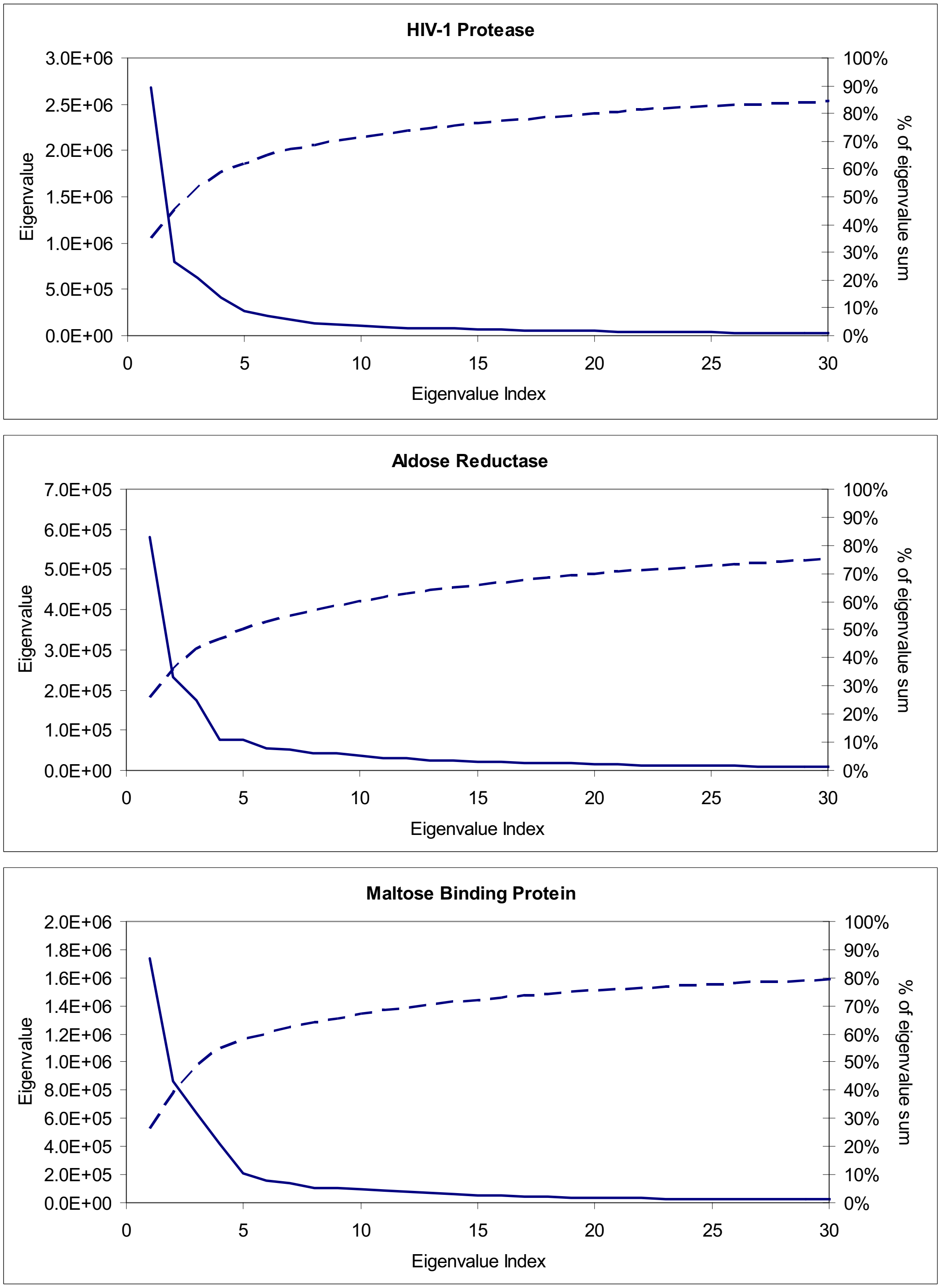

Figure 4.3 – Eigenvalues (continuous line) and percentage of eigenvalue sum (broken line) for the backbone PCA analysis of the molecular dynamics trajectories.

The eigenvalues for the PCA analysis of the three protein models are plotted using a continuous line in Figure 4.3. The absolute values for the eigenvalues are shown on the left axis. The right axis and the broken line indicate the percentage of the eigenvalue sum contributed by the eigenvalues with index less than or equal to the current index. Only the largest 30 eigenvalues are plotted. All the proteins in this study displayed a significant eigenvalue drop with the first few eigenvalues accounting for most of the eigenvalue sum. For the case of HIV-1 protease the first, second, and third eigenvalues account for 34.8%, 45.2%, and 53.2% of the eigenvalue sum. These numbers illustrate the power of the dimensional reduction method. Using only 0.17% of the initial number of degrees of freedom in the system, it is possible to account for more than half of the variance observed during a molecular simulation for this particular system. For the case of aldose reductase the first, second, and third eigenvalues account for 25.6%, 35.8%, and 43.4%. The same numbers for maltose binding protein are 26.1%, 39.0%, and 48.6%, respectively. These numbers are similar to the ones obtained for HIV-1 protease but the differences are relevant. The first aspect to note is that the values for aldose reductase are smaller. This can be explained by the reduced flexibility of this protein in comparison to the other two. HIV-1 protease and especially maltose binding protein undergo large conformational changes upon ligand binding (see Appendix A. for details). In contrast, aldose reductase undergoes little or almost no conformations changes depending on the ligand. Furthermore, this changes happen almost exclusively at the binding site level with the rest of the protein remaining almost unchanged. This difference in overall flexibility can be also observed from the absolute values of the eigenvalues. The sums of the first three eigenvalues for HIV-1 protease, aldose reductase, and maltose binding protein are 4.09×10^{7}, 9.88×10^{6}, and 3.24×10^{7}, respectively. Another important difference is the ratio between the first eigenvalues for the three systems. Whereas for HIV-1 protease, the first eigenvalue clearly dominates the eigenvalue spectrum, for the other proteins there is a more gradual drop in eigenvalues. The ratios between the first and second eigenvalues for HIV-1 protease, aldose reductase, and maltose binding protein are 3.35, 2.50, and 2.02, respectively. These values are of great importance when later we examine the motions corresponding to these eigenvalues. On one hand, due to the large dominance of the first eigenvalue, the first eigenvector for HIV-1 protease can represent a good approximation to a relevant biological motion for this protein. On the other hand, the small difference in first and second eigenvalues for maltose binding protein precludes the interpretation of the first mode of motion for this protein without consideration of the second.

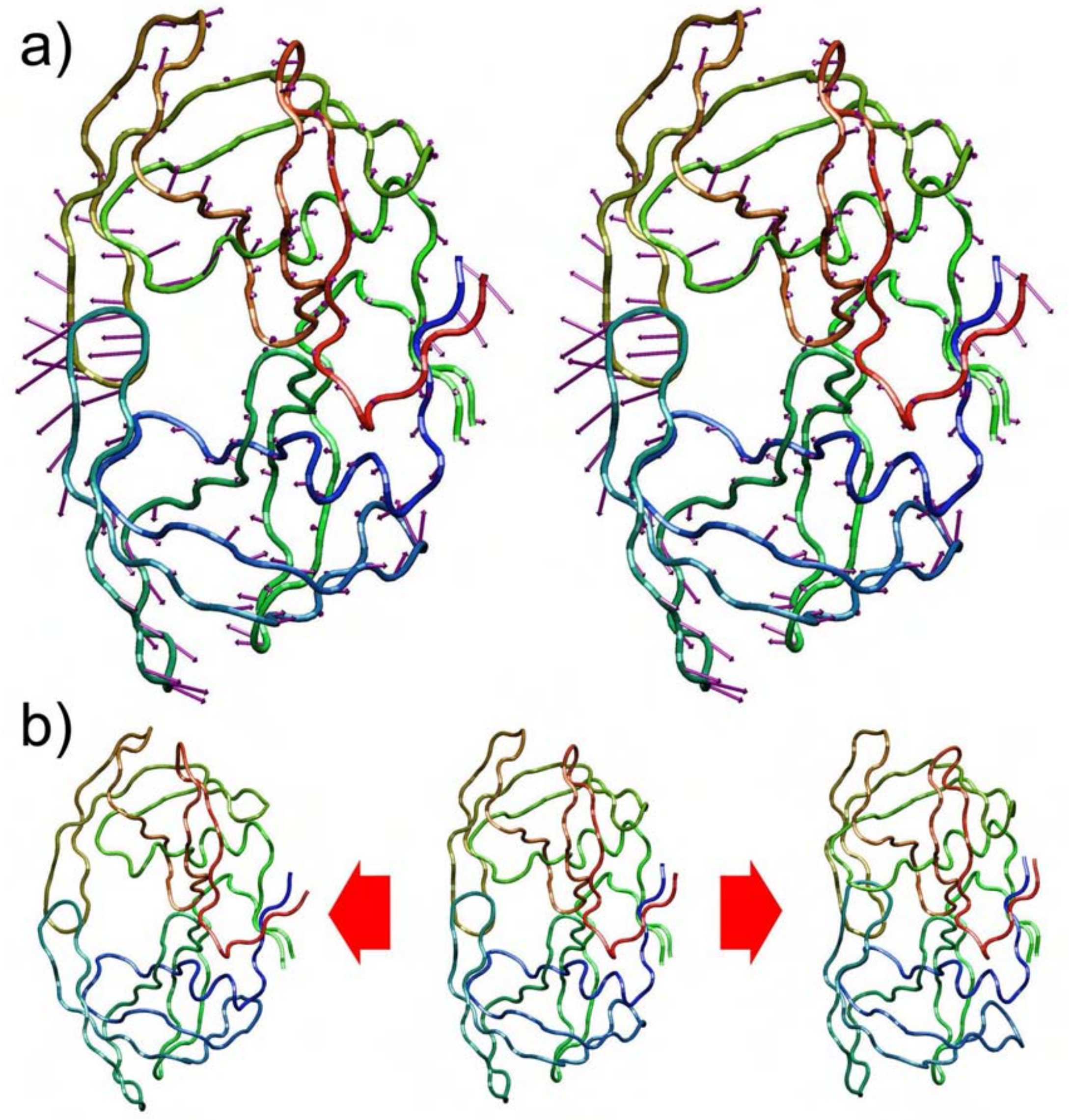

Figure 4.4 – First mode of motion for the backbone of HIV-1 protease. The backbone is colored from red to blue as a function of the residue number. a) Stereoview of the mapping of the first eigenvector on the C-α atoms. The directions of motions are indicated by purple arrows. b) Changes in conformation corresponding to a motion in both directions along the first mode of motion starting from the experimental structure (center).

In the dimensional reduction method using PCA, there is an eigenvector corresponding to each eigenvalue. The eigenvalues provide information about the number of relevant motions and their relative importance. The eigenvectors can be mapped back to the structure of the protein to indicate directions of preferred motion. Given a 3N dimensional eigenvector, corresponding to the N atoms in the protein for which the PCA analysis was carried out, the motions can be readily visualized by partitioning the eigenvector into N Cartesian vectors and mapping each of these to its corresponding atom. Figure 4.4 shows the mapping of the first eigenvector to the backbone of HIV-1 protease. This corresponds to the first mode of motion. The direction of motion is indicated in Figure 4.4 - a) by the Cartesian vectors (purple arrows) for each CA atom. The arrows corresponding to the N and C atom motions were omitted for clarity. The length of the arrows indicates the relative amount of motion for each CA atom. Figure 4.4 - b) shows conformational changes corresponding to a motion in both directions along the first mode of motion starting from the experimental structure. The motion is exaggerated for illustration purposes. The first mode of motion for HIV-1 protease is in excellent accordance to the experimental data available for this protein. The motion occurs mostly in the flaps region and clearly indicates an opening of the flaps in order to expose the binding site. The motion also suggests a transition path between the bound and unbound experimental structures and between alternative bound forms (see Appendix A.1.). For example, the structure shown on the left side of Figure 4.4 - b) is similar to the unbound conformation of HIV-1 protease (Wlodawer, Miller et al. 1989) and to other bounds forms such as 1AID

(Rutenber, Fauman et al. 1993) shown in Figure A.2. The motion is also in good agreement with previous simulation studies using molecular dynamics (Collins, Burt et al. 1995). The mapping of the first eigenvector to the protein structure also shows a significant amount of motion at the level of the 78-83 loop near the binding site. This loop has been shown to undergo significant conformation changes during binding of some HIV-1 protease inhibitors (Munshi, Chen et al. 2000). The core of the protein stays mostly unchanged according to the first mode of motion. This is also in good agreement with the available experimental structures for HIV-1 protease, which show much less conformational variation at the core than at the binding site level.

The second mode of motion for HIV-1 protease is shown in Figure 4.5. This mode is complementary to the first and also explains conformational rearrangements that HIV-1 undergoes when binding to different ligands. While the first mode corresponds to an opening of the flaps region and therefore a change in binding site volume mostly in that direction, the second mode corresponds to a sideways constriction of the binding site allowing for variations in the width of the ligand. Unlike the first mode, there is less variation in the relative size of the arrows. The motion is not restricted to a particular site on the protein but is mostly a change in the relative orientation of the two protein monomers leading to a loosening/tightening of the binding site (see Figure 4.5 – b) left and right).

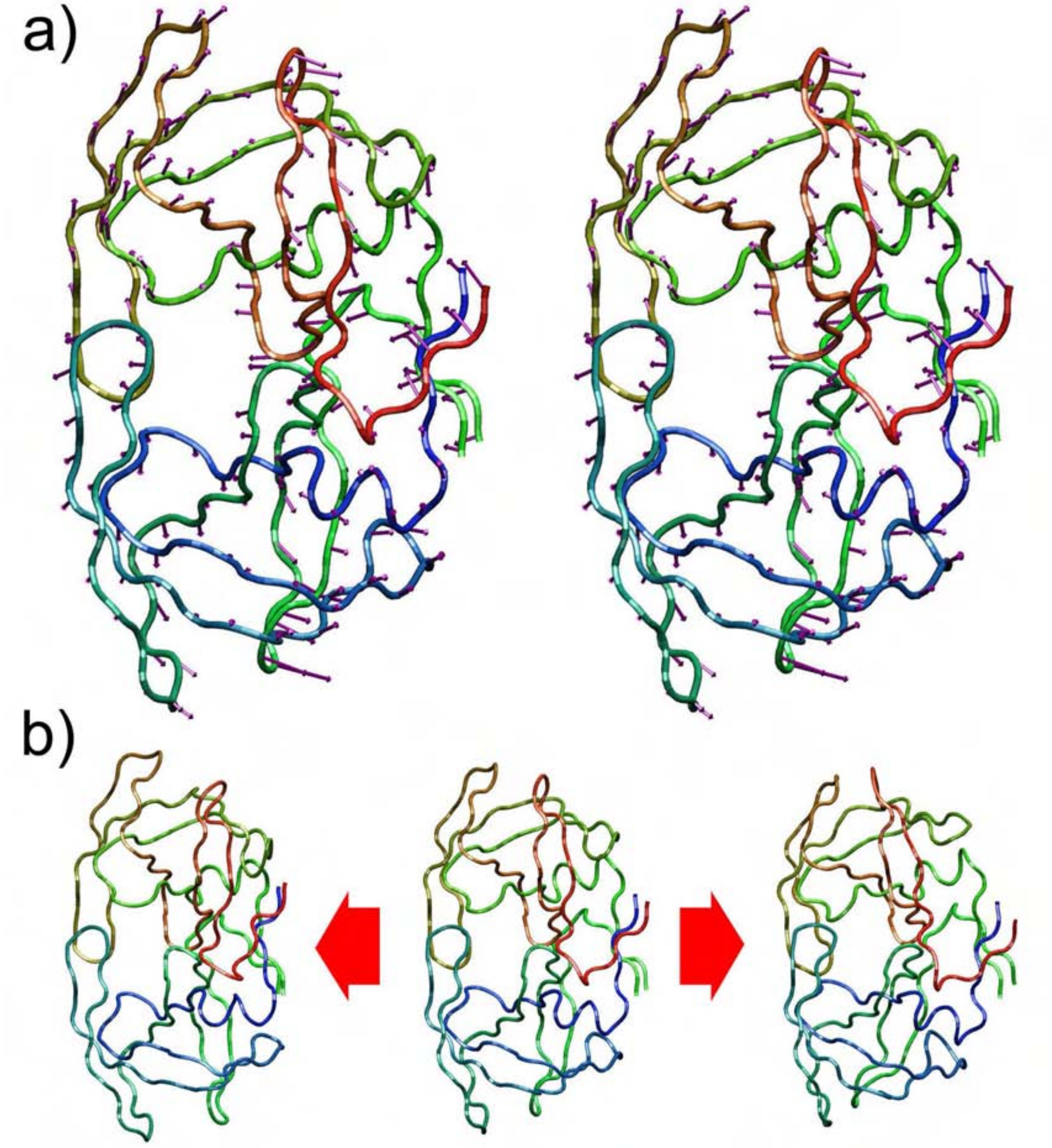

Figure 4.5 - Second mode of motion for the backbone of HIV-1 protease. a) Stereoview of the mapping of the first eigenvector on the C-α atoms. b) Changes in conformation corresponding to a motion in both directions along the second mode of motion starting from the experimental structure (center).

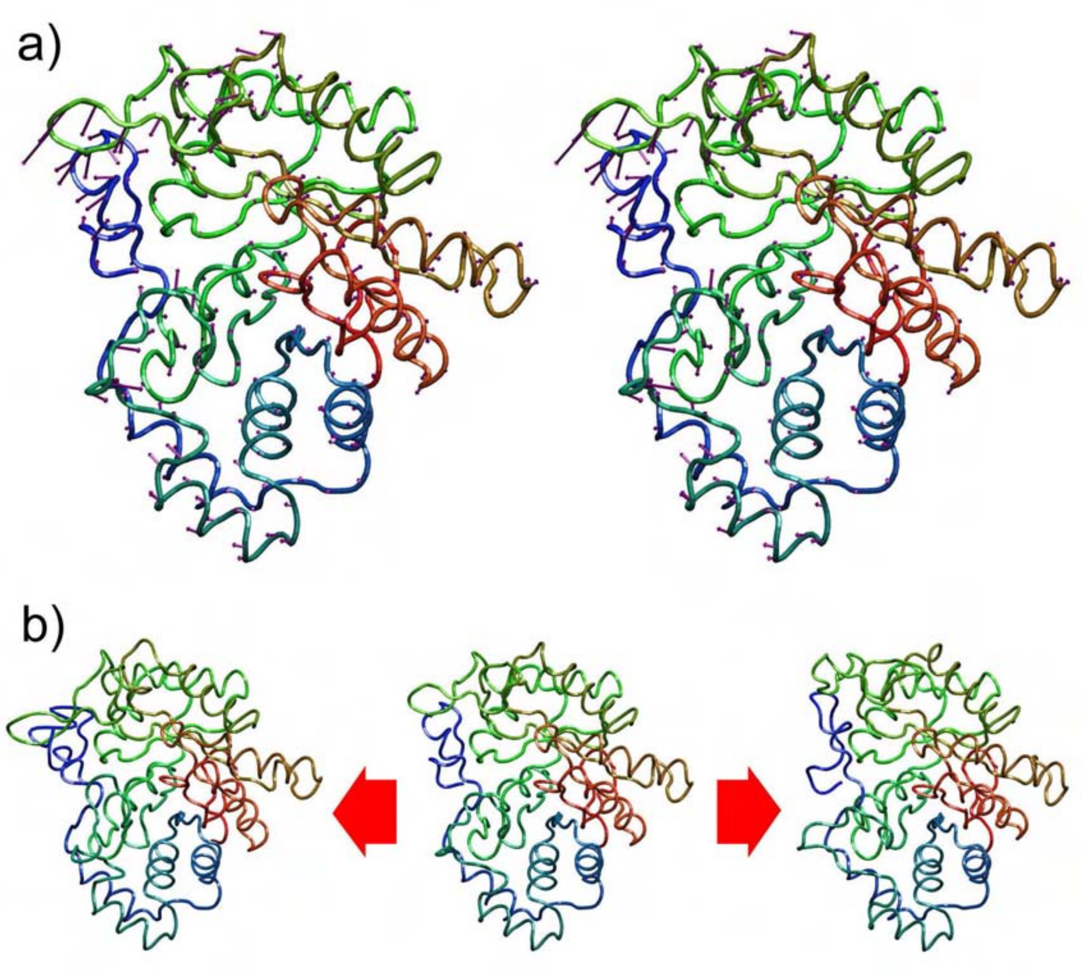

Figure 4.6 - First mode of motion for the backbone of aldose reductase. a) Stereoview of the mapping of the first eigenvector on the C-α atoms. b) Changes in conformation corresponding to a motion in both directions along the first mode of motion starting from the experimental structure (center). Blue arrows indicate the region in the binding site where most of change is observed.

The first mode of motion for aldose reductase is shown in Figure 4.6. As can be observed from the figure, most of the protein is rigid according to the first mode of motion. This is in good accordance with multiple experimental structures available, which shown minimal differences between bound and unbound forms. The regions with larger change as determined by the first mode of motion are indicated by blue arrows in Figure 4.6 – b). These regions include residues 122, 130, 219, 298, 300, 302, and 303. The region constitutes a large portion of the binding site (see also Table 4.1 and Figure 4.1) and is responsible for the opening of the specificity pocket that allows for the binding of larger ligands such as tolrestat and zopolrestat (see also Appendix A and Figure A.4). This is an interesting observation because whereas in the case of HIV-1 protease we had used a bound form as a starting structure for the molecular dynamics, in the case of aldose reductase we used an unbound form. Nevertheless, the PCA analysis was equally capable of capturing conformational rearrangements relevant for the induced fit process. This has important implications for the application of PCA to structure-based drug design methods since it suggests the possibility of obtaining meaningful protein flexibility models independently of the type of structure (bound or unbound) used as a starting model. Often only one is initially available.

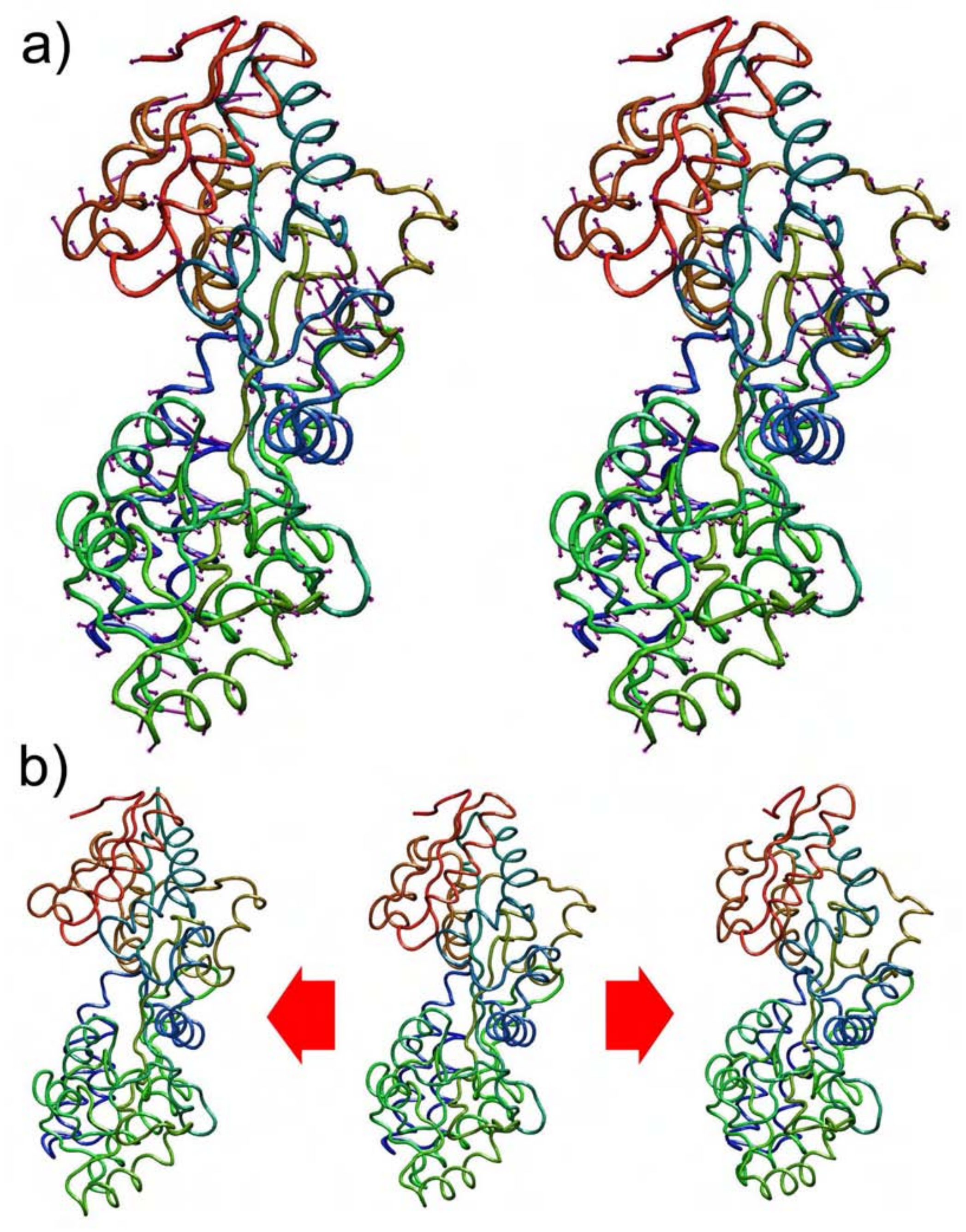

Figure 4.7 - First mode of motion for the backbone of maltose binding protein. a) Stereoview of the mapping of the first eigenvector on the C-α atoms. b) Changes in conformation corresponding to a motion in both directions along the first mode of motion starting from the experimental structure (center).

The first mode of motion for maltose binding protein is shown in Figure 4.7. As can be observed from Figure 4.7 – a) the hinge bending motion that characterizes the conformational transition between the bound and unbound forms of this protein is not clearly observable. Even though there are no intra domain movements in the top and bottom domains (top domain shown mostly in red, yellow, and blue on the top of Figure 4.7 – a) and bottom domain shown mostly in green at the bottom of the figure) which would be indicated by large arrows pointing to mostly different directions within the same domain, there is a clear twisting motion of one domain relative to the other that leads to a moderate opening/closing of the binding site region (see Figure 4.7 – b)). This result was a clear reminder that modes derived from PCA cannot be interpreted by themselves as real modes of protein motion: what they constitute is a reduced dimensional basis for representing motions of proteins. Real protein motion may be a result of the combination of two or more of the PCA modes. As discussed before, one of the main differences between the results of HIV-1 protease and maltose binding protein is the ratio between the first and second eigenvectors. While for HIV-1 protease there is a clear dominance of the first mode in the eigenvalue spectrum, for maltose binding protein there is a much small difference between the first and second modes. As a result, it is important for the case of maltose binding protein to also look at the mode corresponding to the second largest eigenvalue and determine how a combination of the two can result in experimentally observed protein motions. Observation of the second mode of motion revealed a particularly interesting result. The second mode also consists of a twist of one domain relative to the other but in the opposite direction. The motion is equally accompanied by a moderate opening/closing motion about the hinge position near the binding site. The motions are illustrated in Figures 4.8 and 4.9 (note: the figures are stereoviews and should be viewed in portrait mode by looking up and down to give the illusion of motion). The figures are color coded according to the respective collective motion. Red is used for the first mode of motion and blue is used for the second. On Figure 4.8 the motion is for the molecule in red and the blue structure corresponds to the original conformation. On Figure 4.9 the motion is for the molecule in blue using the red conformation as a reference. The first mode corresponds to a counterclockwise rotation of the top domain in relation to the bottom domain (relative dispositions as shown in the figure) around the axis defined by the red arrows. Conversely, the second mode corresponds to a clockwise rotation. Both modes lead to simultaneous opening or closing as they twist in opposite directions. By considering the two modes in conjunction it is possible to obtain an opening and closing of the binding site of maltose binding protein which does not occur in a straight direction but instead takes place in a zigzag motion. Given the results of the PCA analysis this is presently our model for the biologically relevant motion of this protein. Unfortunately, it is not currently possible to experimentally prove or refute this model.

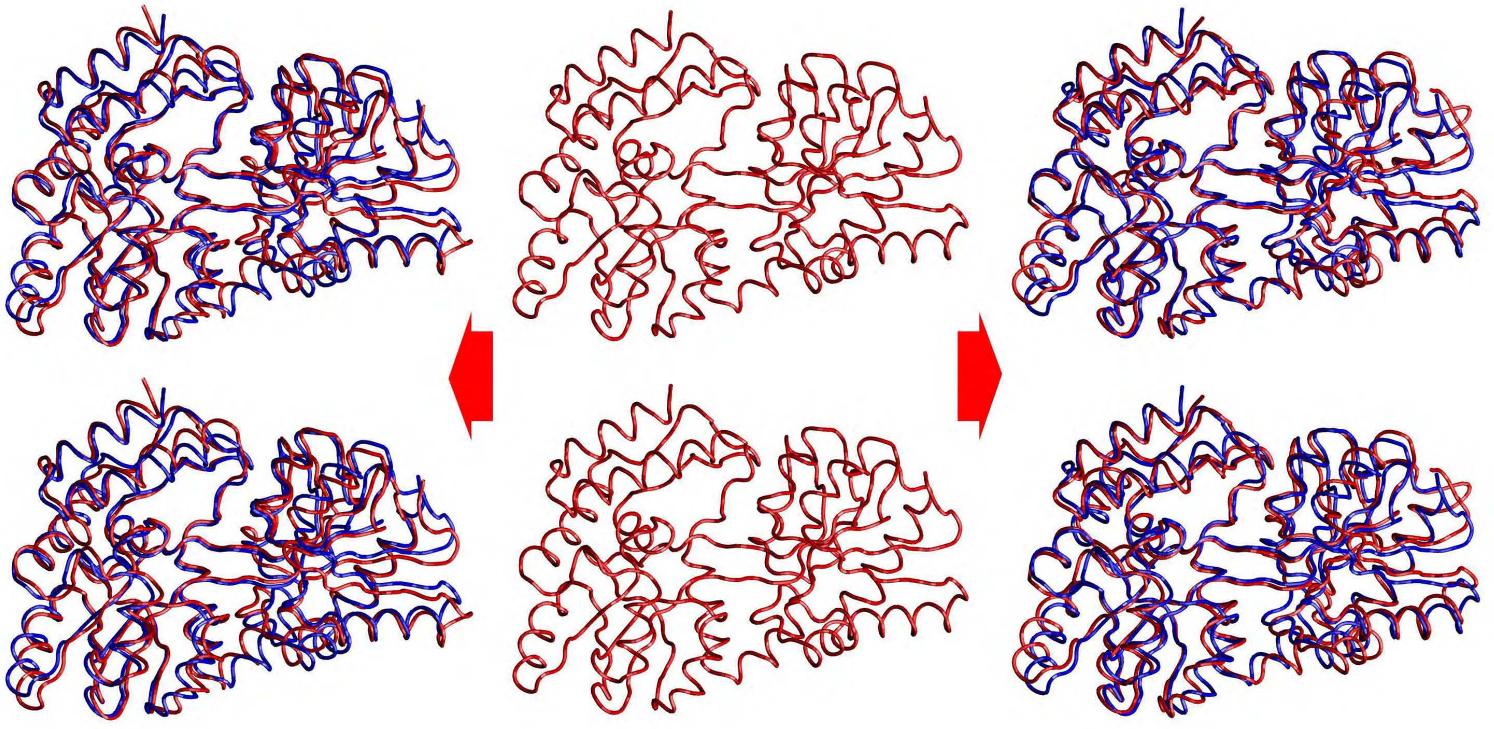

Figure 4.8 – Stereoview of the first mode of motion for the backbone of maltose binding protein. The motion shown is for the red representation. The blue representation is fixed and is used as a reference for visualization of the motion. The figures and should be viewed in portrait mode by looking up and down to give the illusion of motion. The center representation corresponds to the experimental conformation. The top and bottom views represent alternative conformations for the protein as it moves in opposite directions along the first mode of motion.

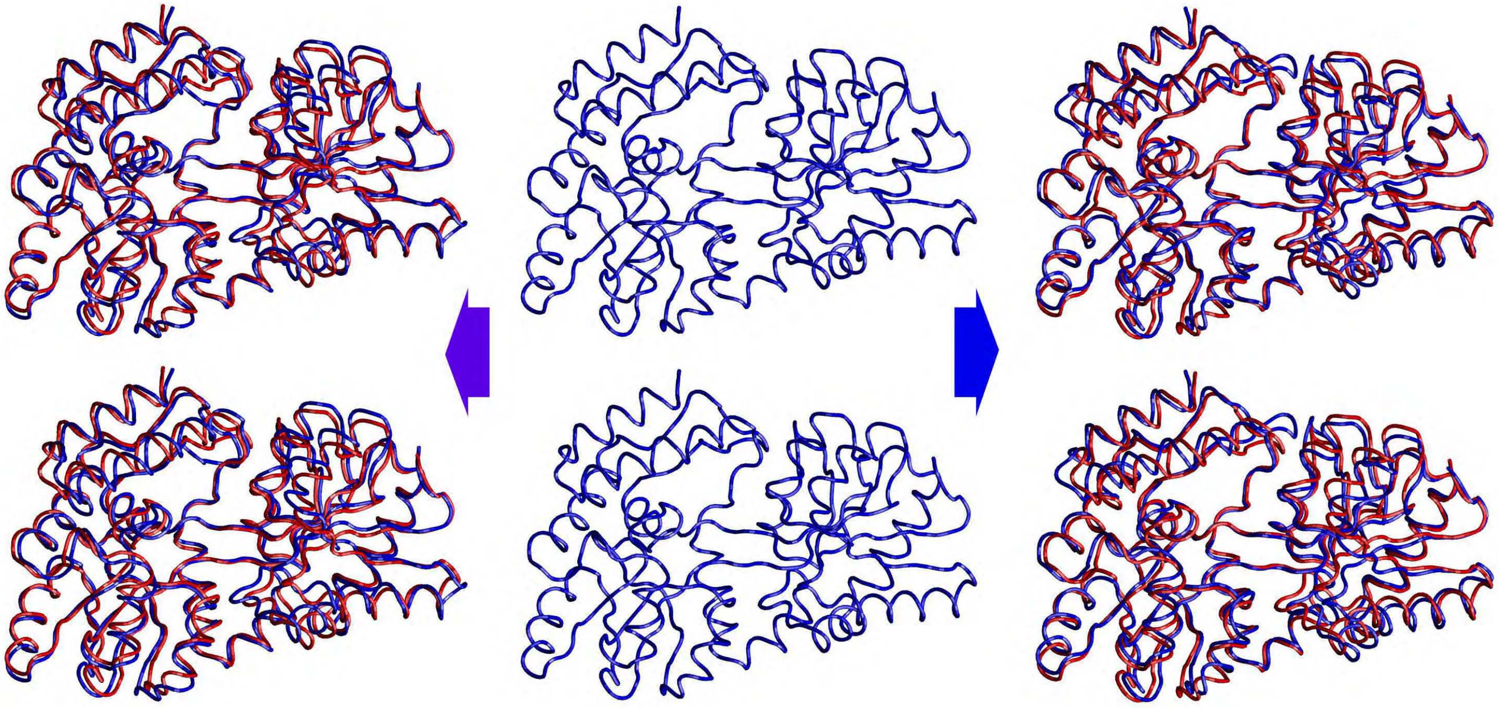

Figure 4.9 -– Stereoview of the second mode of motion for the backbone of maltose binding protein. The motion shown is for the blue representation. The red representation is fixed and is used as a reference for visualization of the motion. The figures and should be viewed in portrait mode by looking up and down to give the illusion of motion. The center representation corresponds to the experimental conformation. The top and bottom views represent alternative conformations for the protein as it moves in opposite directions along the second mode of motion.

Another useful piece of information that can be obtained by carrying out the PCA calculation using the singular value decomposition method is the right singular vectors. The right singular vectors correspond to the reduced coordinate representation in the new basis defined by the left singular vectors. In other words, it is the reduced set of coordinates that represents the original protein motion. For the case of molecular dynamics data, the analysis of this set reveals a set of stable conformational substates that correspond to local energy minima in the conformational energy landscape of the protein. The two and three dimensional plots of the right singular vectors have been previously described as "beads-on-a-string". The beads correspond to low energy regions with long residence times and the string connecting the beads corresponds to fast transitions between metastable substates. For an extensive discussion on the identification and modeling of protein conformational substates see Romo's thesis (Romo 1998).

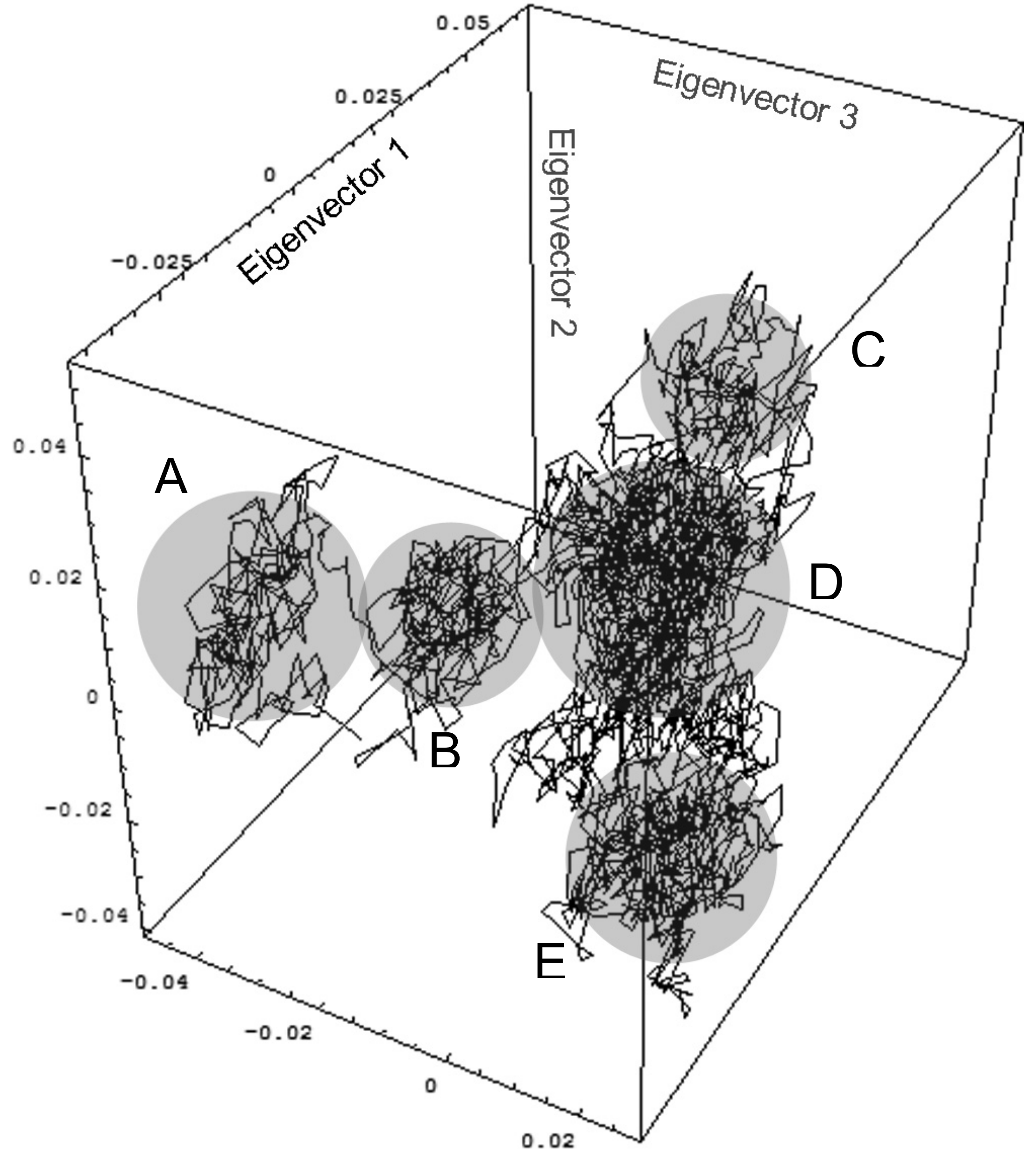

Figure 4.10 – Plot of first three backbone right singular vectors for the 1.4 ns molecular dynamics simulation of HIV-1 protease. These correspond to the projection of the original molecular dynamics trajectory on the three dominant eigenvectors. Protein conformational substates are highlighted using shaded circles and labeled from A to E.

Figure 4.10 shows the plot of first three right singular vectors. These correspond to the projection of the original molecular dynamics trajectory on the three dominant eigenvectors. The plot shows a three dimensional scatter plot in which consecutive points in time are connected by straight lines. In the case of HIV-1 protease 2800 points are plotted in Figure 4.10. As a result each straight line connecting two points corresponds to 5 ps of simulation. It is possible that if we had used a finer time sampling we would observe even more structure in the plots. Such observation would be consistent with the current hierarchical view of ensembles of substates in which each substate can be further divided into another ensemble of substates corresponding to smaller conformational changes. The results show that during the simulation the protein does not change its conformation continuously from the beginning to the end of the simulation but instead jumps between conformational substates. Protein conformational substates are highlighted using shaded circles and labeled from A to E. These correspond to the following approximate time periods: A from 0 ps to 150 ps, B from 150 ps to 325 ps, C from 325 ps to 600 ps, D from 600 ps to 900 ps, and E from 900 ps to 1400 ps. The information obtained from the right singular vectors is also relevant for structure-based drug design because it can hint at certain protein conformations that are more stable in solution and as such should be targeted preferentially in a virtual screening study. This kind of approach allows the use of the power of dimensional reduction methods to include protein flexibility in the drug design process without a large increase in computational expense. This method is going to be explored further in

Chapter 5 when we discuss possible uses of the dimensional reduction methodology in drug design applications.

In order to check if the protein conformational substates correspond in fact to similar backbone conformations we also calculated pairwise backbone RMSD values for the entire trajectory. If this is the case we should see squares of lower RMSD value along the diagonal of the pairwise RMSD matrix. Figure 4.11 shows the backbone RMSD matrix for the 1.4 ns molecular dynamics simulation of HIV-1 protease. The two axes represent 1400 backbone structures sampled every 10 ps. In this plot we can unmistakably verify the existence of the first three conformational substates labeled A, B, and C. The distinctions between substates D and E is not as clearly defined. This reflects the fact than in Figure 4.10, states D and E are close together in the reduced space and there seems to be a lot of interconversion between these. In contrast there is a very clear transition between states A and B with a single path (line) connecting the two states without any interconversion. The comparison of the two plots suggests that analysis of right singular vectors is a better method to identify protein conformational substates.

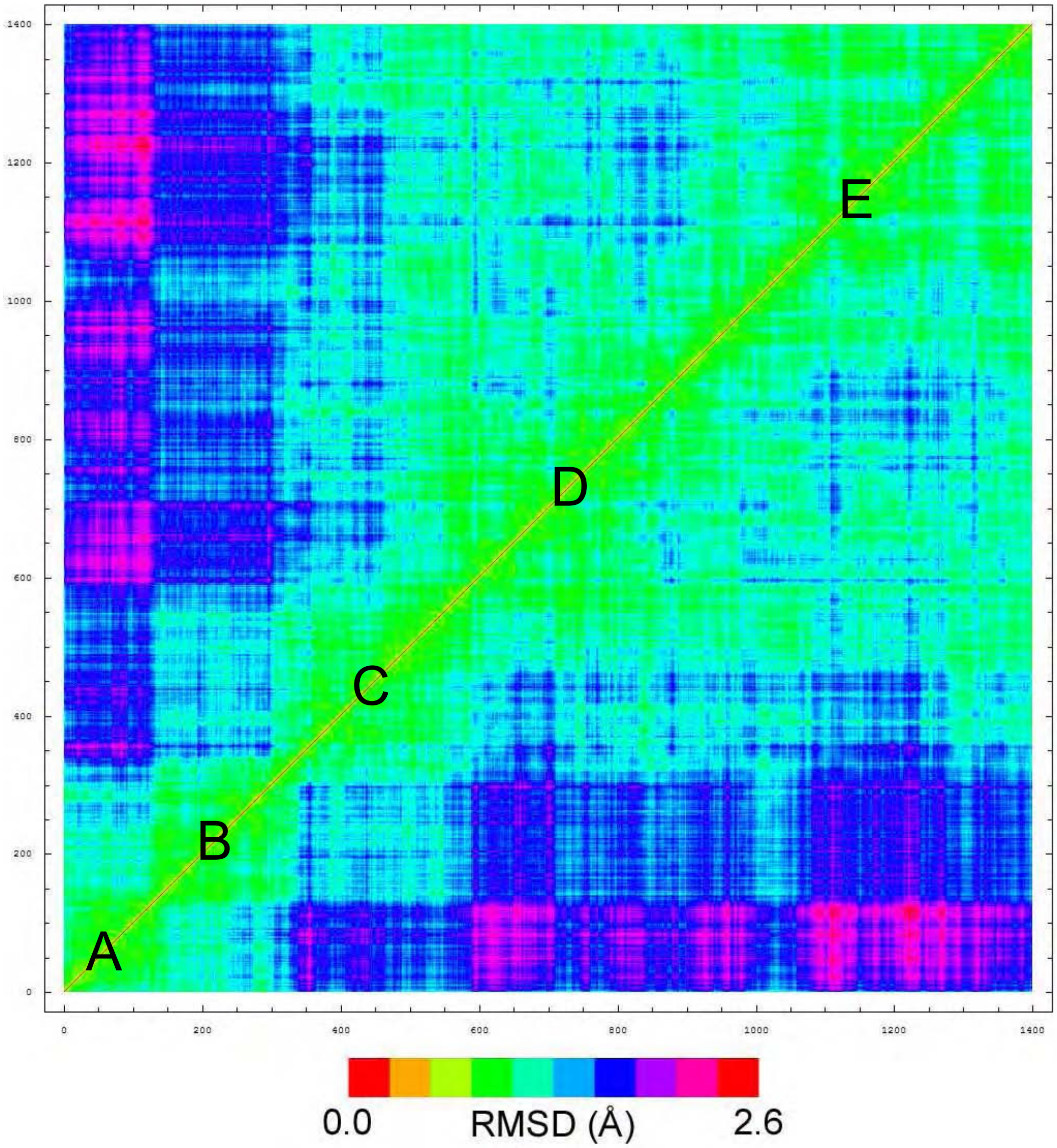

Figure 4.11 – Backbone RMSD matrix for the 1.4 ns molecular dynamics simulation of HIV-1 protease. The two axis represent 1400 backbone structures sampled every 10 ps. The RMSD value between two structures is represented off the diagonal at the intersection of the respective indices (note: the data on the two side of the diagonal is identical). Protein conformational substates identified using Figure 4.10 are labeled from A to E.

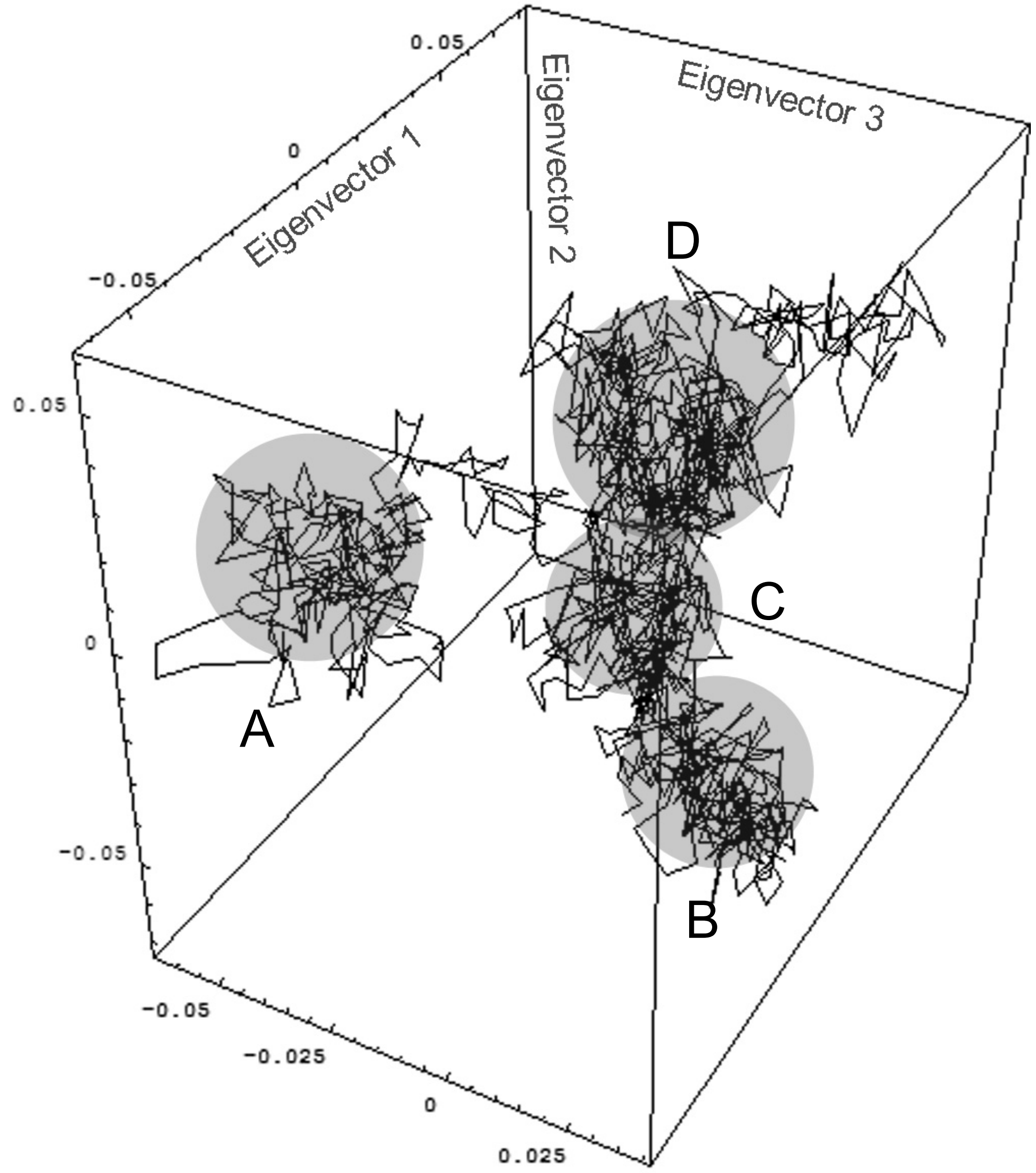

Figure 4.12 - Plot of first three backbone right singular vectors for the 1.0 ns molecular dynamics simulation of aldose reductase. These correspond to the projection of the original molecular dynamics trajectory on the three dominant eigenvectors. Protein conformational substates are highlighted using shaded circles and labeled from A to D.

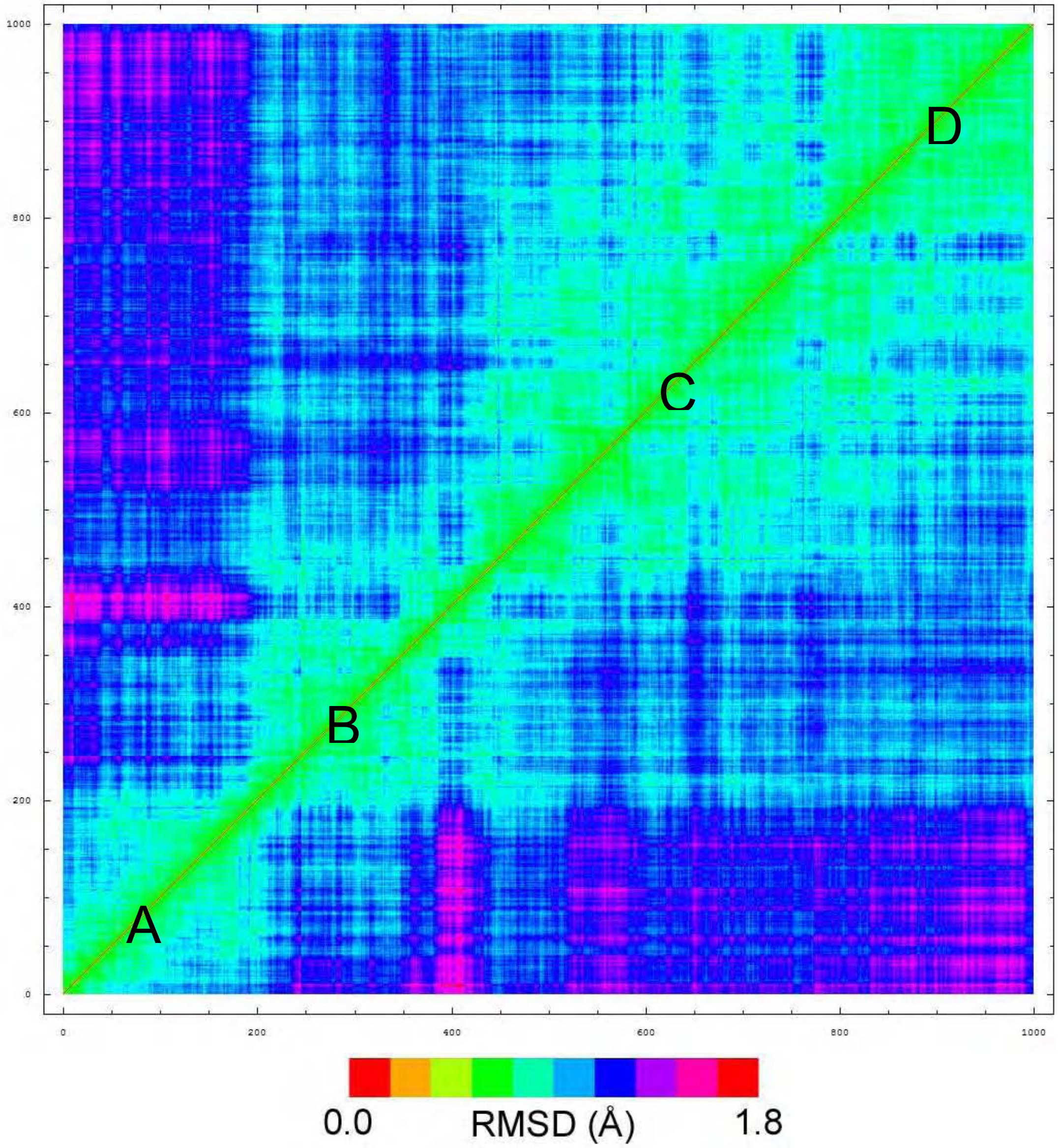

Figure 4.13 - Backbone RMSD matrix for the 1.0 ns molecular dynamics simulation of aldose reductase. The two axis represent 1000 backbone structures sampled every 10 ps. The RMSD value between two structures is represented off the diagonal at the intersection of the respective indices (note: the data on the two side of the diagonal is identical). Protein conformational substates identified using Figure 4.12 are labeled from A to D.

Figure 4.12 shows the three main right singular vectors for the aldose reductase trajectory. In this figure we can see a clearly isolated substate A that later migrates to state B, which is much closer to the following states C and D. The same kind of behavior can also be observed from Figure 4.13 where the conformations in state A are markedly different from the three following substates. An alternative interpretation for this result is to use the hierarchical model and consider only two substates X and Y. X would be composed only of the state A, and Y could be further decomposed in states B, C and D.

Figure 4.14 shows the three main right singular vectors for the maltose binding protein trajectory. The plot visibly isolates three conformational substates labeled A to C. However, when we compare this data to the pairwise RMSD plots in Figure 4.15 these substates cannot be readily identified. This is a case where the right singular vectors are clearly more powerful in the identification of conformational substates.

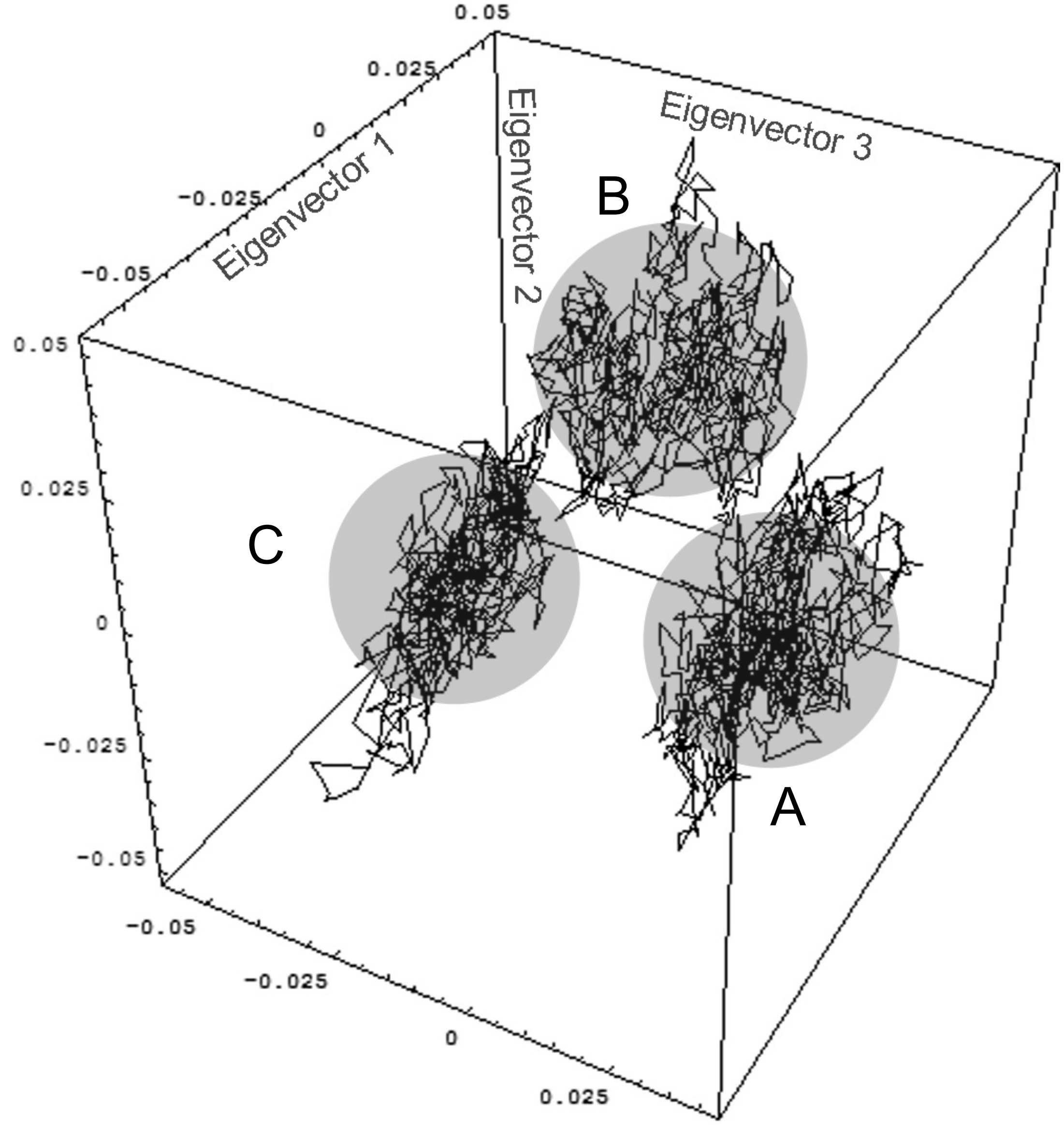

Figure 4.14 - Plot of first three backbone right singular vectors for the 1.6 ns molecular dynamics simulation of maltose binding protein. These correspond to the projection of the original molecular dynamics trajectory on the three dominant eigenvectors. Protein conformational substates are highlighted using shaded circles and labeled from A to C.

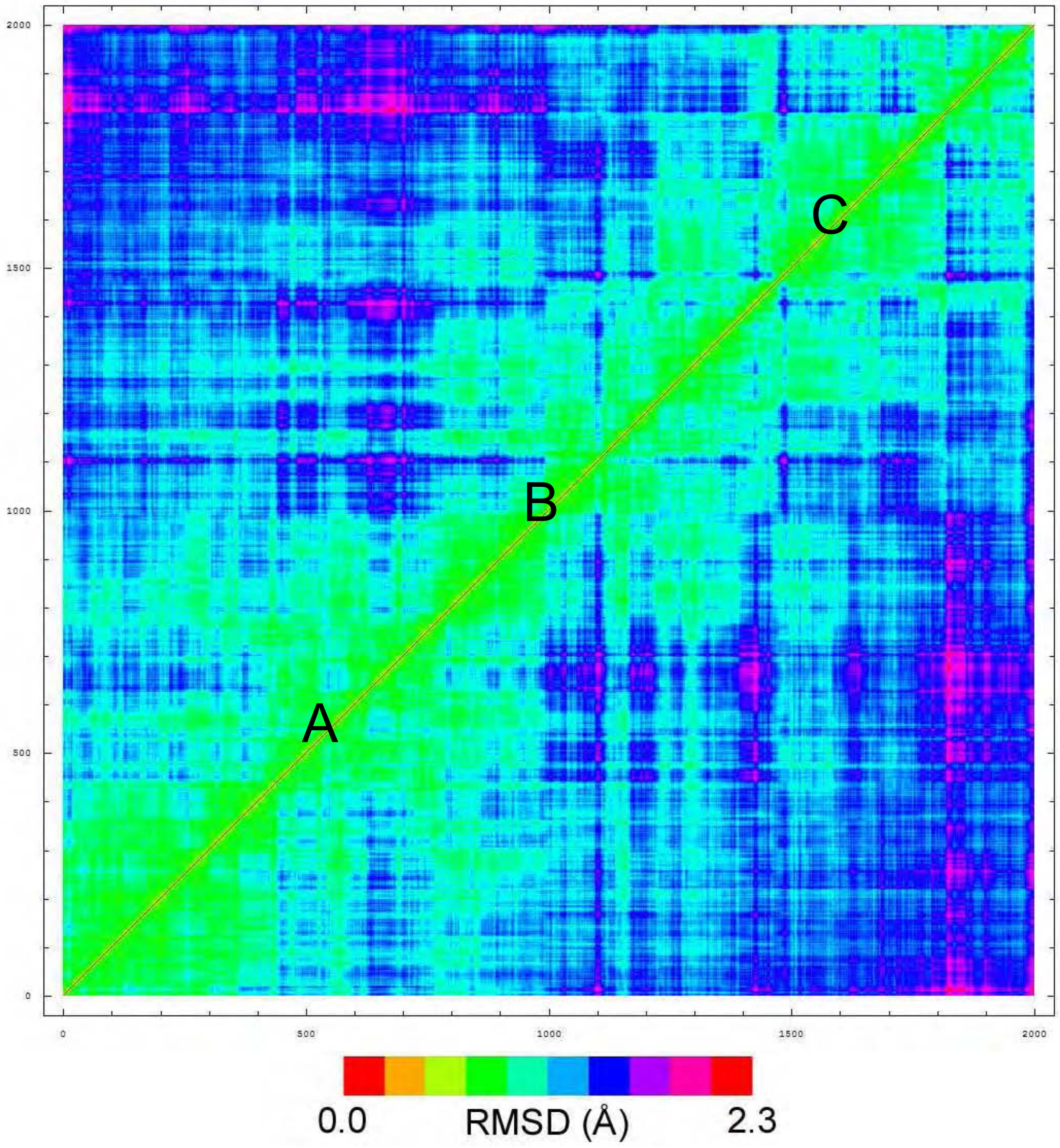

Figure 4.15 - Backbone RMSD matrix for the 1.6 ns molecular dynamics simulation of maltose binding protein. The two axis represent 2000 backbone structures sampled every 8 ps. The RMSD value between two structures is represented off the diagonal at the intersection of the respective indices (note: the data on the two side of the diagonal is identical). Protein conformational substates identified using Figure 4.14 are labeled from A to C.

4.4.3. Binding Site PCA

Changes at the level of the binding site are the most critical in determining the binding of a ligand to the receptor protein. In this section we focused the dimensional reduction analysis on the residues that constitute the binding site (see Figure 4.1). The main advantage from a structure-based drug design point of view in considering only the binding site atoms in the PCA calculation is to avoid the inclusion of motions that are not relevant for ligand binding in the main modes of motion. If non-relevant atomic motions were sufficiently large and well correlated they would mask the results pertinent to induced fit effects at the level of the binding site. This problem will be addressed in more detail in Chapter 5. A second advantage of using only binding site atoms to calculate collective modes of motion for the protein is that, as in the case for the backbone analysis, the initial dimension of the problem is already reduced. If we consider the Cartesian degrees of freedom for each atom in the binding site, the initial number of degrees of freedom is 750 for HIV-1 protease, 426 for aldose reductase, and 426 for maltose binding protein.

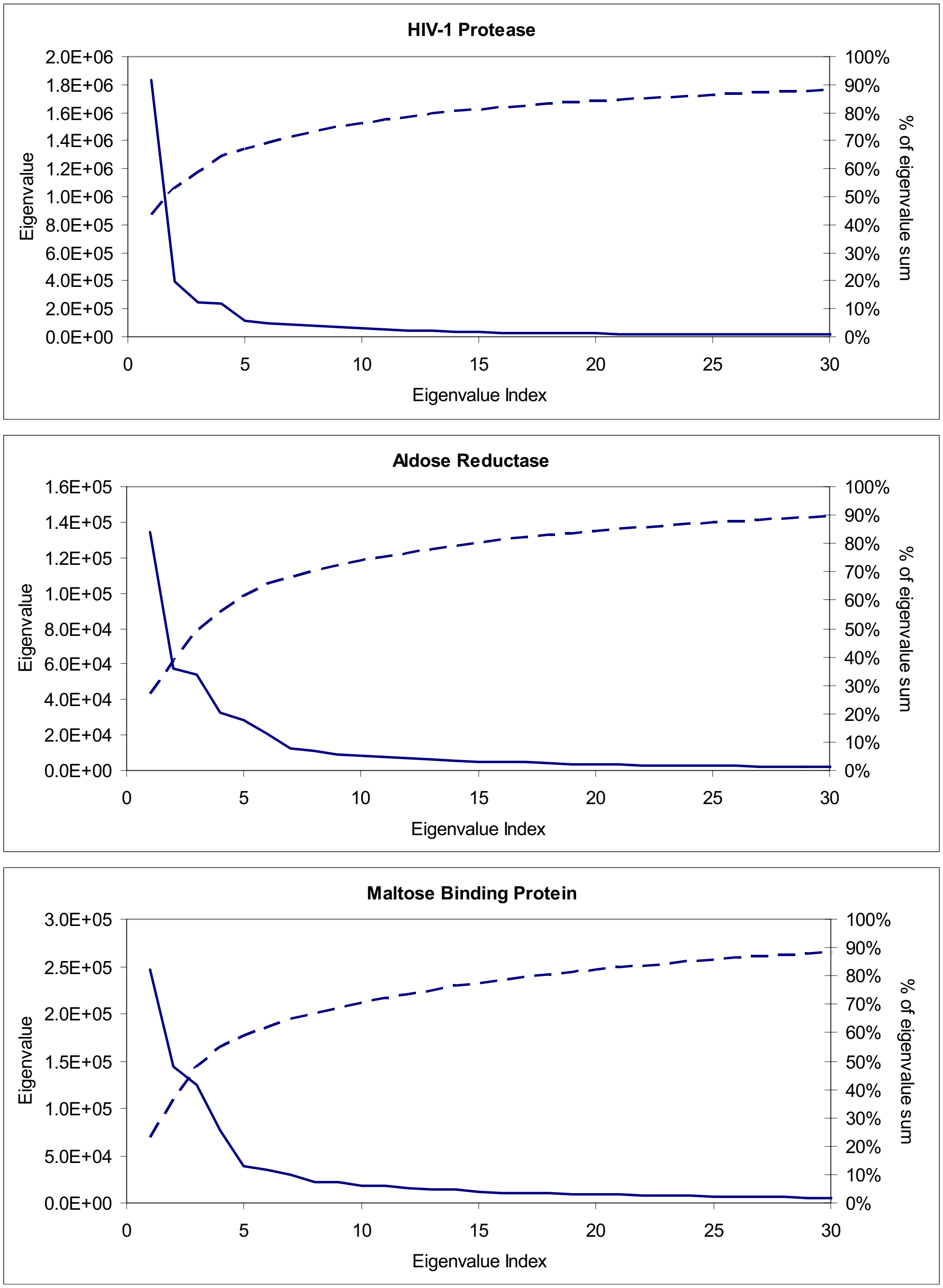

Figure 4.16 - Eigenvalues (continuous line) and percentage of eigenvalue sum (broken line) for the binding site PCA analysis of the molecular dynamics trajectories.

The eigenvalues and eigenvalue sums for the binding site PCA analysis of the three protein models are shown in Figure 4.16. As in the case of the backbone analysis, all the proteins in this study displayed a significant eigenvalue drop with the first few eigenvalues accounting for most of the eigenvalue sum. For the case of HIV-1 protease the first, second, and third eigenvalues account for 43.6%, 53.0%, and 58.9% of the eigenvalue sum. For the case of aldose reductase the first, second, and third eigenvalues account for 27.0%, 38.6%, and 49.4%. The same numbers for maltose binding protein are 23.0%, 36.4%, and 47.9%, respectively. In comparison with the backbone analysis there is now a greater dominance of the main eigenvectors for the cases of HIV-1 protease and aldose reductase. The values for maltose binding protein are very similar to the ones obtained for the binding site analysis. The larger change in results is for the first two proteins because the changes on these proteins were mostly in the binding site region. The changes for maltose binding protein are mainly a reorientation of domains. In this case, the largest atomic displacements are far from the binding site region.

For the case of the binding site analysis, the right singular vectors can indicate binding site conformations that are stable and should be used as target receptors in drug design applications. In comparison with the right singular vectors obtained for the backbone analysis, the ones derived from the binding site should display a cleaner structure, which is easier to interpret. Figure 4.17 to 4.19 show the right singular vector plots for the three proteins. The results for HIV-1 protease shown in Figure 4.17 are comparable to the results shown in Figure 4.10. The first two conformational substates A and B are common to both backbone and binding site analysis. Conformational substate C includes the backbone conformational substates C, D, and E. This indicates that the changes that determined the transitions between these substates are not determined by changes in the binding site. The results for aldose reductase shown in Figure 4.18 are comparable to the results shown in Figure 4.12 and are similar to the results obtained with HIV-1 protease. In this case there are only two major conformational substates A and B. Conformational substate B corresponds to merging states B, C, and D. The results for maltose binding protein shown in Figure 4.19 also show three conformational substates as in Figure 4.14. However the residence time in state B is shorter than in the case of the backbone analysis.

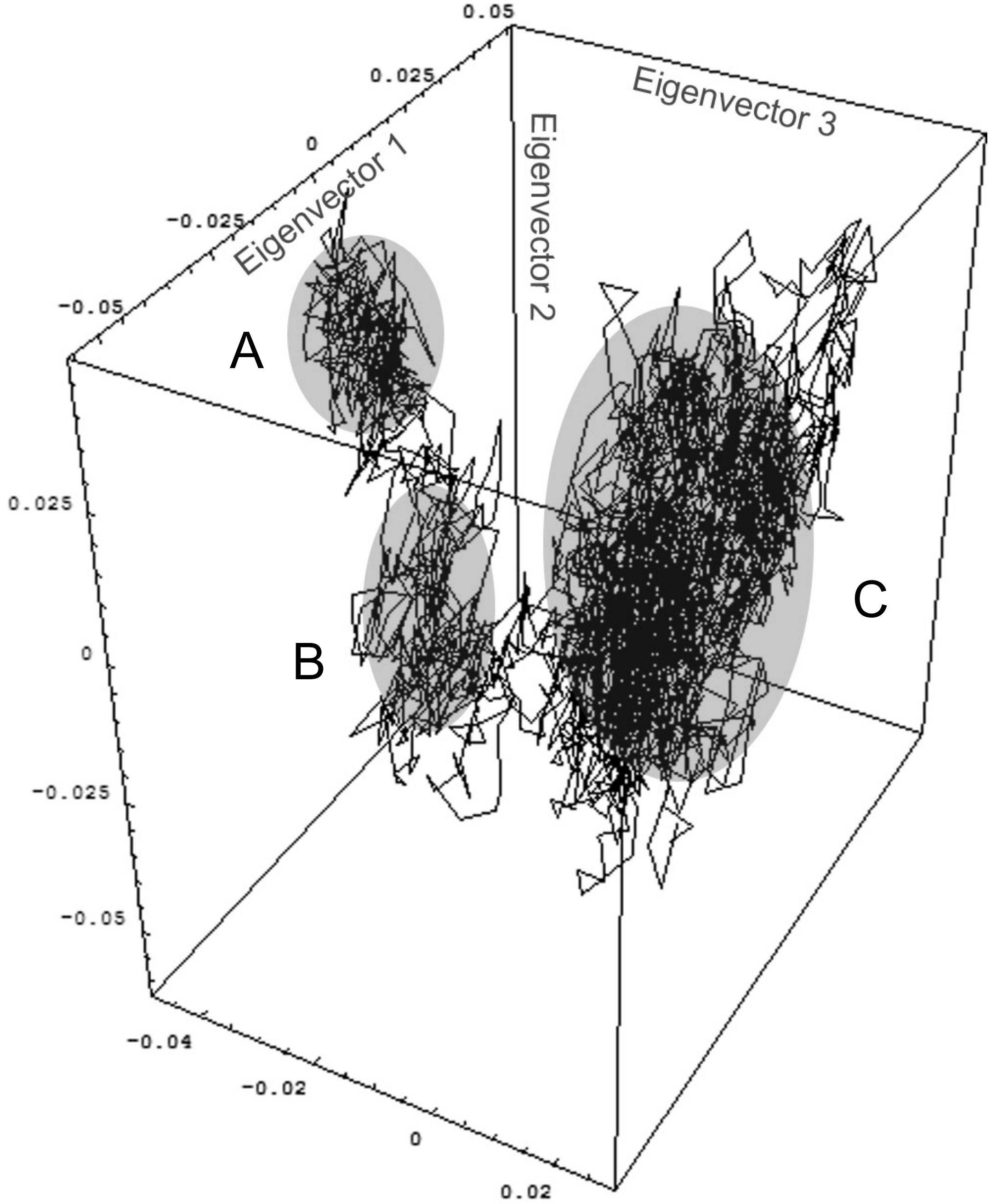

Figure 4.17 - Plot of first three binding site right singular vectors for the 1.4 ns molecular dynamics simulation of HIV-1 protease. These correspond to the projection of the original molecular dynamics trajectory on the three dominant eigenvectors. Protein conformational substates are highlighted using shaded circles and labeled from A to C.

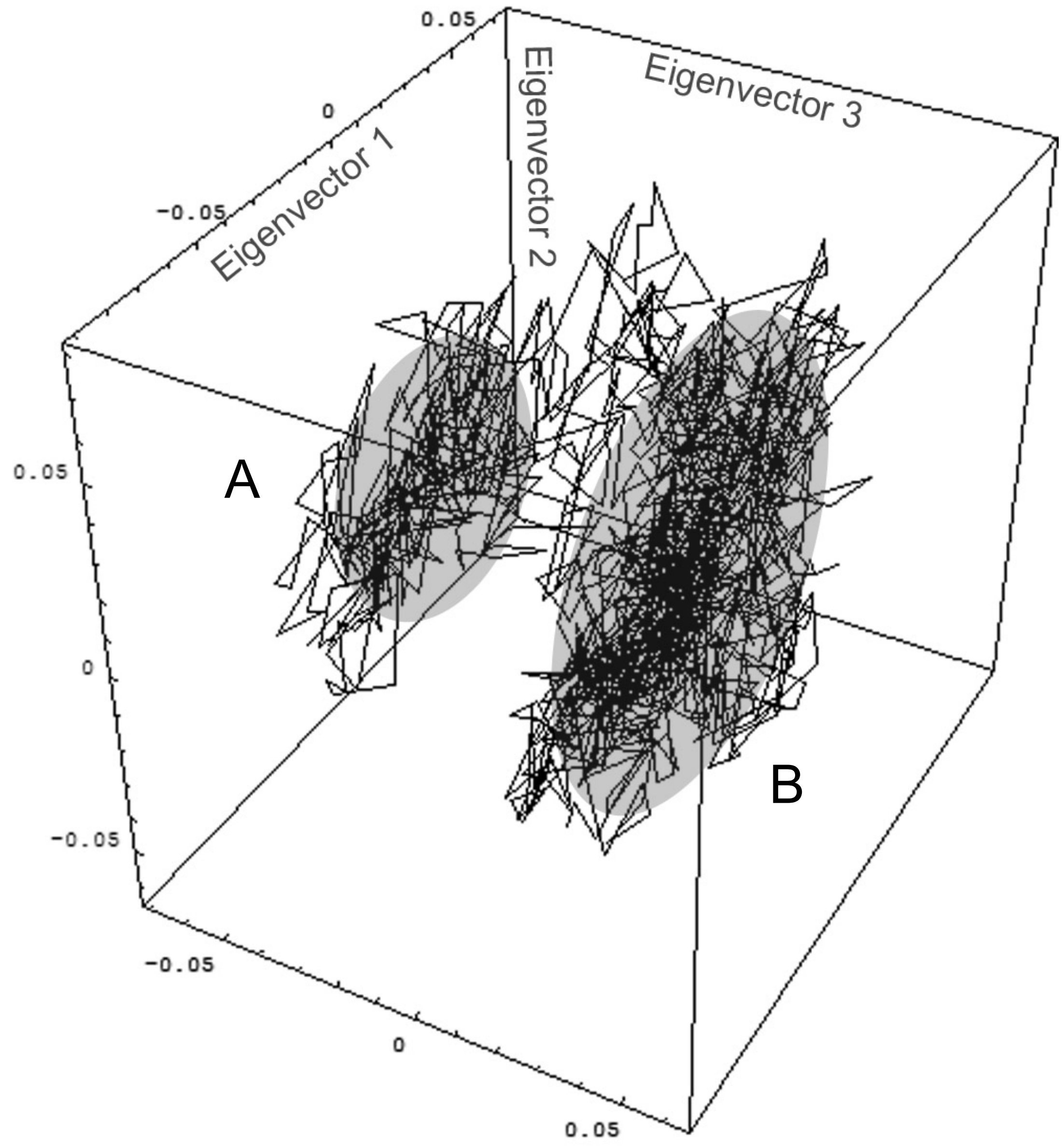

Figure 4.18 - Plot of first three binding site right singular vectors for the 1.0 ns molecular dynamics simulation of aldose reductase. These correspond to the projection of the original molecular dynamics trajectory on the three dominant eigenvectors. Protein conformational substates are highlighted using shaded circles and labeled A and B.

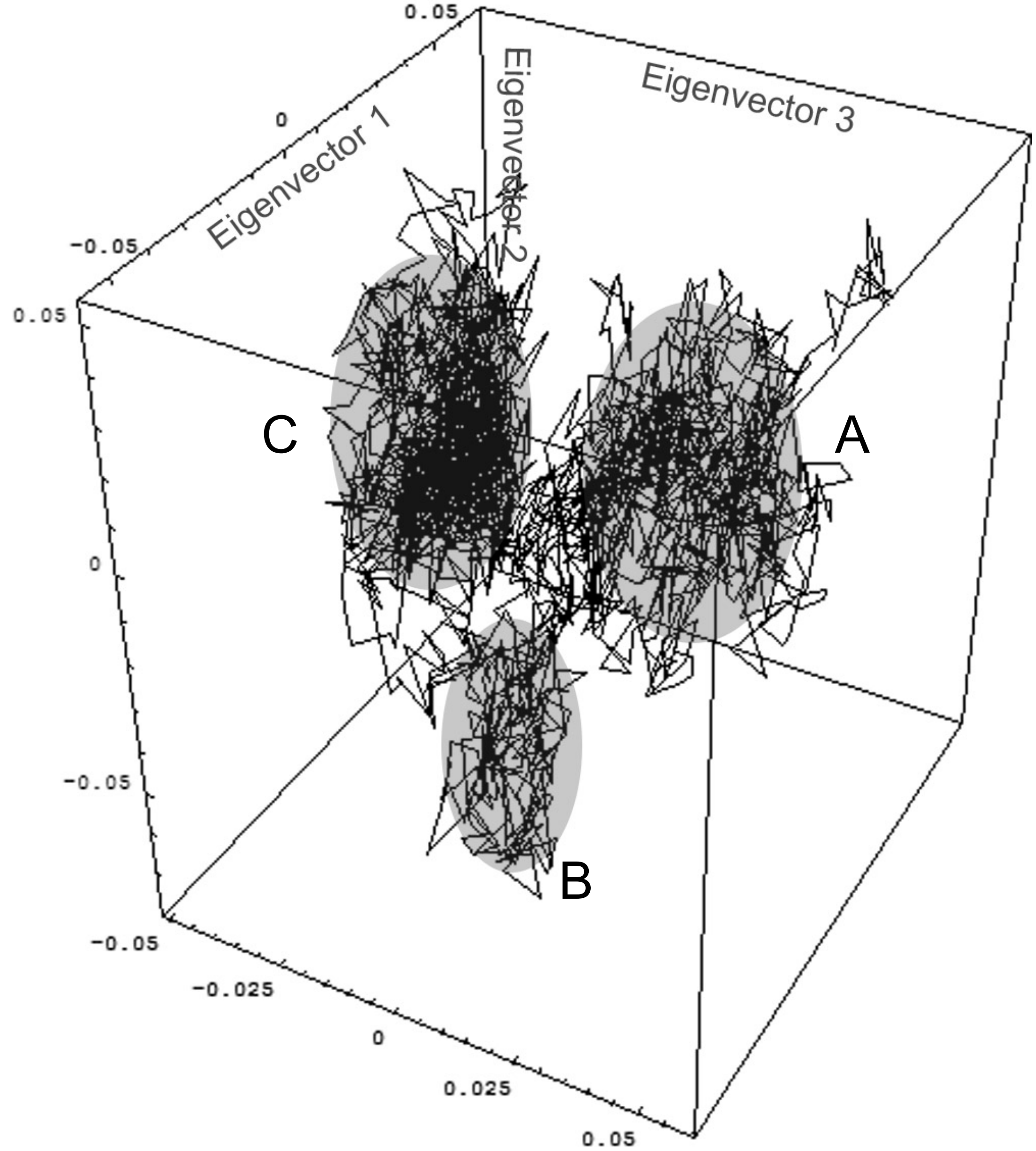

Figure 4.19 - Plot of first three binding site right singular vectors for the 1.6 ns molecular dynamics simulation of maltose binding protein. These correspond to the projection of the original molecular dynamics trajectory on the three dominant eigenvectors. Protein conformational substates are highlighted using shaded circles and labeled from A to C.

4.4.4. All-Atoms PCA

The final level of detail we tested using the PCA method was to include all the atoms in the protein in the calculation. Due to the increase computational requirements for this computation it was carried out only for HIV-1 protease. The computation of the PCA for all atoms of HIV-1 protease has the following memory requirements. The initial data consists of 14,000 data points for 9360 degrees of freedom. Each data point is a single precision floating point number (4 bytes on a 32 bit machine). As a result the initial data occupies approximately 500 MB (megabyte). This data is used for the computation of the covariance matrix of size 9360 by 9360. In order to increase numerical stability, the covariance matrix is computed using double precision floating point numbers (8 bytes on a 32 bit machine). The covariance matrix has size approximately 670 MB. Due to bad memory management, the program *Mathematica* uses approximately four times more memory than what is theoretically required. As a result, the all-atoms PCA computation is not practical using this program because we did not have access to a computer with the required specifications. The use of swap space on hard disk to increase the available virtual memory is also not practical due to the very high latency of accessing the data from hard disk when compared to physical memory or CPU cache. Although using swap space as an alternative solution is possible, it increases the computation time by approximately two orders of magnitude. By reason of the limitations described above we developed the program *svd* that can efficiently manage memory and carry out the above computation on machines with approximately 1 GB (gigabye) of memory. The program is also capable of adapting to smaller physical memory sizes by carrying out matrix computations, such as vector/vector multiplications, in blocks.

The eigenvalues and eigenvalue sums for the all-atoms PCA analysis of the HIV-1 protease is shown in Figure 4.20. As in the case of the backbone and binding site analyses, we observed a significant eigenvalue drop, with the first few eigenvalues accounting for most of the eigenvalue sum. The first, second, and third eigenvalues account for 19.4%, 29.0%, and 36.2% of the eigenvalue sum. The numbers are smaller than for the cases of the backbone and binding site analyses but the total number of degrees of freedom is also much larger (9360 versus 1782 and 750, respectively). Based on visual inspection, the first mode of motion determined for all-atoms is similar to the one calculated for the backbone (result not shown). The motion also corresponds to an opening/closing of the binding site but with extra information regarding aminoacid sidechain positions.

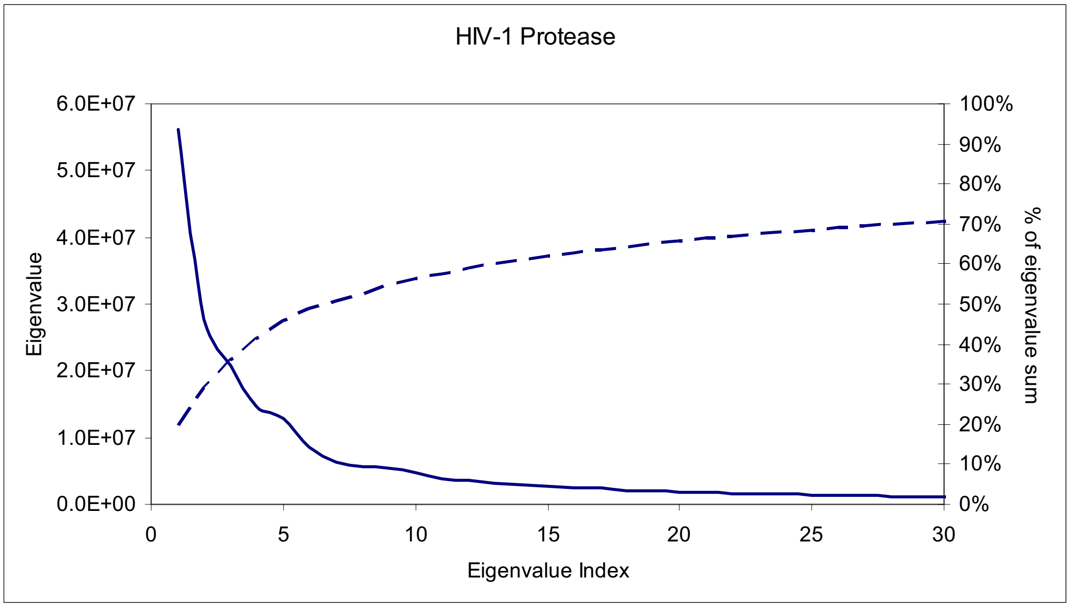

Figure 4.20 - Eigenvalues (continuous line) and percentage of eigenvalue sum (broken line) for the all-atom PCA analysis of the molecular dynamics trajectory for HIV-1 protease.

4.4.5. PCA analysis of experimental structures

In order to validate the results obtained from the PCA analysis of the molecular dynamics data we performed the same type of mathematical analysis for the experimental data obtained using X-ray crystallography. Comparisons done between traditional molecular simulations and experimental techniques (Clarage, Romo et al. 1995; Philippopoulos and Lim 1999) seem to indicate that X-ray crystallography and NMR structures provide better coverage of conformational spaces. As such modes derived using experimental data should also provide a better representation of protein flexibility. Unfortunately, the PCA analysis requires the availability of a large number of conformations in order to calculate accurate correlation coefficients between the initial degrees of freedom of the protein system. The use of experimental data for the purposes of dimensional reduction is therefore limited to a handful of protein systems for which there is a large number of experimentally derived structures available. Although of limited applicability, this test allows a comparison of the results based on computational data to results based purely on experimental data. For this purpose we superimposed 134 structures of HIV-1 protease to the structure determined by Miller *et al* (Miller, Schneider et al. 1989) (see Apendix B. for full list of structures) and extracted the relevant backbone coordinate information to construct matrix A (see section 4.3.3). The results obtained for the eigenvalue spectrum are similar to those obtained when computationally derived data was used (see Figure 4.3). The first 3 and first 20 eigenvalues account for 59% and 85% of the total eigenvalue sum, respectively. These values are slightly higher than for the backbone analysis of the molecular dynamics data. The increased dominance of the main modes of motion is probably related to the increased conformational space that is sampled in the available experimental structures bound to different ligands versus to the simulation of the protein without any ligand bound. The main modes of motion were analyzed by visual inspection and as expected consisted of collective motions that resulted mainly in changes in the binding pocket.

During the course of this experiment we observed an interesting result. When the original protein coordinates were projected on the plane defined by the two dominant eigenvectors we observed that the right singular vectors clustered mainly in three locations (see Figure 4.21). Our initial hypothesis for this observation was the fact that these corresponded to different crystallographic space groups. Out of the 135 experimental structures used for this study there are 18 in $P2_1$, 12 in $P2_12_12$, 81 in $P2_12_12_1$, 21 in $P6_1$, and 3 in $P6_122$ space groups. All unit cells for each of the space groups have approximately the same dimensions. However, the differences in crystallization space groups did not correlate with the observed clustering in the essential subspace. The clustering appears to be the result of different binding modes to different drug classes. This constitutes a positive result because it shows that, at least for the case of HIV-1 protease, differences resulting from different crystal packings do not have a determinant effect on the results of PCA.

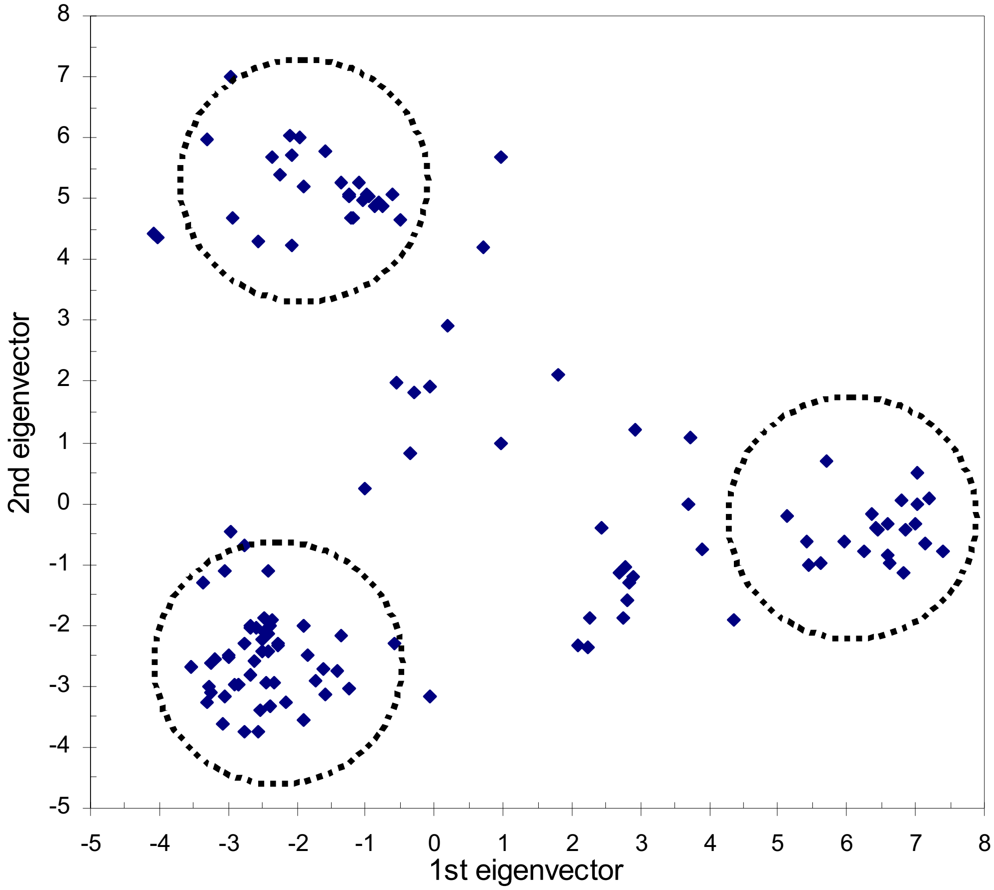

Figure 4.21 - Projection of coordinate vectors of 135 experimental HIV-1 protease structures on the plane defined by the two dominant eigenvectors of the PCA. The circles indicate clustering of structures in the essential subspace.

Although the type of procedure described above using experimental data exclusively is more representative of the conformational flexibility of the model protein when binding to inhibitors of different shapes, it also has several shortcomings. The most important limitation of this approach is that for almost all systems for which determining the main modes of protein flexibility would be beneficial there is not enough experimental data to calculate an accurate correlation matrix. Due to its clinical importance HIV-1 protease is currently a unique case of having a large number of experimentally determined structures. Nevertheless, even the use of 135 experimental structures is likely to introduce a large error. This problem has been analyzed by Genest (Genest 1999) who observed that accurate correlation results could be obtained by using approximately 2000 experimental points for 20 atoms. When the number of experimental samples decreased, the number of false correlations observed increased. In this calculation I used a higher number of atoms (198) and a smaller number of experimental points (135). This is also likely to lead to the observation of correlations that are not present in reality. A second limitation of using experimental data is that we are biasing the conformational space sampled by the main modes of motion to reflect only the binding modes that were already determined experimentally. If for example there is a new binding mode corresponding to a novel class of drugs, the calculated modes of flexibility would likely be of little help in discovering it in an hypothetical flexible-protein / flexible-ligand database screening process. A possible method of testing for errors in our experimental modes would be to a priori exclude part of our experimental data from the dimensional reduction calculations and later check how well the excluded data could be reproduced using the calculated modes of motion. The main limitation to this test is again the reduced number of data available for the calculation of the covariance matrix.

In order to determine the similarity between the modes of motion derived from molecular dynamics data and the modes derived from experimental data we calculated the overlap between the subspaces defined by the most significant principal components. Overlap between two subspaces is calculated as the sum of all of the squared inner products between all pairs of eigenvectors from both essential subspaces, divided by the dimension of that space. When these projections are close to 1.0 for all the eigenvectors of the subspace, the subspaces spanned by the two sets of eigenvectors are the same. However, even if two subspaces are very similar it may happen that two or more eigenvectors in one set are interchanged with respect to the other set resulting in values lower than 1.0. In Figure 4.22 we show the cumulative inner products from the projection of the molecular dynamics eigenvectors onto the first three eigenvectors derived from experimental data. The eigenvectors for both structural sets were calculated using C-α data exclusively. As can be observed from the plot there is a significant amount of overlap between the subspaces defined by the most significant principal components. This result was also confirmed by visual inspection which revealed similar motions for the first mode of motion. The results of this plot are similar to what was previously observed for other proteins (van Aalten, Conn et al. 1997). In this study, the authors compared the collective modes of motion derived from X-ray crystallography experimental structures for eight different proteins. The results showed significant overlap between the subspaces defined by the most significant principal components. Differences between the modes derived by the different methods are probably due to the following factors: 1) Incomplete sampling from the molecular dynamics simulation (Clarage, Romo et al. 1995); 2) different protein environments (solution vs. crystal); 3) insufficient number of structures used in the calculation of the covariance matrix for the X-ray case; 4) limited variability in the ensemble of crystal structures.

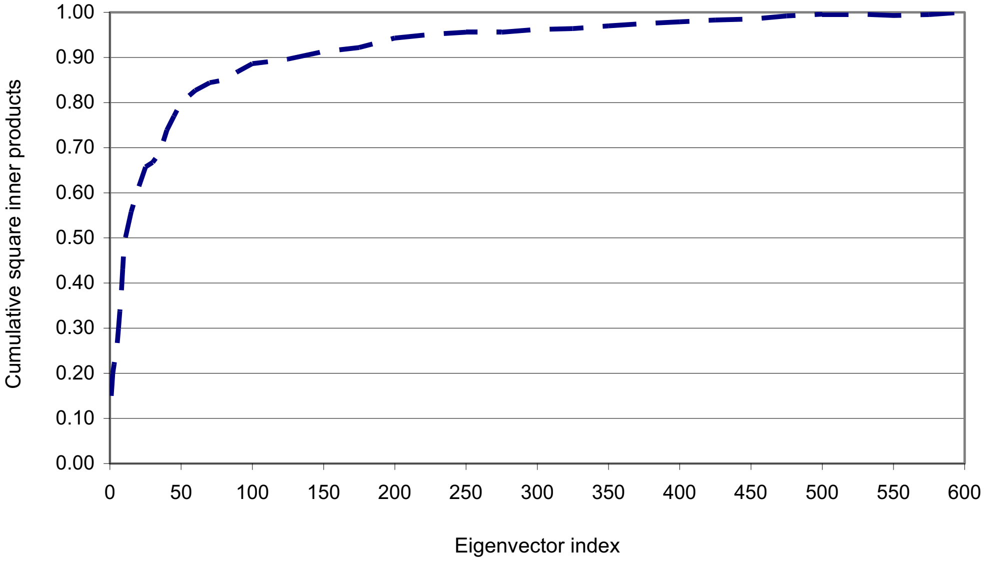

Figure 4.22 - Cumulative inner products from the projection of the molecular dynamics eigenvectors onto the first three eigenvectors derived from experimental data for HIV-1 protease.

Finally, we compared how the modes derived from molecular dynamics data represented the original molecular dynamics data from which they were derived versus the experimentally determined structures. This evaluation was carried out by comparing how much the right singular vectors deviated from a normal distribution. If the modes are a good representation for the data the most significant right singular vectors should have a large deviation from a normal distribution whereas the least significant should be normally distributed with a very small deviation from the mean. The right singular vectors representative of the molecular dynamics data were calculated using the PCA method as described previously and the right singular vectors for the experimental data were determined by calculating the projection of the coordinate vectors of 135 experimentally determined structures on the left singular vectors from the molecular dynamics backbone PCA. The metric used for comparison was the average deviation from the mean. The results for the first 1000 modes are shown in Figure 4.23. The plots show that the average deviation from the mean for the main modes is much larger for the molecular dynamics data than for the experimental data. For the first mode this value is 20.51 for the molecular dynamics data versus 3.15 for the experimental data. The plot for the experimental data shows a decay for the average deviation which would not happen for a random basis, indicating that there is relevant information for HIV-1 protease motion that can be extracted from molecular dynamics data. A more detailed view of these results can be obtained from right singular vector histograms. Figure 4.24 show histograms for the 1st, 2nd, 3rd, and 1000th right singular vector for the molecular dynamics data and the experimental data. It is clear from these plots that the modes are a good representation for the molecular dynamics data but not ideal for the experimental data. The molecular dynamics data shows a much larger deviation from the mean. In conclusion, the results of this section show that modes of motion derived from molecular dynamics represent a valid basis to represent flexibility as observed from experimental structures. However, there is still a significant amount of room for improvement in the quality of modes. Improvement could result from increased accuracy in the computational simulation of biological systems.

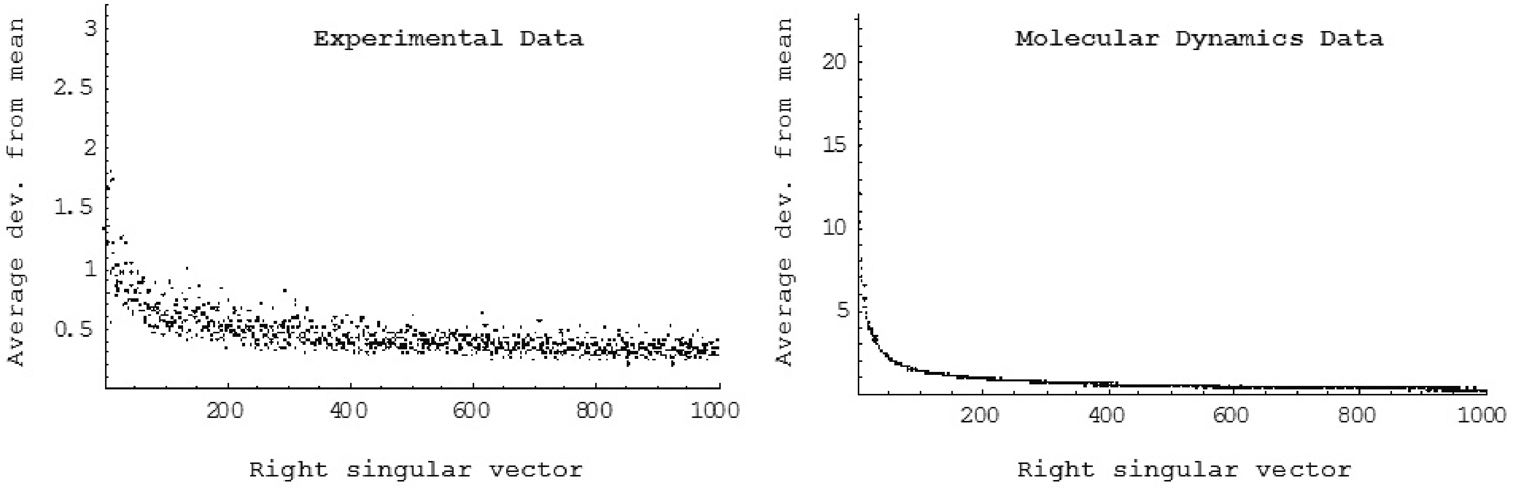

Figure 4.23 - Average deviation from the mean for the right singular vectors of the experimental and MD data.

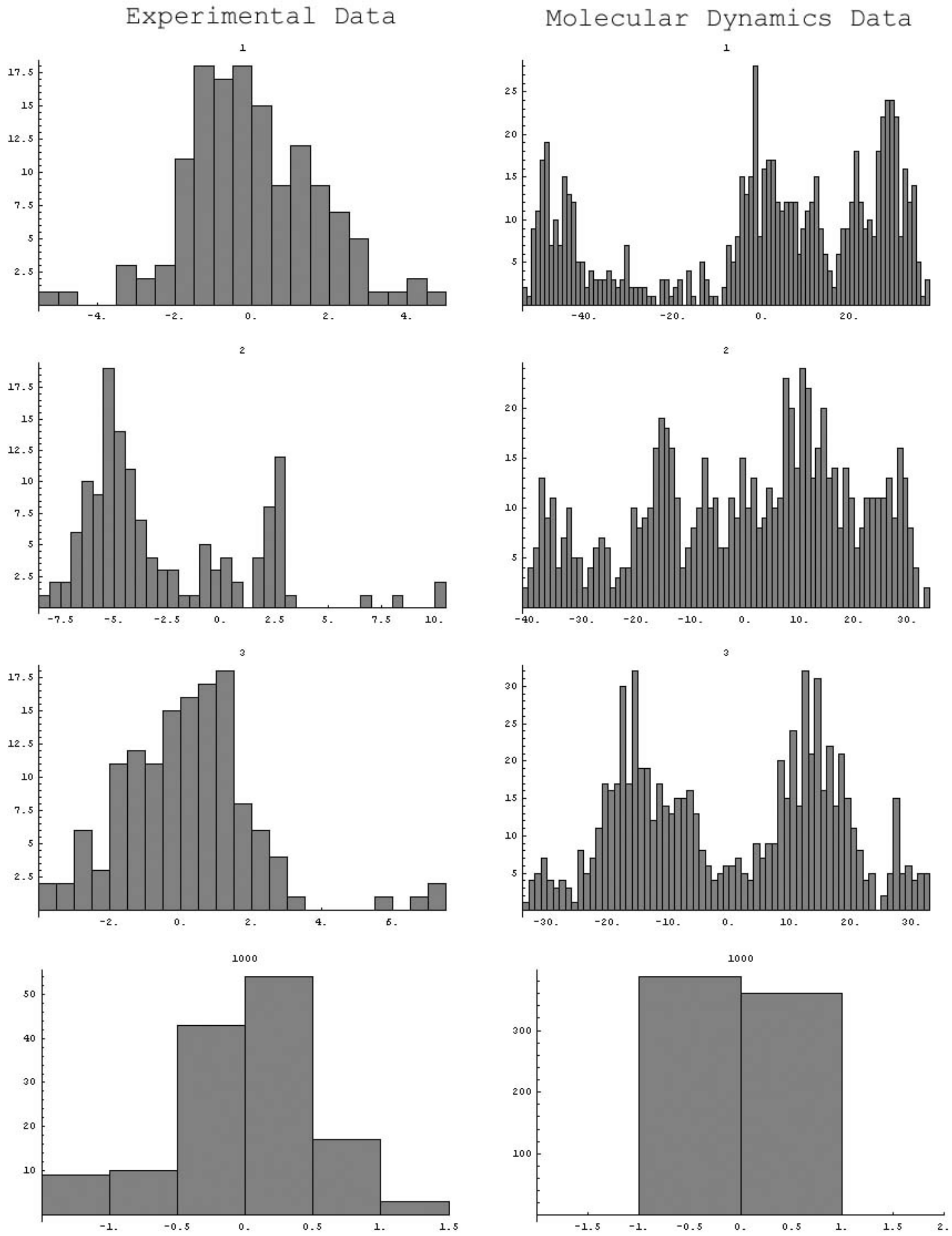

Figure 4.24 - Histogram analysis comparison of the 1st, 2nd, 3rd, and 1000th right singular vectors for the experimental and MD data.

4.5. Summary

In this chapter we show how to use the Principal Component Analysis (PCA) method, a dimensionality reduction technique, to transform the original high-dimensional representation of protein motion into a lower dimensional representation that captures the dominant modes of motions of proteins. The method was applied to HIV-1 protease, aldose reductase, and maltose binding protein. The conformational sampling data used for the PCA calculation was obtained using molecular dynamics techniques. For the case of HIV-1 protease, PCA was also computed using data derived exclusively from experimental methods and the results compared to the molecular dynamics method. One of the advantages of PCA is that it can be carried out at different levels of detail by selecting only a particular set of atoms for a protein. Here we described and compared the results obtained for the PCA analyses of backbone, binding site and all atoms in the protein. The results obtained for the main modes of motion correlate well with experimental data available for these proteins.

Chapter 5.

Applications of Collective Modes of Motion to Pharmaceutical Drug Design

5.1. Introduction

The use of collective modes of motion has been explored previously to include protein flexibility information in structure based drug design (Kolossvary and Guida 1996; Kolossvary and Guida 1999; Zacharias and Sklenar 1999; Kolossvary and Keseru 2001). This previous work was based on collective modes of motion derived from normal mode calculations. The use of normal modes offers some advantages but also a number of important limitations. The main advantage of using a normal modes based method is speed in computing the collective modes of motion. Whereas the PCA approach requires as input conformations obtained from a molecular simulation, which can take several days to obtain, the normal modes approach only requires the computation of the eigendecomposition of the Hessian. The Hessian is the matrix of second derivatives of the potential energy with respect to the mass weighted molecular coordinates. However, the normal modes approach assumes that the system moves about an energy minimum and that the motion is harmonic. This is clearly not the case for induced fit changes occurring at room temperature. In these conditions, the protein will likely go through several conformational substates as it transitions from the bound to the unbound conformation. As a result, the computation of modes from PCA (also called quasi-harmonic analysis) is in our view a better approximation to include collective modes of motion information in modeling induced fit processes.

In this chapter we discuss several approaches to include collective modes of motion information in structure based drug design. In Sections 5.2 and 5.3 we discuss indirect methods in which the SVD information is used to generate a set of conformational samples that represent the flexibility of the protein. The individual structures obtained using this method can later be used in current docking programs that take as input the rigid three dimensional shape of the receptor. In Section 5.4 we investigate the possibility of using the collective degrees of freedom directly to search for alternative protein conformations.

5.2. Generating Docking Targets Using Collective Modes of Motion for Conformational Sampling

One possible method of applying the information derived from the calculation of collective modes of motion to model the flexibility of the protein is to use these to efficiently generate a discrete set of conformations that represents alternative protein conformations. The individual protein conformations can then be used with traditional rigid-protein / flexible-ligand docking software without modifications to the original programs. Protein conformational sampling using collective modes of motion is more efficient because it is done along the degrees of freedom that are responsible for most of the conformational variance observed during a computational simulation (or alternatively in large amount of experimental data). The use of collective modes of motion has been described before as a method to speed up conformational sampling using molecular dynamics (Amadei, Linssen et al. 1996; de Groot, Amadei et al. 1996; de Groot, Amadei et al. 1996). In this previous application, the modes of motion were used as additional constraint forces in the simulation.

A simple method of generating a discrete conformational sampling is to use a reference structure (i.e. experimental structure) and modify it in the direction of a collective mode of motion. This type of perturbation is illustrated in Figures 4.4 to 4.7. More than one direction can be used for the perturbation and more than one structure can be generated along the direction of perturbation. In Figure 5.1 we show an example in which we generate seven conformations along the first mode of motion and five along the second mode of motion. The modes of motion can also be combined by adding or subtracting the corresponding eigenvectors to generate structures along directions diagonal to the original main motions. Although naïve, a grid based sampling can be very easily generated and used for docking. One drawback of using this method is that the structures generated along the modes of motion will display a large increase in internal energy due to the deviations from ideal bond and angle geometry. Nevertheless, this problem can be easily solved using a short conjugate gradient minimization procedure. Our own experiments (results not shown) indicate that a short conjugate gradient minimization protocol that takes less than ten seconds to complete on a current desktop PC is enough to correct the deviation from ideal geometry and restore the internal energy to initial values.

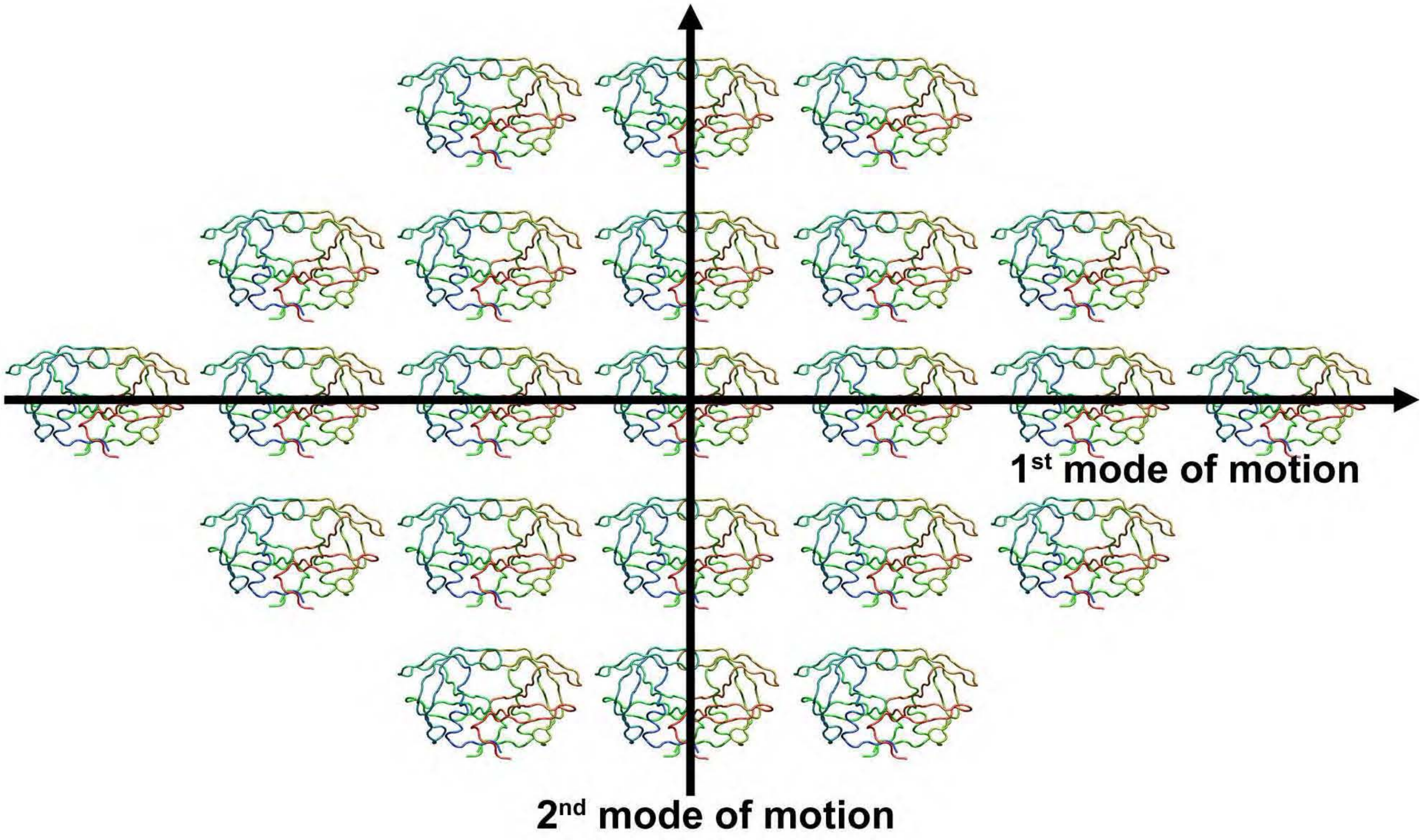

Figure 5.1 - A grid of structure representing the protein flexibility can be generated by sampling along the first two modes of motion.

The main problem of using a discrete grid sampling to represent the flexibility of the protein is that the size of the set will grow exponentially with the number of degrees of freedom used to generate it. Fortunately, there are several factors that limit the severity of this problem. The first factor is that it is not necessary to generate a large number of structures along each mode. Our studies described in Chapter 2 indicate that good docking results can be obtained using current rigid-protein / flexible-ligand docking programs even when there is a non-negligible error (0.6Å – 1.2Å RMSD) in the receptor model relative to the actual experimental structure of the docked receptor. As a result, it is possible to generate a very low sampling along the main modes of motion and rely on the error tolerance of the docking programs to compensate for intermediate conformations that are skipped due to coarseness of the sampling. In addition, it is possible to also modify the docking programs to accommodate for additional accuracy errors relative to the docked conformation (Wojciechowski and Skolnick 2002). A second factor that facilitates the use of the grid method is that, although the problem is larger in size, it can be classified as an embarrassingly parallel problem. This class of problems can be solved in a cost effective way by the use of clusters of commodity type computers, such as common PC desktops.

The structures generated using a grid based approach can be used for applications other than structure-based drug design in which the objective is to dock a small molecule to a large macromolecule. Another potential application of this method is to perform the docking of two macromolecules that undergo some level of conformational change when they interact. Instead of modeling flexibility explicitly using the collective degrees of freedom, the flexibility of the protein is represented by a discrete set of alternative conformations using the grid method. This reduces the complexity of taking into account protein flexibility in modeling protein / protein or protein / DNA interactions by dividing the problem in a series of simpler problems which can be handled using traditional rigid-protein / rigid-protein docking methods. The problem of trying to match two rigid 3D shapes is considerably less complex and very fast Fourier methods for this purpose are currently available (Ten Eyck, Mandell et al. 1995). In order to take into account some inaccuracy in modeling alternative protein conformations using such a reduced number of degrees of freedom it is also possible to combine Fourier docking methods with other approaches that try to minimize the effects of carrying out macromolecular docking using low resolution structures (Vakser 1995).

5.3. Identification of Protein Conformational Substates as Docking Targets

Proteins in solution do not exist in a single conformation. Instead proteins assume a large number of nearly isoenergetic conformations (conformational substates) (Noguti and Go 1989; Noguti and Go 1989; Frauenfelder, Sligar et al. 1991). The analysis of molecular dynamics simulations of proteins using right singular vectors can easily identify a fraction of the available conformational substates (Romo, Clarage et al. 1995; Troyer and Cohen 1995; Garcia, Blumenfeld et al. 1997; Caves, Evanseck et al. 1998; Romo 1998). In this section we describe how to generate a discrete set of conformations that best represents the conformational substates observed for a molecular dynamics simulation. The set of structures can then be used for rigid-protein / flexible-ligand docking.

The right singular vector results for the binding site of HIV-1 protease, aldose reductase and maltose binding protein discussed in Section 4.4.3 clearly show that these proteins do not move at a fixed velocity in conformational space. Instead they hop between stable conformational substates. Using the plots in Figures 4.17 to 4.19 it is possible to identify at what times during the simulation the protein resides in a particular conformational substate. In order to select a representative structure from each of the conformational substates we calculated pairwise root mean square distances between individual structures within the same conformational substate. The distance metric used was not the Cartesian RMSD. Instead distances were calculated in the space defined by the first three modes of motion (Figures 4.17 to 4.19) and the structure with the lowest mean root mean square distance to the other members of the substate was selected to be its representative. It would also be possible to use the Cartesian RMSD as a distance metric to select the representative structure. However such computation would be significantly more expensive because it would require the computation of a distance in a space with 750 dimensions versus 3.

Results for the identification of conformational substate representatives for the three model proteins analyzed in Chapter 4 are shown in Figure 5.2 to 5.4. Figure 5.2 shows the results for HIV-1 protease. The three representative structures corresponding to conformational substates A, B and C are colored using red, yellow and green, respectively. The conformations correspond to largely different binding site shapes. The red conformation displays the smallest binding site and the green conformation the largest. The large differences in binding site volume are consistent with experimentally determined structures which show variations in volume larger than 100%. In Figure 5.2-b) we show a magnified view of the binding site residues show in a). The increase in binding site volume is a result of rotations of some of the residue sidechains but is mostly due to a coordinated motion at the backbone level. The two conformational representatives for aldose reductase are shown in Figure 5.3. In this case the alternative conformations represent more localized changes. In Figure 5.3-b) the white arrow indicates residue LEU 300. Changes in this residue and its vicinity are responsible for most of the opening of the extra cavity that distinguishes the bound conformations with sorbinil and tolrestat (for more information see Appendix A.2). This observation constitutes a positive result for the applicability of the right singular vectors method. Starting from the conformation for one of the ligands it was possible to computationally generate a conformation which could be used successfully to screen a different class of ligands. Finally, in Figure 5.4 we show three different conformational representatives for maltose binding protein. In this case the conformational changes are smaller than in the other two cases but may help understand how maltose binding protein changes its conformation when binding different maltodextrins and cyclodextrins.

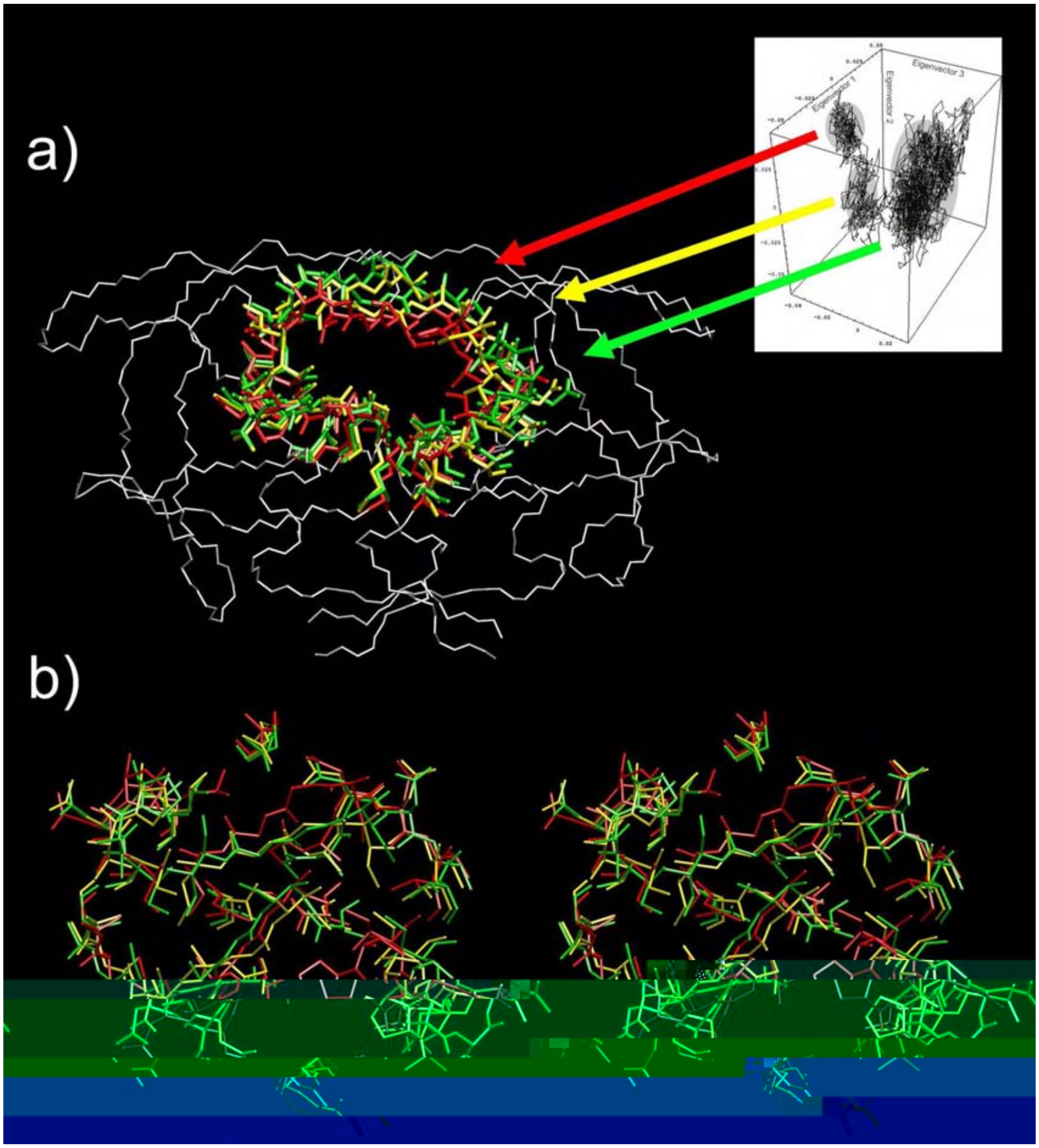

Figure 5.2 – Identification of representative conformations for the binding site of HIV-1 protease. a) Representative conformations for the three conformational substates were identified from the right singular vectors of a molecular dynamics simulation (top right, see also Figure 4.17). The heavy atom positions for the variable regions are shown in red, yellow, and green. The remaining backbone of the protein is shown in white. b) Magnified stereoview of the variable binding site region (note: image is rotated 90º forward relative to the view in a)).

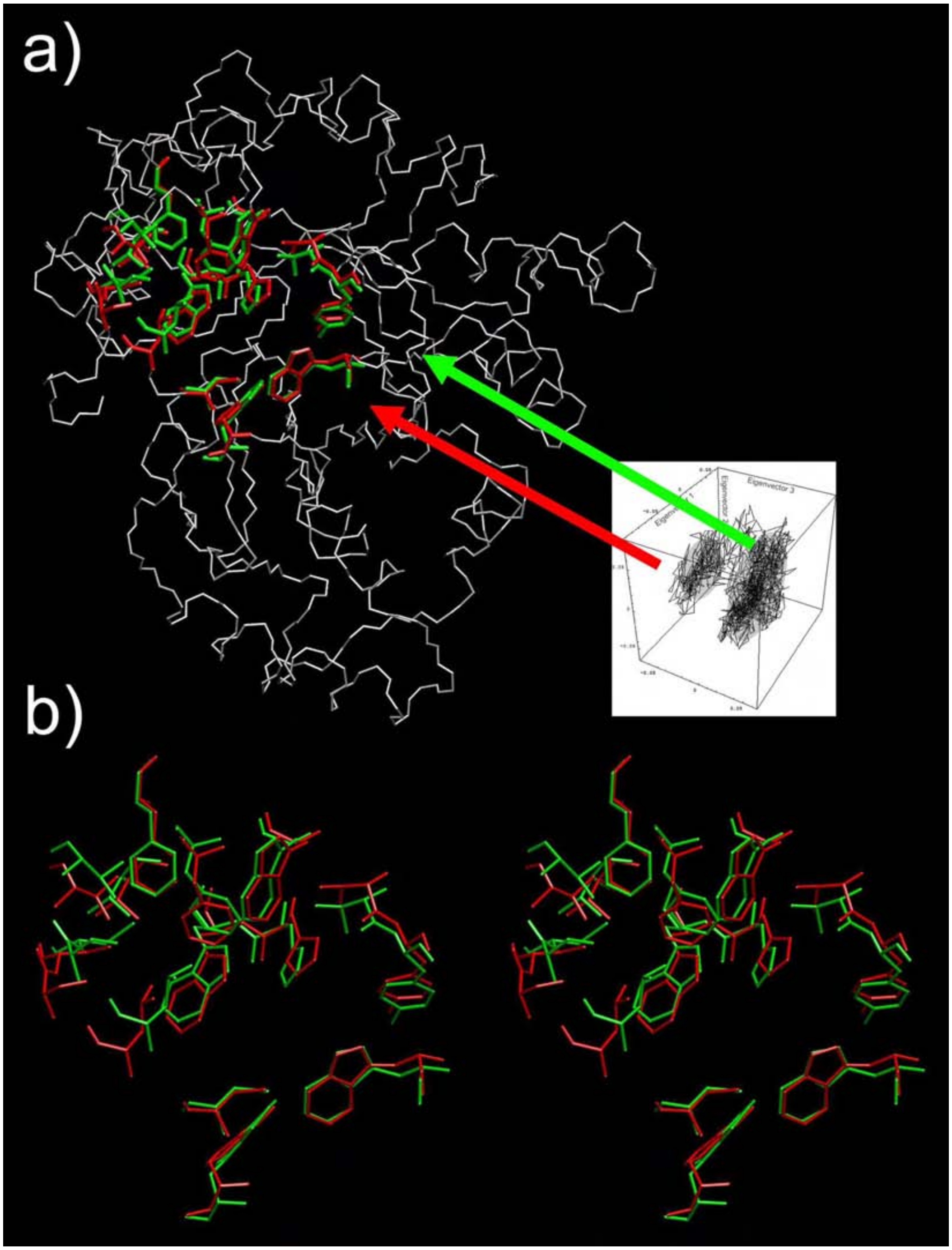

Figure 5.3 – Identification of representative conformations for the binding site of aldose reductase. a) Two conformations were identified using the right singular vectors (top right, see also Figure 4.18). b) Magnified stereoview of the variable binding site region.

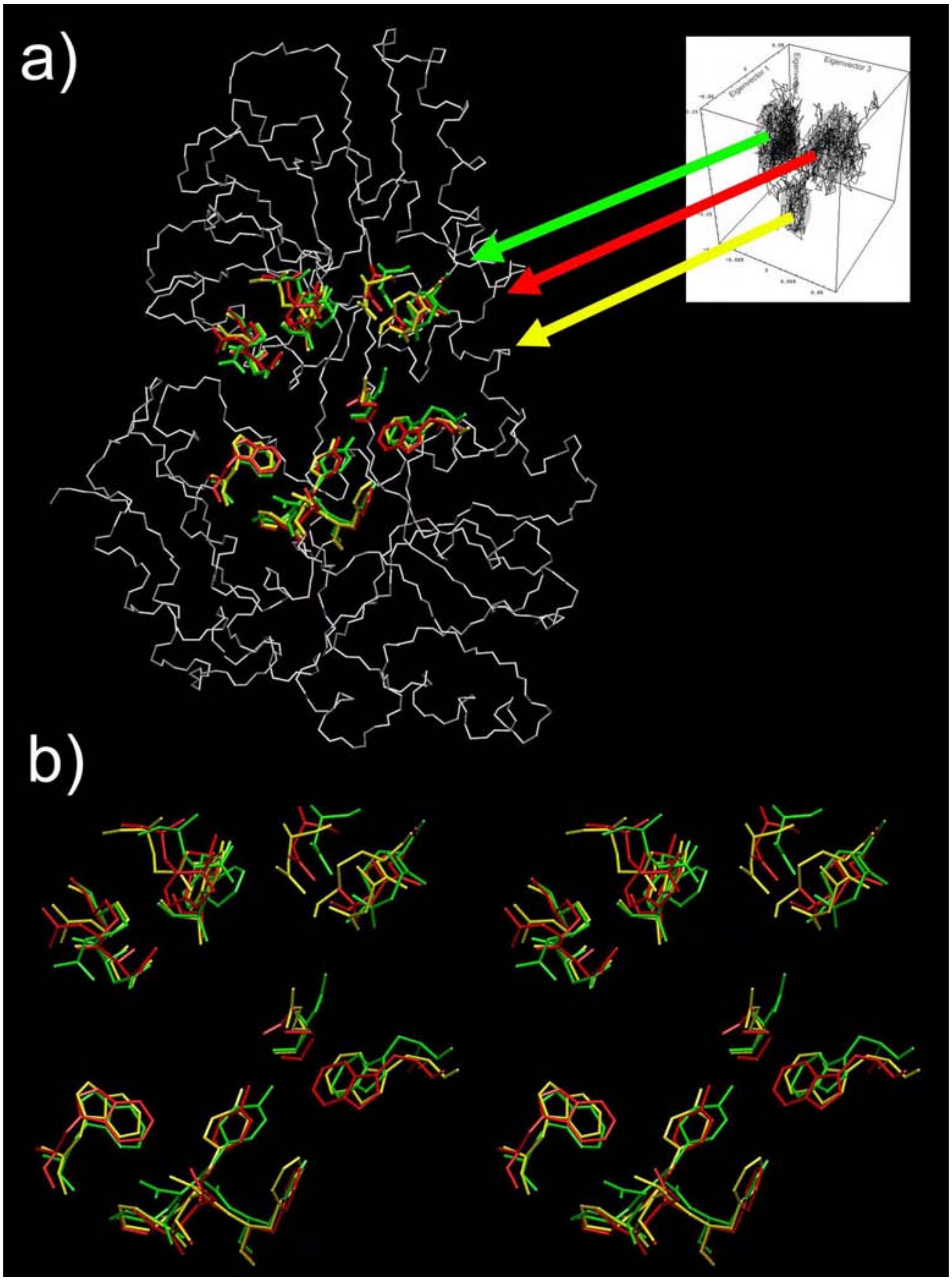

Figure 5.4 - Identification of representative conformations for the binding site of maltose binding protein. a) Two conformations were identified using the right singular vectors (top right, see also Figure 4.18). b) Magnified stereoview of the variable binding site region.

The method described in this section to generate a discrete conformational sampling for the flexibility of the protein has advantages and disadvantages relative to the grid method described in the previous section. The main advantage is that the number of structures generated is much smaller. Furthermore, the structures generated are of better quality in the sense that they correspond to low energy regions of the potential energy landscape. However, the main disadvantage is that even long molecular dynamics simulations only cover a small fraction of the conformational landscape (Clarage, Romo et al. 1995). As such, it is likely that the grid method provides a better coverage of the available conformational space.

An alternative application for the identification of stable conformational substates using the information from the right singular vectors is to improve the design of dynamic pharmacophore models (Carlson, Masukawa et al. 1999; Carlson, Masukawa et al. 2000). The pharmacophore is a three dimensional arrangement of molecular features that is present in all (or most) of the active conformations of a set of drug molecules that interact with a given receptor. Hence, the pharmacophore can be viewed as a geometric invariant of the active conformations of the considered molecules. The dynamic pharmacophore model extends this concept by using as a receptor model several conformations obtained using a molecular dynamics trajectory. The dynamic pharmacophore model is described by binding regions that are conserved over many protein conformations. In their work Carlson *et al* selected conformations from the molecular dynamics trajectory at fixed time intervals. Given the "beads-on-a-string" nature of protein dynamics this is probably not the most effective choice. Fixed time intervals are likely to select more than one structure from each conformational substate (leading to wasted effort) or miss a structure from a particular conformational substate (leading to lack of coverage of the conformational space). A better alternative is to use the right singular vectors to identify protein conformational substates and use representative structures in the pharmacophore calculation.

5.4. Approximating Molecular Conformations Using Low Dimensional Representations for Protein Flexibility

A third method of using the information derived from the calculation of collective modes of motion to model the flexibility of the protein is to use these degrees of freedom directly in the conformational search for the docked ligand. Such a method could be easily included in most current rigid-protein / flexible-ligand docking programs by adding degrees of freedom of the protein to the existing search space. For example, to add protein flexibility capabilities to Autodock (Morris, Goodsell et al. 1998) we would only need to extend the information in the chromosome to include the new degrees of freedom representing the protein (note: Autodock uses a genetic algorithm to search the conformational space of the ligand to find the docked conformation (for more details see Appendix C)). However, if we are to perform the conformational search directly by dealing with the degrees of freedom of the protein in the same manner as the degrees of freedom of the ligand then two important questions arise: "How many degrees of freedom of the protein need to be included in the conformational search?” and “What level of approximation can we obtain using the reduced basis of representation?”. In this section we will address these two questions.

In order to answer the two questions we decided to investigate if using the main modes of motion defined by the principal components and an experimental structure bound to a particular ligand, we could approximate the structure of HIV-1 protease bound to a different ligand. For this experiment we were only concerned with variations in the shape of the binding site and used only the PCA results described in Chapter 4 for this part of the protein. A total of 250 atoms constitute the binding site for HIV-1 protease, which results in an initial search space of 750 dimensions. As the initial reference conformation we chose the same structure we used for the molecular dynamics simulation and as a target structure we used a complex with a large non-peptide inhibitor (Rutenber, Fauman et al. 1993) (PBD access code 1AID). The binding site conformations as well as the inhibitors bound to these are considerably different as shown in Figure A.2. The root mean square deviation (RMSD) between the two proteins is 1.843 Å if we take into account only the atoms that constitute the binding site.

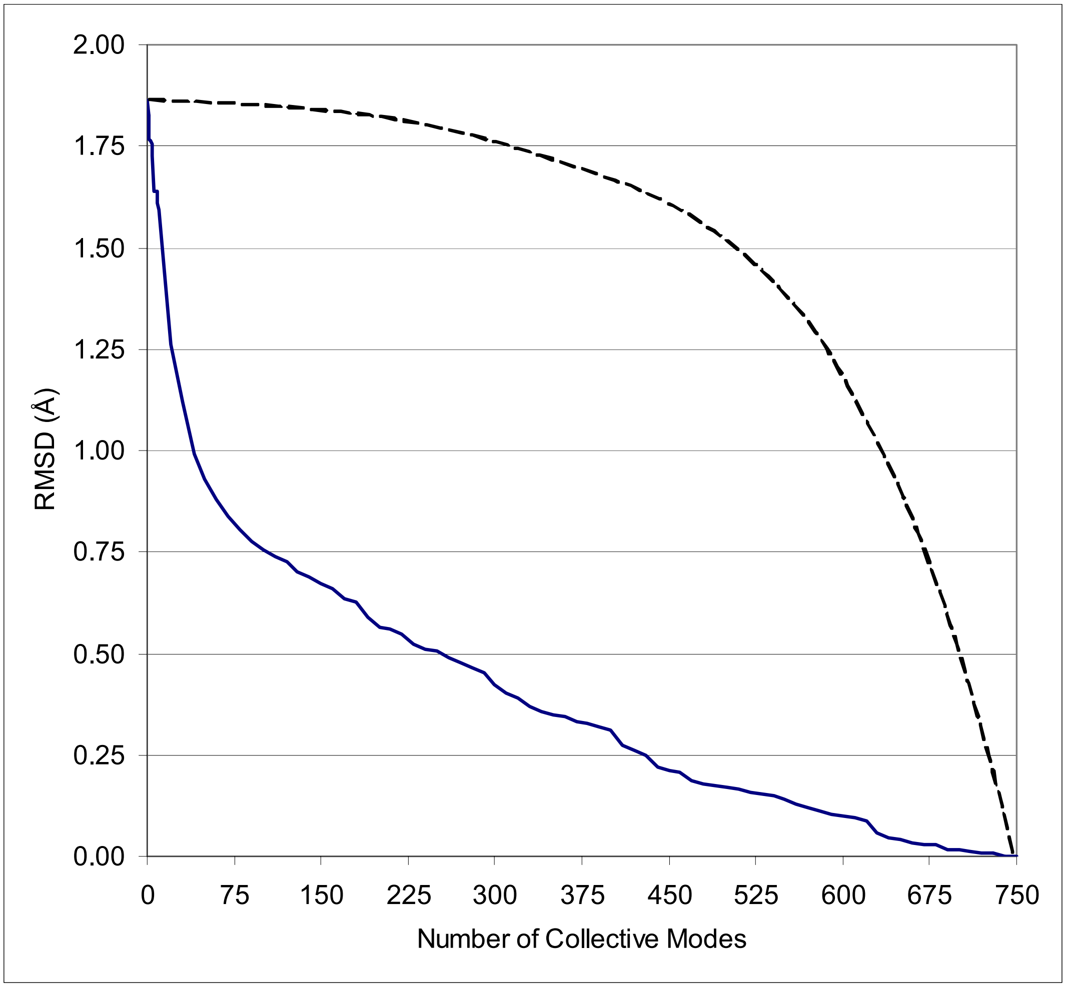

Figure 5.5 - RMSD between a reference (4HVP) and a target structure (1AID) for an approximation of the flexibility of the binding site of HIV-1 protease using an increasing number of collective modes of motion. The solid line uses the collective modes basis determined by the binding site PCA and the broken line uses a random basis defining the same space.

The next step was to calculate the coordinates of the target structure in the new basis. For this we used the definition of the representation basis given by the principal components of the molecular dynamics data and we set the origin of the space to be our reference structure. The coordinates in each of the dimensions are given by the dot product of the atomic displacement vector and the eigenvector defining each dimension. The resulting coordinates will be a solution vector of the form [w_1, w_2, w_3, w_4, …, w_{3N}]. We can now calculate what would be the RMSD between our target structure and our low-dimensional approximation. The approximation corresponds to [w_1, 0, 0, 0, …, 0] if we consider only the first collective mode, [w_1, w_2, 0, 0, …, 0] if we consider the first two and [w_1, w_2, w_3, w_4, …,w_k, 0, …, 0] if we consider the first k collective modes. The RMSD results for an increasing number of collective modes are shown in Figure 5.5. When using the PCA basis we are able to approximate the target structure to an RMSD of less than 1 Å using 40 principal components out of a total of 750. By contrast if we used an approximation with a random orthonormal basis (Wolfram 1999) defining the same space (shown by a broken line in Figure 5.5) we would need more than 650 principal components to obtain the same accuracy. This shows the strength of our method in approximating other conformations of the same protein using a lower dimensional search space and validates the effectiveness of the PCA by comparing it with an approximation carried out using a random basis. Furthermore, the level of approximation achieved is approximately similar to the tolerance level of current docking programs as reported in Chapter 2. It is also important to note that the values that we obtain for the approximation to the target can be further improved. Currently we are using the projection of the target structure on the new basis to estimate a set of coordinates in the reduced space that approximate the target structure. However, the optimal approach is to search the low-dimensional space directly to look for the best match. In this way we can search for alternative coordinate values along the most significant principal components that compensate for the approximation being introduced by the dimensional truncation of the representation basis. We are currently developing search techniques for the purpose of finding these solutions in the reduced space.

Despite the promising results of the previous experiment it is important to note that during the course of our investigation we found two factors which are critical in order to obtain good results using the reduced basis representation for protein flexibility. The first factor is that the PCA should be restricted to the region of interest. For the case of docking applications this would be the binding site region. In Figure 5.6 we show the results of an approximation experiment equal to the one described in the previous paragraph but using the collective modes of motion determined for the all-atoms PCA instead of the binding site PCA. From the comparison of Figures 5.5 and 5.6 we can conclude that although the all-basis atoms also provides a better description of protein flexibility than a random basis, the approximation is significantly worse that for the binding site case. The reason for this is that the all-atoms modes of motion have to account for several changes in conformation that are not relevant at the binding site level.

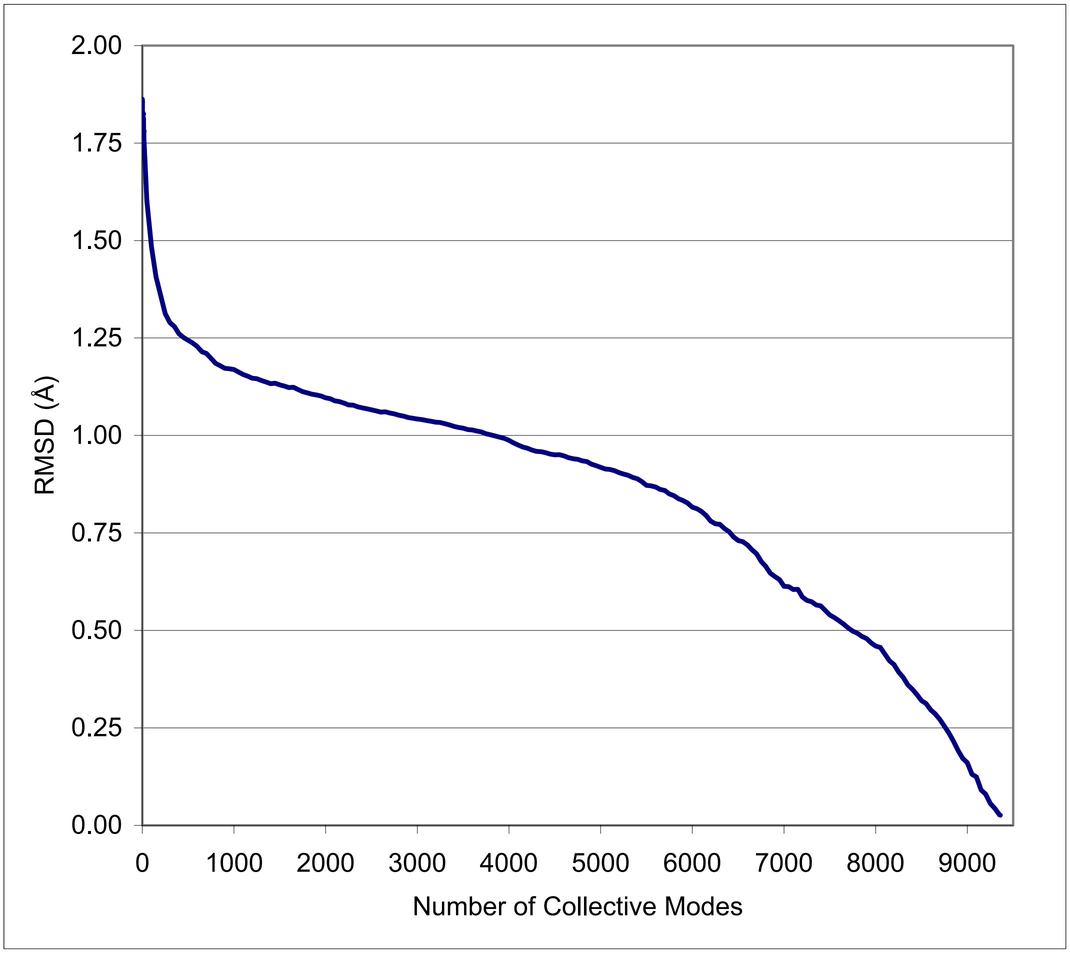

Figure 5.6 - RMSD between a reference (4HVP) and a target structure (1AID) for an approximation of the flexibility of the binding site of HIV-1 protease using an increasing number of collective modes of motion. The solid line uses the collective modes basis determined by all-atoms PCA.

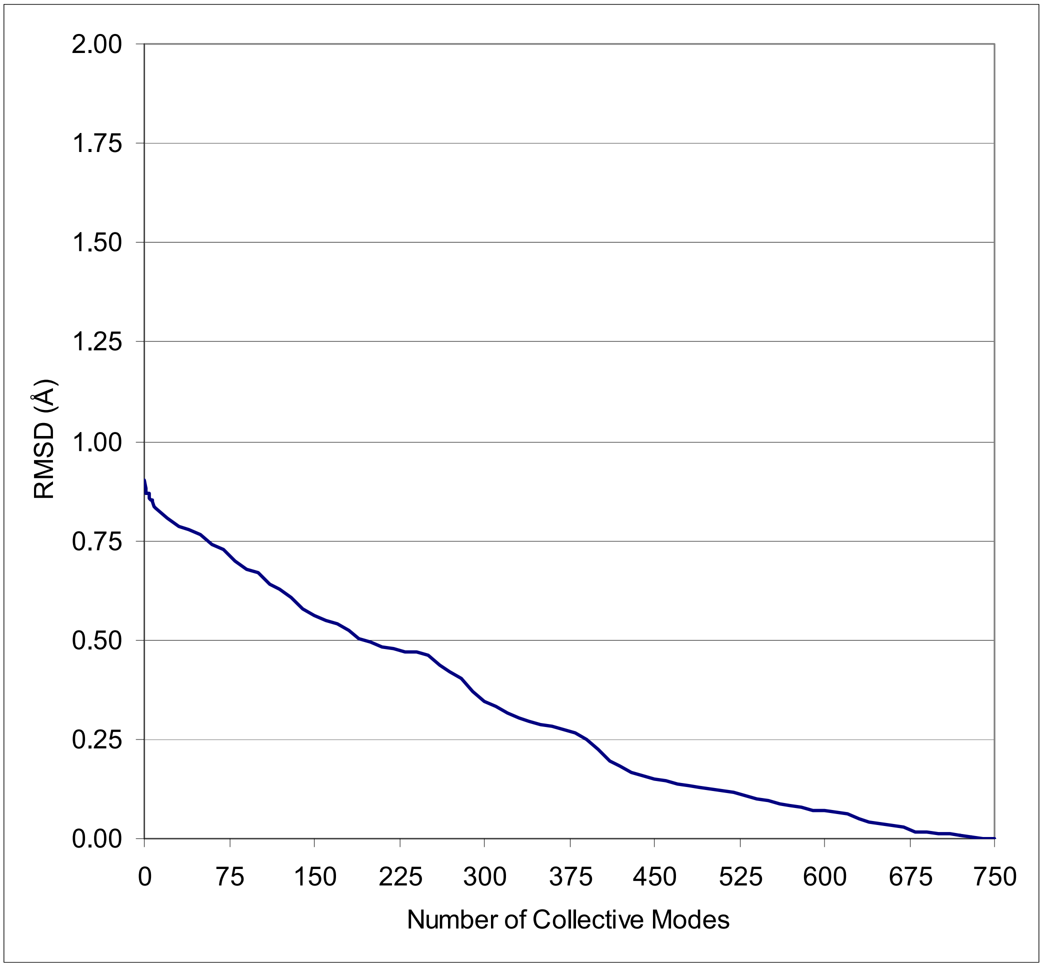

Figure 5.7 - RMSD between a reference (4HVP) and a target structure (9HVP) for an approximation of the flexibility of the binding site of HIV-1 protease using an increasing number of collective modes of motion. The solid line uses the collective modes basis determined by binding site PCA.

The second pitfall we discovered when testing the modes of motion derived from PCA is that they are useful only when modeling conformational rearrangements larger than 1.0Å to 1.2Å. In Figure 5.7 we show an experiment equal to the one described for Figure 5.5 but instead of approximating the binding site structure of 1AID we used the structure with PDB code 9HVP. The initial difference at the level of the binding site for these two structures is 0.9Å RMSD. As can be observed from Figure 5.7 the inclusion of first main modes of motion does not lead to a sharp increase in the level of approximation as was observed in Figures 5.5 and 5.6. On the contrary, the approximation increases almost linearly with the number of degrees of freedom used for modeling. The linear phase is also present in Figure 5.5 starting at approximately 0.9Å RMSD as well as in over 100 other conformations with different initial levels of approximation for which we tested this procedure (results not shown). The main conclusion for all the experiments is that approximately 30-50 main modes of motion are sufficient to generate an approximation at the level of 0.9Å RMSD but beyond this threshold the main modes of motion provide very little useful information. The justification for this result lies in a fundamental limitation of the PCA method. The PCA method relies on the accurate computation of motion correlation between pairs of atoms. If there is a large amount of uncorrelated motion present, such as random thermal motion, it will mask any smaller amplitude correlated motions present in the system and in practice render modes of motion corresponding to very small deviations useless. Fortunately, in light of the results reported in Chapter 2 the 1.0Å approximation threshold is not a major problem for docking applications.

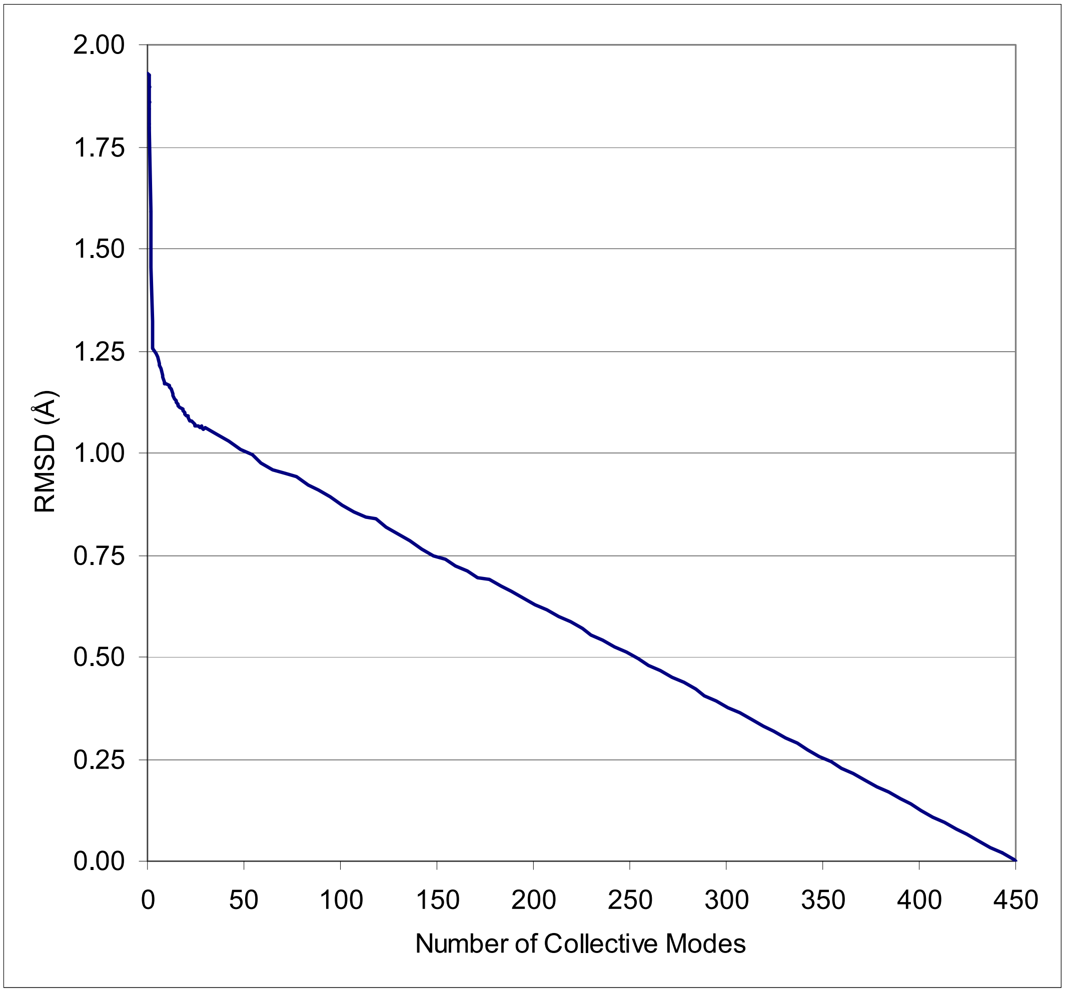

Figure 5.8 - RMSD between a reference (1AH4) and a target structure (1AH3) for an approximation of the flexibility of the binding site of aldose reductase using an increasing number of collective modes of motion. The solid line uses the collective modes basis determined by binding site PCA.

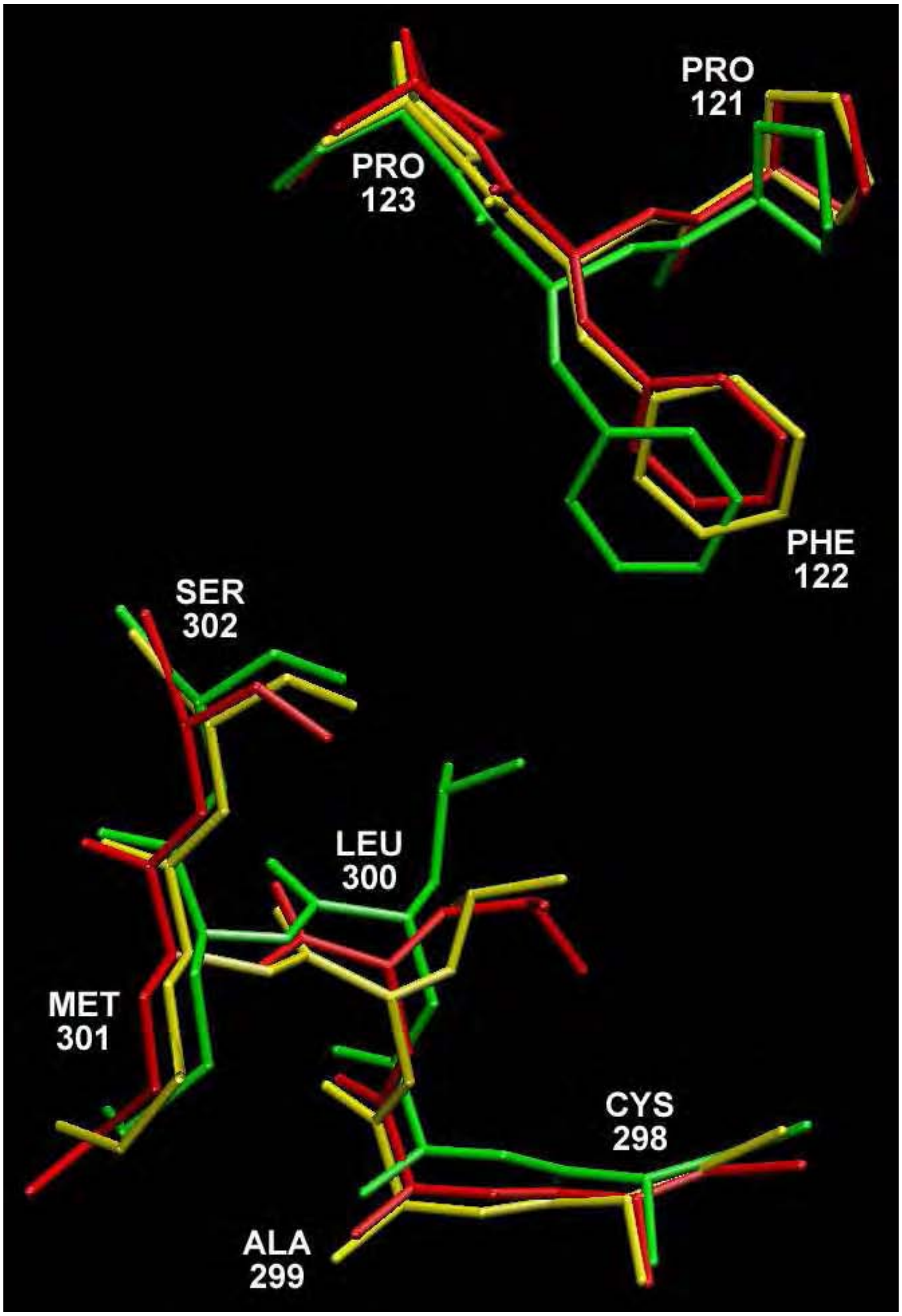

Figure 5.9 - Approximation (yellow) of the binding site bound conformation (red) of aldose reductase using the unbound conformation (green) as a starting point and searching along 40 main modes of collective motion.

In order to test the ability to use PCA modes of motion as degrees of freedom for modeling proteins other than HIV-1 protease we also applied the testing methodology described in this section to aldose reductase. For this we calculated an approximation of the form [w_1, w_2, …, w_{40}, 0, …, 0] as we did for HIV-1 protease using the unbound form as the reference structure (no pocket present) and the bound structure to tolrestat as our target (pocket is present). The RMSD evolution for the binding site residues is shown in Figure 5.8. Figure 5.9 shows the approximation (yellow) of the bound conformation (red) using the unbound conformation (green) as a starting point and searching along 40 main modes of collective motion. The initial difference between the bound and unbound forms is 1.93Å RMSD. Using a 40 degrees of freedom approximation we can reduce this value to 1.03Å. From the figure it is clear that we can obtain a good approximation on the residues that form the top of the specificity pocket with our approximate structure matching almost exactly the experimental structure for the bound form. It is important to note that the approximation is able to capture not only the movement of aminoacid sidechains, such as the rotation of the aromatic ring in PHE 122, but also global displacements caused by a movement at the backbone level, such as shown for the backbone of residues 121 to 123. This contrasts with complexity reduction methods that consider the important flexibility of the protein as being represented only by movements of sidechains and that are unable to represent induced fit conformational changes caused by backbone movements. The bottom part of the specificity pocket does not show a match of similar quality but still shows a trend in the right direction. A good example of this is the change in conformation of LEU 300. In fact the approximated structure already displays the specificity pocket and is large enough to accommodate ligands such as tolrestat or zopolrestat.

5.5. Summary

In this chapter we explore different methods of including the information derived from the dimensional reduction of molecular dynamics trajectories to model protein flexibility in the context of structure-based drug design. The information can be used indirectly to generate a discrete set of conformational samples that represent the flexibility of the protein. The sampled conformations can later be used as target receptors using traditional rigid-protein / flexible-ligand programs. Two methods are described to generate the conformational sampling: one is based on grid sampling along the main modes of motion, and the other is based on the identification of a representative structure of conformational substates using right singular vectors. Alternatively, the modes of motion can be used directly in conjunction with the degrees of freedom in the ligand to search for a flexible-protein / flexible-ligand bound conformation. Although there is inevitably some loss in accuracy, we show that we can obtain conformations that have been observed in laboratory experiments, starting from different initial conformations and working in a drastically reduced search space.

Chapter 6.

Conclusions

In this work we showed how to obtain a reduced basis representation of protein flexibility. Proteins typically have a few hundreds to a few thousands of degrees of freedom. Starting with data obtained from laboratory experiments and/or molecular dynamics simulations, we demonstrate that we can compute a new set of degrees of freedom that are combinations of the original ones and that can be ranked according to significance. Depending on the level of accuracy desired, the k most significant of these new degrees of freedom can be used to model the flexibility of the system. We have observed, in multiple occasions, that the reduced basis representation retains critical information about the directions of preferred motion of the protein. It can thus be used to compute conformational rearrangements of the protein that can further be studied for interaction with novel ligands or other proteins. Our work contributes to the better understanding of how changes in the conformation of a protein affect its ability to bind other molecules and hence its function. We envision that protein databases, such as the Protein Data Bank, would be annotated in the future with principal modes of motion for proteins allowing rapid and detailed analysis of biomolecular interactions. This annotation would allow researchers not only to analyze the static structure of a protein but also its motions and relations between structure, motion and function. The process of determining collective modes of motion could be automated using the methods described in the present work and the information would complement other structural databases such as the Database of Macromolecular Movements (Gerstein and Krebs 1998).

In this work we used PCA as our dimensionality reduction technique. The results obtained are biologically meaningful. Clearly, it is worth investigating the application of non-linear dimensionality reduction techniques to the same problem. For example local PCA (Kambhatla and Leen 1997), locally linear embedding (Roweis and Saul 2000), and multi-layer auto-associative neural networks (Kramer 1991) might be able to provide us with the same kind of information as PCA while using an even further reduced number of degrees of freedom. The application of these dimensionality reduction methods to protein structural data is only practical for modeling if we are able to obtain an inverse mapping from the lower to the higher dimensional space. This mapping can in principle be obtained using machine learning techniques such as neural networks. Carrying out this step efficiently is very difficult and constitutes an open research question. Preliminary work in our group indicates that some of the advantages obtained by performing a non-linear dimensional reduction are outweighed by an increased computational cost and a loss in accuracy due to the approximated inverse mapping. Nevertheless, the advantage of reduced complexity in the representation of molecular motion may justify the increased computational cost of the non-linear dimensionality reduction depending on the application.

All our work was done using the Cartesian coordinates of atoms in the protein. An interesting idea is to perform the dimension reduction in the dihedral and the bond angle space of the system. The advantage of this approach is that the initial dimensionality of the problem is reduced because given certain constraints fewer parameters are necessary to uniquely define a protein structure. The first constraint is that bond lengths are fixed. At a second level of approximation, bond angles between three consecutively bonded atoms can also be considered fixed. As such, it is possible to represent a molecular conformation using only the set of dihedral angles corresponding to torsions around single bonds. The dimensionality of this space is in practice approximately almost an order of magnitude smaller than the Cartesian representation. Initial experiments showed that a dihedral angle-based analysis of conformational data is very sensitive to noise and prone to error. We are currently investigating this problem and improving the general methodology in order to apply the methods described in this work to a dihedral angle representation. Last but not least, we investigate how to effectively explore conformational flexibility of a protein in the reduced basis representation to make approximate but fairly accurate predictions for protein-protein and protein-ligand interactions. This work could be used to predict complex effects such as the induced fit effect during ligand binding in a drug design study in a computationally efficient manner.

Appendix A.

Protein Model Systems

A.1. HIV-1 Protease

HIV-1 protease is a homodimeric aspartyl protease with each subunit containing 99 residues. This protein is encoded in the 5' end of the pol gene and is expressed as part of the gag-pol polyprotein. HIV-1 protease plays a vital role in the maturation of the HIV-1 virus by targeting amino acid sequences in the gag and gag-pol polyproteins (Kramer, Schaber et al. 1986; Graves, Lim et al. 1988; Kohl, Emini et al. 1988; Le Grice, Mills et al. 1988). Cleavage of these polyproteins produces proteins that contribute to the structure of the virion, RNA packaging, and condensation of the nucleoprotein core. In 1988, Le Grice *et al* (Le Grice, Mills et al. 1988) carried out a study in which they demonstrated that proviral DNA lacking functional protease produces immature, noninfectious viral particles. This finding initiated a large concerted effort by the scientific community, from both academia and industry, to develop a small molecule capable of inhibiting proteolytic activity and stop the progression of HIV infection. This research effort marked the start of a new era in which protein structural information and knowledge of energetic interactions at an atomic level led to the discovery of a series of efficient HIV-1 protease inhibitors (Flexner 1998; Wlodawer and Vondrasek 1998). This new method of drug discovery is currently known as rational structure-based drug design.

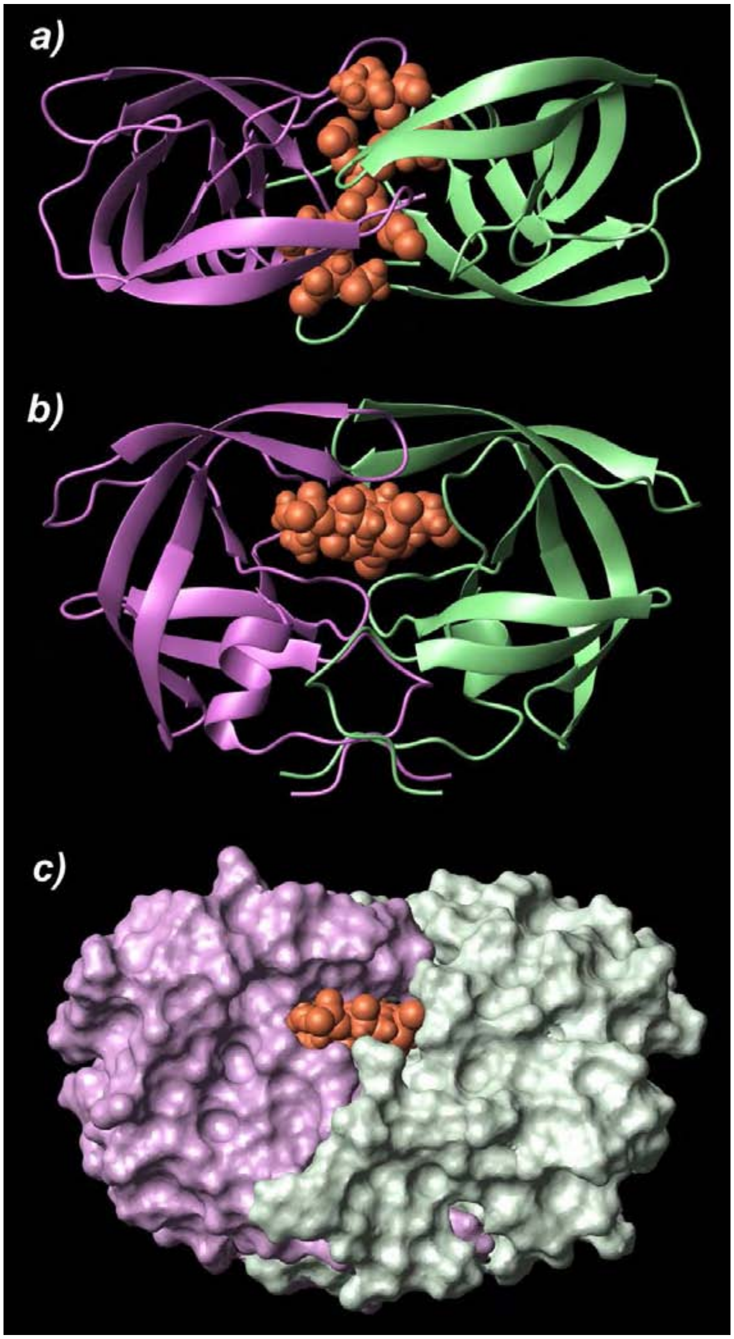

Figure A.1 - 3D structure of HIV-1 protease homodimer complexed with an inhibitor. On the a) top view and b) side view the β-hairpin flaps wrapping around the ligand are shown. c) in a space filling view the tight fit of the ligand in the binding site is shown indicating the need for a protein motion to allow for ligand entry and exit.

The active site of HIV-1 protease is formed by the homodimer interface and is capped by two identical β-hairpin loops from each monomer, which are referred usually as flaps (residues 46-56 and 146-156). The structure of HIV-1 protease complexed with an inhibitor (Miller, Schneider et al. 1989) is shown in Figure A.1. The active site structure for the bound form is significantly different from the structure of the unbound conformation (Wlodawer, Miller et al. 1989). In the bound state the flaps adopt a closed conformation acting as clamps on the bound inhibitors or substrates, whereas in the unbound conformation the flaps are more open. During the binding process the "handedness" of the flaps changes and the positions of the tips of the flaps can vary by as much as 7Å. This constitutes evidence of the importance of large-scale structural rearrangements during the protein-ligand binding process in HIV-1 protease. Further evidence for the importance of flap flexibility comes from experimental observations linking mutations in flap residues to resistance against HIV-1 protease inhibitors (Ho, Toyoshima et al. 1994; Kaplan, Michael et al. 1994).

In this study we used HIV-1 protease as a primary model system to study ligand binding dependent conformational changes. This choice was determined by the following factors:

- There is conclusive evidence that large-scale protein motions play a determinant role in ligand binding to HIV-1 protease (Freedberg, Wang et al. 1998; Piana, Carloni et al. 2002) and in the development of dug resistance (Rose, Craik et al. 1998; Scott and Schiffer 2000; Cecconi, Micheletti et al. 2001).

- HIV-1 protease as been extensively used as a model in computational studies. These studies included flap opening dynamics, protein-ligand complex dynamic flexibility, combined quantum/classical molecular dynamics studies, reaction path free energy calculations (Collins, Burt et al. 1995; Liu, Muller-Plathe et al. 1996; Luo, Kato et al. 1998; Rick, Erickson et al. 1998; Rick, Topol et al. 1998; Ringhofer, Kallen et al. 1999; Piana and Carloni 2000).
- There is extensive information on the mechanism and kinetics of HIV-1 protease (Silva, Cachau et al. 1996; Flexner 1998; Todd and Freire 1999).
- There are close to two hundred structures of HIV-1 protease bound to different ligands available in the Protein Data Bank (Berman, Westbrook et al. 2000). This variety serves as an excellent demonstration of protein plasticity in its optimal adaptation to a flexible ligand (see Figure A.2). Furthermore, it allowed for collective modes of motion to be calculated directly, based on the structural variations observed experimentally.
- Finding more efficient HIV-1 protease inhibitors is of extreme importance, since currently available drugs require a combination therapy to avoid the development of viral resistance and must be taken in very high dosages leading to serious side effects (Flexner 1998; Molla, Granneman et al. 1998; Kaul, Cinti et al. 1999).

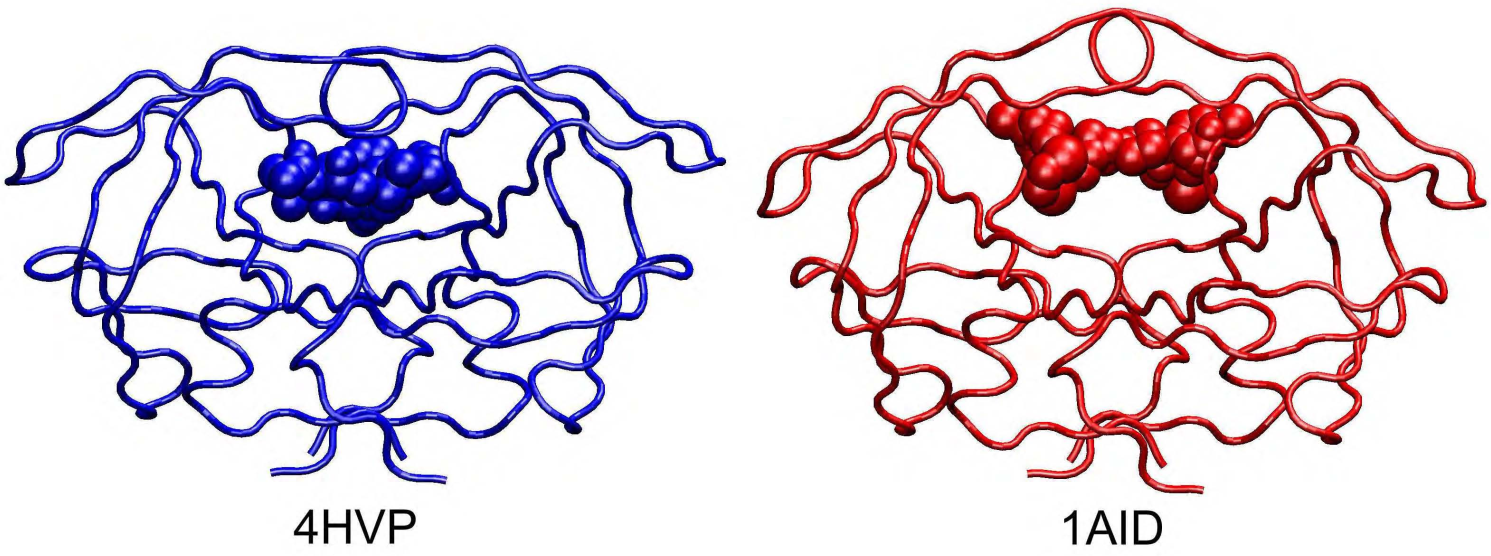

Figure A.2 – Alternative conformations for HIV-1 protease. Tube representation of HIV-1 protease (PDB access codes 4HVP and 1AID) bound to different inhibitors represented by spheres. The plasticity of the binding site of the protein allows the protease to change its shape in order to accommodate ligands with widely different shapes and volumes.

A.2. Aldose Reductase

Aldose reductase is a member of the aldo-keto reductase superfamily and is responsible for the first step of the polyol metabolic pathway to catalyze the reduction of glucose to sorbitol. This reaction uses nicotinamide adenine dinucleotide phosphate (NADPH) as a cofactor. Sorbitol is subsequently transformed to fructose by sorbitol dehydrogenase using a NAD+-dependent oxidation. Aldose reductase is of great pharmacological interest due to its role in the development of complications associated with diabetes mellitus (Oates and Mylari 1999). Namely, the development of retinophaties, cataracts and glaucoma is believed to be due to the osmotic effect caused by an increase in the concentration of sorbitol in the eye (Kinoshita and Nishimura 1988). Moreover, complications such as neuropathy and nephropathy are also caused by the increase flux of glucose in the polyol pathway (Dunlop 2000). The development of inhibitors for aldose reductase has been a goal in the pharmaceutical research field for over 25 years. Some inhibitors, such as epalrestat, have shown positive results in the treatment of diabetic complications. This drug is currently approved and marketed in Japan for treatment of neuropathy associated with diabetes. Unfortunately, several inhibitors such as tolrestat and sorbinil that showed some promise in laboratory and clinical trials have been discarded due to problems associated with efficacy and safety of these drugs. Efforts are still underway to find better inhibitors for aldose reductase that display fewer side effects.

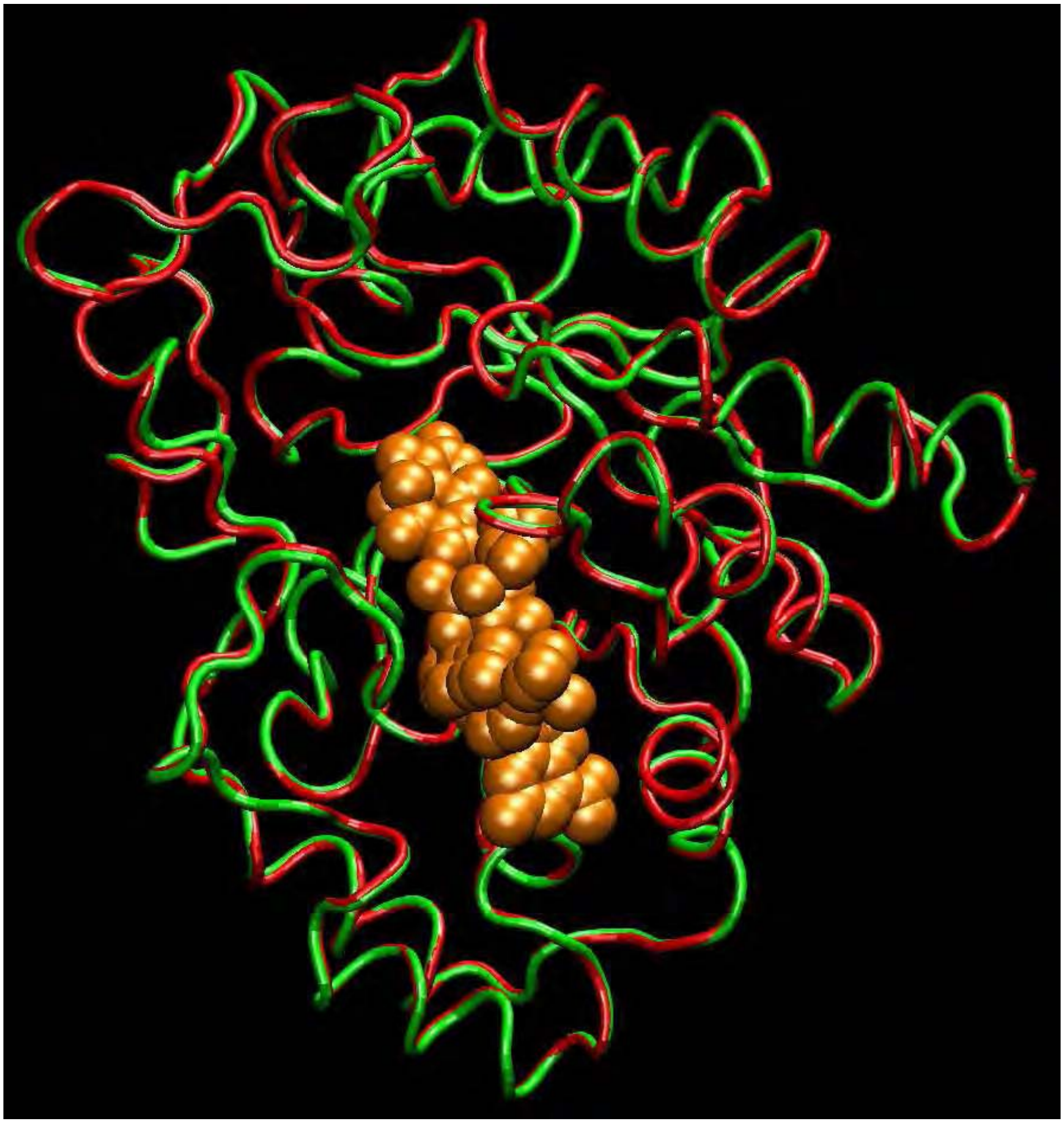

Figure A.3 – Superposition of the unbound (green) and bound (red) forms of aldose reductase. The cofactor NADPH is shown using the orange sphere model. Unlike the other protein models used in the present study, the conformational differences at the backbone level are very small. However, the main changes occur in the binding site region (indicated by B) and play a critical role in determining the binding to inhibitors of different shapes.

Aldose reductase has a molecular weight of approximately 36 KDa. Analysis of the crystal structure of human aldose reductase (Borhani, Harter et al. 1992; Wilson, Bohren et al. 1992) shows that this protein belongs to the family of $(\alpha/\beta)_8$ folding proteins (see Figure A.3). The structure contains eight parallel β-strands forming the core of the barrel with each β-strand alternating with an anti-parallel α-helix. NADPH binds at the carboxy-terminus of the enzyme in an extended conformation, making a total of nineteen hydrogen bonds and three salt links with amino acid residues composing the cofactor binding site.

One of the problems in developing new inhibitors for aldose reductase is that, just like in the case of the other proteins in this study, this enzyme has the capacity to adjust the shape of its binding site depending on the ligand it binds to. As such, a simple small-molecule database screen for potential ligands will miss many potential drug leads if it does not include the protein flexibility in the search process. Several experimental structures of aldose reductase have been solved using X-ray crystallography when bound to different ligands as well as in the unbound form (Figure A.3). It was observed that with some inhibitors such as sorbinil (Urzhumtsev, Tete-Favier et al. 1997), the structure is almost identical to the unbound form. For other inhibitors, such as the tolrestat (Urzhumtsev, Tete-Favier et al. 1997) and zopolrestat (Wilson, Tarle et al. 1993), there is a formation of a specificity pocket resulting in significantly different binding site configurations. This conformational change is shown in A.4 where we compare the shape of the binding site for the unbound form of the enzyme to the bound form with tolrestat. In the unbound form shown on the left of A.4

there are two groups of aminoacids (represented by ball-and-stick models) that come together to close the specificity pocket. In the presence of tolrestat (represented on the right by a van der Waals sphere model) the aminoacids at the top and bottom of the binding site are separated and open the specificity cavity. The movement is caused by both side chain and small backbone rearrangements.

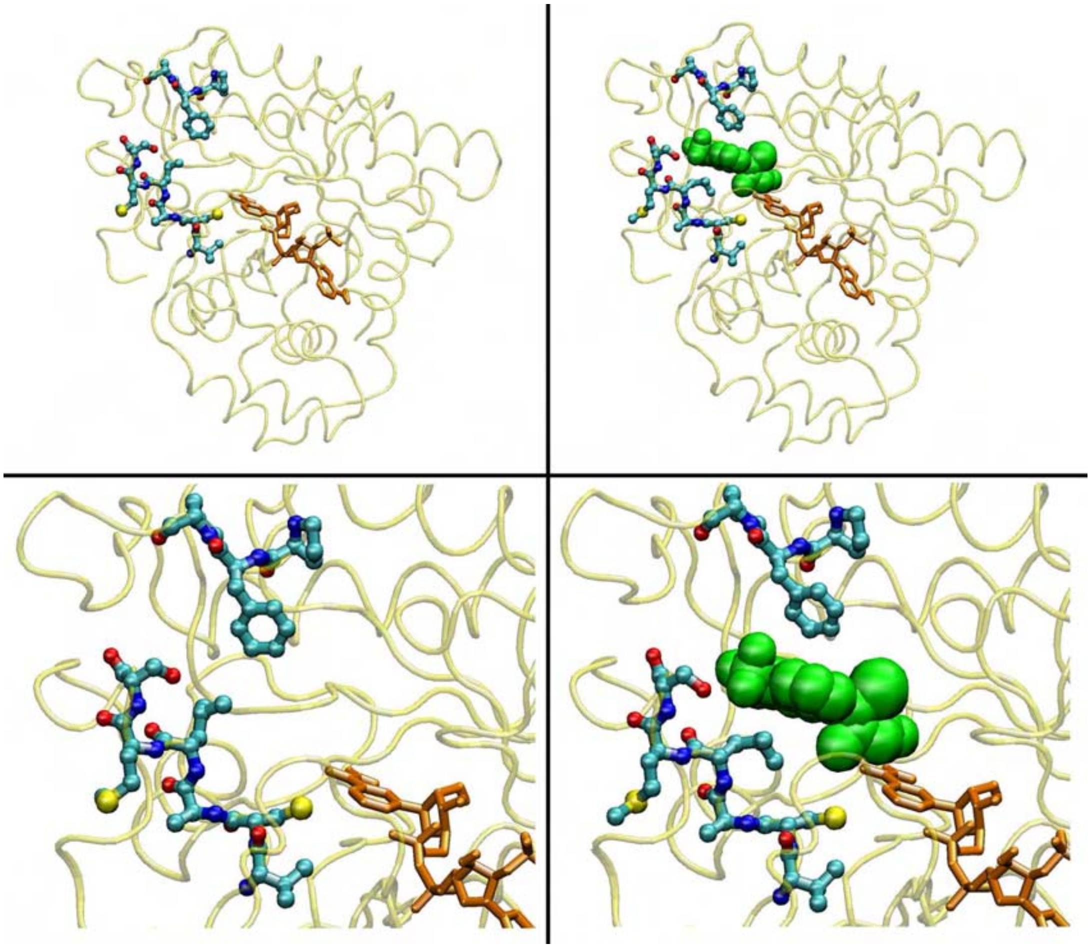

Figure A.4 – Binding site comparison for the unbound and bound forms of aldose reductase. The unbound form of aldose reductase is shown on the left and the bound form is shown on the right. The bottom figures zoom in the corresponding top figures to show aminoacids whose rearrangements open a pocket that make the binding possible. The cofactor NADPH is shown in orange.

A.3. Dihydrofolate Reductase

Dihydrofolate reductase (DHFR) catalyzes the NADPH-dependent reduction of folate to 7,8-dihydrofolate (DHF) and DHF to 5,6,7,8-tetrahydrofolate (THF). In this reaction NADPH is converted to NADP+ and in this process DHFR adds two hydrogens to DHF to create THF. The main biological function of DHFR is to maintain the intracellular concentrations of THF. This molecule is of extreme biochemical importance for living organisms because is essential for the biosynthesis of pyrimidines and purines as well as several amino acids. THF is also a cofactor in a number of one-carbon metabolism processes. Due to its critical role, DHFR has been one of the main targets for structure based drug design. Drugs targeting this protein are used in cancer chemotherapy by inhibiting DNA synthesis in rapidly dividing cancerous cells (Huennekens 1994). The first drug used for cancer chemotherapy was aminopterin. This drug binds to DHFR a thousand times more tightly than folate, therefore blocking the function of the protein. Nowadays, drugs such as methotrexate are most commonly used due to their tighter binding and better clinical characteristics. Additionally, researchers were able to take advantage of small structural differences present in DHFR from different species to developed potent antibacterial drugs (Roth and Stammers 1992). For example, the drug trimethoprim only binds very tightly to the bacterial enzyme.

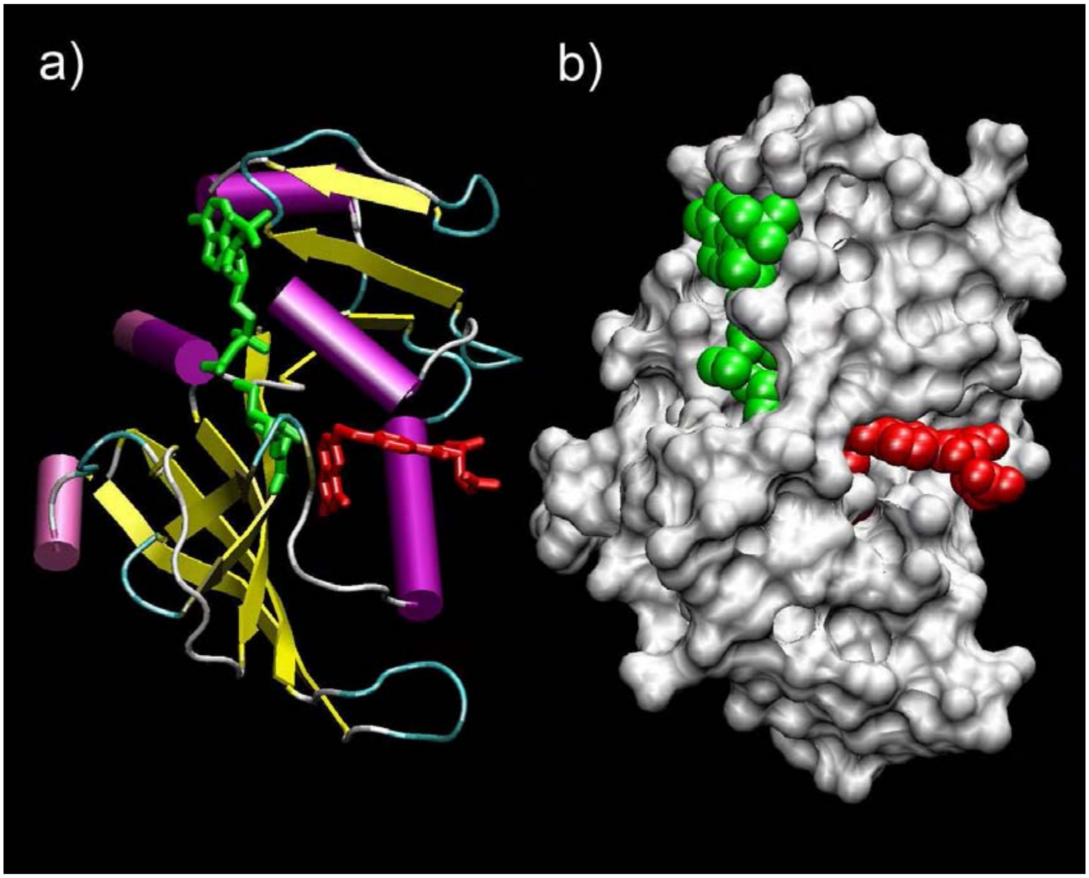

Figure A.5 - Three dimensional structure of DHFR. a) The structure is mostly constituted of β-sheet secondary structure (yellow) and five α-helices (magenta). The position of the large binding site is indicated by the position of the ligands NADPH (green) and folate (red). The two molecules are positioned to facilitate the transfer of hydrogen atoms from NADPH to the folate. b) The surface representation of the protein shows the shape of the binding site and how the catalytic site is protected from the solvent.

DHFR is a monomeric protein with a relatively low molecular weight of approximately 20 kDa. The structure of DHFR consists of 159 amino acid residues which are mostly in a parallel β-sheet conformation. Figure A.5 shows DHFR with α-helices in magenta and beta strands in yellow. The enzyme has a long binding site that binds NADPH at one end and folate at the other. The two molecules are positioned in such a way that transfer of hydrogen atoms from NADPH to the folate is facilitated.

This protein was chosen for this study due to its importance as a clinical target and because it is known to undergo important conformational changes during the binding and release of its substrates. NMR and kinetic studies have shown that DHFR exists in two different unbound conformations (Schweitzer, Dicker et al. 1990; Feeney 2000). The comparison of experimental structures for the bound and unbound forms has revealed structural differences (Cody, Galitsky et al. 1999). Recent computer simulations have also shown that protein flexibility and loop motions were essential to ligand binding, catalysis and release. Figure A.6 shows six different conformations determined experimentally (Sawaya and Kraut 1997) using isomorphous crystal structures for the catalytic cycle of DHFR. The conformations shown correspond to the five detectable kinetic intermediates and to the transition state. These are the holoenzyme, Michaelis complex, ternary product complex, tetrahydrofolate (THF) binary complex, THF•NADPH complex and methotrexate-NADPH complex. Ligands are shown for one of the structures to indentify the binding site. Arrows indicated the regions near the binding site which display the largest amount of variation.

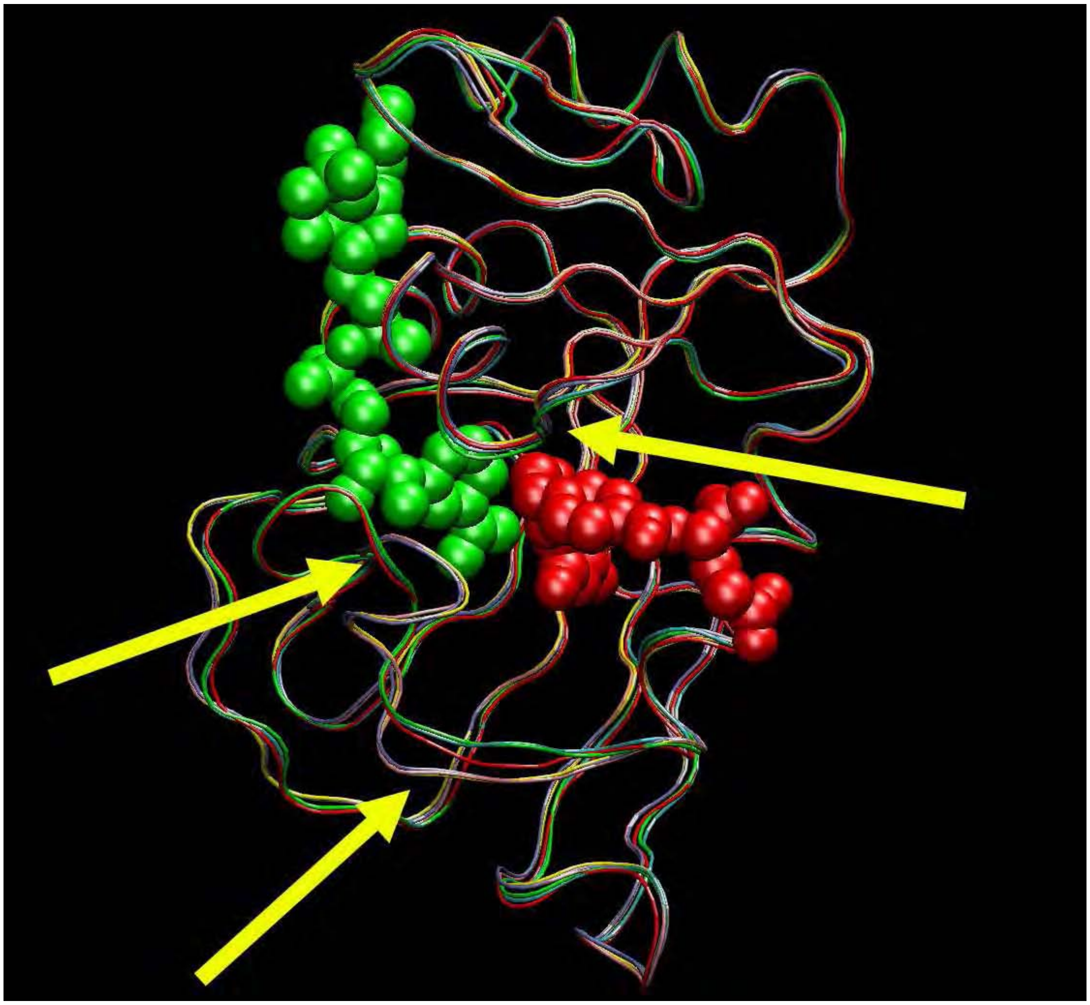

Figure A.6 – Conformational changes during the catalytic cycle of DHFR. The conformations shown in tube representation correspond to the five detectable kinetic intermediates and to the transition state. The location of the binding site is indicated by the VDW representation of NADPH (green) and folate (red). Yellow arrows indicated the regions near the binding site that display the largest amount of variation.

A.4. Maltose Binding Protein

Maltose binding protein exists in the periplasm of Gram-negative bacteria, plays a fundamental role in active transport and also serves as a receptor for chemotaxis. This protein is able to bind maltose, other linear maltodextrins, and cyclodextrins with high affinity, but it binds glucose with low affinity. These maltooligosaccharides traverse the outer bacterial membrane through specific channels (maltoporin LamB) and bind to maltose binding protein. The bound protein then interacts with several components of the cytoplasmatic membrane (MalF, MalG and two molecules of MalK) and initiates the active transport of nutrients across the membrane by hydrolyzing ATP.

The three-dimensional structures of MBP, both bound (Spurlino, Lu et al. 1991) and unbound (Sharff, Rodseth et al. 1992) to maltose, have been determined by X-ray crystallography to 1.8 and 2.3 Å respectively. Maltose binding protein (shown in Figures A.7 and A.8) is a monomeric protein with a molecular weight of 40.6 kDa. The structure of this protein consists of two different globular domains that are separated by a large cleft that forms the binding site. Upon ligand binding, the cleft region acts as an hinge by bringing the two domains close together. The conformational change of maltose binding protein upon addition of maltose has been detected in solution using different experimental methods such as fluorescence (Szmelcman, Schwartz et al. 1976; Hall, Gehring et al. 1997), electron paramagnetic resonance (Hall, Thorgeirsson et al. 1997), small-angle X-rayscattering (Shilton, Flocco et al. 1996), and NMR (Gehring, Zhang et al. 1998). The large conformational rearrangement corresponds almost exclusively to changes in the binding site region. The overall structures of the globular domains stay mostly unchanged. This can be observed in Figure A.7 where the structures of the bound and unbound forms are shown superimposed. The domain displayed on the bottom was used for fitting using a least squares procedure. The conformational rearrangement upon binding for this protein is the largest of all the proteins used as models in this work. As shown in Figure A.7 the atomic displacements for the residues shown at the top of the structure are approximately 15Å. In the unbound form of this protein the binding cleft is exposed to the solvent. Due to the large conformational rearrangement the ligand is engulfed in a tight binding cavity. This dramatic change in solvent exposure of the binding site region is clearly visible in Figure A.8. The binding motion in maltose binding protein is a critical part of its function. Current models for the function of this protein (Duan, Hall et al. 2001) postulate that the closed form of the protein is preferentially recognized by the membrane components responsible for transport and chemotaxis functions.

Although this protein has not been used as a target for structure-based drug design we decided to include maltose binding protein in this study in order to test the dimensional reduction method with larger proteins that undergo large conformational rearrangements.

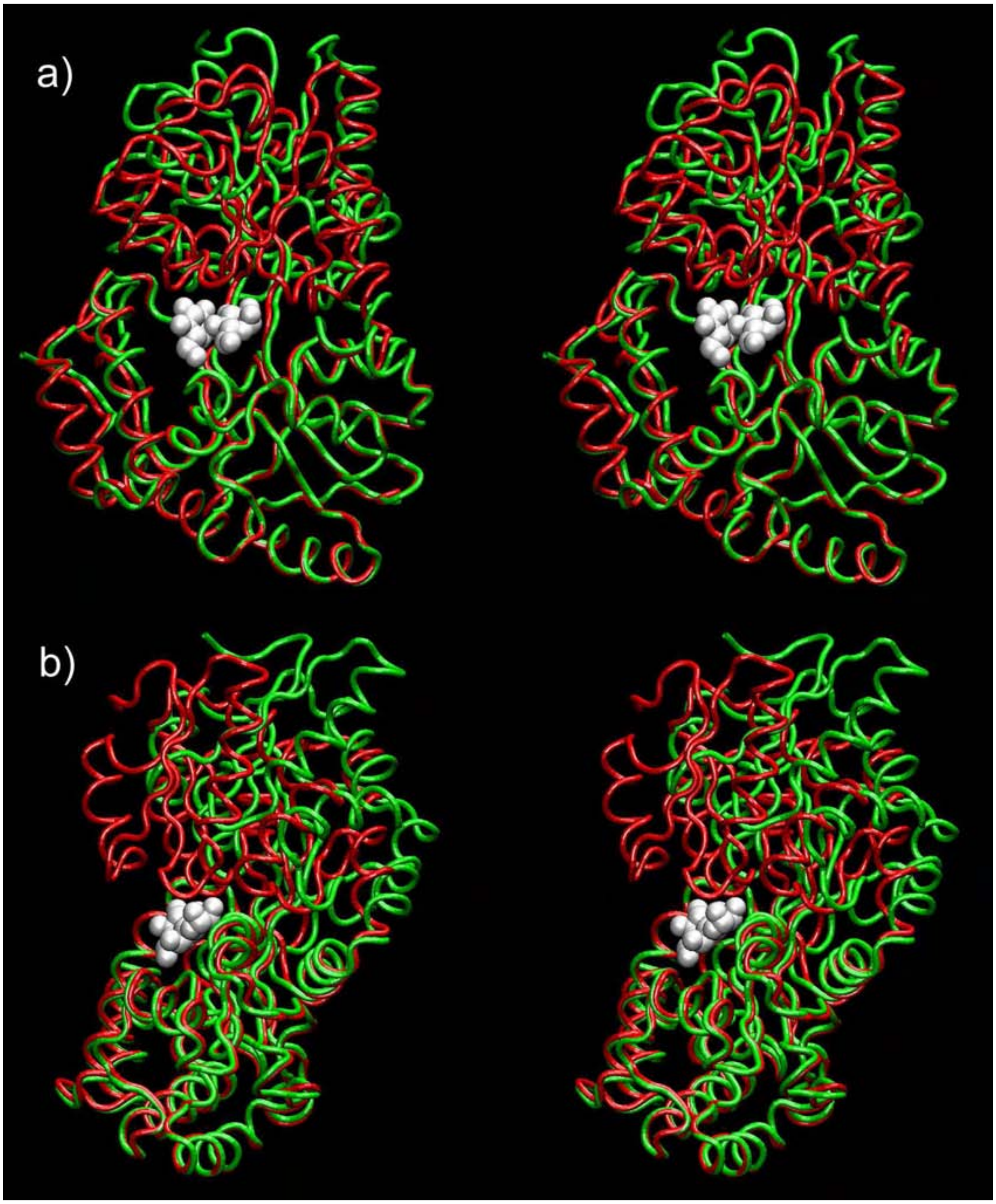

Figure A.7 – a) Front and b) side stereoviews of maltose binding protein. The bound form is shown in red and the unbound form in green. The position of the ligand for the bound structure is shown using the sphere model (white). When the protein binds the ligand the structure bends around an hinge point situated approximately in the center of the protein.

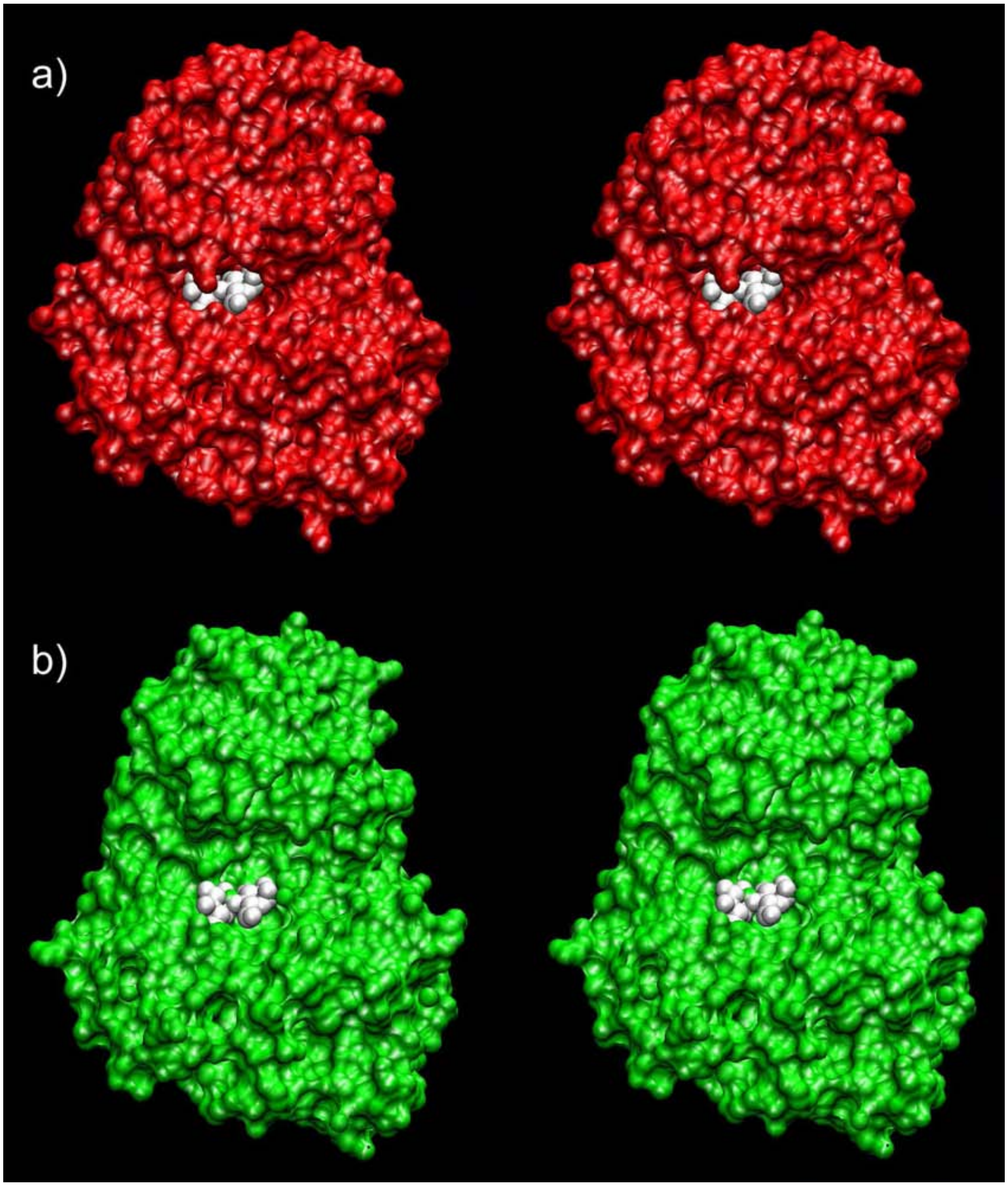

Figure A.8 – Surface representation for the a) bound and b) unbound forms of maltose binding protein (the ligand is shown in the unbound form for comparison purposes). After binding maltose the two domains close around a hinge in the center of the protein and change the solvent exposure of the binding site.

Appendix B.

HIV-1 Protease Structures

System	PDB File	HIVdb File	Company or Laboratory	Year	Inhibitor (Type)
(ARV2/SF2 isolate) unliganded	3hvp	hiv2nci	ABL-BRP, NCI Frederick	1989	N/A
(HXB2 isolate) unliganded	3phv	hiv1bcl	Birkbeck College, Laboratory of Molecular Biology, London	1989	N/A
(synthetic enzyme) with inhibitor MVT101	4hvp	hiv3nci	ABL-BRP, NCI Frederick	1989	MVT101 (Reduced amide isostere)
(BH10 isolate) with inhibitor A74704	9hvp	hiv1abb	Abbott Laboratories Dept. of CAMD	1990	A74704 (hydroxyethylene isostere)
(synthetic enzyme) with inhibitor JG365	7hvp	hiv4nci	ABL-BRP, NCI Frederick	1990	JG365 (hydroxyethylamine isostere)
(NY5 isolate) with acetyl-pepstatin	5hvp	hiv2msd	Merck Sharp and Dohme Res. Lab	1990	(Statine izostere)
(NY5 isolate) with pseudo C2 - symmetry inhibitor L-700,417	4phv	hiv3msd	Merck Sharp and Dohme Res. Lab	1991	L-700,417 (hydroxyethylene isostere)
(synthetic enzyme) with inhibitor U-85548E	8hvp	hiv7nci	ABL-BRP, NCI Frederick	1991	U-85548E (hydroxyethylene isostere)
(BRU isolate) unliganded	1hhp	hiv1pip	Institut Pasteur, Paris	1991	N/A
(BH10 isolate) with inhibitor SKF 108738	1hef	hiv1skb	SmithKline Beecham Pharmaceuticals	1992	SKF 108738 (hydroxyethylene isostere)

System	PDB File	HIVdb File	Company or Laboratory	Year	Inhibitor (Type)
(BH10 isolate) with inhibitor SKF 107457	1heg	hiv2skb	SmithKline Beecham Pharmaceuticalss	1992	SKF 107457 (hydroxyethylene isostere)
(BH10 isolate) with hydroxyethylene inhibitor	1aaq	hiv3skb	SmithKline Beecham Pharmaceuticalss	1992	(hydroxyethylene isostere)
(isolate unknown) with dihydroxyethylene inhibitor U75875	1hiv	hiv8nci	ABL-BRP, NCI Frederick	1992	U75875 (dihydroxyethylene isostere)
(BH10 isolate) with C2 - symmetric phosphinate inhibitor	1hos	hiv4skb	SmithKline Beecham Pharmaceuticalss	1993	SB204144 (perfectly symmetrical phosphinate inhibitor)
(BH10 isolate) with penicillin - derived C2 - symmetric inhibitor	1hte	hiv1glx	Glaxo Group Research Limited	1993	GR123976 (penicillin-derived C2-symmetric inhibitor)
(BH10 isolate) with penicillin - derived C2 - symmetric inhibitor	1htf	hiv2glx	Glaxo Group Research Limited	1993	GR126045 (penicillin-derived C2-symmetric inhibitor)
(BH10 isolate) with inhibitor SB206343	1hps	hiv6skb	SmithKline Beecham Pharmaceuticalss	1994	SB 206343 (hydroxyethylene isostere)
(NY5 isolate) with inhibitor L-735,524 (MK639) [CRIXIVAN (Indinavir)]	1hsg	hiv4msd	Merck & Co., Inc.	1994	L-735,524; MK-639, Indinavir,Crixivan (hydroxyethylene isostere)
(BH10 isolate) with inhibitor SB 203386	1sbg	hiv7skb	SmithKline Beecham Pharmaceuticalss	1994	SB 203386 (hydroxyethylene isostere)

System	PDB File	HIVdb File	Company or Laboratory	Year	Inhibitor (Type)
(BH10 isolate) with C2 - symmetry - based diol inhibitor A77003(R,S)	1hvi	hiv9nci	SAIC, NCI Frederick	1994	A77003 (C2 symmetry-based diol isostere)
(BH10 isolate) with C2 - symmetry - based diol inhibitor A78791(S,-)	1hvj	hiv10nci	SAIC, NCI Frederick	1994	A78791(C2 symmetry-based diol isostere)
(BH10 isolate) with C2 - symmetry - based diol inhibitor A76928(S,S)	1hvk	hiv11nci	SAIC, NCI Frederick	1994	A76928(C2 symmetry-based diol isostere)
(BH10 isolate) with C2 - symmetry - based diol inhibitor A76889(R,R)	1hvl	hiv12nci	SAIC, NCI Frederick	1994	A76889(C2 symmetry-based diol isostere)
(BH10 isolate) with penicillin - derived inhibitor GR137615	1htg	hiv3glx	Glaxo Group Research Limited	1994	GR137615 (penicillin-derived inhibitor)
(LAI isolate) with inhibitor A76928	1hvc	hiv13nci	SAIC, NCI Frederick	1994	A76928 (C2 symmetry-based diol isostere (S,S))
(BH5 isolate) with nonpeptide cyclic ureas as inhibitor XK263	1hvr	hiv1dpm	DuPont Merck Pharmaceuticals Company	1994	XK263 (nonpeptidic ureas inhibitor)
(BH10 isolate) with inhibitor SB203238	1hbv	hiv8skb	SmithKline Beecham Pharmaceuticalss	1995	SB203238 (reduced amide isostere)
(BRU isolate) with inhibitor CGP 53820	1hih	hiv1cgp	Ciba-Geigy Pharmaceuticals Ltd.	1995	CGP53820 (hydroxyethylene isostere)

System	PDB File	HIVdb File	Company or Laboratory	Year	Inhibitor (Type)
(BRU isolate) with inhibitor VX-478,Amprenavir	1hpv	hiv1vpi	Vertex Pharmaceuticalss Incorporated	1995	VX-478;141W94; Amprenavir; Agenerase® (hydroxyethylene isostere,amino sulfonamide inhibitor)
(BH5 isolate) V82A mutant with inhibitor A77003	1hvs	hiv14nci	SAIC, NCI Frederick	1995	A77003 (C2 symmetry-based diol isostere (R,S))
(BRU isolate) with allophenylnorstatine inhibitor KNI - 272	1hpx	hiv15nci	SAIC, NCI Frederick	1995	KNI-272 (allophenylnorstatine analog)
(ARV2/SF2 isolate) with cyclic peptide inhibitor	1cpi	hiv1uba	University of Queensland, Australia	1995	(cyclic peptidomimetic inhibitor)
(BH5 isolate) complex with inhibitor U095438	1upj	hiv5ulk	Upjohn Company, Kalamazoo	1995	U095438 (carboxamide-containing 4-hydroxycoumarin inhibitor)
(BH5 isolate) complex with inhibitor U100313	2upj	hiv6ulk	Upjohn Company, Kalamazoo	1995	U100313 (4-hydroxy-2-pyrones inhibitor)
(unknown isolate) with a difluoroketone containing inhibitor A79285	1dif	hiv16nci	SAIC, NCI Frederick	1996	A79285 (difluoroketone isostere)
(HXB2 isolate) with DMP323, a novel cyclic urea - type inhibitor (mutation C95A)	1bve	hiv1nid	NIDR Bethesda,MD	1996	DMP323 (urea-type inhibitor)
(HXB2 isolate) with DMP323, a novel cyclic urea - type inhibitor (mutation C95A)	1bvg	hiv2nid	NIDR Bethesda,MD	1996	DMP323 (urea-type inhibitor)

System	PDB File	HIVdb File	Company or Laboratory	Year	Inhibitor (Type)
(PV22 isolate) mutant (V82D) with U89360E, a peptidic inhibitor	1gnm	hiv1uoc	University of Oklahoma	1996	U89360E (peptidic inhibitor)
(PV22 isolate) mutant (V82N) with U89360E, a peptidic inhibitor	1gnn	hiv2uoc	University of Oklahoma	1996	U89360E (peptidic inhibitor)
(PV22 isolate) wild type with U89360E, a peptidic inhibitor	1gno	hiv3uoc	University of Oklahoma	1996	U89360E (peptidic inhibitor)
(ARV2/SF2 isolate) (mutant) complexed with a cyclic Phe - Ile - Val peptidomimetic inhibitor	1mtr	hiv2uba	University of Queensland, Australia	1996	Phe-Ile-Val (cyclic peptidomimetic inhibitor)
(Z2 isolate) dimer complex with inhibitor A-98881	1pro	hiv2abb	Abbott Laboratories Dept. of CAMD	1996	A-98881 (urea-type inhibitor)
(HXB-3 isolate) complex with inhibitor RO 31-8959 [INVIRASE (saquinavir)]	1hxb	hiv1hlr	Hoffmann-La Roche	1996	RO 31-8959, saquinavir;Invirase® ; Fortovase®; hydroxyethylamine isostere
(HXB-2 isolate) complex with inhibitor BMS-182193	1odw	hiv17nci	ABL-BRP, NCI Frederick	1996	BMS-182193 aminodiol isostere
(HXB-2 isolate) mutant A71T, V82A with inhibitor BMS-182193	1odx	hiv18nci	ABL-BRP, NCI Frederick	1996	BMS-182193 aminodiol isostere
(SF-2 strain) mutant Q7K with peptide product	1ytg	hiv2ucs	University of CaliforniaSan Francisco	1996	peptide product

System	PDB File	HIVdb File	Company or Laboratory	Year	Inhibitor (Type)
(SF-2 strain) mutant Q7K with peptide product	1yth	hiv3ucs	University of CaliforniaSan Francisco	1996	peptide product
(BH102 isolate) with inhibitor DMP450	1dmp	hiv14dpm	DuPont Merck Pharmaceuticals Company	1996	DMP 450
(BH10 isolate) with cyclic sulfoamide inhibitor AHA006	1ajv	hiv1upp	Uppsala University, Sweden	1997	AHA006 cyclic sulfoamide
(BH10 isolate) with cyclic sulfoamide inhibitor AHA001	1ajx	hiv2upp	Uppsala University, Sweden	1997	AHA001 cyclic urea inhibitor
(SF1 isolate) with a nonpeptide inhibitor THK	1aid	hiv6ucd	University of California San Francisco	1997	THK nonpeptidic inhibitor
with inhibitor A-84538,ABT-538 [NORVIR (Ritonavir)]	1hxw	hiv3abb	Abbott Laboratories	1997	A-84538,ABT-538
(BH102 strain) I84V mutations with inhibitor DMP450	1mer	hiv6dpm	DuPont Merck Pharmaceuticals Company	1997	DMP-450
(BH102 strain) I84V mutations with inhibitor DMP323	1mes	hiv7dpm	DuPont Merck Pharmaceuticals Company	1997	DMP-323
(BH102 strain) V82F mutations with inhibitor DMP323	1met	hiv8dpm	DuPont Merck Pharmaceuticals Company	1997	DMP-323
(BH102 strain) V82F,I84V mutations with inhibitor DMP323	1meu	hiv9dpm	DuPont Merck Pharmaceuticals Company	1997	DMP-323

System	PDB File	HIVdb File	Company or Laboratory	Year	Inhibitor (Type)
(BH102 strain) with cyclic urea amide inhibitor	1qbr	hiv15dpm	DuPont Merck Pharmaceuticals Company	1997	cyclic urea amide inhibitor
(BH102 strain) with cyclic urea amide inhibitor	1qbs	hiv16dpm	DuPont Merck Pharmaceuticals Company	1997	cyclic urea amide inhibitor
(BH102 strain) with cyclic urea amide inhibitor	1qbt	hiv17dpm	DuPont Merck Pharmaceuticals Company	1997	cyclic urea amide inhibitor
(BH102 strain) with cyclic urea amide inhibitor	1qbu	hiv18dpm	DuPont Merck Pharmaceuticals Company	1997	cyclic urea amide inhibitor
(SF2 strain) with a nonpeptide inhibitor	2aid	hiv7ucs	University of California San Francisco	1997	nonpeptide inhibitor
(SF strain) Q7K mutant with an aminimide peptide isostere inhibitor	3aid	hiv8ucs	University of California San Francisco	1997	aminimide peptide isostere inhibitor
(isolate unknown) complexed with AG-1343[Viracept (Nelfinavir)]	1ohr	hiv19aug	Agouron Pharmaceuticals	1997	Nelfinavir Mesylate
(HXB2 isolate) with a hydrophylic tripeptide inhibitor Glu-Asp-Leu	1a30	hiv1nih	National Institute of Health Bethesda	1998	GLU-ASP-LEU hydrophylic tripeptide inhibitorderived from the transframe region of Gag-Pol
G48H mutant with inhibitor U-89360E	1a9m	hiv4uoc	University of Oklahoma	1998	U-89360E
(K7Q, I33L,I63L mutant) with an analog of the conserved Ca-P2 substrate	1a8k	hiv1tju	Thomas Jefferson University Philadelphia	1998	N/A

System	PDB File	HIVdb File	Company or Laboratory	Year	Inhibitor (Type)
T31S, V32I, L33V, E34A, E35G, M36I, S37E mutations with inhibitor SB203386	1bdl	hiv10skb	SmithKline Beecham Pharmaceuticalss	1998	SB203386
T31S, V32I, L33V, E34A, E35G, M36I, S37E, I47V,V82I mutations with inhibitor SB203386	1bdq	hiv11skb	SmithKline Beecham Pharmaceuticalss	1998	SB203386
T31S, L33V, E34T, E35G, M36I, S37E mutations with inhibitor SB203386	1bdr	hiv12skb	SmithKline Beecham Pharmaceuticalss	1998	SB203386
(BH102 strain) I82F, C95A mutations with inhibitor SD146	1bv7	hiv10dpm	DuPont Merck Pharmaceuticals Company	1998	SD146
(BH102 strain) I84V,C95A mutations with inhibitor XV638 (cyclic urea inhibitor)	1bv9	hiv11dpm	DuPont Merck Pharmaceuticals Company	1998	XV638
V82F, I84V mutations with inhibitor XV638 (cyclic urea inhibitor)	1bwa	hiv12dpm	DuPont Merck Pharmaceuticals Company	1998	XV638
(BH102 strain) V82F, I84V mutations with inhibitor SD146	1bwb	hiv13dpm	DuPont MerckPharmaceuticalsCompany	1998	SD146
A28S mutant, with inhibitor U89360E	1axa	hiv5uoc	University of Oklahoma	1999	U89360E
(BH102 strain) with inhibitor Q8261	1hvh	hiv19dpm	DuPont Merck Pharmaceuticals Company	1999	Q8261, Nonpeptide Cyclic Cyanoguanidines

System	PDB File	HIVdb File	Company or Laboratory	Year	Inhibitor (Type)
(BH102 strain) with inhibitor XK216	1hwr	hiv20dpm	DuPont Merck Pharmaceuticals Company	1999	XK216
(HXB2 isolate) with inhibitor LP-130	1ody	hiv20nci	ABL-BRP, NCI Frederick	1999	LP-130
(NY5 isolate) with inhibitor L-738,317	2bpv	hiv12msd	Merck Sharp and Dohme Res. Lab	1999	L-738,317
(NY5 isolate) with inhibitor L-738,317	2bpw	hiv13msd	Merck Sharp and Dohme Res. Lab	1999	L-738,317
(NY5 isolate) with inhibitor L-735,524	2bpx	hiv14msd	Merck Sharp and Dohme Res. Lab	1999	L-735,524,MK-639,Indinavir,Crixivan
(NY5 isolate) with inhibitor L-739,622	2bpy	hiv15msd	Merck Sharp and Dohme Res. Lab	1999	L-739,622
(NY5 isolate) with inhibitor L-739,622	2bpz	hiv16msd	Merck Sharp and Dohme Res. Lab	1999	L-739,622
(synthetic construct SF isolate) with macrocyclic peptidomimetic inhibitor	1d4k	hiv3uba	University of Queensland,Australia	1999	PI9
(synthetic construct SF isolate) mutant with macrocyclic peptidomimetic inhibitor	1d4l	hiv4uba	University of Queensland,Australia	1999	PI9
V82F/I84V Double Mutant/Tipranavir Complex	1d4s	hiv23ulk	Upjohn Company, Kalamazoo	1999	U-140690; PNU-140690;Tipranavir
Q7K, L33I, L63I Triple Mutant/Tipranavir Complex	1d4y	hiv24ulk	Upjohn Company, Kalamazoo	1999	U-140690; PNU-140690;Tipranavir

System	PDB File	HIVdb File	Company or Laboratory	Year	Inhibitor (Type)
(isolate unknown) with inhibitor RO31-8558	N/A	hiv2hlr	Hoffmann-La Roche	1991	RO31-8558 hydroxyethylamine isostere
(isolate unknown) with inhibitor AG1001	N/A	hiv1aug	Agouron Pharmaceuticals	1991	AG1001
(isolate unknown) with inhibitor AG1002	N/A	hiv2aug	Agouron Pharmaceuticals	1991	AG1002
(isolate unknown) with inhibitor AG1004	N/A	hiv3aug	Agouron Pharmaceuticals	1991	AG1004
(isolate unknown) with inhibitor LILLY765	N/A	hiv1lll	Lilly Pharmaceuticals	1991	LILLY765
(isolate unknown) with inhibitor I-BMS-01	N/A	hiv1bms	Bristol-Myers Squibb	1993	I-BMS-01
(isolate unknown) with inhibitor I-BMS-02	N/A	hiv2bms	Bristol-Myers Squibb	1993	I-BMS-02
mutant C95A (BH102 isolate) with inhibitor DMP323	N/A	hiv2dpm	DuPont Merck Pharmaceuticals Company	1996	DMP323 urea based inhibitor
mutant C95A (BH102 isolate) with inhibitor Q8467	N/A	hiv3dpm	DuPont Merck Pharmaceuticals Company	1997	Q8467 cyclic urea amid inhibitor
mutant C95A (BH102 isolate) with inhibitor XV638	N/A	hiv4dpm	DuPont Merck Pharmaceuticals Company	1997	XV638 cyclic urea amid inhibitor
mutant C95A (BH102 isolate) with inhibitor SD146	N/A	hiv5dpm	DuPont Merck Pharmaceuticals Company	1997	SD146 cyclic urea amid inhibitor

System	PDB File	HIVdb File	Company or Laboratory	Year	Inhibitor (Type)
(isolate unknown) with inhibitor	N/A	hiv4glx	Glaxo Group Research Limited	1991	GR-XXXX
(ROD isolate) with inhibitor L-689,502	N/A	hiv7msd	Merck Sharp and Dohme Res. Lab	1992	L-689,502
(BH-10 isolate) with inhibitor MDL 104,168	N/A	hiv1mmd	MMDRI, France	1993	MDL 104,168 difluorostatone inhibitor
(BH-10 isolate) with inhibitor MDL 73,669	N/A	hiv2mmd	MMDRI, France	1993	MDL 73,669 difluorostatone inhibitor
(BH-10 isolate) with inhibitor MDL 73,730	N/A	hiv3mmd	MMDRI, France	1993	MDL 73,730 difluorostatone inhibitor
(BH-10 isolate) with inhibitor MDL 73,881	N/A	hiv4mmd	MMDRI, France	1993	MDL 73,881 difluorostatone inhibitor
(BH-10 isolate) with inhibitor MDL 73,915	N/A	hiv5mmd	MMDRI, France	1993	MDL 73,915 difluorostatone inhibitor
(BH-10 isolate) with inhibitor MDL 74,538	N/A	hiv6mmd	MMDRI, France	1993	MDL 74,538difluorostatone inhibitor
(BH-10 isolate) with inhibitor MDL 75,635	N/A	hiv7mmd	MMDRI, France	1993	MDL 75,635difluorostatone inhibitor
(BH-10 isolate) with inhibitor MDL 75,305	N/A	hiv8mmd	MMDRI, France	1993	MDL 75,305difluorostatone inhibitor
(BH-10 isolate) with inhibitor AHA004	N/A	hiv3upp	Uppsala University, Sweden	1997	AHA004 cyclic urea inhibitor
(BH-10 isolate) with inhibitor AHA009	N/A	hiv4upp	Uppsala University, Sweden	1997	AHA009 sulfoamide inhibitor

System	PDB File	HIVdb File	Company or Laboratory	Year	Inhibitor (Type)
(BH5 isolate) with inhibitor U101935	7upj	hiv11ulk	Upjohn Company, Kalamazoo	1997	U101935
(triple mutant Q7K/L33I/L63I) with inhibitor U103265	1hpo	hiv12ulk	Upjohn Company, Kalamazoo	1997	U103265
(isolate unknown) with inhibitor L-738816	N/A	hiv8msd	Merck Sharp and Dohme Res. Lab	1997	L-738,816
(isolate unknown) with inhibitor L-739622	N/A	hiv9msd	Merck Sharp and Dohme Res. Lab	1997	L-739,622
(isolate unknown) with inhibitor L-771786	N/A	hiv10msd	Merck Sharp and Dohme Res. Lab	1997	L-771,786
(isolate unknown) with inhibitor AP248	N/A	hiv11msd	Merck Sharp and Dohme Res.Lab	1997	AP248
(isolate unknown) with cyclopropan peptidomimetic inhibitor	N/A	hiv19nci	SAIC, NCI Frederick	1998	cyclopropan peptidomimetic inhibitor
with inhibitor U104661	N/A	hiv18ulk	Upjohn Company, Kalamazoo	1998	U104661
with inhibitor U101935	N/A	hiv19ulk	Upjohn Company, Kalamazoo	1998	U101935
with inhibitor U101935	N/A	hiv20ulk	Upjohn Company, Kalamazoo	1998	U101935
(triple mutant Q7K/L33I/L63I) with inhibitor U103695	N/A	hiv21ulk	Upjohn Company, Kalamazoo	1998	U103695

System	PDB File	HIVdb File	Company or Laboratory	Year	Inhibitor (Type)
(triple mutant Q7K/L33I/L63I) with inhibitor U102812	N/A	hiv22ulk	Upjohn Company, Kalamazoo	1998	U102812
(isolate unknown) with inhibitor AG1174	N/A	hiv5aug	Agouron Pharmaceuticals	1999	AG1174
(isolate unknown) with inhibitor AG1204	N/A	hiv6aug	Agouron Pharmaceuticals	1999	AG1204
(isolate unknown) with inhibitor AG1216	N/A	hiv7aug	Agouron Pharmaceuticals	1999	AG1216
(isolate unknown) with inhibitor AG1220	N/A	hiv8aug	Agouron Pharmaceuticals	1999	AG1220
(isolate unknown) with inhibitor AG1221	N/A	hiv9aug	Agouron Pharmaceuticals	1999	AG1221
(isolate unknown) with inhibitor AG1225	N/A	hiv10aug	Agouron Pharmaceuticals	1999	AG1225
(isolate unknown) with inhibitor AG1232	N/A	hiv11aug	Agouron Pharmaceuticals	1999	AG1232
(isolate unknown) with inhibitor AG1235	N/A	hiv12aug	Agouron Pharmaceuticals	1999	AG1235
(isolate unknown) with inhibitor AG1240	N/A	hiv13aug	Agouron Pharmaceuticals	1999	AG1240
(isolate unknown) with inhibitor AG1254	N/A	hiv14aug	Agouron Pharmaceuticals	1999	AG1254

System	**PDB File**	**HIVdb File**	**Company or Laboratory**	**Year**	**Inhibitor (Type)**
(isolate unknown) with inhibitor AG1256	N/A	hiv15aug	Agouron Pharmaceuticals	1999	AG1256
(isolate unknown) with inhibitor AG1274	N/A	hiv16aug	Agouron Pharmaceuticals	1999	AG1274
(isolate unknown) with inhibitor AG1276	N/A	hiv17aug	Agouron Pharmaceuticals	1999	AG1276
(isolate unknown) with inhibitor AG1284	N/A	hiv18aug	Agouron Pharmaceuticals	1999	AG1284

Table B.1. – HIV-1 protease structures used for the PCA analysis (note: Data was obtained from the HIV Protease Database (http://srdata.nist.gov/hivdb/)).

Appendix C.

Molecular Modeling and Rigid Protein Docking

C.1. Molecular Modeling

A molecule is characterized by a pair (A; B), in which A represents a collection of atoms, and B represents a collection of bonds between pairs of atoms. Information used for kinematic and energy computations is associated with each of the atoms and bonds. Each atom carries standard information, such as its van der Waals radius. Three pieces of information are associated with each bond: (i) bond length, is the distance between atom centers; (ii) bond angle, is the angle between two consecutive bonds; (iii) whether the bond is rotatable or not. Since bond lengths and angles do not change significantly, it is common practice to consider them fixed. Thus the degrees of freedom of the molecule arise from the rotatable bonds. The three dimensional embedding of a molecule defined when we assign values to its rotatable bonds is called the conformation of the molecule. Ligands typically have 3-15 rotatable bonds, while receptors have 1,000-2,000 rotatable bonds. The dimension of the combined search space makes the docking problem computationally intractable.

One key aspect of molecular modeling is calculating the energy of conformations and interactions. This energy can be calculated with a wide range of methods ranging from quantum mechanics to purely empirical energy functions. The accuracy of these functions is usually proportional to its computational expense and choosing the correct energy calculation method is highly dependent on the application. Computation times for different methods can range from a few milliseconds on a workstation to several days on a supercomputer.

In the context of docking, energy evaluations are usually carried out with the help of a scoring function and developing these is a major challenge facing structure based drug design (Vieth, Hirst et al. 1998; Muegge and Rarey 2001; Halperin, Ma et al. 2002). No matter how efficient and accurate the geometric modeling of the binding process is, without good scoring functions it is impossible to obtain correct solutions. The two main characteristics of a good scoring function are selectivity and efficiency. Selectivity enables the function to distinguish between correctly and incorrectly docked structures and efficiency enables the docking program to run in a reasonable amount of time.

A large number of current scoring functions are based on forcefields that were initially designed to simulate the function of proteins (Cornell, Cieplak et al. 1995; MacKerell, Bashford et al. 1998). A forcefield is an empirical fit to the potential energy surface in which the protein exists and is obtained by establishing a model with a combination of bonded terms (bond distances, bond angles, torsional angles, etc.) and non-bonded terms (van der Waals and electrostatic). The relative contributions of these terms are adjusted for the different types of atoms in the simulated molecule by adjusting a series of empirical parameters. Some scoring functions used in molecular docking have been adapted to include terms such as solvation and entropy (Morris, Goodsell et al. 1998). A separate approach is to use statistical scoring functions that are derived using experimental data (Muegge and Martin 1999).

C.2. Rigid Protein Docking

Most of the docking methods used at the present moment in academic and industrial research assume a rigid protein. To illustrate the methodology used by these methods we will briefly discuss three of the most common programs used for docking: Autodock (Morris, Goodsell et al. 1998), Dock (Ewing and Kuntz 1997) and FlexX (Kramer, Rarey et al. 1999).

Autodock uses a kinematic model for the ligand based on rotations around single bonds. The ligand begins the search process randomly outside the binding site and by exploring the values for translations, rotations and its internal degrees of freedom, it will eventually reach the bound conformation. Distinction between good and bad docked conformations is carried out by the scoring function. Autodock is able to use Monte Carlo methods or simulated annealing (SA) in the search process and in its last version introduced the ability to use genetic algorithms (GA). The routine implemented in the recent release is a Lamarkian genetic algorithm (LGA), in which a traditional GA is used for global search and is combined with a Solis and Wets local search procedure. Morris *et al* show that the new LGA is able to handle ligands with a larger number of degrees of freedom than SA or traditional GA.

FlexX and Dock both use an incremental construction algorithm which attempts to reconstruct the bound ligand by first placing a rigid anchor in the binding site and later using a greedy algorithm to add fragments and complete the ligand structure. Although these programs are more efficient than Autodock in the sense that they require fewer energy evaluations there exist some tradeoffs. One of main problems is that it is not trivial to choose the anchor fragment and its choice will determine what solutions can be obtained. Also the greedy algorithm propagates errors resulting from initial bad choices that lead to missing final conformations of lower energy.

In order to solve the docking problem conformation methods using standard robotics techniques such as probabilistic roadmap planning have been recently described[8,9]. In addition to being successful in finding the correct docking conformation these methods are useful in identifying possible binding sites and in providing a computational efficient description of the dynamics of ligand binding.

References

Abseher, R. and Nilges, M. (1998). "Are there non-trivial dynamic cross-correlations in proteins?" Journal of Molecular Biology **279**(4): 911-20.

Abseher, R. and Nilges, M. (2000). "Efficient sampling in collective coordinate space." Proteins: Structure, Function, and Genetics **39**(1): 82-8.

Althaus, E., Kohlbacher, O., Lenhof, H. P. and Muller, P. (2002). "A combinatorial approach to protein docking with flexible side chains." Journal of Computational Biology **9**(4): 597-612.

Amadei, A., Ceruso, M. A. and Di Nola, A. (1999). "On the convergence of the conformational coordinates basis set obtained by the essential dynamics analysis of proteins' molecular dynamics simulations." Proteins: Structure, Function, and Genetics **36**(4): 419-24.

Amadei, A., Linssen, A. B. and Berendsen, H. J. (1993). "Essential dynamics of proteins." Proteins: Structure, Function, and Genetics **17**(4): 412-25.

Amadei, A., Linssen, A. B., de Groot, B. L., van Aalten, D. M. and Berendsen, H. J. (1996). "An efficient method for sampling the essential subspace of proteins." Journal of Biomolecular Structure and Dynamics **13**(4): 615-25.

Amit, A. G., Mariuzza, R. A., Phillips, S. E. and Poljak, R. J. (1986). "Three-dimensional structure of an antigen-antibody complex at 2.8 A resolution." Science **233**(4765): 747-53.

Anderson, A. C., O'Neil, R. H., Surti, T. S. and Stroud, R. M. (2001). "Approaches to solving the rigid receptor problem by identifying a minimal set of flexible residues during ligand docking." Chemical Biology **8**(5): 445-57.

Andrews, B. K., Romo, T., Clarage, J. B., Pettitt, B. M. and Phillips, G. N., Jr. (1998). "Characterizing global substates of myoglobin." Structure **6**(5): 587-94.

Apostolakis, J., Pluckthun, A. and Caflisch, A. (1998). "Docking small ligands in flexible binding sites." Journal of Computational Chemistry **19**(1): 21-37.

Appelt, K. (1993). "Crystal structures of HIV-1 protease-inhibitor complexes." Perspectives in Drug Discovery and Design **1**: 23–48.

Auzat, I., Gawlita, E. and Garel, J. R. (1995). "Slow ligand-induced transitions in the allosteric phosphofructokinase from Escherichia coli." Journal of Molecular Biology **249**(2): 478-92.

Bahar, I., Erman, B., Jernigan, R. L., Atilgan, A. R. and Covell, D. G. (1999). "Collective motions in HIV-1 reverse transcriptase: examination of flexibility and enzyme function." Journal of Molecular Biology **285**(3): 1023-37.

Banner, D. W. and Hadvary, P. (1991). "Crystallographic analysis at 3.0-A resolution of the binding to human thrombin of four active site-directed inhibitors." Journal of Biological Chemistry **266**(30): 20085-93.

Berendsen, H. J. C., Postma, J. P. M., van Gunsteren, W. F., DiNola, A. and Haak, J. R. (1984). "Molecular dynamics with coupling to an external bath." Journal of Chemical Physics **81**(8): 3684-3690.

Berg, B. A. and Neuhaus, T. (1992). "Multicanonical ensemble: A new approach to simulate first-order phase transitions." Physical Review Letters **68**: 9-12.

Berman, H. M., Westbrook, J., Feng, Z., Gilliland, G., Bhat, T. N., Weissig, H., Shindyalov, I. N. and Bourne, P. E. (2000). "The Protein Data Bank." Nucleic Acids Research **28**(1): 235-242.

Betts, M. J. and Sternberg, M. J. (1999). "An analysis of conformational changes on protein-protein association: implications for predictive docking." Protein Engineering **12**(4): 271-83.

Bishop, C. M., Svensen, M. and Williams, C. K. (1998). "GTM:the Generative Topographic Mapping." Neural Computation **10**(1): 215 -234.

Blow, D. M. (1976). "Structure and Mechanism of Chymotrypsin." Accounts Chemical Research **9**: 145-152.

Bolin, J. T., Filman, D. J., Matthews, D. A., Hamlin, R. C. and Kraut, J. (1982). "Crystal structures of Escherichia coli and Lactobacillus casei dihydrofolate reductase refined at 1.7 A resolution. I. General features and binding of methotrexate." Journal of Biological Chemistry **257**(22): 13650-62.

Borhani, D. W., Harter, T. M. and Petrash, J. M. (1992). "The crystal structure of the aldose reductase.NADPH binary complex." Journal of Biological Chemistry **267**(34): 24841-7.

Bouzida, D., Rejto, P. A., Arthurs, S., Colson, A. B., Freer, S. T., Gehlhaar, D. K., Larson, V., Luty, B. A., Rose, P. W. and Verkhivker, G. M. (1999). "Computer simulations of ligand-protein binding with ensembles of protein conformations:

A Monte Carlo study of HIV-1 protease binding energy landscapes." International Journal of Quantum Chemistry **72**: 73-84.

Brooks, C. L. I., Montgomery, B. and Karplus, M. (1988). Proteins : A Theoretical Perspective of Dynamics, Structure and Thermodynamics. New York, John Wiley & Sons.

Broughton, H. B. (2000). "A method for including protein flexibility in protein-ligand docking: improving tools for database mining and virtual screening." Journal of Molecular Graphics and Modeling **18**(3): 247-57, 302-4.

Bruccoleri, R. E. and Karplus, M. (1990). "Conformational sampling using high-temperature molecular dynamics." Biopolymers **29**(14): 1847-62.

Brünger, A. T. (1992). X-PLOR Version 3.1: A system for X-ray crystallography and NMR. New Haven, Yale University Press.

Bursavich, M. G. and Rich, D. H. (2002). "Designing non-peptide peptidomimetics in the 21st century: inhibitors targeting conformational ensembles." Journal of Medicinal Chemistry **45**(3): 541-58.

Bystroff, C. and Kraut, J. (1991). "Crystal structure of unliganded Escherichia coli dihydrofolate reductase. Ligand-induced conformational changes and cooperativity in binding." Biochemistry **30**(8): 2227-39.

Caflisch, A., Fischer, S. and Karplus, M. (1997). "Docking by Monte Carlo Minimization with a Solvation Correction: Application to an FKBP-Substrate Complex." Journal of Computational Chemistry **18**(6): 723-743.

Cao, Y., Musah, R. A., Wilcox, S. K., Goodin, D. B. and McRee, D. E. (1998). "Protein conformer selection by ligand binding observed with crystallography." Protein Science **7**(1): 72-8.

Carlson, H. A. (2002). "Protein flexibility and drug design: how to hit a moving target." Current Opinion in Chemical Biology **6**(4): 447-52.

Carlson, H. A. (2002). "Protein Flexibility is an Important Component of Structure-Based Drug Discovery." Current Pharmaceutical Design **8**(17): 1571-8.

Carlson, H. A., Masukawa, K. M. and McCammon, J. A. (1999). "Method for Including the Dynamic Fluctuations of a Protein in Computer-Aided Drug Design." Journal of Chemical Information and Computer Science **103**: 10213-10219.

Carlson, H. A., Masukawa, K. M., Rubins, K., Bushman, F. D., Jorgensen, W. L., Lins, R. D., Briggs, J. M. and McCammon, J. A. (2000). "Developing a dynamic pharmacophore model for HIV-1 integrase." Journal of Medicinal Chemistry **43**(11): 2100-14.

Carlson, H. A. and McCammon, J. A. (2000). "Accommodating protein flexibility in computational drug design." Molecular Pharmacology **57**(2): 213-8.

Case, D. A. (1994). "Normal Mode Analysis of Protein Dynamics." Current Opinion in Structural Biology **4**: 285-290.

Caves, L. S., Evanseck, J. D. and Karplus, M. (1998). "Locally accessible conformations of proteins: multiple molecular dynamics simulations of crambin." Protein Science **7**(3): 649-66.

Cecconi, F., Micheletti, C., Carloni, P. and Maritan, A. (2001). "Molecular dynamics studies on HIV-1 protease drug resistance and folding pathways." Proteins: Structure, Function, and Genetics **43**(4): 365-72.

Chillemi, G., Falconi, M., Amadei, A., Zimatore, G., Desideri, A. and Di Nola, A. (1997). "The essential dynamics of Cu, Zn superoxide dismutase: suggestion of intersubunit communication." Biophysical Journal **73**(2): 1007-18.

Clarage, J. B., Romo, T., Andrews, B. K., Pettitt, B. M. and Phillips, G. N., Jr. (1995). "A sampling problem in molecular dynamics simulations of macromolecules." Proceedings of the National Academy of Sciences USA **92**(8): 3288-92.

Claussen, H., Buning, C., Rarey, M. and Lengauer, T. (2001). "FlexE: efficient molecular docking considering protein structure variations." Journal of Molecular Biology **308**(2): 377-95.

Cody, V., Galitsky, N., Rak, D., Luft, J. R., Pangborn, W. and Queener, S. F. (1999). "Ligand-induced conformational changes in the crystal structures of Pneumocystis carinii dihydrofolate reductase complexes with folate and NADP+." Biochemistry **38**(14): 4303-12.

Collins, J. R., Burt, S. K. and Erickson, J. W. (1995). "Flap opening in HIV-1 protease simulated by 'activated' molecular dynamics." Nature Structural Biology **2**(4): 334-8.

Cornell, W. D., Cieplak, P., Bayly, C. I., Gould, I. R., Merz, K. M., Ferguson, D. M., Spellmeyer, D. C., Fox, T., Caldwell, J. W. and Kollman, P. A. (1995). "A second generation force field for the simulation of proteins and nucleic acids." Journal of the American Chemical Society **117**: 5179-5197.

Darden, T. A., York, D. and Pedersen, L. (1993). "Particle Mesh Ewald: An N log(N) method for Ewald sums in large systems." Journal of Chemical Physics **98**: 10089.

David, L., Luo, R. and Gilson, M. K. (2001). "Ligand-receptor docking with the Mining Minima optimizer." Journal of Computer Aided Molecular Design **15**(2): 157-71.

de Groot, B. L., Amadei, A., Scheek, R. M., van Nuland, N. A. and Berendsen, H. J. (1996). "An extended sampling of the configurational space of HPr from E. coli." Proteins: Structure, Function, and Genetics **26**(3): 314-22.

de Groot, B. L., Amadei, A., van Aalten, D. M. and Berendsen, H. J. (1996). "Toward an exhaustive sampling of the configurational spaces of the two forms of the peptide hormone guanylin." Journal of Biomolecular Structure and Dynamics **13**(5): 741-51.

de Groot, B. L., Hayward, S., van Aalten, D. M., Amadei, A. and Berendsen, H. J. (1998). "Domain motions in bacteriophage T4 lysozyme: a comparison between molecular dynamics and crystallographic data." Proteins: Structure, Function, and Genetics **31**(2): 116-27.

DesJarlais, R. L., Sheridan, R. P., Seibel, G. L., Dixon, J. S., Kuntz, I. D. and Venkataraghavan, R. (1988). "Using shape complementarity as an initial screen in designing ligands for a receptor binding site of known three-dimensional structure." Journal of Medicinal Chemistry **31**(4): 722-9.

Desmet, J., DeMaeyer, M., Hazes, B. and Lasters, I. (1992). "The dead-end elimination theorem and its use in protein side-chain positioning." Nature **356**: 539-542.

Di Nola, A., Roccatano, D. and Berendsen, H. J. (1994). "Molecular dynamics simulation of the docking of substrates to proteins." Proteins: Structure, Function, and Genetics **19**(3): 174-82.

Duan, X., Hall, J. A., Nikaido, H. and Quiocho, F. A. (2001). "Crystal structures of the maltodextrin/maltose-binding protein complexed with reduced oligosaccharides: flexibility of tertiary structure and ligand binding." Journal of Molecular Biology **306**(5): 1115-26.

Dunbrack, R. (2002). "Rotamer Libraries in the 21(st) Century." Current Opinion in Structural Biology **12**(4): 431.

Dunlop, M. (2000). "Aldose reductase and the role of the polyol pathway in diabetic nephropathy." Kidney Int Suppl **77**: S3-12.

Essman, U., Perera, L., Berkowitz, M. L., Darden, T., H., L. and L.G., P. (1995). "A smooth particle mesh Ewald method." Journal of Chemical Physics **103**: 8577-8593.

Ewing, T. J. A. and Kuntz, I. D. (1997). "Critical evaluation of search algorithms for automated molecular docking and database screening." Journal of Computational Chemistry **18**: 1175-1189.

Feeney, J. (2000). "NMR Studies of Ligand Binding to Dihydrofolate Reductase." Angew Chem Int Ed Engl **39**(2): 290-312.

Fenton, W. A., Kashi, Y., Furtak, K. and Horwich, A. L. (1994). "Residues in chaperonin GroEL required for polypeptide binding and release." Nature **371**(6498): 614-9.

Finn, P. and Kavraki, L. E. (1999). "Computational Approaches to Drug Design." Algorithmica **25**: 347-371.

Fischer, E. (1894). "Einfluss der Configuration auf die Wirkung der Enzyme." Ber. Dtsch. Chem. Ges. **27**: 2985.

Fless, G. M., Furbee, J., Jr., Snyder, M. L. and Meredith, S. C. (1996). "Ligand-induced conformational change of lipoprotein(a)." Biochemistry **35**(7): 2289-98.

Flexner, C. (1998). "HIV-protease inhibitors." New England Journal of Medicine **338**(18): 1281-92.

Fradera, X., Cruz, X., Silva, C. H. T. P., Gelpi, J. L., Luque, F. J. and Orozco, M. (2002). "Ligand-induced changes in the binding site of proteins." Bioinformatics **18**(7): 939-948.

Frauenfelder, H., Sligar, S. G. and Wolynes, P. G. (1991). "The energy landscapes and motions of proteins." Science **254**(5038): 1598-603.

Freedberg, D. I., Wang, I. X., Stahl, S. J., Kaufman, J. D., Wingfield, P. T., Kiso, Y. and Torchia, D. A. (1998). "Flexibility and function in HIV protease: dynamics of the HIV-1 protease bound to the asymmetric inhibitor kinostatin-272 (kni-272)." Journal of the American Chemical Society **120**(31): 7916-7923.

Gane, P. J. and Dean, P. M. (2000). "Recent advances in structure-based rational drug design." Current Opinion in Structural Biology **10**(4): 401-4.

Garcia, A. E. (1992). "Large-amplitude nonlinear motions in proteins." Physical Review Letters **68**(17): 2696-2699.

Garcia, A. E., Blumenfeld, R., Hummer, G. and Krumhasl, J. A. (1997). "Multi-basin dynamics of a protein in a crystal environment." Physica D **107**(2-4): 225-239.

Gasteiger, J. and Marsili, M. (1980). "Iterative Partial Equalization of Orbital Electronegativity- A Rapid Access to Atomic Charges." Tetrahedron **36**: 3219-3288.

Gehring, K., Zhang, X., Hall, J., Nikaido, H. and Wemmer, D. E. (1998). "An NMR study of ligand binding by maltodextrin binding protein." Biochem Cell Biol **76**(2-3): 189-97.

Genest, D. (1999). "Correlated motion analysis from molecular dynamics trajectories: statistical accuracy on the determination of canonical correlation coefficients." Journal of Computational Chemistry **20**: 1571-1576.

Gerstein, M. and Krebs, W. (1998). "A database of macromolecular motions." Nucleic Acids Research **26**(18): 4280-90.

Given, J. A. and Gilson, M. K. (1998). "A hierarchical method for generating low-energy conformers of a protein-ligand complex." Proteins: Structure, Function, and Genetics **33**(4): 475-95.

Go, N., Noguti, T. and Nishikawa, T. (1983). "Dynamics of a small globular protein in terms of low-frequency vibrational modes." Proceedings of the National Academy of Sciences USA **80**(12): 3696-700.

Gogonea, V., Suarez, D., van der Vaart, A. and Merz, K. M., Jr. (2001). "New developments in applying quantum mechanics to proteins." Current Opinion in Structural Biology **11**(2): 217-23.

Gohlke, H. and Klebe, G. (2001). "Statistical potentials and scoring functions applied to protein-ligand binding." Current Opinion in Structural Biology **11**(2): 231-5.

Graves, M. C., Lim, J. J., Heimer, E. P. and Kramer, R. A. (1988). "An 11-kDa form of human immunodeficiency virus protease expressed in Escherichia coli is sufficient for enzymatic activity." Proceedings of the National Academy of Sciences USA **85**(8): 2449-53.

Hall, J. A., Gehring, K. and Nikaido, H. (1997). "Two modes of ligand binding in maltose-binding protein of Escherichia coli. Correlation with the structure of ligands and the structure of binding protein." Journal of Biological Chemistry **272**(28): 17605-9.

Hall, J. A., Thorgeirsson, T. E., Liu, J., Shin, Y. K. and Nikaido, H. (1997). "Two modes of ligand binding in maltose-binding protein of Escherichia coli. Electron paramagnetic resonance study of ligand-induced global conformational changes by site-directed spin labeling." Journal of Biological Chemistry **272**(28): 17610-4.

Halperin, I., Ma, B., Wolfson, H. and Nussinov, R. (2002). "Principles of docking: An overview of search algorithms and a guide to scoring functions." Proteins: Structure, Function, and Genetics **47**(4): 409-43.

Hart, P. E., N.J., N. and Raphael, B. (1968). "A formal basis for the heuristic determination of minimum cost paths." IEEE Transactions on Systems Science and Cybernetics **4**: 100–114.

Hastie, T. and Stuetzle, W. (1989). "Principal curves." Journal of the American Statistical Association **84**: 502 -516.

Hayward, S. and Go, N. (1995). "Collective Variable Description of Native Protein Dynamics." Annual Reviews in Physical Chemistry **46**: 223-250.

Hayward, S., Kitao, A. and Berendsen, H. J. (1997). "Model-free methods of analyzing domain motions in proteins from simulation: a comparison of normal mode analysis and molecular dynamics simulation of lysozyme." Proteins: Structure, Function, and Genetics **27**(3): 425-37.

Hayward, S., Kitao, A., Hirata, F. and Go, N. (1993). "Effect of solvent on collective motions in globular protein." Journal of Molecular Biology **234**(4): 1207-17.

Ho, D. D., Toyoshima, T., Mo, H., Kempf, D. J., Norbeck, D., Chen, C. M., Wideburg, N. E., Burt, S. K., Erickson, J. W. and Singh, M. K. (1994). "Characterization of human immunodeficiency virus type 1 variants with increased resistance to a C2-symmetric protease inhibitor." Journal of Virology **68**(3): 2016-20.

Holtje, H. D. and Kier, L. B. (1974). "Sweet taste receptor studies using model interaction energy calculations." Journal of Pharmaceutical Sciences **63**(11): 1722-5.

Hotelling, H. (1933). "Analysis of a complex of statistical variables into principal components." Journal of Educational Psychology **24**: 441.

Hubbard, S. J., Campbell, S. F. and Thornton, J. M. (1991). "Molecular recognition. Conformational analysis of limited proteolytic sites and serine proteinase protein inhibitors." Journal of Molecular Biology **220**(2): 507-30.

Huber, R. and Bode, W. (1978). "Structural basis of the activation and action of trypsin." Accounts Chemical Research **11**: 114-122.

Huennekens, F. M. (1994). "The methotrexate story: a paradigm for development of cancer chemotherapeutic agents." Adv Enzyme Regul **34**: 397-419.

Ibragimova, G. T. and Wade, R. C. (1998). "Importance of explicit salt ions for protein stability in molecular dynamics simulation." Biophysical Journal **74**(6): 2906-11.

Jacobs, D. J., Rader, A. J., Kuhn, L. A. and Thorpe, M. F. (2001). "Protein flexibility predictions using graph theory." Proteins: Structure, Function, and Genetics **44**(2): 150-65.

Jaqaman, K. and Ortoleva, P. J. (2002). "New space warping method for the simulation of large-scale macromolecular conformational changes." Journal of Computational Chemistry **23**(4): 484-91.

Jiang, F. and Kim, S. H. (1991). ""Soft docking": matching of molecular surface cubes." Journal of Molecular Biology **219**(1): 79-102.

Jones, G., Willett, P., Glen, R. C., Leach, A. R. and Taylor, R. (1997). "Development and validation of a genetic algorithm for flexible docking." Journal of Molecular Biology **267**(3): 727-48.

Kabsch, W. (1976). "A solution for the best rotation to relate two sets of vectors." Acta Crystallographica **32**: 922-923.

Kairys, V. and Gilson, M. K. (2002). "Enhanced docking with the mining minima optimizer: acceleration and side-chain flexibility." Journal of Computational Chemistry **23**(16): 1656-70.

Kalé, L., Skeel, R., Bhandarkar, M., Brunner, R., Gursoy, A., Krawetz, N., Phillips, J., Shinozaki, A., Varadarajan, K. and Schulten, K. (1999). "NAMD2: Greater scalability for parallel molecular dynamics." Journal of Computational Physics **151**: 283-312.

Kambhatla, N. and Leen, T. K. (1997). "Dimension reduction by local principal component analysis." Neural Computation **9**(7): 1493 -1516.

Kaplan, A. H., Michael, S. F., Wehbie, R. S., Knigge, M. F., Paul, D. A., Everitt, L., Kempf, D. J., Norbeck, D. W., Erickson, J. W. and Swanstrom, R. (1994). "Selection of multiple human immunodeficiency virus type 1 variants that encode viral proteases with decreased sensitivity to an inhibitor of the viral protease." Proceedings of the National Academy of Sciences USA **91**(12): 5597-601.

Karplus, M. and McCammon, J. A. (2002). "Molecular dynamics simulations of biomolecules." Nature Structural Biology **9**(9): 646-52.

Kastenholz, M. A., Pastor, M., Cruciani, G., Haaksma, E. E. and Fox, T. (2000). "GRID/CPCA: a new computational tool to design selective ligands." Journal of Medicinal Chemistry **43**(16): 3033-44.

Katritch, V., Totrov, M. and Abagyan, R. (2003). "ICFF: A new method to incorporate implicit flexibility into an internal coordinate force field." Journal of Computational Chemistry **24**(2): 254-65.

Kaul, D. R., Cinti, S. K., Carver, P. L. and Kazanjian, P. H. (1999). "HIV protease inhibitors: advances in therapy and adverse reactions, including metabolic complications." Pharmacotherapy **19**(3): 281-298.

Keseru, G. M. and Kolossvary, I. (2001). "Fully flexible low-mode docking: application to induced fit in HIV integrase." Journal of the American Chemical Society **123**(50): 12708-9.

Kier, L. B. and Aldrich, H. S. (1974). "A theoretical study of receptor site models for trimethylammonium group interaction." Journal of Theoretical Biology **46**(2): 529-41.

Kinoshita, J. H. and Nishimura, C. (1988). "The involvement of aldose reductase in diabetic complications." Diabetes Metab Rev **4**(4): 323-37.

Kitao, A. and Go, N. (1999). "Investigating protein dynamics in collective coordinate space." Current Opinion in Structural Biology **9**(2): 164-169.

Kitao, A., Hayward, S. and Go, N. (1998). "Energy landscape of a native protein: jumping-among-minima model." Proteins: Structure, Function, and Genetics **33**(4): 496-517.

Klebe, G. (2000). "Recent developments in structure-based drug design." Journal of Molecular Medicine **78**(5): 269-81.

Knegtel, R. M., Kuntz, I. D. and Oshiro, C. M. (1997). "Molecular docking to ensembles of protein structures." Journal of Molecular Biology **266**(2): 424-40.

Kohl, N. E., Emini, E. A., Schleif, W. A., Davis, L. J., Heimbach, J. C., Dixon, R. A., Scolnick, E. M. and Sigal, I. S. (1988). "Active human immunodeficiency virus protease is required for viral infectivity." Proceedings of the National Academy of Sciences USA **85**(13): 4686-90.

Kolossvary, I. and Guida, W. C. (1996). "Low Mode Search. An Efficient, Automated Computational Method for Conformational Analysis: Application to Cyclic and Acyclic Alkanes and Cyclic Peptides." Journal of the American Chemical Society **118**: 5011-5019.

Kolossvary, I. and Guida, W. C. (1999). "Low-Mode Conformational Search Elucidated: Application to C39H80 and Flexible Docking of 9-Deazaguanine Inhibitors into PNP." Journal of Computational Chemistry **20**(15): 1671-1684.

Kolossvary, I. and Keseru, G. M. (2001). "Hessian-Free Low-Mode Conformational Search for Large-Scale Protein Loop Optimization: Application to c-jun N-Terminal Kinase JNK3." Journal of Computational Chemistry **22**(1): 21-30.

Koshland, D. E. (1958). "Application of a theory of enzyme specificity to protein synthesis." Proceedings of the National Academy of Sciences USA **44**(2): 98-104.

Kramer, B., Rarey, M. and Lengauer, T. (1999). "Evaluation of the FLEXX incremental construction algorithm for protein-ligand docking." Proteins: Structure, Function, and Genetics **37**(2): 228-41.

Kramer, M. A. (1991). "Nonlinear principal component analysis using autoassociative neural networks." AIChE Journal **37**(2): 233 -243.

Kramer, R. A., Schaber, M. D., Skalka, A. M., Ganguly, K., Wong-Staal, F. and Reddy, E. P. (1986). "HTLV-III gag protein is processed in yeast cells by the virus pol-protease." Science **231**(4745): 1580-4.

Kruskal, J. B. (1964). "Nonmetric multidimensional scaling : a numerical method." Psychometrika **29**: 115-129.

Kua, J., Zhang, Y. and McCammon, J. A. (2002). "Studying enzyme binding specificity in acetylcholinesterase using a combined molecular dynamics and multiple docking approach." Journal of the American Chemical Society **124**(28): 8260-7.

Kuntz, I. D., Blaney, J. M., Oatley, S. J., Langridge, R. and Ferrin, T. E. (1982). "A geometric approach to macromolecule-ligand interactions." Journal of Molecular Biology **161**(2): 269-88.

Lafontaine, I. and Lavery, R. (1999). "Collective variable modelling of nucleic acids." Current Opinion in Structural Biology **9**(2): 170-6.

Lam, P. Y., Jadhav, P. K., Eyermann, C. J., Hodge, C. N., Ru, Y., Bacheler, L. T., Meek, J. L., Otto, M. J., Rayner, M. M., Wong, Y. N. and et al. (1994). "Rational design of potent, bioavailable, nonpeptide cyclic ureas as HIV protease inhibitors." Science **263**(5145): 380-4.

Le Grice, S. F., Mills, J. and Mous, J. (1988). "Active site mutagenesis of the AIDS virus protease and its alleviation by trans complementation." Embo Journal **7**(8): 2547-53.

Leach, A. R. (1994). "Ligand docking to proteins with discrete side-chain flexibility." Journal of Molecular Biology **235**(1): 345-56.

Leach, A. R. and Lemon, A. P. (1998). "Exploring the conformational space of protein side chains using dead-end elimination and the A* algorithm." Proteins: Structure, Function, and Genetics **33**(2): 227-39.

Lehoucq, R., Sorensen, D. C. and Yang, C. (1998). Arpack User's Guide: Solution of Large-Scale Eigenvalue Problems With Implicitly Restorted Arnoldi Methods. Philadelphia, SIAM.

Lehoucq, R. B. and Sorensen, D. C. (1996). "Deflation techniques for an implicitly restarted Arnoldi iteration." SIAM Journal on Matrix Analysis and Applications **17**(4): 789-821.

Levitt, M., Sander, C. and Stern, P. S. (1985). "Protein normal-mode dynamics: trypsin inhibitor, crambin, ribonuclease and lysozyme." Journal of Molecular Biology **181**(3): 423-47.

Levy, R. M. and Karplus, M. (1979). "Vibrational Approach to the Dynamics of an alpha-Helix." Biopolymers **18**: 2465-2495.

Lin, J. H., Perryman, A. L., Schames, J. R. and McCammon, J. A. (2002). "Computational drug design accommodating receptor flexibility: the relaxed complex scheme." Journal of the American Chemical Society **124**(20): 5632-3.

Liu, H., Muller-Plathe, F. and van Gunsteren, W. F. (1996). "A combined quantum/classical molecular dynamics study of the catalytic mechanism of HIV protease." Journal of Molecular Biology **261**(3): 454-69.

Lovell, S. C., Word, J. M., Richardson, J. S. and Richardson, D. C. (2000). "The penultimate rotamer library." Proteins: Structure, Function, and Genetics **40**(3): 389-408.

Luo, X., Kato, R. and Collins, J. R. (1998). "Dynamic flexibility of protein-inhibitor complexes: a study of the HIV-1 protease/KNI-272 complex." Journal of the American Chemical Society **120**: 12410-12418.

Luong, C., Miller, A., Barnett, J., Chow, J., Ramesha, C. and Browner, M. F. (1996). "Flexibility of the NSAID binding site in the structure of human cyclooxygenase-2." Nature Structural Biology **3**(11): 927-33.

Luty, B. A., Wasserman, R., Stouten, P., Hodge, C. N., Zacharias, M. and McCammon, J. A. (1995). "A Molecular Mechanics/Grid Method for Evaluation of Ligand-Receptor Interactions." Journal of Computational Chemistry **16**: 454-464.

Ma, B., Kumar, S., Tsai, C. J. and Nussinov, R. (1999). "Folding funnels and binding mechanisms." Protein Engineering **12**(9): 713-20.

Ma, B., Shatsky, M., Wolfson, H. J. and Nussinov, R. (2002). "Multiple diverse ligands binding at a single protein site: a matter of pre-existing populations." Protein Science **11**(2): 184-97.

Ma, B., Wolfson, H. J. and Nussinov, R. (2001). "Protein functional epitopes: hot spots, dynamics and combinatorial libraries." Current Opinion in Structural Biology **11**(3): 364-9.

MacKerell, A. D., Bashford, D., Bellott, M., Dunbrack Jr., R. L., Evanseck, J. D., Field, M. J., Fischer, S., Gao, J., Guo, H., Ha, S., Joseph-McCarthy, D., Kuchnir, L., Kuczera, K., Lau, F. T. K., Mattos, C., Michnick, S., Ngo, T., Nguyen, D. T., Prodhom, B., Reiher, I., W.E., Roux, B., Schlenkrich, M., Smith, J. C., Stote, R., Straub, J., Watanabe, M., Wiorkiewicz-Kuczera, J., Yin, D. and Karplus, M. (1998). "All-atom empirical potential for molecular modeling and dynamics studies of proteins." Journal of Physical Chemistry B **102**: 3586-3616.

Mangoni, M., Roccatano, D. and Di Nola, A. (1999). "Docking of flexible ligands to flexible receptors in solution by molecular dynamics simulation." Proteins: Structure, Function, and Genetics **35**(2): 153-62.

Meinicke, P. and Ritter, H. (1999). Local PCA Learning with Resolution-Dependent Mixtures of Gaussians. ICANN99 Ninth Int. Conf. on Artificial Neural Networks, Edinburgh, U.K.

Miller, M., Schneider, J., Sathyanarayana, B. K., Toth, M. V., Marshall, G. R., Clawson, L., Selk, L., Kent, S. B. and Wlodawer, A. (1989). "Structure of complex of synthetic HIV-1 protease with a substrate-based inhibitor at 2.3 A resolution." Science **246**(4934): 1149-52.

Molla, A., Granneman, G. R., Sun, E. and Kempf, D. J. (1998). "Recent developments in HIV protease inhibitor therapy." Antiviral Research **39**(1): 1-23.

Moreno, E. and Leon, K. (2002). "Geometric and chemical patterns of interaction in protein-ligand complexes and their application in docking." Proteins: Structure, Function, and Genetics **47**(1): 1-13.

Morris, G. M., Goodsell, D. S., Halliday, R. S., Huey, R., Hart, W. E., Belew, R. K. and Olson, A. J. (1998). "Automated docking using a Lamarckian genetic algorithm and an empirical binding free energy function." Journal of Computational Chemistry **19**(14): 1639-1662.

Muegge, I. and Martin, Y. C. (1999). "A general and fast scoring function for protein-ligand interactions: a simplified potential approach." Journal of Medicinal Chemistry **42**(5): 791-804.

Muegge, I. and Rarey, M. (2001). "Small Molecule Docking and Scoring." Reviews in Computational Chemistry **17**: 1-60.

Munshi, S., Chen, Z., Yan, Y., Li, Y., Olsen, D. B., Schock, H. B., Galvin, B. B., Dorsey, B. and Kuo, L. C. (2000). "An alternate binding site for the P1-P3 group of a class of potent HIV- 1 protease inhibitors as a result of concerted structural change in the 80s loop of the protease." Acta Crystallographica Section D - Biological Crystallography **56**(Pt 4): 381-8.

Murray, C. W., Baxter, C. A. and Frenkel, A. D. (1999). "The sensitivity of the results of molecular docking to induced fit effects: Application to thrombin, thermolysin and neuraminidase." Journal of Computer Aided Molecular Design **13**: 547-562.

Najmanovich, R., Kuttner, J., Sobolev, V. and Edelman, M. (2000). "Side-chain flexibility in proteins upon ligand binding." Proteins: Structure, Function, and Genetics **39**(3): 261-8.

Nakajima, N., Higoa, J., Kiderab, A. and Nakamura, H. (1997). "Flexible docking of a ligand peptide to a receptor protein by multicanonical molecular dynamics simulation." Chemical Physics Letters **278**(4-6): 297-301.

Nakajima, N., Nakamura, H. and Kidera, A. (1997). "Multicanonical Ensemble Generated by Molecular Dynamics Simulation for Enhanced Conformational Sampling of Peptides." Journal of Physical Chemistry B **101**(5): 817-824.

Noguti, T. and Go, N. (1985). "Efficient Monte Carlo method for simulation of fluctuating conformations of native proteins." Biopolymers **24**(3): 527-46.

Noguti, T. and Go, N. (1989). "Structural basis of hierarchical multiple substates of a protein. I: Introduction." Proteins: Structure, Function, and Genetics **5**(2): 97-103.

Noguti, T. and Go, N. (1989). "Structural basis of hierarchical multiple substates of a protein. V: Nonlocal deformations." Proteins: Structure, Function, and Genetics **5**(2): 132-8.

Oates, P. J. and Mylari, B. L. (1999). "Aldose reductase inhibitors: therapeutic implications for diabetic complications." Expert Opin Investig Drugs **8**(12): 2095-2119.

Oshiro, C. M. and Kuntz, I. D. (1998). "Characterization of receptors with a new negative image: use in molecular docking and lead optimization." Proteins: Structure, Function, and Genetics **30**(3): 321-36.

Osterberg, F., Morris, G. M., Sanner, M. F., Olson, A. J. and Goodsell, D. S. (2002). "Automated docking to multiple target structures: incorporation of protein mobility and structural water heterogeneity in AutoDock." Proteins: Structure, Function, and Genetics **46**(1): 34-40.

Ota, N. and Agard, D. A. (2001). "Binding mode prediction for a flexible ligand in a flexible pocket using multi-conformation simulated annealing pseudo crystallographic refinement." Journal of Molecular Biology **314**(3): 607-17.

Pak, Y. and Wang, C. (2000). "Application of a Molecular Dynamics Simulation Method with a Generalized Effective Potential to the Flexible Molecular Docking Problems." Journal of Physical Chemistry B **104**: 354-359.

Pang, Y. P. and Kozikowski, A. P. (1994). "Prediction of the binding sites of huperzine A in acetylcholinesterase by docking studies." Journal of Computer Aided Molecular Design **8**(6): 669-81.

Pastor, M. and Cruciani, G. (1995). "A novel strategy for improving ligand selectivity in receptor-based drug design." Journal of Medicinal Chemistry **38**(23): 4637-47.

Paul, N. and Rognan, D. (2002). "ConsDock: A new program for the consensus analysis of protein-ligand interactions." Proteins: Structure, Function, and Genetics **47**(4): 521-33.

Pearson, K. (1901). "On lines and planes of closest fit to systems of points in space." The London, Edinburgh and Dublin Philosophical Magazine and Journal of Science **2**: 572.

Pfeiffer, S., Fushman, D. and Cowburn, D. (1999). "Impact of Cl- and Na+ ions on simulated structure and dynamics of betaARK1 PH domain." Proteins: Structure, Function, and Genetics **35**(2): 206-17.

Philippopoulos, M. and Lim, C. (1999). "Exploring the dynamic information content of a protein NMR structure: comparison of a molecular dynamics simulation with the NMR and X-ray structures of Escherichia coli ribonuclease HI." Proteins: Structure, Function, and Genetics **36**(1): 87-110.

Piana, S. and Carloni, P. (2000). "Conformational flexibility of the catalytic Asp dyad in HIV-1 protease: An ab initio study on the free enzyme." Proteins: Structure, Function, and Genetics **39**(1): 26-36.

Piana, S., Carloni, P. and Parrinello, M. (2002). "Role of conformational fluctuations in the enzymatic reaction of HIV-1 protease." Journal of Molecular Biology **319**(2): 567-83.

Rarey, M., Kramer, B., Lengauer, T. and Klebe, G. (1996). "A fast flexible docking method using an incremental construction algorithm." Journal of Molecular Biology **261**(3): 470-89.

Raymer, M. L., Punch, W. F., Goodman, E. D., Kuhn, L. A. and Jain, A. K. (2000). "Dimensionality Reduction Using Genetic Algorithms." IEEE Transactions on Evolutionary Computation **4**: 164-171.

Rhodes, G. (1993). Crystallography Made Crystal Clear. London, Academic Press.

Rich, D. H., Bursavich, M. G. and Estiarte, M. A. (2002). "Discovery of nonpeptide, peptidomimetic peptidase inhibitors that target alternate enzyme active site conformations." Biopolymers **66**(2): 115-25.

Rick, S. W., Erickson, J. W. and Burt, S. K. (1998). "Reaction path and free energy calculations of the transition between alternate conformations of HIV-1 protease." Proteins: Structure, Function, and Genetics **32**(1): 7-16.

Rick, S. W., Topol, I. A., Erickson, J. W. and Burt, S. K. (1998). "Molecular mechanisms of resistance: free energy calculations of mutation effects on inhibitor binding to HIV-1 protease." Protein Science **7**(8): 1750-6.

Ringhofer, S., Kallen, J., Dutzler, R., Billich, A., Visser, A. J., Scholz, D., Steinhauser, O., Schreiber, H., Auer, M. and Kungl, A. J. (1999). "X-ray structure and conformational dynamics of the HIV-1 protease in complex with the inhibitor SDZ283-910: agreement of time-resolved spectroscopy and molecular dynamics simulations." Journal of Molecular Biology **286**(4): 1147-59.

Roitberg, A. and Elber, R. (1991). "Modeling side chains In peptides and proteins: Application of the locally enhanced sampling and the simulated annealing methods to find minimum energy conformations." Journal of Chemical Physics **95**(12): 9277-9287.

Romo, T. (1998). Identification and modeling of protein conformational substates. Department of Biochemistry and Cell Biology. Houston, Rice University**:** 235.

Romo, T. D., Clarage, J. B., Sorensen, D. C. and Phillips, G. N., Jr. (1995). "Automatic identification of discrete substates in proteins: singular value decomposition analysis of time-averaged crystallographic refinements." Proteins: Structure, Function, and Genetics **22**(4): 311-21.

Rose, R. B., Craik, C. S. and Stroud, R. M. (1998). "Domain flexibility in retroviral proteases: structural implications for drug resistant mutations." Biochemistry **37**(8): 2607-21.

Roth, B. and Stammers, D. K. (1992). The Design of Drugs to Macromolecular Targets. The Design of Drugs to Macromolecular Targets. Beddell, C. R. New York, John Wiley & Sons Ltd.**:** 85-118.

Roweis, S. and Saul, L. (2000). "Nonlinear dimensionality reduction by locally linear embedding." Science **290**(5500): 2323--2326.

Rutenber, E., Fauman, E. B., Keenan, R. J., Fong, S., Furth, P. S., Ortiz de Montellano, P. R., Meng, E., Kuntz, I. D., DeCamp, D. L., Salto, R., Rose, J. R., Craik, C. S. and Stroud, R. M. (1993). "Structure of a non-peptide inhibitor complexed with HIV-1 protease. Developing a cycle of structure-based drug design." Journal of Biological Chemistry **268**(21): 15343-15346.

Ryckaert, J. P., Ciccotti, G. and Berendsen, H. J. C. (1977). "Numerical-Integration of Cartesian Equations of Motion of a System with Constraints - Molecular-Dynamics of N-Alkanes." Journal of Computational Physics **23**(3): 327-341.

Sandak, B., Nussinov, R. and Wolfson, H. J. (1995). "An automated computer vision and robotics-based technique for 3-D flexible biomolecular docking and matching." Computer Applications in the Biosciences **11**(1): 87-99.

Sandak, B., Nussinov, R. and Wolfson, H. J. (1998). "A method for biomolecular structural recognition and docking allowing conformational flexibility." Journal of Computational Biology **5**(4): 631-54.

Sandak, B., Wolfson, H. J. and Nussinov, R. (1998). "Flexible docking allowing induced fit in proteins: insights from an open to closed conformational isomers." Proteins: Structure, Function, and Genetics **32**(2): 159-74.

Sawaya, M. R. and Kraut, J. (1997). "Loop and subdomain movements in the mechanism of Escherichia coli dihydrofolate reductase: crystallographic evidence." Biochemistry **36**(3): 586-603.

Schaffer, L. and Verkhivker, G. M. (1998). "Predicting structural effects in HIV-1 protease mutant complexes with flexible ligand docking and protein side-chain optimization." Proteins: Structure, Function, and Genetics **33**(2): 295-310.

Schnecke, V., Swanson, C. A., Getzoff, E. D., Tainer, J. A. and Kuhn, L. A. (1998). "Screening a peptidyl database for potential ligands to proteins with side-chain flexibility." Proteins: Structure, Function, and Genetics **33**(1): 74-87.

Schweitzer, B. I., Dicker, A. P. and Bertino, J. R. (1990). "Dihydrofolate reductase as a therapeutic target." Faseb J **4**(8): 2441-52.

Scott, W. R. and Schiffer, C. A. (2000). "Curling of flap tips in HIV-1 protease as a mechanism for substrate entry and tolerance of drug resistance." Structure with Folding and Design **8**(12): 1259-65.

Sharff, A. J., Rodseth, L. E., Spurlino, J. C. and Quiocho, F. A. (1992). "Crystallographic evidence of a large ligand-induced hinge-twist motion between the two domains of the maltodextrin binding protein involved in active transport and chemotaxis." Biochemistry **31**(44): 10657-63.

Shepard, R. N. (1962). "The analysis of proximities: multidimensional scaling with an unknown distance function." Psychometrika **27**(2): 125-140.

Shilton, B. H., Flocco, M. M., Nilsson, M. and Mowbray, S. L. (1996). "Conformational changes of three periplasmic receptors for bacterial chemotaxis and transport: the maltose-, glucose/galactose- and ribose-binding proteins." Journal of Molecular Biology **264**(2): 350-63.

Shoichet, B. K., McGovern, S. L., Wei, B. and Irwin, J. J. (2002). "Lead discovery using molecular docking." Current Opinion in Chemical Biology **6**(4): 439-46.

Silva, A. M., Cachau, R. E., Sham, H. L. and Erickson, J. W. (1996). "Inhibition and catalytic mechanism of HIV-1 aspartic protease." Journal of Molecular Biology **255**(2): 321-46.

Spurlino, J. C., Lu, G. Y. and Quiocho, F. A. (1991). "The 2.3-A resolution structure of the maltose- or maltodextrin-binding protein, a primary receptor of bacterial active transport and chemotaxis." Journal of Biological Chemistry **266**(8): 5202-19.

Stultz, C. M. and Karplus, M. (1999). "MCSS functionality maps for a flexible protein." Proteins: Structure, Function, and Genetics **37**(4): 512-29.

Sudbeck, E. A., Mao, C., Vig, R., Venkatachalam, T. K., Tuel-Ahlgren, L. and Uckun, F. M. (1998). "Structure-based design of novel dihydroalkoxybenzyloxopyrimidine derivatives as potent nonnucleoside inhibitors of the human immunodeficiency virus reverse transcriptase." Antimicrobial Agents and Chemotherapy **42**(12): 3225-3233.

Szmelcman, S., Schwartz, M., Silhavy, T. J. and Boos, W. (1976). "Maltose transport in Escherichia coli K12. A comparison of transport kinetics in wild-type and lambda-resistant mutants as measured by fluorescence quenching." Eur J Biochem **65**(1): 13-9.

Tame, J. R. (1999). "Scoring functions: a view from the bench." Journal of Computer Aided Molecular Design **13**(2): 99-108.

Ten Eyck, L. F., Mandell, J., Roberts, V. A. and Pique, M. E. (1995). Surveying molecular Interactions with DOT. 1995 ACM/IEEE Supercomputing Conference, San Diego, California, USA, IEEE Press.

Tenenbaum, J. B., de Silva, V. and Langford, J. C. (2000). "A Global Geometric Framework for Nonlinear Dimensionality Reduction." Science **290**(5500): 2319-2323,.

Teodoro, M. L. and Kavraki, L. E. (2003). "Conformational Flexibility Models for the Receptor in Structure Based Drug Design." Current Pharmaceutical Design **9**: 1419-1431.

Teodoro, M. L., Phillips, G. N., Jr. and Kavraki, L. E. (2003). "Understanding Protein Flexibility Through Dimensionality Reduction." Journal of Computational Biology **10**(3-4): 617-634.

Teodoro, M. L., Phillips, G. N. J. and Kavraki, L. E. (2000). Singular Value Decomposition of Protein Conformational Motions. Currents in Computational Molecular Biology. Satoru, M., Shamir, R. and Tagaki, T. Tokyo, Universal Academy Press, Inc.**:** 198-199.

Teodoro, M. L., Phillips, G. N. J. and Kavraki, L. E. (2001). Molecular Docking: A Problem with Thousands of Degrees of Freedom. IEEE International Conference on Robotics and Automation, Seoul, Korea, IEEE Press.

Tibshirani, R. (1992). "Principal curves revisited." Statistics and Computing **2**: 183 - 190.

Tipping, M. E. and Bishop, C. M. (1999). "Mixtures of Probabilistic Principal Component Analysers." Neural Computation **11**(2): 443-482.

Todd, M. J. and Freire, E. (1999). "The effect of inhibitor binding on the structural stability and cooperativity of the HIV-1 protease." Proteins: Structure, Function, and Genetics **36**(2): 147-56.

Totrov, M. and Abagyan, R. (1997). "Flexible protein-ligand docking by global energy optimization in internal coordinates." Proteins: Structure, Function, and Genetics **Suppl**(1): 215-20.

Trosset, J. Y. and Scheraga, H. A. (1998). "Reaching the global minimum in docking simulations: a Monte Carlo energy minimization approach using Bezier splines." Proceedings of the National Academy of Sciences USA **95**(14): 8011-5.

Trosset, J. Y. and Scheraga, H. A. (1999). "Flexible docking simulations: scaled collective variable Monte Carlo minimization approach using Bezier splines, and comparison with a standard Monte Carlo algorithm." Journal of Computational Chemistry **20**(2): 244-252.

Trosset, J. Y. and Scheraga, H. A. (1999). "PRODOCK: Software Package for Protein Modeling and Docking." Journal of Computational Chemistry **20**(4): 412-427.

Troyer, J. M. and Cohen, F. E. (1995). "Protein conformational landscapes: energy minimization and clustering of a long molecular dynamics trajectory." Proteins: Structure, Function, and Genetics **23**(1): 97-110.

Tuffery, P., Etchebest, C., Hazout, S. and Lavery, R. (1991). "A new approach to the rapid determination of protein side chain conformations." Journal of Biomolecular Structure and Dynamics **8**(6): 1267-89.

Urzhumtsev, A., Tete-Favier, F., Mitschler, A., Barbanton, J., Barth, P., Urzhumtseva, L., Biellmann, J. F., Podjarny, A. and Moras, D. (1997). "A 'specificity' pocket inferred from the crystal structures of the complexes of aldose reductase with the pharmaceutically important inhibitors tolrestat and sorbinil." Structure **5**(5): 601-612.

Vakser, I. A. (1995). "Protein docking for low-resolution structures." Protein Engineering **8**(4): 371-7.

van Aalten, D. M., Conn, D. A., de Groot, B. L., Berendsen, H. J., Findlay, J. B. and Amadei, A. (1997). "Protein dynamics derived from clusters of crystal structures." Biophysical Journal **73**(6): 2891-2896.

van Aalten, D. M., de Groot, B. L., Findlay, J. B., Berendsen, H. J. and Amadei, A. (1997). "A Comparison of Techniques for Calculating Protein Essential Dynamics." Journal of Computational Chemistry **18**(2): 169-181.

Vazquez-Laslop, N., Zheleznova, E. E., Markham, P. N., Brennan, R. G. and Neyfakh, A. A. (2000). "Recognition of multiple drugs by a single protein: a trivial solution of an old paradox." Biochemical Society Transactions **28**(4): 517-20.

Verkhivker, G. M., Bouzida, D., Gehlhaar, D. K., Rejto, P. A., Freer, S. T. and Rose, P. W. (2002). "Complexity and simplicity of ligand-macromolecule interactions: the energy landscape perspective." Current Opinion in Structural Biology **12**(2): 197-203.

Verkhivker, G. M., Rejto, P. A., Bouzida, D., Arthurs, S., Colson, A. B., Freer, S. T., Gehlhaar, D. K., Larson, V., Luty, B. A., Marrone, T. and Rose, P. W. (2001). "Parallel simulated tempering dynamics of ligand–protein binding with ensembles of protein conformations." Chemical Physics Letters **337**(1-3): 181-189.

Vieth, M., Hirst, J. D., Kolinski, A. and Brooks, C. L. I. (1998). "Assessing energy functions for flexible docking." Journal of Computational Chemistry **19**(14): 1612-1622.

Wasserman, Z. R. and Hodge, C. N. (1996). "Fitting an inhibitor into the active site of thermolysin: a molecular dynamics case study." Proteins: Structure, Function, and Genetics **24**(2): 227-37.

Weber, P. C., Ohlendorf, D. H., Wendoloski, J. J. and Salemme, F. R. (1989). "Structural origins of high-affinity biotin binding to streptavidin." Science **243**(4887): 85-8.

Weichsel, A. and Montfort, W. R. (1995). "Ligand-induced distortion of an active site in thymidylate synthase upon binding anticancer drug 1843U89." Nature Structural Biology **2**(12): 1095-101.

Wilson, D. K., Bohren, K. M., Gabbay, K. H. and Quiocho, F. A. (1992). "An unlikely sugar substrate site in the 1.65 A structure of the human aldose reductase holoenzyme implicated in diabetic complications." Science **257**(5066): 81-4.

Wilson, D. K., Tarle, I., Petrash, J. M. and Quiocho, F. A. (1993). "Refined 1.8 A structure of human aldose reductase complexed with the potent inhibitor zopolrestat." Proceedings of the National Academy of Sciences USA **90**(21): 9847.

Wlodawer, A., Miller, M., Jaskolski, M., Sathyanarayana, B. K., Baldwin, E., Weber, I. T., Selk, L. M., Clawson, L., Schneider, J. and Kent, S. B. (1989). "Conserved folding in retroviral proteases: crystal structure of a synthetic HIV-1 protease." Science **245**(4918): 616-21.

Wlodawer, A. and Vondrasek, J. (1998). "Inhibitors of HIV-1 protease: a major success of structure-assisted drug design." Annual Reviews Biophysics and Biomolecular Structure **27**: 249-84.

Wojciechowski, M. and Skolnick, J. (2002). "Docking of Small Ligands to Low-Resolution and Theoretically Predicted Receptor Structures." Journal of Computational Chemistry **23**(1): 189-197.

Wolfram, S. (1999). The Mathematica Book. New York, Cambridge University Press.

Wüthrich, K. (1986). Nmr of Proteins and Nucleic Acids. New York, J. Wiley & Sons.

Zacharias, M. and Sklenar, H. (1999). "Harmonic Modes as Variables to Approximately Account for Receptor Flexibility in Ligand-Receptor Docking Simulations: Application to DNA Minor Groove Ligand Complex." Journal of Computational Chemistry **20**(3): 287-300.

Zhao, S., Goodsell, D. S. and Olson, A. J. (2001). "Analysis of a data set of paired uncomplexed protein structures: new metrics for side-chain flexibility and model evaluation." Proteins: Structure, Function, and Genetics **43**(3): 271-9.

Zhu, J., Fan, H., Liu, H. and Shi, Y. (2001). "Structure-based ligand design for flexible proteins: application of new F-DycoBlock." Journal of Computer Aided Molecular Design **15**(11): 979-96.